In vivo application of magnetic resonance methods to study the substrate for disability in multiple sclerosis

by

Sridar Narayanan

Department of Neurology and Neurosurgery
McGill University, Montreal

May 2003

A thesis submitted to the Faculty of Graduate Studies and Research in partial fulfillment of the requirements for the degree of

Doctor of Philosophy

Abstract

This dissertation presents a series of studies aimed at elucidating the relationship between clinical disability and central nervous system pathology in multiple sclerosis (MS) using multiple magnetic resonance (MR) surrogates of pathology. MR spectroscopic (MRS) measurement of the neuronal-specific metabolite N-acetylaspartate provides an index of neuronal/axonal integrity. Magnetization transfer (MT) imaging provides measures related to myelination. Visualization of brain regions that become activated while performing a given task is possible using functional MRI (fMRI). Sophisticated image processing techniques allow more of the information contained in MR data to be extracted, such as the degree of atrophy of the brain or spinal cord.

We generated lesion probability images in stereotaxic space for relapsing-remitting (RR) and secondary progressive (SP) MS patients and demonstrated that the greater axonal damage per unit lesion volume previously observed in SP patients was not due to differences in lesion distribution between the two groups. Average NAA/Cr images in stereotaxic space showed that axonal injury extended into regions of low lesion probability, providing evidence for axonal injury in the normal-appearing white matter (NAWM). We showed that a portion of the axonal injury in NAWM was due to chronic metabolic dysfunction by observing recovery of chronically low central brain NAA in patients treated with interferon β-1b. Combining MRS and fMRI, we presented convincing evidence that cortical adaptations to injury could augment recovery from relapse in early stage MS, potentially masking underlying axonal injury. A combined

quantitative MT and MRS study showed that while diffuse axonal damage and demyelination in the NAWM were not linked, lesion volume weighted by an index of demyelination within lesions correlated well with diffuse axonal damage, suggesting that wallerian degeneration of axons damaged within lesions contributes to diffuse axonal injury in the NAWM. However, diffuse axonal and tissue injury were demonstrated in non-disabled patients with very low lesion burden and no brain atrophy, suggesting that a direct mechanism of NAWM injury also exists. Cerebral axonal injury was shown to be relevant to disability from the early stages of MS, while spinal cord atrophy was strongly linked to disability in late stage MS. Prolonged axonal dysfunction may eventually lead to axonal degeneration and tissue loss.

Résumé

Ce doctorat presénte une série d'études utilisant diverses techniques d'imagerie par résonance magnétique effectuées dans le but d'élucider la relation entre le déficit clinique et la pathologie du système nerveux central dans la sclérose en plaques. La mesure du métabolite neuronal N-acetylaspartate (NAA) par la technique de résonance magnétique spectroscopique fournit un index d'intégrité neuronale et axonale. L'imagerie par transfert de magnétisation permet d'évaluer la myélinisation. La résonance magnétique fonctionelle permet la visualisation des régions du cerveau qui s'activent suite à une tâche donnée. En outre, les techniques avancées de traitement des images permettent l'extraction d'informations complémentaires de celles contenues dans les données d'imagerie par résonance magnétique, telles que le degré d'atrophie du cerveau ou de la moelle épinière.

Nous avons généré des images de probabilités de lésions dans l'espace stéréotaxique chez les malades atteints de la forme cyclique et de la forme progressive secondaire. Nous avons ainsi démontré que l'atteinte axonale par unité de volume lésionnel, qui est plus marquée chez les patients atteints de la forme cyclique, n'était pas due à des differences dans la distribution des lésions entre les deux groupes. Les images de probabilités de NAA/Cr dans l'espace stéréotaxique ont démontré que les atteintes axonales s'étendaient dans les régions o_ la probabilité de trouver des lésions est faible, en particulier dans la matière blanche d'apparence normale. En observant une remontée du taux de NAA chez des patients présentant un déficit chronique de ce métabolite, et

traités par l'interferon ß-1b, nous avons démontré qu'une partie de l'atteinte axonale dans la matière blanche d'apparence normale était due à un dysfonctionnement métabolique chronique. L'utilisation combinée des techniques d'imagerie par résonance magnétique spectroscopique et fonctionnelle nous a permis de démontrer que l'adaptation corticale suite à une atteinte du système nerveux pouvait accélérer la guérison après une rechute durant la phase précoce de la sclérose en plaques, masquant ainsi éventuellement l'atteinte axonale sous-jacente. L'utilisation combinée des techniques d'imagerie par résonance magnétique spectroscopique et par transfert de magnétisation nous a permis d'observer que l'atteinte axonale étendue et la démyelinisation dans la matière blanche d'apparence normale n'etaient pas liées. Cependant, nous avons trouvé une corrélation entre l'atteinte axonale diffuse et le volume total des lésions pondéré par un index de démyelinisation à l'intérieur de ces lésions. Ceci nous a permis de suggérer que la dégénérescence wallerienne des axones malades au sein des lésions contribue à l'atteinte axonale diffuse dans la matière blanche d'apparence normale. D'autre part, la mise en évidence d'atteintes axonales et tissulaires diffuses chez les patients encore valides (chez qui la masse lésionnelle est minime et qui n'ont pas d'atrophie cérébrale) suggère un mécanisme direct pouvant être responsable des anomalies observées dans la matière blanche d'apparence normale. Nous avons démontré que l'atteinte axonale diffuse joue un rôle important dans les phases précoces de la sclérose en plaques, tandis qu'une atrophie de la moelle épinière est fortement liée au déficit clinique observé dans les phases tardives de la maladie. Un dysfonctionnement axonal prolongé pourrait ultimement entraîner une dégénéréscence axonale et une perte tissulaire.

Table of Contents

Acknowledgements

Modern research has become an intensely collaborative endeavour, particularly in the field of neuroimaging. The work presented in this thesis would have been impossible without the contributions of many people.

First and foremost, I would like to thank Professor Douglas Arnold, my supervisor and mentor, for nurturing my research career and providing the environment and means to conduct my studies. Not only has he taught me a great deal about magnetic resonance spectroscopy and multiple sclerosis, but he has helped me hone my abilities to think critically, pose scientifically interesting questions that are answerable by the techniques at hand, and design successful experiments. I am also grateful for the confidence he has shown in allowing me to conduct my research with a remarkable degree of independence, while still giving me the benefit of his incredible insight and rather particular view of things.

I would also like to thank the members of my advisory committee, Drs. Bruce Pike and Jack Antel. I have always been impressed with Dr. Pike's knowledge of MR physics, and am indebted to him for his advice and thoughts regarding all things MR, as well as his trademark ability to cut through the fluff to the heart of the matter. Dr. Antel has provided me with an invaluable "biological perspective" on my work, and his critical reading of my manuscripts has been extremely helpful. I would also like to acknowledge the help of Dr. Gordon Francis, who was originally part of my advisory committee, but has since left McGill for Boston.

My friend and collaborator, Dr. Nicola De Stefano, has been an important figure in the work contained in this thesis. From the many late nights poring over data (both in Montreal and Siena), to lively discussions over results, interpretations and manuscripts, and our continual exchange of ideas, expertise, food and wine, it has always been a pleasure. I am grateful to Professor Paul Matthews for his keen insights and remarkable ability to think "out of the box", particularly when revising the discussion of a manuscript, and to Dr. Louis Collins for help and advice on image processing issues.

From the Graduate Program in Neurosciences, I would like to thank my administrative mentor, Dr. Guy Debonnel, for ensuring that I jumped through all the hoops necessary to arrive at this stage, Monique Ledermann, for administrative help and keeping tabs on my complicated situation, and Dr. Heather Durham, for advice and encouragement.

I would like to thank the many bright young minds that have passed through the MRS Unit over the years for their friendship, support and camaraderie. The assistance of Simon Francis, Carmela Tartaglia, Zografos Caramanos, Carlos Santos, Samson Antel and Jacqueline Chen in data collection and analysis was invaluable and is greatly appreciated. Special thanks go to Carmie and Jacqueline for last-minute help in getting things done under the wire on more than one occasion, and for their long-standing friendship and moral support. I would also like to thank Li Li Min, Tanja Taivassalo, Neda and Andrea Bernasconi, Wolfgang Serles and Sanjay Kalra for sharing the good times and the bad. Special thanks go to the amazingly multi-lingual Neda for translating the abstract to French.

The MRS Unit would not function without the efficient administrative assistance of Ellie Tobman; her readily offered help, friendship and coffee are greatly appreciated.

Many thanks go to the students and alumni of the Brain Imaging Centre for friendship and collaboration: Dr. Rick Hoge, Dr. John Sled, Dr. David MacDonald, Dr. Alan Evans, Ives Levesque, Jennifer Campbell, Najma Khalili and, of course, Dr. Roch Comeau, who has been my buddy for 17 years and counting (and thanks for the colour prints!).

Special thanks go to my fiancée, Aman Badhwar, for love and encouragement when I needed it most, and for helping with some of the drudgery involved in putting together this thesis. To my parents and brothers, thanks for being there.

I would like to thank the MR technologists for help in performing the scans (particularly André Cormier and Gilles Leroux), the neurologists and staff of the MS Clinic and the Clinical Research Unit of the MNI (particularly Rozie Arnaoutelis) for their assistance in recruiting patients and coordinating our studies and, finally, to the patients themselves, for so generously donating their time.

Contributions to original knowledge

This thesis contains seven manuscripts, five of which have already been published or accepted for publication in internationally known, peer-reviewed journals. The important and original contributions to scientific knowledge are outlined below.

Manuscript 1: *Imaging axonal damage in multiple sclerosis: spatial distribution of magnetic resonance imaging lesions.* This combined lesion volumetry and MRS study describes the novel application of stereotaxic methods (registration and transformation of segmented lesion maps and metabolite ratio images into a standardized brain-based coordinate system) to (i) quantitatively define the spatial probability distribution of lesions in relapsing-remitting and secondary progressive MS patients, which was only qualitatively described before, and show that only the quantity of lesions and not their spatial distribution differed between the two MS subgroups, (ii) demonstrate that axonal injury extended beyond regions of high lesion probability into lesions of low probability across this group of MS patients, providing evidence for axonal injury in the normal-appearing white matter (NAWM). A follow-up study using sophisticated spatial statistics confirmed the existence of axonal damage in the NAWM in both RR and SP patients, with the SP group exhibiting greater NAWM damage (Fu et al., 1998). These results have often been quoted in subsequent literature, particularly by pathologists who may have been motivated by it to search for and find conclusive evidence that significant axonal damage occurs in MS.

Manuscript 2: *Axonal metabolic recovery in multiple sclerosis patients treated with interferon b-1b.* After establishing that axonal pathology existed in NAWM, we pursued a number of avenues to elucidate the possible mechanisms for this. Previous MRS studies showed that transient axonal metabolic dysfunction could occur within acute plaques, so we hypothesized that chronic axonal dysfunction could contribute to low NAWM NAA. In this paper, we were the first to describe the striking result that cerebral NAA could recover in chronic MS patients following treatment with interferon β-1b. The implication is that axons can experience chronic metabolic dysfunction, and that this can be partially reversed with interferon treatment, at least for a time.

Manuscript 3: *Relating axonal injury to functional recovery in multiple sclerosis.* The mismatch between clinical disability and the pathology visualized with brain MRI has been commented upon by many authors. We questioned whether cortical reorganization to injury could mask the clinical impact of white matter injury. In this combined functional MRI and spectroscopy study, we observed and quantified enlarged and bilateral areas of cortical activation in conjunction with recovery of hand motor function following an acute attack of hemiparesis referable to a new acute lesion. Recovery of hand function preceded recovery of NAA within the lesion. This was a seminal article in that it was the first to clearly demonstrate that cortical adaptations to acute white matter injury could aid recovery of function in MS. In a follow-up study (Reddy et al., 2000a), we demonstrated that the extent of cortical adaptation to a hand motor task in a group of patients with normal hand function was strongly correlated to the degree of axonal injury, confirming the hypothesis that cortical adaptations could mitigate the clinical impact of white matter injury and potentially mask early damage. Since axonal damage accumulates and eventually will have clinical consequences, this

result substantiates the rationale for early treatment even for patients with mild symptoms.

Manuscript 4: *Assessment of axonal injury and demyelination in the cerebral normal-appearing white matter of patients with multiple sclerosis.* Continuing to probe the mechanisms of axonal injury in NAWM, we applied the quantitative magnetization transfer imaging techniques developed by John Sled and Bruce Pike along with MR spectroscopic imaging to study the relationships between the fractional size of the bound water pool (F), a putative marker of myelination, and NAA/Cr in the cerebral normal-appearing white matter of MS patients. We found that demyelination and axonal injury in the NAWM were not linked, but that NAWM axonal injury correlated with total lesion volume weighted by mean lesion F (an index of the extent of demyelination within lesions), suggesting (i) that wallerian degeneration of axons damaged in lesions contributes to axonal damage in NAWM and (ii) lesion volume weighted by an index of the destructiveness of the lesions may provide a better measure of the burden of disease.

Manuscript 5: *Evidence of axonal damage in the early stages of multiple sclerosis and its relevance to disability.* Axonal damage and loss had previously been thought to be late events in MS, occurring only after substantial demyelination had accumulated. In this MRS study, we showed that cerebral axonal damage is evident from the early stages of MS and shows greater declines with increasing disability than in the later stages of the disease. Axonal damage showed good correlation with EDSS both in low disability and low duration patients. These results demonstrate that axonal damage is not a late event in MS, but occurs right from the beginning of the disease, motivating early therapeutic interventions to preserve axons. The lack of correlation between cerebral NAA and EDSS late in the disease, combined with the evidence from

Manuscript 2 for widespread axonal dysfunction being present in RR patients, led us to hypothesize that the early-stage declines of NAA were due in large part to increasing axonal dysfunction, while in later stage MS, mechanisms of axonal degeneration and loss predominated. Concomitant brain volume loss would mitigate decreases of cerebral NAA, consistent with the lack of correlation between cerebral NAA and EDSS in late stage MS. The following two studies were designed to test this hypothesis.

Manuscript 6: *Disease duration influences the relationship between brain axonal injury, spinal cord atrophy and disability in multiple sclerosis.* We combined MRS assessment of axonal injury with measurement of spinal cord atrophy in a group of patients with a wide range of disability scores to extend and clarify previous findings and better define the substrate for disability over the course of the disease. We found that cerebral axonal injury correlated strongly with disability early in the disease, while spinal cord atrophy correlated strongly with disability late in the disease. These results suggest that chronic axonal dysfunction is the prime determinant of disability early in MS (perhaps mediated by chronic low-level inflammation), but that in the later stages the disease takes on a more degenerative character typified by axonal loss and atrophy.

Manuscript 7: *Diffuse axonal and tissue injury is already present in MS patients with low cerebral lesion load and no disability.* This study combined MRS, magnetization transfer imaging and measurements of brain atrophy in patients with low lesion load and without disability to help clarify the mechanisms of NAWM injury in early stage MS. We showed that diffuse axonal and tissue damage (low NAA/Cr and NAWM MTR) occurs even in very mildly affected patients. Brain volume was normal in the two subgroups with particularly low disease duration or lesion volume, but showed a trend toward atrophy for the whole group. The important implications of this study are

that (i) diffuse axonal and tissue damage can occur to some degree independently of focal inflammatory demyelination, suggesting the existence of some other "slow burning" pathological process and (ii) NAA loss and brain atrophy do not necessarily occur in parallel, and should be measured in concert to assess the full extent of axonal injury and loss. These data remain consistent with the evidence from Manuscript 2 for widespread axonal metabolic dysfunction being present in relapsing MS, perhaps due to low-level inflammation or subtle myelin pathology. The lack of clinical disability associated with these brain abnormalities is likely the result of the type of cortical adaptations seen in Manuscript 3.

Contributions of Authors

In accordance with the *Guidelines for Thesis Preparation* of the Faculty of Graduate Studies and Research of McGill University, the contributions of individual authors to the work described in each manuscript contained in this thesis is described below.

Manuscript 1: *Imaging Axonal Damage in Multiple Sclerosis: Spatial Distribution of Magnetic Resonance Imaging Lesions*

Authors: Sridar Narayanan MSc, Liqun Fu MSc, Erik Pioro MD, DPhil, Nicola De Stefano MD, D. Louis Collins PhD, Gordon S. Francis MD, Jack P. Antel MD, Paul M. Matthews MD, DPhil, Douglas L. Arnold MD

Contributions: This paper presents a unique analysis of data acquired as part of an ongoing study in the MRS Unit initiated by Dr. Arnold. The idea for this analysis arose during conversations between Drs. Collins, Arnold and myself. I performed computer-assisted segmentation of MS lesions on MRI, registration of MRI images to a standard brain in stereotaxic space, transformation of MRIs, segmented lesion maps and metabolite images into stereotaxic space and generated lesion probability distributions and average metabolite maps. I did the initial interpretation of the data and wrote the manuscript. The software to perform these analyses was developed by Dr. Collins and colleagues in the Brain Imaging Centre under Dr. Alan Evans. Drs. Pioro and De Stefano supervised the acquisition of the MRS and MRI data and Dr. De Stefano performed

metabolite quantitation using software written by Liqun Fu. Liqun Fu also performed the Monte Carlo simulations to test for significant differences in risk ratio. I performed the other, more standard statistical tests. Drs. Francis, Antel, Matthews and Arnold recruited the patients in the study and performed clinical disability assessments. All coauthors contributed to the critical review of the manuscript.

Manuscript 2: *Axonal metabolic recovery in multiple sclerosis patients treated with interferon b-1b.*

Authors: Sridar Narayanan, MSc, Nicola De Stefano, MD, PhD, Gordon S. Francis, MD, Rozie Arnaoutelis, BSc, Zografos Caramanos, MA, D. Louis Collins, PhD, Daniel Pelletier, MD, Barry G. W. Arnason, MD, Jack P. Antel, MD and Douglas L. Arnold, MD

Contributions: The original idea for this study arose out of discussions between Drs. Arnold and Arnason. The design of the study was established in a meeting between Dr. Arnold, Dr. De Stefano, Dr. Antel, Dr. Francis, Rozie Arnaoutelis and myself. I established the scanning protocols, supervised the bulk of the MRI/MRS acquisitions and performed MRS quantitation and lesion volumetry. Dr. Pelletier supervised the remainder of the MRI/MRS acquisitions. Rozie Arnaoutelis coordinated the study and contacted patients. Drs. Francis and Antel performed clinical assessments and Dr. Collins performed brain atrophy measurements. Zografos Caramanos performed the bulk of the statistical analysis. I wrote the manuscript, which was critically reviewed by Dr. De Stefano and Dr. Arnold, with input from all authors.

Manuscript 3: *Relating axonal injury to functional recovery in multiple sclerosis.*

Authors: Hasini Reddy, MD, Sridar Narayanan, MSc, Paul M. Matthews, MD, DPhil, Richard D. Hoge, PhD, G. Bruce Pike, PhD, Pierre Duquette, MD, Jack Antel, MD, Douglas L. Arnold, MD

Contributions: This is a combined fMRI and MRS study of a patient with acute hemiplegia due to several large, confluent acute plaques. The patient was first seen by Dr. Duquette who referred her to Dr. Arnold for MRS study of her acute plaque. Dr. Arnold and I performed the initial MRI/MRS scanning according to protocols that I had established, and Dr. Arnold suggested that an fMRI would be revealing. I devised an appropriate fMRI "boxcar" activation paradigm consisting of a simple finger-thumb tapping task with auditory cueing at a frequency roughly 75% of her maximum tapping rate at the time. The acquisitions were performed using pulse sequences written by Drs. Pike and Hoge. I did the MRS quantitation and performed the fMRI analysis using software written by Dr. Hoge. Dr. Reddy identified the corticospinal tract on MRI, labeled regions of activation above the critical *t*-statistic threshold and wrote the first draft of the manuscript. Dr. Matthews and I critically reviewed and revised the manuscript, with final review and input from all authors.

Manuscript 4: *Assessment of axonal injury and demyelination in the cerebral normal-appearing white matter of patients with multiple sclerosis.*

Authors: Sridar Narayanan, MSc, Simon J. Francis, BSc, John G. Sled, PhD, A. Carlos Santos, MD, Samson Antel, MSc, Ives Levesque, BSc, Steven Brass, MD, Yves Lapierre, MD, Dominique Sappey-Marinier, PhD, G. Bruce Pike, PhD and Douglas L. Arnold, MD

Contributions: This was an intensely collaborative study combining MRS and quantitative magnetization transfer imaging (QMTI), a technique developed by Dr. Sled

as part of his PhD work, supervised by Dr. Pike. Drs. Pike, Sled, Arnold and myself established the overall goals and design of the QMTI study. I added a parallel MRS analysis, as these were patients we were following as part of ongoing MRS protocols. Dr. Santos and I supervised the MRS scans and performed MRS quantitation. Ives Levesque and Dr. Santos performed the QMTI acquisitions and Ives Levesque and Dr. Sled performed the QMTI analyses and generated the parametric images. Simon Francis performed lesion and tissue segmentation on the MRI data from the MRS acquisitions, and Dr. Santos performed the analysis of the anatomical images from the QMT scanning sessions. I performed the NAWM regression analysis using software developed by Samson Antel, Dr. Sappey-Marinier and myself. Drs. Brass, Lapierre and Arnold performed clinical assessments. I drafted the manuscript, which has been reviewed so far by Drs. Pike, Sled and Arnold.

Manuscript 5: *Evidence of axonal damage in the early stages of multiple sclerosis and its relevance to disability.*

Authors: Nicola De Stefano, MD, Sridar Narayanan, MSc, Gordon S. Francis, MD, Rozie Arnaoutelis, BSc, M. Carmela Tartaglia, BSc, Jack P. Antel, MD, Paul M. Matthews, MD, Douglas L. Arnold, MD

Contributions: This is a cross-sectional study of 88 patients spanning the EDSS range using combined MRI/MRS. Dr. De Stefano and I supervised the acquisitions and, along with Carmela Tartaglia, analyzed the MRS data. I performed lesion volumetry. Drs. Francis, Antel and Arnold performed clinical assessments and Rozie Arnaoutelis coordinated the study. Dr. De Stefano performed the statistical analyses in consultation with me, and drafted the manuscript. I critically reviewed and revised the manuscript, as did Drs. Matthews, Antel and Arnold.

Manuscript 6: *Disease duration influences the relationship between brain axonal injury, spinal cord atrophy and disability in multiple sclerosis.*

Authors: Sridar Narayanan, MSc, Nicola De Stefano, MD, PhD, Simon Francis, BSc, M. Carmela Tartaglia, BSc, Rozie Arnaoutelis, BSc, Yves Lapierre, MD and Douglas L. Arnold, MD

Contributions: I had the idea to expand our brain MRI/MRS acquisition protocols with spinal cord imaging, inspired to a large part by the work of Dr. Losseff and the Queen Square group. I devised a high-resolution imaging protocol suitable for reliable measurements of spinal cord cross-sectional area that could be implemented on our Philips ACS II scanner with the coils available. I then established the post-processing procedure to reliably and reproducibly quantify spinal cord cross-sectional area at the level of C2. This paper reports a cross-sectional study of 56 patients. I supervised the MRI/MRS scanning including the spinal cord acquisitions. Carmela Tartaglia and I performed the MRS quantitation, and Simon Francis and I performed the spinal cord cross-sectional area analyses. Drs. Lapierre and Arnold performed clinical assessments, and Rozie Arnaoutelis coordinated the study. I performed the statistical analysis in consultation with Dr. De Stefano and drafted the manuscript.

Manuscript 7: *Diffuse axonal and tissue injury is already present in MS patients with low cerebral lesion load and no disability*

Authors: Nicola De Stefano, MD, Sridar Narayanan, MSc, Simon J. Francis, BSc, Steve Smith, DPhil, Marzia Mortilla, MD, M. Carmela Tartaglia, BSc, Maria L. Bartolozzi, MD, Leonello Guidi, MD, Antonio Federico, MD and Douglas L. Arnold, MD

Contributions: This is a cross-sectional combined MRI/MRS study measuring NAA, MTR and brain atrophy in 60 MS patients without disability (EDSS < 2) in two centres,

the MNI and the Institute of Neurological Sciences of the University of Siena. Dr. De Stefano devised and planned this study to see whether diffuse axonal or tissue damage were present in non-disabled patients with low lesion load. Drs. De Stefano and Mortilla supervised the scanning in Siena, while I supervised the scanning in Montreal. Dr. De Stefano analyzed the MRS data in Siena while Carmela Tartaglia and I analyzed the Montreal MRS data. Simon Francis performed tissue segmentation and lesion volumetry for data from both sites. Dr. Smith developed software for the measurement of brain atrophy (SIENAX).

Chapter 1

Introduction

Elucidating the relationship between clinical disability and disease pathology is essential for understanding the natural history of multiple sclerosis (MS) and evaluating new therapeutic strategies for this disease. Magnetic resonance imaging (MRI) can directly visualize pathology in the central nervous system and has had a major impact on the diagnosis and study of MS. However, the lack of pathological specificity of lesions on conventional MRI has limited its utility as a surrogate for pathology. The lack of a strong correlation between the conventional measure of MRI lesion load, the total lesion volume seen on T2-weighted MRI, and clinical disability in either cross-sectional or longitudinal studies highlight this difficulty. Neuroimaging measures are needed that are specific for particular aspects of MS pathology in order to better understand the substrates for disability. The combined use of multiple magnetic resonance (MR) techniques having different pathological specificities allows for better characterization of the disease processes *in vivo*.

Magnetic resonance spectroscopy (MRS) is particularly well suited for the study of axonal damage *in vivo* as it allows noninvasive quantification of axonal dysfunction

and loss based on the signal intensity of N-acetylaspartate (NAA), a compound localized exclusively in neurons and axons in normal adult brain. Other advanced MR techniques such as magnetization transfer (MT) imaging, T1W lesion analysis, and quantitative relaxometry also offer more specific pathological information than that obtained by conventional MRI and may provide data that account for variance not explained by T2-weighted lesion volume. Quantification of brain or spinal cord atrophy may provide a pathologically nonspecific measure of tissue loss and advanced disease changes that correlate with axonal loss and disability. Finally, functional MRI (fMRI) may help to understand the relationship between axonal loss and disability by demonstrating whether functional reorganization compensates for chronic axonal loss. The theory and application of magnetic resonance methods to the study of MS will be summarized in the review of relevant literature.

The general rationale for my doctoral work was the idea that combined application of multiple *in vivo* MR techniques that reflect different aspects of disease pathology and pathophysiology could yield important new insights into the pathological substrate for disability in MS. Under this rather broad umbrella, the following specific questions are addressed in this dissertation.

1. Are pathological changes outside of visible lesions a general feature of MS, and does the degree of pathology relate to the amount of visible lesion or to the clinical stage of the disease?
2. Is potentially reversible axonal metabolic dysfunction present in MS, and do therapeutic agents aid axonal recovery?
3. Does functional reorganization of neuronal circuitry occur in MS, and can this mitigate the neurological impairment associated with axonal injury?

4. How does axonal injury relate to demyelination?
5. Is the relationship between axonal damage and clinical disability constant, or does it vary with the stage of MS?
6. How does spinal cord pathology relate to disability, and does this relationship change over the course of the disease?
7. Is axonal pathology already present in early stage MS, or is it strictly a feature of late stage disease?

This thesis is organized as a series of manuscripts that address each of these questions in turn, employing the appropriate neuroimaging modalities to the task. The rationale and objectives of each study will be discussed in the preface to its respective chapter. Since questions 5, 6 and 7 are strongly interrelated, the manuscripts addressing these questions have been organized into one chapter with a unified preface. The final chapter of this thesis summarizes the entire body of work and draws overall conclusions from it.

Chapter 2

Review of the literature

2.1 Epidemiology of MS

Multiple sclerosis (MS) is an idiopathic inflammatory disease of the central nervous system characterized by deficits referable to multiple lesions (also called "plaques") disseminated in the CNS that arise independently at different times. The natural history of the disease is marked by two general stages. For most patients the early phase of the disease is characterized by recurrent attacks with neurological deficits that resolve completely or partially. This form of the disease is classified as "relapsing-remitting" (RR). Eventually the remissions diminish or cease completely while the disease progresses continuously (McAlpine et al., 1955). This is referred to as the secondary progressive (SP) phase. In addition, a small percentage of MS patients (about 10-15%) have a progressive course from onset, in the absence of attacks. This form of MS is termed primary progressive (PP) MS (Thompson et al., 2000).

2.2 Pathology

Pathological examination of the brains of patients with MS reveals multiple, diffusely scattered lesions of different ages. Recent lesions show inflammation and edema with loss of myelin, relatively modest degeneration of oligodendrocytes and large numbers of macrophages, whereas longstanding, severe lesions show profound loss of myelin and oligodendrocytes with astrogliosis (Matthews et al., 1991b). A relative sparing of axons in the center of lesions has been a characteristic emphasized by pathologists, as it is helpful in discriminating them from those of a more generally destructive process, such as encephalitis. However, this does not imply that axonal damage does not occur. Axons show changes in size, shape, and morphology (Prineas and Connell, 1978; Raine and Cross, 1989; Rodriguez and Scheithauer, 1994) and estimates suggest that there may be loss of 1/3 - 2/3 or more of the axons traversing severe, chronic lesions (Barnes et al., 1991; Prineas and Connell, 1978).

Focal lesions in MS are usually thought to begin with acute increases in the permeability of the blood brain barrier (BBB) and infiltration of fluid and inflammatory cells associated with acute swelling. The cells secrete a large variety of soluble factors that aid in the destruction of myelin. Although the attack is primarily directed against myelin, other cells such as axons are also injured. Recent MR evidence based on magnetization transfer, diffusion and spectroscopy suggests that focal lesions in MS actually may begin to form months to years before they enter the acute phase described above (Filippi et al., 1998; Goodkin et al., 1998; Pike et al., 2000; Richert et al., 2001; Tartaglia et al., 2002; Werring et al., 2000).

The acute inflammatory phase subsides after weeks to months and repair processes occur. Myelin can regenerate (Raine, 1997b) in both acute (Prineas et al., 1993;

Raine and Wu, 1993) and chronic (Prineas and Connell, 1979) lesions, but the regeneration of myelin is not complete and may become less efficient over time. The causes of this failure of remyelination in the later stages of MS are unclear, but may include progressive damage to oligodendrocytes by inflammation or glutamate excitotoxicity, inhibitory influences on oligodendrocyte proliferation and migration, the effects of age or changes in their axonal substrate (Chang et al., 2002; Pitt et al., 2000; Raine, 1997b; Werner et al., 2000).

2.3 Pathophysiology

Nervous system dysfunction in MS has generally been attributed to the consequences of demyelination (Quarles et al., 1993). Myelin, acting both directly as an electrical insulator and indirectly in organization of axonal membrane ion channels, allows the saltatory conduction necessary for normal myelinated nerve conduction. Demyelination leads to conduction block acutely because of failure of propagation of locally generated axonal membrane potentials due to sodium channels being clustered at the previous nodes of Ranvier while internodal repolarizing potassium channels are unmasked. Because at least partial remyelination of MS lesions has been described pathologically (Prineas et al., 1993), one possible explanation for the remission of symptoms is remyelination of previously demyelinated axonal segments. However, there are also other potential explanations. In acute optic neuritis, serial examination using visual evoked potentials revealed recovery of the P100 amplitude with recovery of visual acuity, but with persistently prolonged latency (Youl et al., 1991). In another study (Jones, 1993), although some recovery of latency had been observed (attributable to remyelination), 70% of patients still had abnormal latencies more than 2 years after the initial episode. These findings and the observation that recovery of axonal function

parallels an increase in the density of internodal sodium channels over time (Rivera-Quinones et al., 1998) (Waxman, 1998) suggests that adaptation of axonal sodium channels is an important determinant of axonal functional recovery (McDonald, 1994).

The available experimental evidence supports the possible involvement of multiple mechanisms in recovery by emphasizing that there is not a simple relationship between demyelination and conduction block (Rasminsky, 1984). In nerve that is chronically denervated by diphtheria toxin (Rasminsky and Sears, 1972) or in the dystrophic mouse model (Rasminsky et al., 1978), conduction may be preserved across even several millimeters of demyelinated axon.

2.4 Selected questions regarding the pathology and pathophysiology of MS

A key component for understanding the natural history of MS and evaluating new therapeutic strategies is the relationship between clinical disability and disease pathology. The problem is complicated by limitations of the measurement "instruments" for both disability and pathology. It is hoped that the MS functional composite (MSFC) (Fischer et al., 1999) score will overcome some of the weaknesses of the traditional Kurtzke expanded disability status scale (EDSS) (Kurtzke, 1983). Modern quantitative neuropathological techniques are also improving our understanding of MS pathology, particularly with respect to axonal damage in lesions and so-called normal-appearing white matter (NAWM).

To say that MS is an enigmatic disease would be an understatement. Many questions remain regarding the pathophysiology of lesion formation and evolution, the pathological substrate for chronic impairment and disability, and the mechanisms underlying secondary progression. A number of these questions can be approached using

in-vivo magnetic resonance techniques, and a selection of these will be addressed in the body of this thesis.

As evidence accumulates that demyelination alone is insufficient to explain chronic nervous system dysfunction, the role of axonal damage is being increasingly appreciated. Careful examination of postmortem material, particularly using recent technical advances for observing axons, has demonstrated clearly that sparing of axons in MS is only relative: axonal transection (Trapp et al., 1998), chronic damage (Ferguson et al., 1997), and substantial loss of axons (Raine, 1997a) having all been demonstrated.

Irreversible loss of axons must be associated with chronic neurological impairment and disability to the extent that central nervous system redundancy and plasticity cannot compensate. The hypothesis that chronic axonal damage and loss (rather than demyelination) is primarily responsible for chronic impairment and disability in MS is termed the "Axonal Hypothesis".

Figure 2-1 illustrates the hypothetical relationship between disability, chronic axonal loss, and MRI activity in MS. MRI reveals, on average, about 10 times more new lesions (white peaks) than there are clinical exacerbations (gray peaks) (Barkhof et al., 1997; Miller and Frank, 1998). This may occur, in part, because the T2 changes are not necessarily associated with significant myelin or axon damage. Even those lesions that do produce neurological dysfunction may still remain subclinical because they do not produce sufficient dysfunction of eloquent regions of brain to exceed a "threshold" for clinical expression. In the early phase of the disease, recovery may appear to be complete because recovery of acute axonal dysfunction may predominate over permanent axonal damage (De Stefano et al., 1995a), and/or because sufficient axons remain such that cerebral plasticity and functional reorganization are able to compensate. Axonal damage

and associated accumulated burden of neurological dysfunction at this stage of disease, therefore, remain subclinical. However, this apparent clinical recovery does not necessarily mean that axonal damage is not significant at this early stage of the disease. Assessment of the amount of axonal injury and loss at various stages of MS is necessary in order to better understand the substrate for disability and progression in MS.

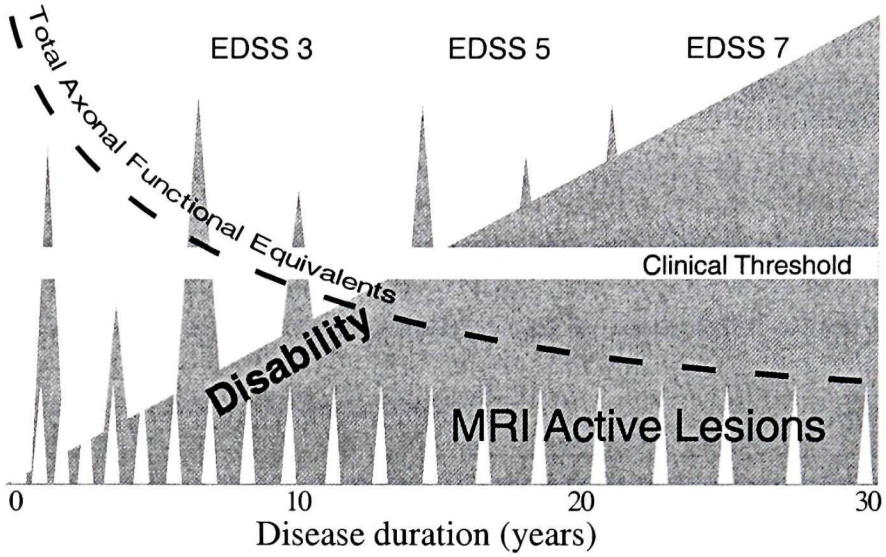

Figure 2-1. Hypothetical relationship between MRI activity (white peaks), accumulated irreversible disability (gray), clinical exacerbations (gray peaks), and axonal loss and functional impairment (black dotted line) in MS.

Clearly, if the hypothetical relationship between axonal pathology and disability described above is correct, it has major implications for treatment – arguing that treatment should be started as early as possible and be directed, not only at controlling inflammation, but also at axonal protection.

Since multifocal lesions are the hallmark of MS, most studies in this disease have naturally focused on lesions and lesion pathology. However, combined histological and histochemical studies have revealed abnormalities in the macroscopically "normal" appearing white matter (Allen et al., 1981; Allen and McKeown, 1979), either suggesting that the white matter in MS patients may be more susceptible to the disease process, or

that there could be primary pathology affecting the white matter at a level below that required to form a lesion. An initial magnetic resonance spectroscopy (MRS) study showed decreases of NAA in large single-voxels out of proportion to the lesion content of the voxels, suggesting that NAWM abnormalities contributed to the NAA decreases (Arnold et al., 1990a). A subsequent serial MR spectroscopic imaging (MRSI) study of a large demyelinating lesion demonstrated abnormal metabolite signals extending beyond the border of the plaque as seen on MRI (Arnold et al., 1992). The general relevance of pathology in the macroscopically normal-appearing white matter to clinical impairment in MS is an important question that should be addressed *in-vivo* in patients with MS.

Given this backdrop, a number of questions can be formulated which are testable using in-vivo magnetic resonance (MR) methods.

1. Are pathological changes outside of visible lesions a general feature of MS, and does the degree of pathology relate to the amount of visible lesion or to the clinical stage of the disease?
2. Is potentially reversible axonal metabolic dysfunction present in MS, and do therapeutic agents aid axonal recovery?
3. Does functional reorganization of neuronal circuitry occur in MS, and can this mitigate the neurological impairment associated with axonal injury?
4. How does axonal injury relate to demyelination?
5. Is axonal pathology already present in early stage MS, or is it strictly a feature of late stage disease?
6. Is the relationship between axonal damage and clinical disability constant, or does it vary with the stage of MS?

7. How does spinal cord pathology relate to disability, and does this relationship change over the course of the disease?

The remainder of this chapter will summarize published work using conventional and newer, more advanced MR techniques that begin to answer these questions, including some discussion on the basic principles behind these techniques. Subsequent chapters of this thesis will present, in detail, studies conducted by myself and colleagues that employ advanced MR methods to further elucidate the answers to these questions and contribute new knowledge to the study of MS.

2.5 Magnetic resonance techniques for investigating pathology and pathophysiology

2.5.1 Conventional imaging

MRI takes advantage of the fact that certain nuclei, in particular the nuclei of the hydrogen atoms in water molecules, have a property known as nuclear spin. Placing a water-containing sample in a strong magnetic field gives rise to a net magnetization, which can be manipulated via pulses of radiofrequency (RF) energy at their resonant frequency. The system returns to its equilibrium state with time constants dependent upon the local chemical environment of the water molecules, re-emitting RF energy as it does so. By measuring the dynamic properties of the emitted signal, we can non-invasively probe the chemical environment of the water molecules. In a living organism, images of great anatomical detail based on differences in proton density and spin-lattice (longitudinal, or T1) and spin-spin (transverse, or T2) relaxation rates between different tissue types can be generated by the judicious application of RF pulses and magnetic field gradients. On standardized imaging sequences, healthy tissues exhibit fairly stereotyped

relative MR intensities across normal subjects. Pathologies that disturb the resonance properties of water will change the locally observed signal and thus can be visualized as regions of changed MRI intensity.

Conventional MR images reflect a combination of the three basic MRI parameters of proton density, T1 and T2. Sequences are generally designed to provide images that have a greater weighting of one of these parameters. A T1-weighted image is one in which differences in T1 between tissues are maximized, and in human brain provides good grey matter / white matter contrast. Similarly, T2-weighted sequences highlight differences in T2 between tissues, and are effective at visualizing pathologies that strongly affect local T2 relaxation rates, such as those associated with inflammation or edema. In particular, MS plaques appear as hyperintense regions on T2-weighted (T2W) images. A true proton density-weighted sequence attempts to minimize the effects of T1 and T2 relaxation, producing images that more or less reflect the distribution of water protons. However, what is generally referred to as a proton density-weighted scan actually produces images with an intermediate weighting to T1 or T2-weighted images, with relatively bright lesions and dark CSF. Note that none of these three types of imaging sequence produce "pure" images, in that there always remains some contribution from the other two parameters to the resulting contrast. Methods exist for producing quantitative parametric images, but these are time-consuming techniques employed at a few specialized centres, and are not generally available.

T2 lesion load

The notion of a measure of the "burden of disease" to reflect the accumulated extent of pathological damage due to MS is an attractive concept. One measure of disease burden is the total volume of lesion quantified on T2-weighted MRI (Paty, 1993). Several

studies have demonstrated that T2W lesion volume increases by about 10%/year in MS patients (Kastrukoff et al., 1990; Paty and Li, 1993), and T2W lesion volume has been shown to be useful as an additional outcome measure in clinical trials. For example, in the β-interferon 1b trial (Paty and Li, 1993), RR patients demonstrated significantly greater accumulation of lesion burden when on placebo than when treated with β-interferon.

T1 lesion load

T2-weighted lesions can also be associated with regions of hypointense signal on T1-weighted images. A T1-weighted lesion can be defined by specifying an intensity threshold (for example, 75% of the intensity of surrounding white matter, or, alternatively, the intensity of grey matter) below which voxels are considered lesion. A T1 lesion usually represents some fraction of the volume of the corresponding T2W lesion, and total T1W lesion loads are substantially smaller than T2W lesion loads. T1W imaging is less sensitive to MS lesions than T2W imaging, but may be more specific for tissue destruction as opposed to inflammation or edema (van Walderveen et al., 1999; van Walderveen et al., 1998).

Limitations of lesion volume

A major concern with using lesion volume as a measure of the burden of disease in MS is that it has been difficult to demonstrate a strong correlation between MRI cerebral lesion load and clinical status in either cross-sectional or longitudinal studies (Filippi et al., 1994b; Filippi et al., 1995b; Khoury et al., 1994; Miller, 1994). Using T1 lesion volume measures instead of T2 lesion volume improves the correlation with disability (Lycklama à Nijeholt et al., 1998), particularly in longitudinal studies of SP

patients (Truyen et al., 1996), but a large proportion of the variance in EDSS remains unexplained by cerebral lesion volume (van Walderveen et al., 2001). One possibility is that spinal cord lesions may account for a failure to find strong correlations between cerebral lesion load and disability. Another is that the scoring of disability is heavily weighted towards motor dysfunction whereas the lesion volume is measured over the whole brain, most of which is not directly involved in motor function. Perhaps more important, though, is the lack of pathological specificity of the conventionally defined MRI lesions. As noted above, it is clear from classical pathological studies that there is considerable heterogeneity between lesions in brains of MS patients.

2.5.2 Advanced MR techniques for improved characterization of MS pathology in vivo

A key component for understanding the natural history of MS and evaluating new therapeutic strategies is the relationship between clinical disability measures and abnormalities on MR imaging. There is a need for neuroimaging measures that are more specific for irreversible nervous system injury and also for better clinical measures of disability. Newer imaging techniques and integrated data analysis could provide a clearer reflection of the natural history of the disease and provide further insight into the biological basis of observed clinical deficits.

Newer MR techniques such as MRS, magnetization transfer ratio (MTR) imaging (Gass et al., 1994) and quantitative T1 or T2 imaging (MacKay et al., 1994) may offer more specific pathological information than that obtained by conventional T2W MRI. For example, myelin water content in lesion and NAWM can be computed using quantitative T2 imaging (Vavasour et al., 1998). In addition, image processing techniques providing measures of atrophy of the brain (Fox et al., 2000; Losseff et al., 1996a; Rudick et al.,

1999) and spinal cord (Liu et al., 1999; Losseff and Miller, 1998; Losseff et al., 1996b; Stevenson et al., 1998) may provide pathologically nonspecific measures of tissue loss and advanced disease changes that correlate with axonal loss and disability. Finally, functional MRI (fMRI) may help us understand the relationship between axonal loss and disability by demonstrating whether functional reorganization dilutes this relationship, as has been suggested in stroke (Cifelli and Matthews, 2002; Weiller et al., 1993; Yousry et al., 1998).

Proton Magnetic Resonance Spectroscopy

Magnetic resonance spectroscopy is a method of probing the chemical environment of nuclei based on their nuclear spin reorientation in an applied magnetic field, by taking advantage of shifts in resonance frequency as a function of chemical environment. The metabolic products of biological reactions can be measured, elucidating the details of both normal function and disease processes. MRS is promising as it can define simultaneously a number of chemical correlates of pathological change. In particular, MRS measurement of the neuronal marker NAA, which is found exclusively in neurons and neuronal processes in the mature brain, has an advantage over water-based measurements as it is pathologically specific for neuronal/axonal changes (Birken and Oldendorf, 1989; Moffett et al., 1991; Simmons et al., 1991).

Basic Principles of Nuclear Magnetic Resonance

Certain atomic nuclei, such as ^{1}H and ^{31}P, possess a property known as spin [the information and equations in this section and the next, "Chemical Shift" are drawn mainly from David Gadian's excellent book, *NMR and its applications to living systems* (Gadian, 1995)]. Associated with this spin are an angular momentum **p** and a nuclear

magnetic moment $\boldsymbol{\mu}$ that can interact with applied magnetic fields. Both $\mathbf{p}$ and $\boldsymbol{\mu}$ are generated by the nuclear spin, and point in the same direction. From quantum mechanics, the magnitude p of the angular momentum is quantized, as is the component of $\mathbf{p}$ relative to any axis. By placing the nucleus in a strong magnetic field and defining the z-axis as pointing in the same direction, the z-component of $\mathbf{p}$ can be specified and is given by

$$p_z = m\hbar$$

where m for spin-1/2 nuclei such as ^{1}H and ^{31}P is $\pm 1/2$, and $\hbar$ is Planck's constant / 2π. From the Heisenberg uncertainty principle, having specified p_z exactly, p_x and p_y must remain completely indeterminate, which can be visualized as a precession of $\mathbf{p}$ about the z-axis. The z-component of the magnetic moment is given by

$$\mu_z = \gamma\hbar m$$

where γ is the gyromagnetic ratio, an intrinsic property of the nucleus. In a strong magnetic field ($\mathbf{B_0}$, oriented along the z-axis), the nuclear magnetic moment can orient itself in one of several configurations with respect to $\mathbf{B_0}$. The number of allowable orientations corresponds to the number of allowable energy levels given the spin quantum number of the nucleus. Again, the number of energy levels available to spin 1/2 nuclei such as ^{1}H and ^{31}P is $(2I + 1) = 2$. These two energy levels correspond to the magnetic moment being aligned with or against the applied magnetic field, with the first orientation being of lower energy. The energy gap between these two levels is given by

$$\Delta E = \gamma\hbar B_0$$

Transitions between these two energy states can be induced by applying a magnetic field B_1 in the xy-plane, oscillating at a frequency ν_0 specified by

$$\Delta E = h\nu_0$$

Thus ν_0 is given by

$$\nu_0 = \frac{\gamma B_0}{2\pi}$$

and the angular frequency ω_0 is

$$\omega_0 = \gamma B_0$$

This is the resonance condition for NMR. Since γ is characteristic of a nucleus, different nuclei resonate at different frequencies in the same magnetic field. It is interesting to note that since ΔE is much smaller than the thermal energy kT at the temperatures found in biological samples, a classical description of NMR treating $\boldsymbol{\mu}$ as a magnetic dipole with angular momentum in an applied field yields the same resonance condition, given by the Larmor frequency of precession. However, γ can only be determined from quantum mechanics. The gyromagnetic ratios for the two most commonly studied nuclei in biological NMR are 17.23 MHz/T for ^{31}P and 42.55 MHz/T for ^{1}H.

If we consider a macroscopic sample in a strong magnetic field, we have an ensemble of nuclei with magnetic moments precessing about $\mathbf{B_0}$. If we define the z-axis to lie in the direction of $\mathbf{B_0}$, then the net magnetization, or magnetic moment per unit volume, in the transverse plane will be zero, since the x and y components of the individual magnetic moments are randomly distributed. However, there is a net magnetization in the z-direction, due to the difference in spin populations given by the Boltzmann distribution. The ratio of the number of nuclei in the spin-down state (m = -1/2) to the number of nuclei in the spin-up state (m = +1/2) is

$$\frac{n^{m=-\frac{1}{2}}}{n^{m=+\frac{1}{2}}} = e^{-\frac{\Delta E}{kT}} = e^{-\frac{\gamma \hbar B_0}{kT}}$$

There are slightly more nuclei in the lower energy state with positive z-components ($m = +1/2$), i.e., pointing in the direction of $\mathbf{B_0}$, than nuclei with negative z-components ($m = -1/2$). At $B_0 = 1$ T and at room temperature, this population difference is on the order of 1 part in 10^7. The population difference increases with increasing magnetic field strength. The result is a net magnetization **M** in the positive z-direction.

Detection of **M** is accomplished via the application of a magnetic field $\mathbf{B_1}$ rotating at the nuclear precession frequency in the xy plane. In a reference frame also rotating at this frequency, $\mathbf{B_1}$ will be static. If we consider it directed along the x'-axis of the rotating frame, then the nuclear spins will precess about $\mathbf{B_1}$ with angular frequency γB_1. After a time t_p, the net magnetization vector **M** will rotate about x' by an angle

$$\theta = \gamma B_1 t_p$$

A B_1 pulse of magnitude and duration to give $\theta = 90°$ is called a 90° pulse, and serves to rotate **M** into the $x'y'$ plane. An RF pulse oscillating at the Larmor frequency in the xy plane produces the necessary B_1 field. After a 90° pulse, a net transverse magnetization $\mathbf{M}_{xy}$ is produced which rotates in the xy plane of the fixed frame at the Larmor frequency. This is due to the coherence of nuclear spins rotating about $\mathbf{B_0}$. This rotating magnetization vector induces a voltage in the receiver coil and produces the NMR signal.

Chemical Shift

The resonant frequency of a nucleus depends upon its gyromagnetic ratio, which is a constant for that nucleus, and the effective magnetic field to which it is subjected. The applied main magnetic field B_0 induces electronic currents in atoms and molecules,

which in turn produce small magnetic fields opposing B_0. This serves to modify the effective magnetic field felt by the nucleus

$$B_{eff} = B_0(1-\sigma)$$

where σ is the diamagnetic screening constant, so-called because the electronic currents prevent the nuclei from experiencing the full applied field. As a result, the resonant frequency of a given nucleus also depends on σ, which in turn depends on the local chemical environment, ranging from 10^{-6} to 10^{-3} in biological samples.

$$\nu_0 = \frac{\gamma}{2\pi} B_0(1-\sigma)$$

It is this dependence of the nuclear magnetic resonant frequency on chemical environment that forms the basis of NMR spectroscopy as a chemical probe, since the resonant frequency of a nucleus will shift depending on its molecular environment. This difference in resonant frequency from a chosen reference is called the chemical shift. When expressed in Hz, the chemical shift is B_0 dependent. As a convenience, the chemical shift δ is usually expressed in parts-per-million (ppm), which is independent of B_0.

$$\delta = \frac{\nu_{sample} - \nu_{reference}}{\nu_{reference}} \times 10^6$$

Figure 2-2 shows a simple ^1H spectrum of a sample of acetic acid (Gadian, 1995). The resonance of the ^1H nuclei in the COOH group is shifted with respect to that of the nuclei in the CH_3 group. The area under the CH_3 peak is three times that of the COOH peak, since there are 3 protons in CH_3 for every proton in COOH.

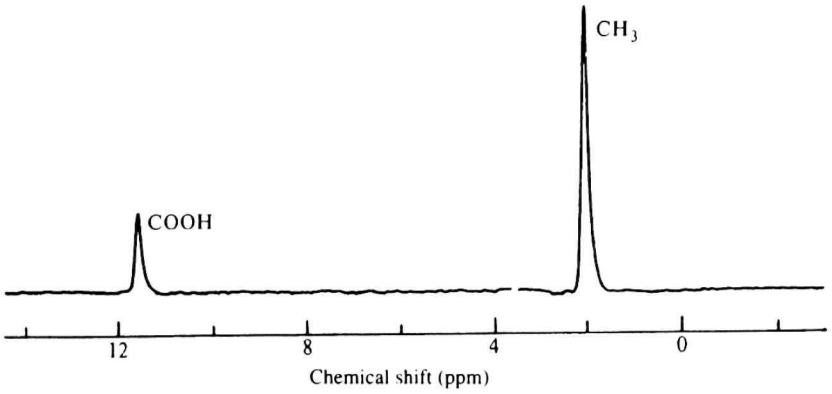

Figure 2-2: 1H NMR spectrum of acetic acid (CH_3COOH). The relative areas of the two signals are 3:1. The frequencies of the signals are expressed in terms of ppm relative to the signal from the reference compound tetramethylsilane (TMS). From Gadian, *NMR and its applications to living systems* (Gadian, 1995).

Measurable metabolites at long echo times

Resonances in MR spectra are identified primarily by their frequency, i.e., position in the spectrum, expressed as the shift in frequency in parts-per-million (ppm) relative to a standard (tetramethylsilane). Water-suppressed, localized proton MR spectra of normal human brain at 'long' echo times (TE 136 or TE 272 msec) reveal 4 major resonances (Figure 2-3):

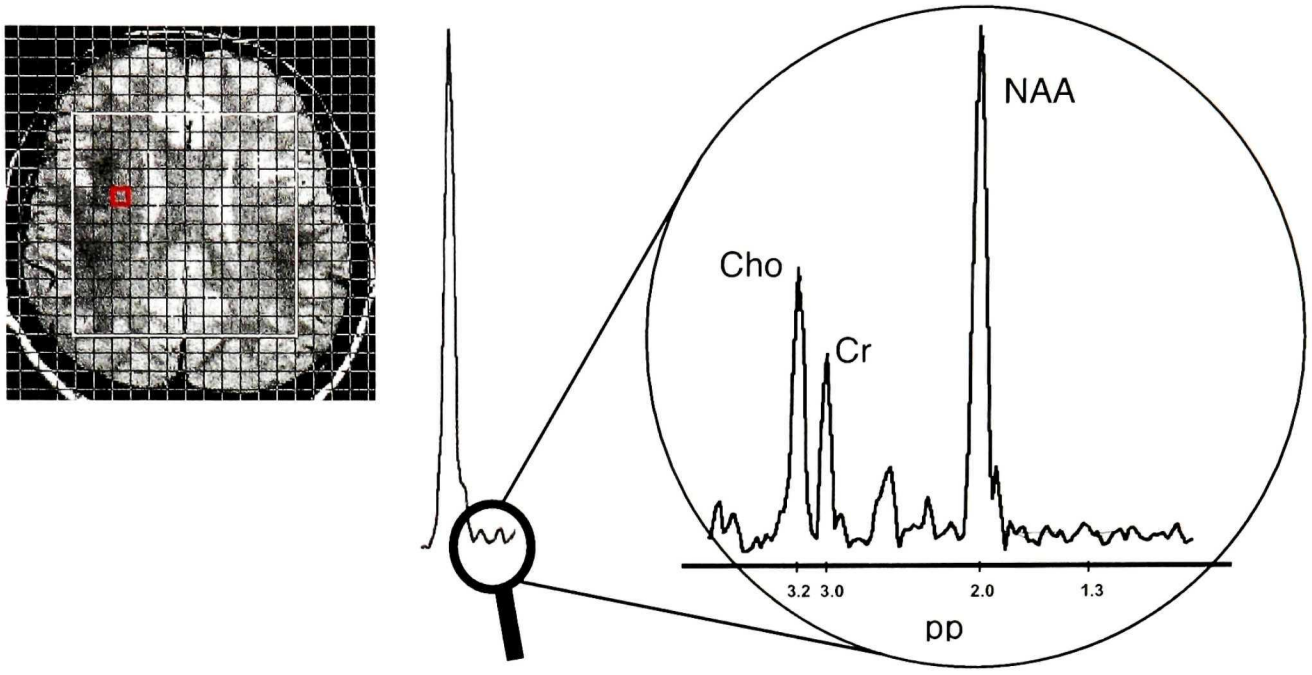

Figure 2-3: The image on the right is a conventional proton density-weighted MRI of a normal subject's brain. Superimposed on the MRI is the phase-encoding grid for an MRS exam (TE=272ms), as well as the excited volume-of-interest (large white box). A spectrum from the highlighted voxel is shown in the centre and right. Without water-supression, the spectrum would be dominated by the water signal (centre), with the metabolite peaks lost in the noise. After water-suppression, a normal white-matter spectrum is shown on the right, containing peaks corresponding to NAA, Cho and Cr. The LA peak at 1.3 ppm is not normally visible above the noise at this echo time, but can be seen in certain pathologies.

- one, at 3.2 ppm, arises mainly from tetramethylamines, especially choline-containing phospholipids (Cho);
- one, at 3.0 ppm, arises primarily from creatine (Cr), either alone or as phosphocreatine;
- one, at 2.0 ppm, arises from N-acetyl groups, especially N-acetylaspartate (NAA); and
- one, at 1.3 ppm, arises from the methyl resonance of lactate (LA) and is normally barely visible above the baseline noise. In certain pathological conditions, a methyl resonance from lipids or alanine can also be detected in this region.

Shorter echo times are better for detecting compounds with short T2- relaxation times, such as lipids, myo-inositol, glutamate, and GABA. The advantage of using longer echo times is that the resulting spectra are simpler, presenting fewer problems due to overlapping peaks and difficulties in baseline estimation. Quantitation of the major resonances such as NAA and Cr is, therefore, more robust.

Cho

Changes in the resonance intensity of Cho appear to result mainly from increases in the steady-state levels of soluble choline compounds including choline, phosphocholine, glycerophosphocholine and, in some cases, betaine (Brenner et al., 1993; Miller et al., 1996). In demyelinating lesions, these may be released from membranes in which they are normally bound too tightly to give a detectable MR signal.

Cr

Total Cr concentration is relatively constant throughout the brain and tends to be fairly resistant to change. Therefore, Cr is often used as an internal standard to which the resonance intensities of other metabolites are normalized. Care must be taken, however, not to use local Cr signals as an internal standard for pathologies in which Cr may change. These include some destructive pathologies such as malignant tumors (Preul et al., 1996), acute demyelinating plaques (De Stefano et al., 1995a), or mitochondrial encephalopathies (De Stefano et al., 1995b) which can result in focal decreases of measured Cr. In these cases it is often appropriate to standardize metabolite resonances to Cr signals in voxels homologous to the region under study, assuming the absence of Cr-modifying pathology in the homologous region.

Significant changes in 'apparent' brain Cr concentrations have been reported in MS patients in some MRS studies attempting absolute quantitation. A clinically practical yet accurate procedure for absolute quantification of *in vivo* MRS data is unlikely to become available soon due to technical difficulties and the necessity to make assumptions (e.g., about relaxation times) that may not be valid for pathological brain tissue in individual patients. In fact, quantitative MRS studies of MS patients have shown discrepant results in terms of Cr changes, reporting increases, decreases and absence of Cr resonance intensity changes in MRI lesions and in the normal appearing WM (Davies et al., 1995; Husted et al., 1994; Pan et al., 1996; Rooney et al., 1997; Sarchielli et al., 1999). In a post-mortem study performed using high-resolution proton NMR spectroscopy *in vitro*, decreases in Cr were limited to MS plaques, whereas Cr levels were unchanged in the normal-appearing WM (Davies et al., 1995). Such in vitro studies do not depend on the assumptions required for *in vivo* measurements. A meta-analysis of all the published quantitative MRS studies reporting Cr concentrations reveals that, across all studies, there is no significant change in NAWM Cr (Zografos Caramanos, personal communication).

Lactate

LA is the end product of glycolysis and accumulates when oxidative metabolism is unable to meet energy requirements. LA also accumulates in the extracellular environment of necrotic tissue, fluid-filled cysts, and with inflammation.

NAA

The resonance from NAA is arguably the most important proton MRS signal in the characterisation of brain pathologies. NAA is found essentially exclusively in neurons

and neuronal processes such as axons in mature brain (Moffett et al., 1991; Simmons et al., 1991), and therefore has been used as a marker of neuronal and axonal integrity (Matthews et al., 1998). Decreases in the relative NAA concentrations are observed in pathologies well known to involve neuronal loss, such as degenerative disorders, stroke, and glial tumors. Low NAA signals also are observed in other pathologies in which the loss or damage to neurons and axons is less well-known and less evident, such as MS. The ability to quantify neuronal loss or damage *in vivo* is one of the most important applications of MRS in the study of cerebral disorders.

Specificity of NAA to neuronal/axonal pathology

Studies in cell culture have suggested that NAA may not be expressed solely in neurons and their processes (Urenjak et al., 1993). Along with neurons, NAA is expressed in O2A-progenitor cells, which can be cultured from foetal rat brain and induced to differentiate into either oligodendroglial- or neuron-like cells *in vitro* (Urenjak et al., 1992). Strictly defined, these cells have been characterised only in culture. Related cells are believed to occur *in vivo*, on the basis of observations of shared surface antigens. Their abundance *in situ* has been estimated to be less than 1 in 100 cells in adult human brain (Scolding et al., 1999). Thus, NAA from O2A-like cells is not likely to make a measurable contribution to total NAA concentrations in mature brain, but caution should be exercised when interpreting NAA changes in developing brain.

A recent report has demonstrated that mature oligodendrocytes derived in culture from rat O2A progenitor cells can be induced to express NAA *in vitro* with stimulation by ciliary neurotrophic factor (CNTF) (Bhakoo and Pearce, 2000). While acknowledging the pitfalls of extending these results obtained in very specific *in vitro* conditions to adult human brain *in vivo*, these findings did raise concerns about the specificity of NAA

changes as a measure of axonal injury. This is in contrast to earlier observations that antibodies directed against NAA or NAAG stain neurons strongly but do not stain glial cells (Moffett et al., 1991; Simmons et al., 1991). Recently, however, Bjartmar et al measured NAA and NAAG in transected rat optic nerves via high-performance liquid chromatography, and the density of axons, oligodendrocytes and oligodendrocyte precursor cells using immunohistochemistry (Bjartmar et al., 2002). In *adult* rat optic nerve, they found that NAA and NAAG levels progressively decreased to zero in parallel with axonal degeneration, while non-proliferating oligodendrocyte progenitor cells, oligodendrocytes and myelin remained abundant. These results confirm the specificity of NAA to axons in *adult* white matter.

Developing rat optic nerves exhibit small quantities of NAA (~6% that of age-matched controls) following axonal transection and complete axonal degeneration, while still containing high densities of proliferating (BrdU+) NG2+ oligodendrocyte progenitor cells (Bjartmar et al., 2002). To the extent that developing rat optic nerve can be considered a model for acute, potentially remyelinating lesions, this suggests that the contribution of proliferating oligodendrocyte progenitor cells to the observed NAA resonance intensity even within *acute* plaques is relatively small, and in fact would cause the degree of axonal damage to be slightly underestimated (Bjartmar et al., 2002). In *chronic* lesions, most oligodendrocyte progenitor cells appear to be non-proliferating (Wolswijk, 1998), and should not contribute to the observed NAA signal.

Mechanisms of decreased NAA in MS

Reduced NAA has been demonstrated in both acute and chronic T2-hyperintense lesions in MS brains, as well as in the surrounding normal-appearing white matter (NAWM). Decreased NAA in voxels of MR spectra can be due to either: 1) decreases in

axonal density with axon loss, 2) axonal shrinkage with decreases in the partial volume of axoplasm per unit volume of brain tissue, or 3) axonal metabolic dysfunction leading to decreased concentrations of NAA in the persisting axons.

As the pathological changes of MS may result in different combinations of these changes, it may be useful to consider decreases in NAA as decreases in axonal "functional equivalents", an expression of axonal integrity. This approach recognises our current inability to confidently distinguish between the different mechanisms (at least with measurements performed at a single time). A 10% decrease of NAA could be the result of, for example, either a 10% decrease in axon density, a 10% decrease in the volume of persisting (demyelinated) axons, or a 10% decrease in the concentration of NAA in remaining axons (e.g., from impaired synthesis of NAA in the presence of soluble inflammatory mediators). As the latter two mechanisms are to a variable extent reversible, some index of their relative contribution can be inferred from serial studies defining recovery of NAA levels after reduction associated with acute lesions.

Measurement of NAA levels thus is complementary to measures of brain atrophy. Brain atrophy reflects loss of axons (along with myelin and other tissue components). In contrast, NAA decreases occur with a reduction in the *functional density* of axons, including axon loss that is not associated with a compensatory amount of atrophy (Evangelou et al., 2000), as well as axonal metabolic dysfunction and volume change. It follows that both measures of changes in brain volume loss and axon density are needed to assess the total axonal damage (or, more precisely, the loss of axonal functional equivalents). In pathological studies of NAWM of the corpora callosa of patients with chronic MS, for example, both axon density and cross-sectional area were found to be

decreased by 35%. Thus, the true extent of axon loss was (35% + (35%x65%)) = 58% (Evangelou et al., 2000).

The relationship between axonal dysfunction, density and volume loss with the *in vivo* -observable quantities of NAA decrease and brain atrophy have yet to be defined. It is not clear that these measures should show a simple relationship with each other that is constant over time. Axon calibre and density might decrease before there is measurable loss of brain parenchymal volume, for example. In addition, as NAA decreases can occur with metabolic dysfunction (despite gross structural integrity), under some conditions, decreases in NAA could be independent of any structural changes in axons or atrophy.

Progression of chronic axonal changes in MS

Significant decreases in NAA are also present in chronic lesions and NAWM as shown in Figure 2-4. Involvement of the NAWM was suggested from the very first MRS studies of brains of MS patients, which demonstrated substantial decreases in NAA from large volumes that included primarily NAWM (Arnold et al., 1990a). Subsequent studies also found NAA levels to be lowered in the NAWM of MS patients (Davie et al., 1995; Davie et al., 1994; Husted et al., 1994; Peters et al., 1995) providing further evidence that axon injury results from a diffuse process in the white matter, in addition to changes associated with focal lesions. Perhaps surprisingly, it is the progression of NAA changes in the NAWM rather than in lesions that is most strongly correlated with the progression of disability in longitudinal follow-up (Fu et al., 1998). The observed correlations between decreases of NAA in NAWM and increased disability in both longitudinal and cross-sectional studies strongly suggest that axonal damage is the primary pathological feature determining disability (De Stefano et al., 1998; Fu et al., 1998). Such relationships have been easier to detect within groups of patients with relapsing-remitting

MS than with secondary progressive MS, suggesting that the relationship between relative brain NAA/Cr and disability is likely not linear.

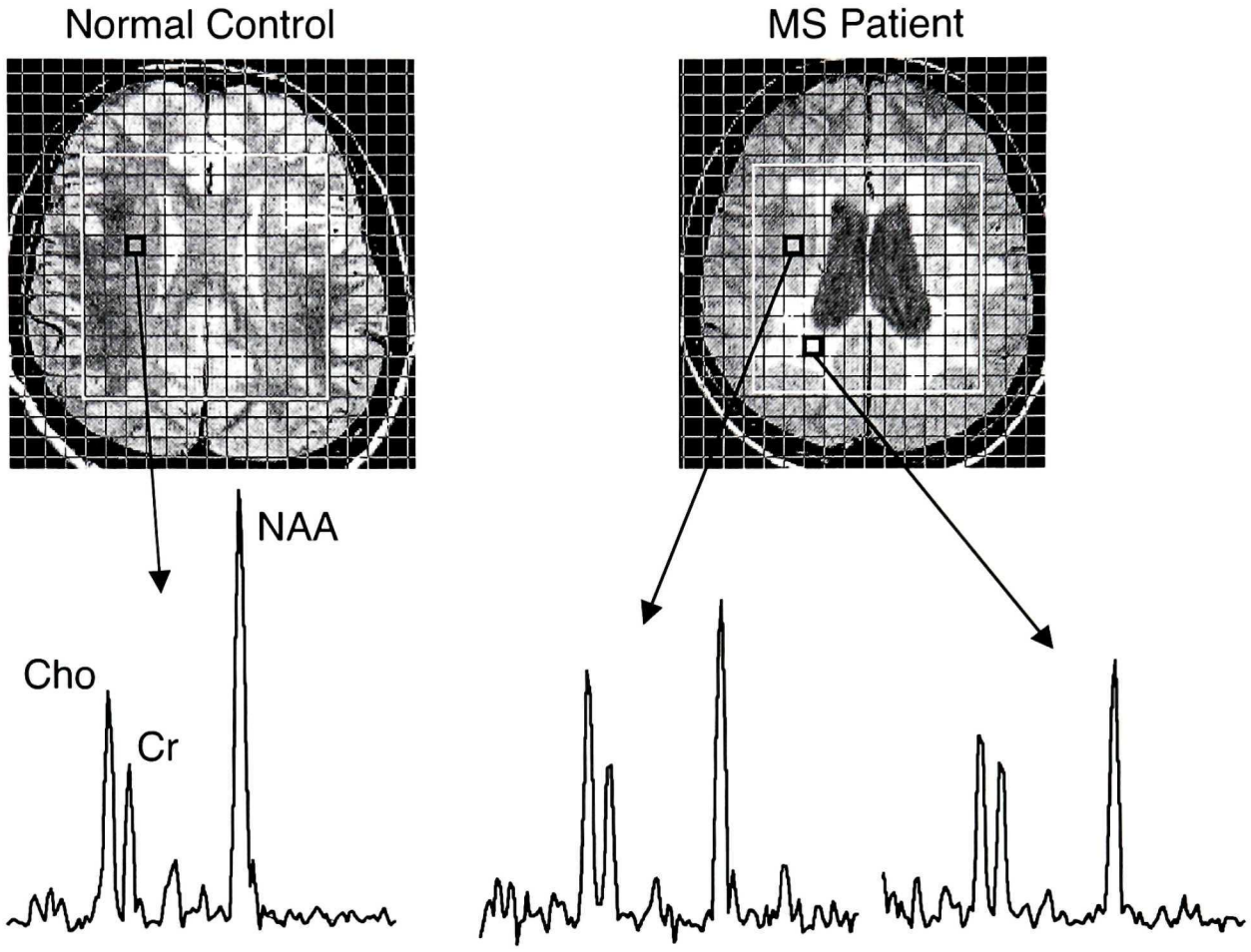

Figure 2-4: The top two images are MRIs of a normal control (left) and an MS patient (right). The spectra in the bottom row depict lower NAA/Cr in the NAWM of the MS patient (bottom, centre) relative to the corresponding location in control white matter (bottom, left), as well as a further reduction in NAA/Cr in the chronic plaque (bottom, right).

NAA and disability in MS

As described above, decreases of NAA are strongly correlated with neurological dysfunction. However, although much stronger than the correlation of, for example, T2 lesion volume or T1 lesion volume with clinical disability (Miller et al., 1998), the correlation is far from perfect. It is instructive to consider in more detail what factors may be responsible for the unexplained variance in the relationship.

First, it must be considered that decreases in NAA due to axonal metabolic dysfunction may not be functionally equivalent to decreases of the same magnitude that are due to axonal loss. That is, a 10% decrease of NAA concentration in axons may not have the same clinical impact as a 10% loss of axons. Second, the location of axonal damage is also important. Although the diffuse decrease in NAWM tends to be relatively homogeneous in the hemispheres, the relative importance of spinal cord pathology to disability may increase in the later stages of MS and is not strongly reflected by changes in hemispheric NAA. Third, the brain has reserve capacity that could be recruited to compensate for focal injury. This "plasticity" may mask the accumulation of axonal loss and damage, at least early in the course of MS.

Magnetization transfer imaging

Conventional MRI produces images based on the distribution and relaxation properties of hydrogen nuclei with relatively unrestricted motion, mainly those in water and fat. The MR signals from hydrogen nuclei bound to macromolecules such as the proteins of myelin decay too rapidly to be directly imaged. However, one can take advantage of the fact that nuclei can exchange magnetization to indirectly image the relative distributions of macromolecules by observing their effect on the free water signal.

Basic Principles

Magnetization transfer (MT) is the MR phenomenon in which spins in two or more distinct environments exchange their magnetization via cross relaxation and/or chemical exchange (Edzes and Samulski, 1978; Wolff and Balaban, 1989). In a two-pool tissue model, protons may exist in a highly mobile liquid state associated with water (free

pool) or in semi-solid macromolecular sites of relatively restricted motion, such as protein matrices or cell membranes (restricted pool) (Wolff and Balaban, 1989). The difference in mobility (correlation time) between a water molecule and a macromolecule results in the liquid protons having a relatively long T2 ($T2_f > 10$ ms) and the semi-solid spins having a very short T2 ($T2_r < 100$ μs). In conventional imaging experiments, the semi-solid magnetization pool is not directly observed as the minimum echo times used (TE) are at least an order of magnitude longer than the T2 of the semi-solid pool. However, by altering the magnetization state of the semi-solid pool selectively (e.g., by saturating its magnetization), the semi-solid pool can be studied via its exchange with directly observable, liquid spins.

The majority of human MT imaging has been performed using shaped off-resonance RF pulses (Pierce et al., 1991; Schneider et al., 1993) or short, intense on-resonance binomial RF pulses (Hu et al., 1992; Pike, 1996; Pike et al., 1993; Pike et al., 1992; Yeung and Aisen, 1992). In either case, the pulses are designed to selectively saturate (at least partially) the short T2 semi-solid spins without any direct effect on the liquid component(s) (Graham and Henkelman, 1997; Henkelman et al., 2001). In an attempt to isolate MT effects, acquisitions are often performed with and without saturation pulses, and ratio or percent difference images (so called MTR images) are calculated (Grossman et al., 1994). The resulting semi-quantitative images reflect a complex combination of sequence and relaxation parameters in addition to MT (Henkelman et al., 2001; Pike, 1996).

Specificity for myelin pathology

Although the exact mechanisms of MT in WM are not definitively known, its importance has been clearly established (Dousset et al., 1992; Fralix et al., 1991; Koenig

et al., 1990; Kucharczyk et al., 1994). The most comprehensive in vitro analysis has been performed by Kucharczyk et al., who studied all the major lipid components of WM in a multilamellar vesicle model system and measured T1, T2, and MT at varying pH (Kucharczyk et al., 1994). They observed that galactocerebroside had the greatest effect on relaxivity, and that MT was 2 to 3 times greater than with either cholesterol or sphingomyelin alone.

Measures of spinal cord disease

Spinal cord lesion volume

MS is a disease that involves both the brain and the spinal cord. Despite early technical difficulties, spinal cord lesions have been documented on MRI (Kidd et al., 1993; Thomas et al., 1993; Thorpe et al., 1993), and the presence of spinal cord lesions can be diagnostically useful when cerebral lesions are absent (Thorpe et al., 1996b). It was hoped that spinal cord lesions would help explain some of the variance in clinical disability not explained by cerebral lesions. Spinal cord lesion load, however, was found not to correlate well with clinical disability (Kidd et al., 1993; Lycklama à Nijeholt et al., 1998), although new lesions in the spinal cord, though infrequent, were often symptomatic (Thorpe et al., 1996a). The small diameter of the spinal cord would argue against differences in lesion location between clinically silent and eloquent areas being responsible for this, once again pointing to the lack of pathological specificity of lesions on T2-weighted MRI.

Spinal cord atrophy

Atrophy of the spinal cord is known to occur in MS, and early work by the Queen Square group showed an association between spinal cord atrophy and clinical disability

(Kidd et al., 1993). This group went on to refine the technique, using high-resolution, T1-weighted volumetric imaging of the second cervical spinal segment (C2) and computer-assisted methods of cross-sectional area measurement (Losseff et al., 1996b). Spinal cord atrophy measured in this way proved to be highly reproducible and strongly correlated to clinical disability (Losseff and Miller, 1998; Losseff et al., 1996b; Stevenson et al., 1998). The high reproducibility of this technique is related to the fact that the cross-sectional area of the cord around C2 is fairly uniform compared to other levels of the spinal cord, so that, within limits, the measurement is not critically dependent on position along the cord. The cord is well centred in the surrounding CSF pool at C2, facilitating delineation of the cord boundary on appropriately acquired MRI images. Semi-automated identification of the cord-CSF boundary reduces the variability of the area measurement. Ideally, the MRI images should be acquired using a high-resolution, 3D sequence that allows the stack to be reformatted to yield images truly orthogonal to the cord, and with a strong T1-weighting to obtain good contrast between the cord and surrounding CSF (Losseff and Miller, 1998; Narayanan et al., 2000).

The amount of accumulated spinal cord atrophy is greater in patients with secondary progressive MS than in patients with relapsing-remitting disease (Liu et al., 1999; Losseff et al., 1996b; Lycklama à Nijeholt et al., 1998; Stevenson et al., 1998), which is consistent with the notion that SPMS is a more advanced stage of MS than RRMS. The *rate* of cross-sectional area loss, however, appears to be faster in patients with RRMS, perhaps indicating a more active disease process in the earlier, relapsing-remitting stage of MS (Stevenson et al., 1998). Since both demyelination and axonal loss can contribute to spinal cord atrophy, one could speculate that the cross sectional area loss seen in the RR group is linked more to demyelination and associated axonal

shinkage, while in the more disabled SP group, the atrophy represents a greater proportion of axonal loss. This idea is supported by the stronger correlation between spinal cord atrophy and disability seen in later stages of MS versus earlier stages (Narayanan et al., 2000), and will be discussed further in Chapter 6.

Functional MRI

Basic Principles

The primary goal of functional MRI (fMRI) is to detect brain areas that are "activated" when a subject performs a given task, analogously to positron emission tomography (PET) activation studies. The great advantage of fMRI over PET in this type of application is the ability to use endogenously generated contrast mechanisms rather than injected radionuclides. The most widely used fMRI contrast mechanism takes advantage of the small change in T2* (a measure of the rate of spin dephasing that includes both the intrinsic T2 of the tissue as well as local magnetic field inhomogeneity) resulting from the difference in magnetic susceptibility of deoxyhemoglobin and oxyhemoglobin, and is termed the blood oxygenation level-dependent (BOLD) response (Ogawa et al., 1993). Deoxyhemoglobin is a paramagnetic molecule with a relatively high magnetic susceptibility, whereas oxyhemoglobin is a diamagnetic molecule with a relatively low magnetic susceptibility. As a result, deoxyhemoglobin has a greater ability to dephase neighbouring hydrogen nuclei, leading to a local loss of signal. Cortical activation leads to increased local capillary blood flow, far in excess of what is needed to satisfy local oxygen demand, resulting in an increased ratio of oxyhemoglobin to deoxyhemoglobin. This hemodynamic response in turn leads to increased signal on T2*-weighted images.

The typical fMRI experiment is to rapidly and repeatedly acquire T2*-weighted images during alternating steady-state periods of rest and "activity", where "activity" can be a motor, visual or cognitive task, or any task which can elicit an appropriate cerebral hemodynamic change. This is the so-called block design. Because the difference in signal intensity between the two states is quite small, many runs are averaged together to build up a sufficient contrast to noise ratio to obtain meaningful results. This, and the fact that the hemodynamic response to activation occurs on the order of seconds, imposes the requirement for very rapid imaging. Echo-planar imaging (EPI) is typically employed in fMRI, and can provide multi-slice data with good brain coverage in 1-2 seconds or less.

An alternative experimental design is the so-called "event-related" paradigm, where the responses to individual, isolated events are measured. The advantage of this paradigm is that issues of fatigue or habituation due to the repetitive execution of a task are avoided. However, an event-related paradigm does require precise knowledge of the temporal profile of the hemodynamic response, and is operationally more difficult. The block design has been the more widely used method to date.

Findings in MS

Recovery from relapse in MS may be mediated by multiple mechanisms, including axonal adaptations and remyelination. Functional recovery from stroke and mass lesions compressing functionally important pathways has been associated with local cortical reorganisation (Weiller et al., 1993). There also is clinical, electrophysiological and imaging evidence for increased recruitment of ipsilateral cortical areas for movement after such brain injury (Cao et al., 1998; Caramia et al., 1996; Green et al., 1999; Nudo and Friel, 1999; Seitz et al., 1999). In children it is felt that this capacity is substantial, allowing limb function even after excision of the contralateral hemisphere (Muller et al.,

1998). It has been a matter of debate how much this contributes to recovery in adults. If this occurs in MS, then it may provide a mechanism of functional recovery that would complicate the relationship between axon loss or injury and disability. One of the first studies demonstrating a dynamic cortical response to a relapse of MS is contained within this thesis, and the topic is addressed in detail in Chapter 5.

Summary

Magnetic resonance imaging (MRI) has dramatically improved our ability to visualize abnormalities in living patients with MS and has provided surrogate outcome measures that are more sensitive to change and to therapeutic efficacy than are current clinical measures. Newer MR techniques offer increased pathological specificity and enable the study of specific pathological and adaptive processes in MS patients. Understanding the relationships between these MR surrogates and clinical and pathological outcomes will provide important new insights into the evolution of MS, as well as improved methods for the evaluation of drug efficacy.

Chapter 3

Imaging axonal injury in multiple sclerosis and its relationship to lesion distribution

3.1 Preface

The majority of MS patients initially have a relapsing-remitting (RR) course of MS. Most RR patients then go on to the secondary-progressive (SP) phase of MS, for reasons that have not been fully elucidated. SP patients as a group tend to experience greater disability, and by definition, their condition worsens even in the absence of attacks. SP patients tend to have a greater lesion burden, but the volume of lesion on T2-weighted MRI often does not explain their level of disability. It is known that lesions identified on T2-weighted MRI are pathologically heterogeneous, containing varying amounts of edema, demyelination, gliosis and axonal loss (McDonald, 1994; Newcombe et al., 1991). Given the relevance of axonal damage to clinical impairment and disability, an important question regarding the observed clinical differences between RR and SP MS is whether lesions in SPMS are associated with a greater degree of axonal damage than lesions in RRMS.

Our group initially addressed this question in a cross-sectional study of 29 MS patients, 11 with RR and 18 with SP disease, using single-voxel MRS to assess axonal integrity in a region encompassing the corpus callosum, and using computer-assisted techniques to quantify lesion volume on concurrently acquired PD/T2 weighted images (Matthews et al., 1996). The RR and SP patient groups were roughly matched for disability in order to focus on differences in lesion volume and axonal/neuronal integrity. This criterion had the effect of selecting RR patients with rather large lesion volumes and SP patients with relatively modest lesion volumes, despite the fact that the SP patients had a considerably longer mean duration of disease, and were in a more advanced stage of MS. We found, however, that both subgroups had similarly low NAA/Cr compared to normal controls, suggesting a similar degree of axonal injury in the two groups. We used the ratio of total lesion volume to NAA/Cr in the spectroscopic volume of interest as an index of the degree of axonal damage associated with lesions. The mean ratio of lesion volume to NAA/Cr was markedly (about double) and significantly higher in the RR patients than in the SP patients, suggesting that the amount of axonal damage per unit volume of lesion was greater in the SP group (Matthews et al., 1996).

Another possible explanation for the lower ratio of lesion volume to NAA/Cr in the RR group was that their lesions were distributed more peripherally relative to the SP group. There actually was a greater volume of lesion within the MRS volume in the RR group. However, since the spectroscopic VOI was centred on the corpus callosum, it was conceivable that NAA/Cr levels could be more affected by nearby, often confluent periventricular lesions (with a high degree of connectivity to the white matter in the VOI) than peripheral lesions, which would have a greater "dilution factor" for axons traversing both the distant lesions and the spectroscopic VOI.

Thus, one of the motivations behind performing the study described in this chapter was to determine whether the relative distribution of peripheral and periventricular lesions was different between RR and SP patients. In addition, the novel idea of defining a spatial probability map for lesion occurrence in a standardized coordinate space could yield some insight into the spatial pattern of lesion formation.

Finally, the question of whether axonal damage in the normal appearing white matter is diffusely present in MS was addressed by generating average MR spectroscopic images from the multivoxel MRSI acquisitions performed on this patient cohort. This larger spectroscopic volume contained a greater proportion of normal-appearing white matter than the previous single-voxel, and also had a greater intersection with descending white matter tracts in addition to the corpus callosum. The mean NAA/Cr within this VOI calculated for each subject thus provided a representative measure of axonal injury in the brains of these patients, and could differentiate the control, RR and SP groups.

3.2 Manuscript 1

Published in Annals of Neurology 1997;41:385-391

Imaging Axonal Damage in Multiple Sclerosis: Spatial Distribution of Magnetic Resonance Imaging Lesions

S. Narayanan MSc, L. Fu* MSc, E. Pioro† MD, DPhil,
N. De Stefano MD, D. L. Collins PhD, G. S. Francis MD,
J. P. Antel MD, P. M. Matthews**‡ MD, DPhil, D. L. Arnold MD

Dept. of Neurology and Neurosurgery, Montreal Neurological Institute,
*Dept. of Epidemiology and Biostatistics, and **Dept. of Human Genetics,
McGill University, Montreal, Quebec
†Current address: Dept. of Neurology, Cleveland Clinic, Cleveland, OH
‡Current address: Centre for Functional Magnetic Imaging of the Brain, Dept. of Clinical Neurology, University of Oxford, England

Address for Correspondence:
Dr. D. L. Arnold, 3801 University Street,
Montreal, Quebec, Canada H3A 2B4.
Tel: (514) 398-8185. Fax: (514) 398-2975

Keywords: multiple sclerosis, nuclear magnetic resonance, MRI, MRSI, magnetic resonance spectroscopy, axons, image processing

Abstract

We performed magnetic resonance imaging (MRI) and magnetic resonance spectroscopic imaging (MRSI) on 28 patients with multiple sclerosis stratified for disability and clinical course (relapsing with at least partial remissions or secondary progressive disease). Lesions were segmented on the conventional proton density and T2-weighted MR images, and lesion distribution images were generated for each patient. The conventional MR and spectroscopic images were transformed into a standard brain-based stereotaxic coordinate space, allowing comparison of images from different patients on a voxel-by-voxel basis. The spatial distribution of lesions in the transformed MR images did not differ significantly between the relapsing and the progressive patient groups. We then generated from the individual data sets, group lesion probability distribution images for the relapsing and the progressive patient groups. The spatial distribution of metabolites was characterized with respect to lesion distribution using the magnetic resonance spectroscopic images transformed into stereotaxic space and averaged. The neuronal marker, N-acetylaspartate, was diffusely lower in the MS patients than in normal control subjects. Comparison of the averaged metabolite and T2-weighted lesion probability images confirmed loss of N-acetylaspartate both in regions of high and low lesion probability. This suggests that diffuse axonal volume loss or dysfunction extends beyond the inflammatory lesions of MS, perhaps due to microscopic disease or Wallerian degeneration along projection pathways of axons traversing the lesions.

Introduction

Proton magnetic resonance (MR) spectroscopy (MRS) allows noninvasive evaluation of regional chemical-pathological changes *in vivo* in the brains of patients with various neurological disorders (Arnold et al., 1990a; Arnold et al., 1990b; Cendes et al., 1994; Graham et al., 1992; Lee et al., 1994; Matthews et al., 1993; Menon et al., 1990). By measuring the relative resonance intensity of N-acetyl groups (primarily N-acetylaspartate (NAA), found only in neurons in the mature brain (Moffett et al., 1991; Simmons et al., 1991)) with respect to creatine (Cr) (which is relatively evenly distributed throughout the brain) an index of neuronal damage can be obtained (Arnold et al., 1990a). MRS imaging (MRSI) uses phase encoding to show the spatial distribution of these metabolites. Signal-to-noise ratio (SNR) is intrinsically low due to the small volume of tissue in each voxel, but can be improved by averaging data obtained from many individuals. However, due to the variability in the size and shape of individual brains, simple voxel-by-voxel averaging of data from different subjects would lead to averaging of non-homologous voxels. This difficulty can be overcome by mapping each individual data set to a standard brain-based stereotaxic coordinate space (Evans et al., 1992; Evans et al., 1991; Fox, 1989; Fox et al., 1988; Fox et al., 1985). This procedure maps anatomically equivalent locations in the data space of each subject to standard locations in stereotaxic space, compensating for individual variations in size and shape.

Although multiple sclerosis (MS) is a primary demyelinating disease, axonal dysfunction and loss occur and may have important functional consequences (McDonald, 1994; Raine and Cross, 1989). The relationship between brain MS lesion volume and brain axonal dysfunction or loss may reflect the clinical evolution of the disease. We found in MRS studies using a large, central volume of interest that the amount of axonal

damage per unit lesion volume on MR imaging (MRI) is significantly less in MS patients with relapsing (R) disease with little fixed clinical deficit than in patients with secondary progressive (P) disease and fixed neurological deficits (Matthews et al., 1996). This could be the result either of pathological heterogeneity of the lesions between the two groups or of differences in the spatial distributions of the lesions, with a greater proportion of central, periventricular lesions in the P group. A recent study suggests that lesion distribution may indeed be different in R and P MS, with greater accumulation of plaque in the periventricular region in P MS and a greater predisposition for new lesions to occur more peripherally in R MS (Paty et al., 1994).

To determine whether the difference in the relationship of axonal damage to lesion volume between R and P MS patients reflects pathological heterogeneity or differences in lesion distribution, we generated average brain NAA and MRI lesion probability images for R and P MS patients with similar neurological disability.

Methods

Patient Population

Twenty-eight patients (16 men, 12 women) aged 26 to 58 years (42.7 ± 10.3 yrs, mean ± standard deviation [SD]) with definite MS and evidence of periventricular white matter disease were selected from the Multiple Sclerosis Clinic at the Montreal Neurological Hospital. The patients were divided into two groups roughly matched for disability but differentiated with regard to recurrences or relapses. One group consisted of patients with recurrent relapses and partial remissions (R) while the second had chronically progressive disease without discrete relapses, after an earlier history of relapsing and partially remitting disease (P). Concurrent clinical evaluations of each patient included the recording of expanded disability status scale (EDSS) scores and any

recent exacerbations. A group of 13 healthy laboratory and hospital workers served as normal control subjects. The study was approved by the ethics committee of the Montreal Neurological Institute and informed consent was obtained from all participants.

Magnetic Resonance Spectroscopic and Conventional Imaging

MR imaging and spectroscopy were performed on a Philips Gyroscan S15 HP 1.5T combined imaging and spectroscopy system (Philips Medical Systems, The Netherlands). MRI data were acquired using a double spin-echo sequence (TR = 2116 ms, TE = 30, 78 ms), yielding a set of proton density images and a set of T2-weighted images. Twenty 5.5 mm thick transverse slices, with a 0.5 mm interslice gap, were collected parallel to the line joining the anterior and posterior commissures (the AC-PC line) for each echo time. The field of view was 250 mm with a matrix size of 256 × 256. These images, along with a sagittal scout image, were used to select a large central volume of interest (VOI) for spectroscopic imaging measuring approximately 10 × 10 × 2.2 cm^3. This was positioned parallel to the transverse slices and centered on the corpus callosum. Proton spectra were obtained using a 90°-180°-180° (PRESS) sequence for volume selection with T1-nulling of water (TR = 2 sec, TE = 272 ms, FOV = 250 × 250 mm^2, 32 × 32 phase encoding steps and 1 average per phase-encoding step). Non-water-suppressed spectra were acquired using TR = 850 ms, TE = 272 ms, FOV = 250 × 250 mm^2 and 16 × 16 phase encoding steps. To correct for artifacts arising from magnetic field inhomogeneities, the water-suppressed MRSI was divided by the unsuppressed MRSI, after the latter was zero-filled to 32 × 32 profiles.

Results are expressed as the ratio NAA/Cr, which assumes that Cr is relatively constant in the volume studied. This is probably true, although some authors have

suggested that Cr might increase and others that it might decrease in chronic MS (Bruhn et al., 1992; Husted et al., 1994). Absolute quantitation was not attempted as this is technically difficult and involves multiple assumptions that are unconfirmed for pathological tissue.

Post-processing of MRSI data was performed on a Sun SPARCstation IPX computer using Sunspec1 software (Philips, Netherlands) and locally developed imaging software. Water was further suppressed by left shifting the time domain data and subtracting it from itself. This procedure modulates the amplitude of the spectrum and increases the ratio of NAA/Cr, but by an amount proportional to the true NAA/Cr ratio in each voxel. After filtering and Fourier transforming the time domain signal, metabolite images for N-acetylaspartate (NAA) and creatine (Cr) were reconstructed by integration between automatically chosen frequency limits surrounding each peak. The nominal voxel size of the MRSIs was $7.8 \times 7.8 \times 22$ mm^3. However, simulations modeling the effects of the point spread function of our acquisition and post-processing indicate a resolution of about $12 \times 12 \times 22$ mm^3.

Image Analysis

Image data for each subject were registered in stereotaxic space using manual homologous landmark matching between the MRI volume and an average ($n > 300$) 3D MRI brain volume that is co-extensive with the Talairach atlas (Evans et al., 1992; Talairach and Tournoux, 1988). Lesion classification on the original MRI data was performed by a single observer (SN) using a manually controlled edge-following algorithm on a lesion-by-lesion basis. The lesion outlines were manually edited when necessary. Locally developed software with the ability to toggle between the proton

density and T2-weighted images provided the operator with convenient access to the information in both data sets while defining lesions (Kamber, 1991). Although not rigorously validated, this method has shown good reproducibility (~2%) on a subset of our data. The outlined plaque data were then transformed into stereotaxic space using the transformation parameters (three translations and three rotations) obtained from the registration of the MRI images to the average MRI brain. Once in stereotaxic space, the data were averaged to yield lesion frequency distributions for each clinical sub-group, as well as for the patient group as a whole. Average patient MRI image volumes were computed as well.

The spectroscopic images were similarly transformed into stereotaxic space, where they were then averaged voxel-by-voxel to yield average metabolite images for the patient group and the normal control group.

Test for difference in lesion distribution between R and P groups

To determine whether there was a difference in the probability of lesions being in the periventricular *vs.* more peripheral regions of the brain in R *vs.* P MS patients, we divided the brain into two regions: a periventricular region and a region remote from the ventricles. The periventricular region was defined based on a ventricular probability distribution created by averaging the segmented lateral ventricles of all the patients in stereotaxic space. This average voxelated ventricle was blurred using a three-dimensional gaussian blurring function with a full-width at half-maximum (FWHM) of 24 mm in each direction. A near-zero probability boundary of the resulting region was obtained which encompassed the ventricles as well as most of the periventricular plaque (Figure 3-1). The remote region was then simply defined as the rest of the brain.

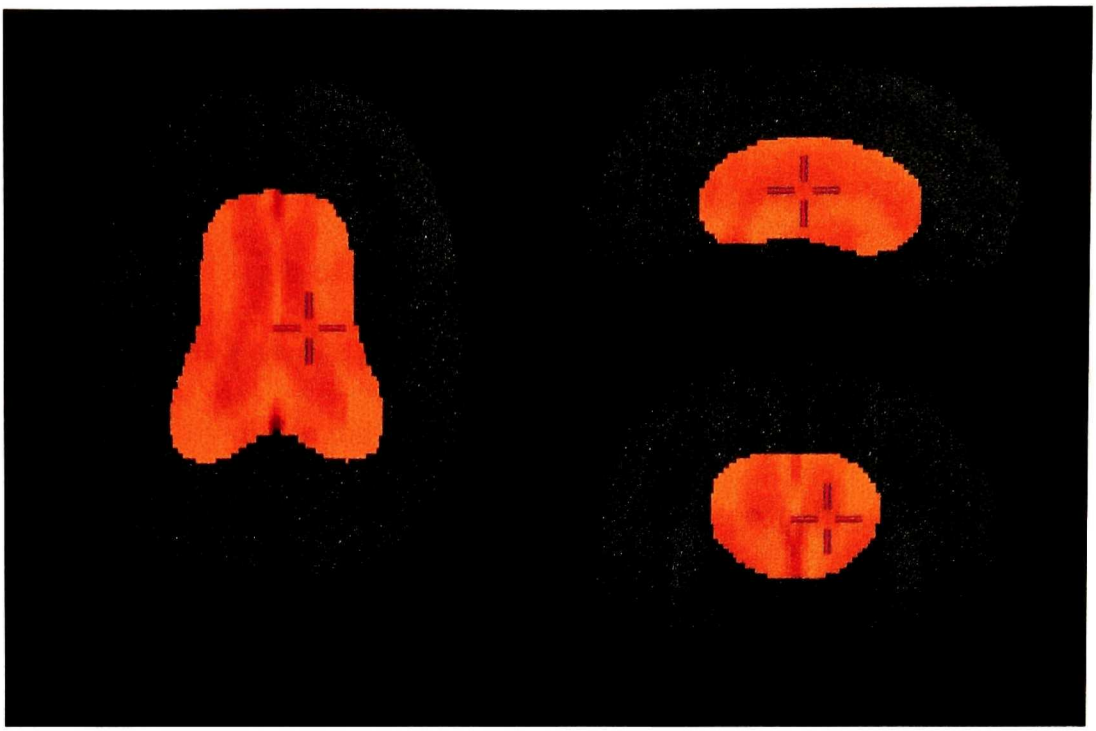

Figure 3-1: Tri-plane view of the periventricular region mask. The mask was generated by averaging the segmented ventricles of all the patients in stereotaxic space, blurring the result with a three-dimensional gaussian blurring function with a full width at half maximum of 24 mm along each axis, and taking the boundary of the resulting distribution. The remote region was defined as the rest of the brain.

We used the risk of the existence of MS plaque in each region as a measure of lesion distribution. The *risk* of the existence of plaque was defined as the number of voxels showing plaque in each region divided by the total number of voxels in that region. The risk of the existence of plaque for the P group divided by the risk of the existence of plaque for the R group (*risk ratio*) in each region was used for sub-group comparisons. Because of the correlation between voxels within individual images, the conventional χ^2 test for the comparison of risk is inappropriate (Manly, 1991). We employed a Monte Carlo simulation to incorporate the cluster property of the lesions. In this simulation, the distributions of the risk ratios in the two regions, under the null hypothesis of no difference existing between R and P patients, were obtained after

$$C_m^n = \frac{n!}{m!(n-m)!}$$

permutations, where n is the total number of subjects in the analysis, and m is the number of R patients. The *p* value for each risk ratio was obtained by taking the integral of the respective distribution from zero to the risk ratio (Manly, 1991) (Figure 3-2). The distributions are the result of plotting the number of occurrences of a given risk ratio *vs.* the risk ratio, for all possible permutations of the data. That is, taking the entire patient group, we arbitrarily divide the patients into the two sub-groups, calculate the risk ratios, permute the data and continue until all possible groupings are accounted for. Consequently, the one-tailed *p* value for the risk ratio measurement in each region is the area under the probability distribution curve from zero to the risk ratio, and indicates the probability of the risk ratio being obtained by chance.

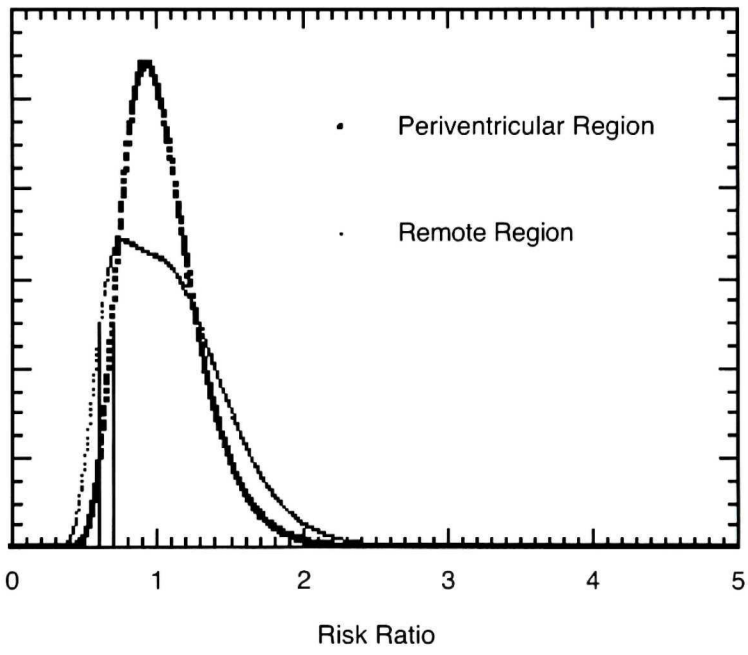

Figure 3-2: The risk ratio probability distribution for T2-weighted lesions in relapsing *vs.* secondary progressive patients. The *risk* of developing a lesion in each region is defined as the number of voxels showing MS plaque divided by the total number of voxels in that region. The *risk ratio* in a given region is the ratio of the risk of developing plaque in the secondary progressive MS subgroup to the risk of developing plaque in the relapsing MS sub-group. The risk ratio (vertical bars) is 0.7 for the periventricular region and 0.6 for the remote region.

A non-parametric Mann-Whitney U test (Dawson-Saunders and Trapp, 1990) was then used to compare the ratios of the risk of the existence of plaque for the P sub-group to the R sub-group in the periventricular and remote regions.

Results

Patient Demographics

The mean age of the 11 patients (6 men, 5 women) in the R sub-group was 33.1 ± 6.3 years (mean ± SD). Their EDSS ratings ranged from 3.0 to 6.5 (median 5.0). The most recent attack in R patients ranged from 2-36 months (15.6 ± 10.7, mean ± SD) prior to MRI examination. Their mean duration (± SD) of disease was 8.7 ± 5.4 years.

The 17 patients in the P sub-group (10 men, 7 women) had a mean age (± SD) of 48.9 ± 7.2 years, with EDSS ratings ranging from 4.0 to 7.0 (median 6.0). Their mean duration (± SD) of disease was 19.8 ± 6.2 years.

Plaque Distribution

Segmenting lesions on individual patient scans, transforming the segmented lesion volumes into a standard brain space, and then adding up the segmented lesion volumes together in standard space produces an image in which the intensity in each voxel is proportional to the fraction of patients having a lesion in that location (Figure 3-3). Such an averaged segmented lesion image thus defines a probability model of lesion distribution for a patient group in a standard anatomical space. In both patient groups, the highest probability voxels (shown brighter in the "hot metal" scale in Figure 3-3) were found to correspond to the corpus callosum and the outline of the body and occipital horns of the lateral ventricles. There was a predilection for the lesions to occur in the periventricular white matter and the minor (anterior) and major (posterior) forceps.

Figure 3-3 also emphasizes the involvement of the internal capsule and the tapetum. The low intensity of voxels in the corona radiata and sub-cortical white matter shows that the probability of lesions decreases with distance from the lateral ventricles. Such probability models in standard space are useful for defining lesion distribution, as significant involvement of specific regions may not be apparent in images from any single subject since the probability of a lesion occurring in a given location is relatively low in an individual.

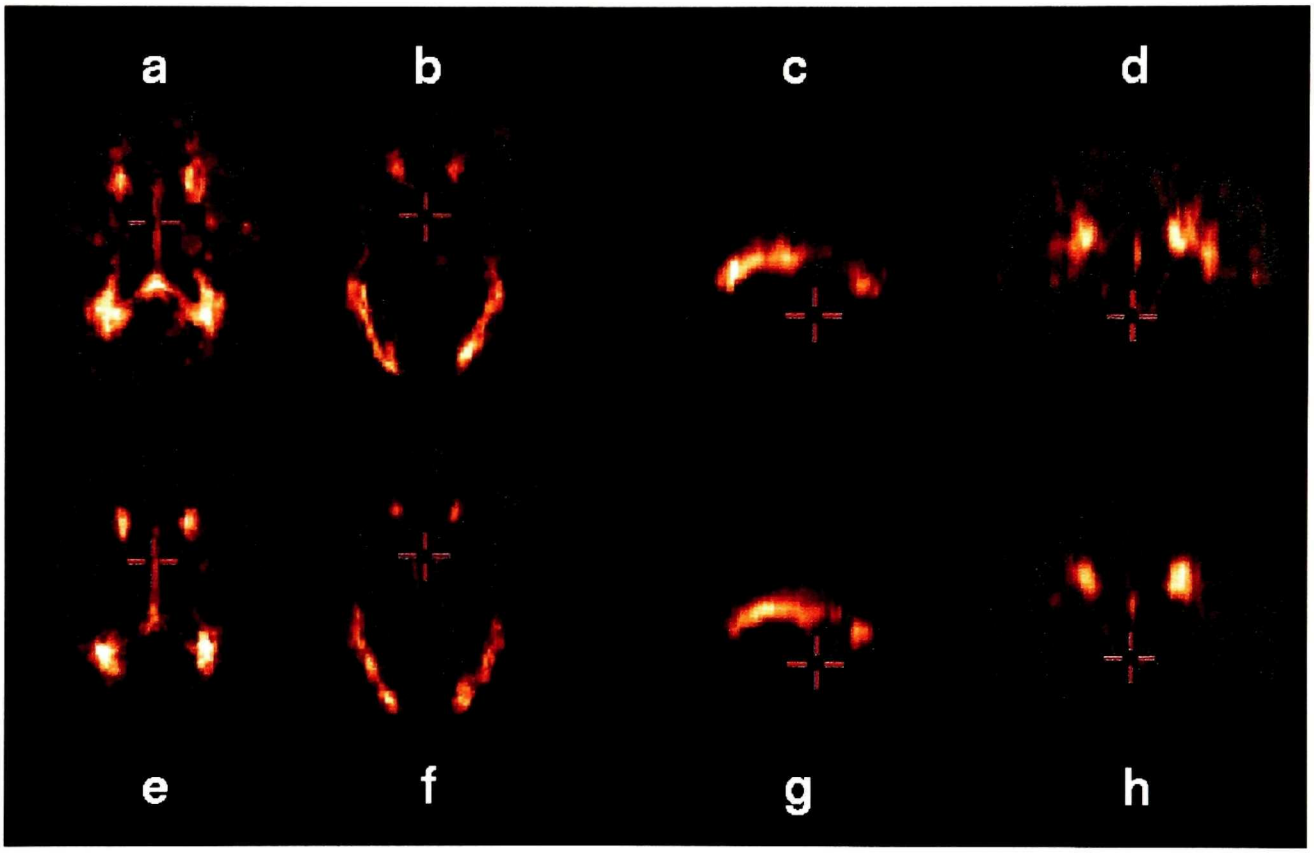

Figure 3-3: Lesion probability distributions in stereotaxic space (hot metal colour scale) for relapsing (top row) and secondary progressive (bottom row) MS patients, superimposed on their respective average MRIs (in greyscale). The lesion probability distributions are bright in regions of high lesion probability and dim in region of low lesion probability. The greater amount of plaque in the relapsing MS group is evident, but gives the appearance of there being more peripheral plaque relative to periventricular plaque in the relapsing MS group than in the secondary progressive MS group. This perception was shown to be false. There is more plaque in *both* regions in the average relapsing MS group image than in the secondary progressive MS group. These average images also show the low frequency involvement of the tapetum (b, f) and the internal capsule (d, h) in both groups.

The average lesion load (± SD) for R patients (32.5 ± 20.9 cc) was significantly higher ($p < 0.04$) than for P patients (16.6 ± 9.0 cc). This difference persisted even when comparing lesion volumes from the 6 R patients with EDSS scores below 5 or after excluding values for the 2 R patients who had experienced attacks 2 and 4 months prior to MR examination.

The relative risk of a voxel containing plaque in P *vs.* R patients (risk ratio) was 0.7 in the periventricular region and 0.6 in the remote region. The p value for the risk ratio was 0.066 in the periventricular region, and 0.064 for the remote region, indicating that the values for the two risk ratios were borderline significantly different from 1.0. This suggests that there was a lower risk of lesion occurrence for the P patient group than for the R group in both regions. The difference between the risk ratios for the periventricular and remote regions (0.7 and 0.6) was not significant ($p > 0.8$) based on the non-parametric Mann-Whitney U test. This indicates that the risk of lesion occurrence in the P group *relative* to the R group is the same in both brain regions.

Proton Magnetic Resonance Spectroscopic Imaging

A limitation of spectroscopic imaging is low sensitivity because of an inherently low SNR. This problem can be redressed for certain applications by averaging the data in a standard anatomical space. The spectroscopic image for each individual contains the ratio of NAA to Cr intensity at each voxel location in space. Once these data are transformed and resampled into stereotaxic space, metabolite ratios at corresponding locations in the standardized brain space can be averaged to improve the SNR and to examine regional trends across a group. The averaged NAA/Cr image of control subjects is relatively uniform outside the ventricles, with some decrease of signal within voxels containing significant proportions of CSF due to difficulties in peak quantitation

associated with lower signal-to-noise ratio in these voxels. The averaged NAA/Cr image for the patient group shows a generalized decrease in signal across the VOI, with greater decreases in regions having high lesion probability.

Average N-Acetylaspartate–Cr Ratio over Volume of Interest

A global value of NAA/Cr ratio for each subject can be obtained by averaging NAA/Cr for all the voxels in the spectroscopic VOI for each subject. In essence, this reduces the information contained in each MRSI to a result analogous to a single-voxel measurement. In this form, the results are amenable to simple statistical analyses.

The average ratio of NAA/Cr in the MRSI VOI was computed for each subject. Group differences were compared using Student's unpaired *t* test. We found that NAA/Cr was significantly lower in the P sub-group (3.2 ± 0.8, mean ± SD) than in the normal control group (4.6 ± 0.7, $p = 0.0007$). NAA/Cr was reduced by a lesser amount in the R sub-group (3.9 ± 0.6, $p = 0.03$) compared to the normal group. The lower NAA/Cr in the P sub-group relative to the R sub-group was also significant ($p = 0.04$).

Discussion

Transformation of images into a standard anatomical coordinate space has allowed us to generate lesion probability models and average MRSIs. The lesion probability images showed the low frequency but systematic involvement of the tapetum and internal capsule, which would not have been noted on images from individual patients. Averaging the MRSI images in standard space improved the SNR and helped demonstrate the decrease in NAA/Cr in both regions of high and low lesion probability. The use of standard space also allowed us to define our periventricular and remote regions and apply them to individual images in standard space. We consider the use of

average images in standard space to be a complementary approach to the analysis of individual data sets, which requires complex statistical techniques only now being developed (Fu et al., 1996).

While the risk ratios in the periventricular (0.7) and remote (0.6) regions differed slightly, this difference was found not to be significant. The difference of each risk ratio from unity, however, was borderline significant. Thus, although the lesion volume in R patients was significantly greater than in P patients in both brain regions, the *spatial distribution* was not significantly different between the two groups, despite the appearance of there being more peripheral plaque relative to periventricular plaque in the MRI scans of R patients. The lower plaque load in the remote region makes the additional lesions in the R group more conspicuous than in the periventricular region, where the density of plaque in both groups is high. Therefore, differences in lesion distribution cannot explain the differences in the relationship of total NAA/Cr to lesion volume in P *vs*. R MS patients. This reinforces the view that the lesions and associated white matter in the two sub-groups are pathologically different, on average, with a higher density of axonal damage in the MRI lesions and surrounding white matter of P patients. One explanation for this could be that there is a greater proportion of edema and inflammation without axonal damage in the MRI lesions of R MS.

The MRSI findings demonstrate a decrease of NAA/Cr even in regions with a low probability of MRI-detected plaque in the brains of these MS patients. We previously showed that decreased NAA/Cr in MS does not result from changes in the relaxation times of either NAA or Cr (Matthews et al., 1991a), and that marked decreases in Cr intensity are likely seen in acute plaques only (Arnold et al., 1992; De Stefano et al., 1995a). While increases in Cr in non-acute MS lesions have been reported (Husted et al.,

1994), these changes are small relative to decreases in NAA. We thus consider the decreases of NAA/Cr in our group of patients as being primarily due to decreases in NAA, reflecting neuronal or axonal damage or loss. We cannot exclude the possibility that the widespread decreases in NAA/Cr are caused by microscopic plaques in the normal-appearing white matter (NAWM). However, axonal volume change, dysfunction or loss (wallerian degeneration), transmitted in an anterograde and retrograde fashion away from lesions visible on MRI, may also be an important mechanism. A practical consequence of this is that positioning of the spectroscopic VOI to include the corpus callosum and deep central white matter (where axonal projections converge) effectively allows sampling that reflects axonal damage in a much larger proportion of the brain than is included in the VOI itself.

The significantly greater amount of axonal damage relative to MRI lesion load in patients with P MS vs. those with R MS emphasizes the limitations of MRI-derived lesion volume alone as a surrogate marker of nervous system injury in MS. Lesions on conventional MRI examinations represent variable combinations of edema, inflammation, and tissue damage. More sophisticated MR protocols may be able to produce more pathologically specific information (e.g., magnetization transfer imaging (Gass et al., 1994; Grossman, 1994) or analysis of T2 behavior (Barnes et al., 1991; Filippi et al., 1994a)), but development of these sequences and characterization of their specificity is still in the early stages. MRSI, although limited by low SNR and low spatial resolution, has the unique ability to specifically image axonal damage, which may have a more direct relationship to impairment in MS than is generally appreciated (De Stefano et al., 1995a; McDonald, 1994).

Acknowledgments

The study was supported by grants from the Multiple Sclerosis Society and the Medical Research Council of Canada. Dr. Matthews thanks the Medical Research Council of Canada for personal support.

The authors gratefully acknowledge Dr. Alan Evans and his group in the NeuroImaging Laboratory of the Montreal Neurological Institute for the development of segmentation and registration software. We are grateful to Ms. Arlene Cohen for coordinating the study, to Mr. Gilles Leroux and Mr. André Cormier for providing excellent technical support, and to Dr. G. B. Pike for constructive comments regarding this manuscript.

References

Arnold DL, Matthews PM, Francis G, Antel J. Proton magnetic resonance spectroscopy of human brain *in vivo* in the evaluation of multiple sclerosis: assessment of the load of disease. Magnetic Resonance in Medicine 1990a; 14: 154-159.

Arnold DL, Matthews PM, Francis GS, O'Connor J, Antel JP. Proton magnetic resonance spectroscopic imaging for metabolic characterization of demyelinating plaques. Ann Neurol 1992; 31: 235-41.

Arnold DL, Shoubridge EA, Villemure JG, Feindel W. Proton and phosphorus magnetic resonance spectroscopy of human astrocytomas *in vivo*. Preliminary observations on tumor grading. NMR Biomed 1990b; 3: 184-189.

Barnes D, Munro PMG, Youl BD, Prineas JW, McDonald WI. The longstanding MS lesion; a quantitative MRI and electron microscopic study. Brain 1991; 114: 1271-1280.

Bruhn H, Frahm J, Merboldt KD, Hanicke W, Hanefeld F, Christen HJ, et al. Multiple sclerosis in children: cerebral metabolic alterations monitored by localized proton magnetic resonance spectroscopy in vivo. Ann Neurol 1992; 32: 140-50.

Cendes F, Andermann F, Preul MC, Arnold DL. Lateralization of temporal lobe epilepsy based on regional metabolic abnormalities in proton magnetic resonance spectroscopic images. Annals of Neurology 1994; 35: 211-216.

Dawson-Saunders B, Trapp RG. Basic and Clinical Biostatistics. Norwalk, CT: Appleton and Lange, 1990.

De Stefano N, Matthews PM, Antel JP, Preul M, Francis G, Arnold DL. Chemical pathology of acute demyelinating lesions and its correlation with disability. Annals of Neurology 1995; 38: 901-909.

Evans AC, Marrett S, Neelin P, Collins L, Worsley KJ, Dai W, et al. Anatomical mapping of functional activation in stereotactic coordinate space. NeuroImage 1992; 1: 43-63.

Evans AC, Marrett S, Torrescorzo J, Ku S, Collins L. MRI-PET correlation in three dimensions using a volume-of-interest (VOI) atlas. Journal of Cerebral Blood Flow & Metabolism 1991; 11: A69-A78.

Filippi M, Barker GJ, Horsfield MA, Sacares PR, MacManus DG, Thompson AJ, et al. Benign and secondary progressive multiple sclerosis: a preliminary quantitative MRI study. Journal of Neurology 1994; 241: 246-251.

Fox PT. Functional brain mapping with positron emission tomography. [Review]. Seminars in Neurology 1989; 9: 323-329.

Fox PT, Mintun MA, Reiman EM, Raichle ME. Enhanced detection of focal brain responses using intersubject averaging and change-distribution analysis of subtracted PET images. Journal of Cerebral Blood Flow & Metabolism 1988; 8: 642-653.

Fox PT, Perlmutter JS, Raichle ME. A stereotactic method of anatomical localization for positron emission tomography. Journal of Computer Assisted Tomography 1985; 9: 141-153.

Fu L, Wolfson C, Worsley KJ, De Stefano N, Collins DL, Narayanan S, et al. Statistics for investigation of multimodal MR imaging data and an application to multiple sclerosis patients. NMR Biomed 1996; 9: 339-46.

Gass A, Barker GJ, Kidd D, Thorpe JW, MacManus D, Brennan A, et al. Correlation of magnetization transfer ratio with clinical disability in multiple sclerosis. Annals of Neurology 1994; 36: 62-67.

Graham GD, Blamire AM, Howseman AM, Rothman DL, Fayad PB, Brass LM, et al. Proton magnetic resonance spectroscopy of cerebral lactate and other metabolites in stroke patients. Stroke 1992; 23: 333-40.

Grossman RI. Magnetization transfer in multiple sclerosis. Annals of Neurology 1994; 36 Suppl: S97-S99.

Husted CA, Goodin DS, Hugg JW, Maudsley AA, Tsuruda JS, de Bie SH, et al. Biochemical alterations in multiple sclerosis lesions and normal-appearing white matter detected by in vivo 31P and 1H spectroscopic imaging. Annals of Neurology 1994; 36: 157-165.

Kamber M. Automated Detection of Multiple Sclerosis Lesions in Magnetic Resonance Images of the Human Brain. Montreal, Quebec: Master's thesis, Dept. of Computer Science, Concordia University, 1991.

Lee JH, Arcinue E, Ross BD. Brief report: organic osmolytes in the brain of an infant with hypernatremia. N Engl J Med 1994; 331: 439-42.

Manly BFJ. Randomization and Monte Carlo Methods in Biology. New York: Chapman and Hall, 1991.

Matthews PM, Andermann F, Silver K, Karpati G, Arnold DL. Proton MR spectroscopic characterization of differences in regional brain metabolic abnormalities in mitochondrial encephalomyopathies. Neurology 1993; 43: 2484-90.

Matthews PM, Francis G, Antel J, Arnold DL. Proton magnetic resonance spectroscopy for metabolic characterization of plaques in multiple sclerosis. Neurology 1991; 41: 1251-1256.

Matthews PM, Pioro E, Narayanan S, De Stefano N, Fu L, Francis G, et al. Assessment of lesion pathology in multiple sclerosis using quantitative MRI morphometry and magnetic resonance spectroscopy. Brain 1996; 119: 715-22.

McDonald WI. Rachelle Fishman-Matthew Moore Lecture. The pathological and clinical dynamics of multiple sclerosis. [Review]. Journal of Neuropathology & Experimental Neurology 1994; 53: 338-343.

Menon DK, Baudouin CJ, Tomlinson D, Hoyle C. Proton MR spectroscopy and imaging of the brain in AIDS: evidence of neuronal loss in regions that appear normal with imaging. J Comput Assist Tomogr 1990; 14: 882-5.

Moffett JR, Namboodiri MAA, Cangro CB, Neale JH. Immunohistochemical localization of N-acetylaspartate in rat brain. NeuroReport 1991; 2: 131-134.

Paty DW, Li DK, Oger JJ, Kastrukoff L, Koopmans R, Tanton E, et al. Magnetic resonance imaging in the evaluation of clinical trials in multiple sclerosis. Annals of Neurology 1994; 36 Suppl: S95-S96.

Raine CS, Cross AH. Axonal dystrophy as a consequence of long-term demyelination. Laboratory Investigation 1989; 60: 714-725.

Simmons ML, Frondoza CG, Coyle JT. Immunocytochemical localization of N-acetyl-aspartate with monoclonal antibodies. Neuroscience 1991; 45: 37-45.

Talairach J, Tournoux P. Co-planar stereotactic atlas of the human brain: 3-dimensional proportional system: an approach to cerebral imaging. Stuttgart: Georg Thieme Verlag, 1988.

Chapter 4

Can axonal dysfunction be chronic and reversible?

4.1 Preface

The data presented in the previous chapter demonstrated that decreased NAA/Cr extended beyond regions of high lesion probability into regions of low lesion probability, suggesting that chronic axonal injury existed in the NAWM of MS patients. Our group went on to confirm and extend these findings in a longitudinal study using sophisticated statistical methods that allowed estimation of NAA/Cr in NAWM and lesions of patient groups despite the variable location of the lesions and despite the substantial partial volume effects present (Fu et al., 1998). We showed that NAA/Cr in the NAWM was lower in RR patients versus controls, and lower in SP patients than in RR patients (Fu et al., 1998). We found that NAA/Cr was lower still within lesions compared to NAWM, and that lesion NAA/Cr was similar between the RR and SP groups. Thus, combining the results of these three studies (Fu et al., 1998; Matthews et al., 1996; Narayanan et al., 1997), the difference in central brain NAA/Cr between the RR and SP patient groups

(roughly matched for disability) that we originally described in the Matthews paper (Matthews et al., 1996) can now be ascribed to lower NAWM NAA/Cr in the SP group.

Decreased NAA (both absolute estimates and ratios to Cr) in the cerebral normal-appearing white matter of MS patients has now been widely noted (Davie et al., 1997; Davie et al., 1994; Foong et al., 1999; Kapeller et al., 2001; Leary et al., 1999; Lee et al., 2000b; Peters et al., 1995; Schiepers et al., 1997; Suhy et al., 2000; Tourbah et al., 1999; Tourbah et al., 1996; van Walderveen et al., 1999). In our 30-month longitudinal study (Fu et al., 1998), we found that chronic levels (i.e., measured between attacks) of NAA/Cr in the NAWM decreased by 6.2% per year in the RR subgroup, and correlated with EDSS changes over time. Lesion NAA/Cr did not show this temporal correlation with EDSS, suggesting that diffuse axonal injury outside of visible lesions contributes significantly to chronic disability.

Previous reports had documented the recovery of NAA over time after initial decreases associated with *acute* demyelinating plaques (Arnold, 1992; Davie et al., 1994; De Stefano et al., 1995a; De Stefano et al., 1995b; Narayana et al., 1998). Along with supporting *in vitro* work (Matthews et al., 1995), this provided evidence that NAA decreases could be transient, most likely due to mitochondrial metabolic dysfunction (Bates et al., 1996; Dautry et al., 2000; Patel and Clark, 1979; Truckenmiller et al., 1985). Furthermore, in a 6-year longitudinal MRS study of one patient with relapsing-progressive MS, we observed that NAA/Cr decreased with severe relapse and recovered with remission, and correlated strongly with clinical disability (Spearman rank order coefficient = –0.73, $p < 0.001$) (De Stefano et al., 1997). Since NAA was measured in a large single voxel containing predominantly NAWM, this provided evidence that axonal dysfunction could extend beyond visible lesions in acute, severe relapses. We went on to

show similar results in a group of RR patients followed longitudinally for 30 months using a similar single-voxel MRS volume. Again, NAA/Cr correlated significantly with EDSS in the RR patient group, particularly in a subgroup who experienced significant relapses during the study, whereas lesion volume did not correlate with EDSS (De Stefano et al., 1998). Relapse in RRMS patients appears to be associated with widespread, reversible axonal metabolic dysfunction.

We questioned whether a portion of the NAA decreases seen in *chronic* MS (measured in periods of clinical stability between attacks) could be due to chronic metabolic dysfunction, not spontaneously reversible, but perhaps reversible with therapeutic intervention. Interferon β-1b therapy has been shown to be beneficial in MS, assessed by both clinical (The IFNB multiple sclerosis study group, 1993) and MRI indices (Paty and Li, 1993) (Stone et al., 1995), but its effect on axonal integrity was largely unknown. In this context, we studied a small group of RR patients starting interferon β-1b therapy with MRSI to investigate the effects of treatment on axonal integrity.

4.2 Manuscript 2

Published in Journal of Neurology 2001;248:979-986

Axonal Metabolic Recovery in Multiple Sclerosis Patients Treated with Interferon β-1b

*Sridar Narayanan, MSc, †*Nicola De Stefano, MD, PhD, *Gordon S. Francis, MD, *Rozie Arnaoutelis, BSc, *Zografos Caramanos, MA, *D. Louis Collins, PhD, *Daniel Pelletier, MD, ‡Barry G. W. Arnason, MD, *Jack P. Antel, MD and *Douglas L. Arnold, MD

*Department of Neurology and Neurosurgery, Montreal Neurological Institute and Hospital, Montreal, Quebec, Canada, (514) 398-8185,

†Institute of Neurological Sciences, Neurometabolic Unit University of Siena, Italy, 39-0577-585-111 and

‡Department of Neurology, Pritzker School of Medicine, and the Brain Research Institute, University of Chicago, Chicago Illinois, USA, (773) 702-9076 (FAX)

Reprint requests and correspondence to:

Dr. Douglas L. Arnold,
Montreal Neurological Institute,
3801 University Street, Montreal,
Quebec, Canada, H3A 2B4
Tel: (514) 398-8185
Fax: (514) 398-2975
E-mail: doug@mrs.mni.mcgill.ca

Key words: Interferon-beta, multiple sclerosis, N-acetylaspartate, axons, magnetic resonance spectroscopy

Abstract

Patients with multiple sclerosis (MS) can benefit from treatment with interferon β-1b. However, the mechanisms of action of this drug are incompletely understood and effects of interferon β-1b on axonal injury are not known. A measure of axonal injury can be obtained *in vivo* using magnetic resonance spectroscopy to quantify the resonance intensity of the neuronal marker, N-acetylaspartate (NAA).

In a small pilot study, we performed combined magnetic resonance imaging (MRI) and magnetic resonance spectroscopic imaging (MRSI) on 10 patients with relapsing-remitting MS before and 1 year after starting treatment with subcutaneous interferon β-1b. Resonance intensities of NAA relative to creatine (Cr) were measured in a large, central brain volume. These measurements were compared to those made in a group of 6 untreated patients selected to have a similar range of scores on the Expanded Disability Status Scale and mean NAA/Cr at baseline.

NAA/Cr in the treated group [2.74 (0.16), mean (SD)] showed an increase of 5.5% 12 months after the start of therapy [2.89 (.24), $p = 0.05$], while NAA/Cr in the untreated group decreased, but not significantly [2.76 (0.1) at baseline, 2.65 (0.14) at 12 months, $p > 0.1$]. NAA/Cr had become significantly higher in the treated group at 12 months than in the untreated group ($p = 0.03$).

Our data suggest that, in addition to losing axons, patients with chronic multiple sclerosis suffer from chronic, sublethal axonal injury that is at least partially reversible with interferon β-1b therapy.

Introduction

Multiple sclerosis (MS) is an inflammatory disease of the central nervous system (CNS) characterized by deficits referable to multiple lesions disseminated in the CNS in both space and time. While the primary target of the immunologic attack appears to be myelin / oligodendrocytes, secondary axonal damage also occurs and may be the substrate for chronic, irreversible neurological impairment. Although axonal pathology in MS has been recognized since the initial descriptions of Charcot (Charcot, 1868), emphasis generally has been placed on the relative sparing of axons traversing lesions. Recent magnetic resonance spectroscopy (MRS) and pathology studies have stressed the importance of axonal pathology in multiple sclerosis in addition to demyelination (Ferguson et al., 1997; Matthews et al., 1998; McDonald, 1994; Trapp et al., 1998; Waxman, 1998). MRS and magnetic resonance spectroscopic imaging (MRSI) offer the unique ability to noninvasively assess the integrity of neurons and neuronal processes in diseased brain based on levels of N-acetylaspartate (NAA), a neuronal marker localized primarily in neurons in mature brain (Moffett et al., 1991; Simmons et al., 1991).

Early MRS studies revealed decreased NAA in patients with MS, with more disabled patients exhibiting lower brain NAA (Arnold et al., 1990a; Bruhn et al., 1992; Larsson et al., 1991; Matthews et al., 1991a). Subsequent studies have demonstrated that decreases of NAA could be partially reversible in acute demyelinating lesions (Arnold, 1992; Davie et al., 1994; De Stefano et al., 1995b; Narayana et al., 1998).

Several lines of evidence suggest that potentially reversible axonal metabolic dysfunction may contribute to observed decreases and increases of NAA *in vivo*. NAA is synthesized by neuronal mitochondria, which are sensitive to injury from many sources (Bates et al., 1996; Patel and Clark, 1979; Truckenmiller et al., 1985). Reversible

decreases of NAA can be produced in cultures of a neuronal cell line by transient serum deprivation (Matthews et al., 1995) and in primate striatum by the mitochondrial toxin 3-nitropropionate (Dautry et al., 2000). Reduction of NAA has been reported in acute experimental allergic encephalomyelitis (EAE), in which inflammation rather than axonal loss or demyelination is evident (Brenner et al., 1993). Thus, it appears that both axonal loss and potentially reversible axonal metabolic dysfunction may contribute to the decreases of NAA observed in the brains of patients with MS.

The decreases of NAA that occur in MS are not restricted to lesions but are also present in normal-appearing white matter (NAWM). Group metabolite maps averaged in a standardized coordinate space have shown loss of NAA extending beyond regions of high lesion probability into surrounding regions of low lesion probability (Narayanan et al., 1997). Other studies have specifically demonstrated decreased NAA/Cr in NAWM (Fu et al., 1998; Husted et al., 1994). Importantly, the NAA loss in NAWM correlates strongly with disability in patients with relapsing-remitting MS, suggesting that axonal injury in NAWM is an important determinant of disability (Fu et al., 1998).

In patients with relapsing-remitting MS, interferon β-1b (IFNβ-1b) reduced attack frequency, mean attack duration (The IFNB multiple sclerosis study group, 1993), annual accrual of lesion burden, the occurrence of new lesions (Paty and Li, 1993) and the frequency of gadolinium enhancement on MRI (Stone et al., 1995). However, the mechanisms of action of IFNβ-1b in the brains of MS patients, and the effect of IFNβ-1b on axonal injury specifically, are still unclear.

We questioned whether IFNβ-1b could permit recovery of sublethally-injured axons, either by reducing chronic low-level inflammation, or via some other unknown neuroprotective effect. To determine this, we studied a small group of patients with

relapsing-remitting MS embarking upon IFNβ-1b therapy using MRI and MRSI to examine changes in the neuronal marker, NAA, after treatment. An untreated group was studied for comparison.

Methods

Patients:

Patients followed in the MS Clinic of the Montreal Neurological Hospital with relapsing-remitting MS who were about to start IFNβ-1b therapy were asked to enter the study. Inclusion criteria included at least two exacerbations in the preceding two years, but none in the month preceding the first scan. Patients were excluded if they had received steroids in the month prior to starting treatment or if they had previously been on immunosuppressive therapy. Ten patients were enrolled in the study.

Interferon beta-1b (Betaseron®, Berlex Laboratories, Richmond, CA) was self-injected subcutaneously at a dose of 8 MIU every other day. Combined MRI/MRSI scanning was performed immediately prior to the first injection, and again after one year. Interim data also were acquired 6 months after the initiation of treatment in a subgroup of 8 patients. Neurological examinations and EDSS assessments were performed on the same day as the MR examinations.

Given the availability of approved therapies for relapsing-remitting MS, we could not randomly select placebo or non-treatment control groups for our study. Therefore, we have compared our serial observations in patients treated with IFNβ-1b with those made in a non-randomized control group of patients who either elected to remain untreated or who did not have the requisite number of attacks to qualify for treatment. These patients were scanned twice, one year apart, over a similar period as the treated patients, except for two who were scanned as part of a previous study. In order to avoid the confounding

factor of increases in NAA associated with recovery from attacks, MR examinations were performed only if patients had been free from clinically-defined attacks in the previous month. As a whole, this untreated group had relatively more benign disease than the patients in the treated group. We tried to mitigate this bias by selecting a subgroup of untreated patients to have group mean EDSS and NAA/Cr at baseline equivalent to those of the treated group. Six patients comprised the final untreated group.

The Ethics Committee of the Montreal Neurological Institute and Hospital approved the study and informed consent was obtained from all participants prior to their inclusion.

Proton MRI/MRSI

Combined proton MRI and MRSI examinations of the brain were obtained in a single session for each examination using a Philips Gyroscan ACS II operating at 1.5 T (Philips Medical Systems, Best, The Netherlands). A transverse dual-echo, turbo spin-echo sequence (TR/TE1/TE2 = 2075/32/90 ms, 256x256 matrix, 1 signal average, 250mm field of view) yielding proton density-weighted (PDW) and T2-weighted (T2W) images with 50 contiguous 3 mm slices was acquired parallel to the line connecting the anterior and posterior commissures (AC-PC line), followed by a matching T1-weighted (T1W) fast field-echo (FFE) sequence (TR/TE = 35/10 ms). Two patients in the untreated group were scanned as part of a previous study using a dual spin-echo sequence (TR/TE1/TE2 = 2100/30/78 ms, 256x256 matrix, 1 signal average, 250 mm field of view) yielding PDW and T2W images with 20 slices (5.5 mm thick, 0.5 mm gap) parallel to the AC-PC line. In each individual, the same slice thickness was used for both the baseline and follow-up scans.

These conventional MR images were used to position a spectroscopic volume of interest (VOI) of approximately 90x90x20 mm^3 to include the corpus callosum and adjacent white matter (Figure 1). In each subject, the size and location of the VOI was kept constant for the follow-up examination. MR spectroscopic images parallel to the AC-PC line were acquired (32x32 phase-encodes, 250x250 mm field-of-view, 20 mm slab thickness) using a double spin-echo excitation method (TR 2000, TE 272ms) (Ordidge et al., 1987). To suppress the intense water resonance, frequency selective excitation pulses were placed at the beginning of the MRSI sequence (Haase and Frahm, 1985). A quick MRSI without water-suppression was also acquired (TR 850ms, TE 272ms, 16x16 phase-encodes, 250x250 mm field-of-view and 1 signal average) to allow for correction of B_0 inhomogeneity during post-processing.

Post-Processing

Post-processing of the raw MRSI data was performed as previously described (Fu et al., 1998), with the exception that in the present study the residual water signal was fitted and removed from the water-suppressed data using the Hankel singular-value decomposition procedure (de Beer and van Ormondt, 1992). The nominal voxel size in-plane was approximately 8x8 mm, which yielded a spatial resolution of approximately 12x12 mm after filtering.

Metabolite resonance intensities were determined automatically from fitted peak areas using in-house software (AVIS, Samson Antel, MNI). Metabolite signals were expressed as ratios to creatine (Cr) in the same voxel and then averaged over the entire VOI to obtain mean metabolite ratios for each examination. Using this procedure, we have obtained a test-retest variation in NAA/Cr of about 5% in 6 normal controls.

Lesions were manually segmented using locally-developed software (Display, David MacDonald, Brain Imaging Centre, MNI) which provides simultaneous access to PD, T2 and T1-weighted image sets. Lesion boundaries were primarily determined on the PD images.

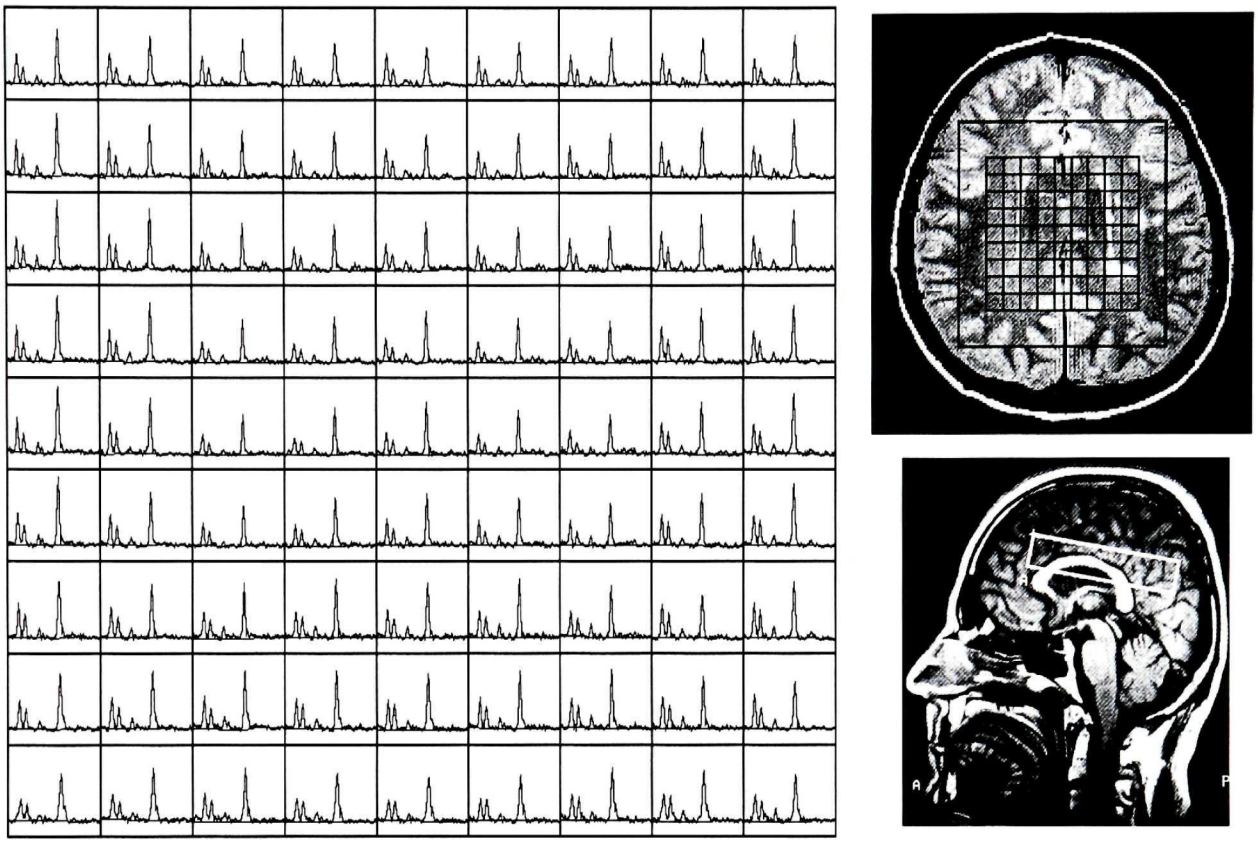

Figure 4-1: MRI images of a patient with multiple sclerosis illustrating the volume of interest (VOI) used for spectroscopic imaging (right), and the resulting spectra (left). Voxels at the edge of the VOI were omitted from analysis since they can show artifactual relative amplitudes. The ratio of NAA to intravoxel Cr in the remaining voxels were averaged to obtain one value for each examination.

Statistics

We applied the non-parametric Kruskal-Wallis test to confirm the comparability of EDSS in the two groups at baseline, and the non-parametric Friedman test to probe for change in EDSS over time. We then applied a repeated-measures, multivariate analysis-of-variance (MANOVA) with one between-subjects grouping factor, **Group** [(i) Treated vs. (ii) Untreated] and two within-subject factors, **Measure** [(i) NAA/Cr, and (ii) lesion

volume] and **Time Point** [(i) Prior to treatment and (ii) 12 months into treatment]. Since NAA/Cr and lesion volume were measured using different scales, we standardized the data using a z-transform prior to performing the MANOVA. Post-hoc analysis was performed using the Least Significant Difference (LSD) test with Bonferroni correction for multiple comparisons.

For the subgroup of treated patients who had interim examinations 6 months after the start of treatment, we performed a repeated-measures analysis-of-variance (ANOVA) on NAA/Cr, followed by Tukey's HSD post-hoc testing, to examine the time course of the NAA/Cr changes.

To determine whether changes in lesion volume could drive changes in NAA/Cr, we performed Pearson correlation between the difference in NAA/Cr and the difference in T2-weighted lesion volume between baseline and 1 year.

The statistical analyses were carried out using STATISTICA for Windows, version 5.1a (StatSoft Inc, Tulsa, OK), and SYSTAT for Windows, version 7.0.1 (SPSS Inc, Chicago, IL.).

Results

The data are summarized in the Table and Figure 2. The EDSS of the two groups did not differ at baseline (Mann-Whitney $U = 29, p > 0.9$), or at 12 months ($U = 22.5, p > 0.4$). There was no significant change in EDSS over time for either the treated (Friedman test statistic = 1.6, $p > 0.2$) or untreated (Friedman test statistic = 0.17, $p > 0.6$) patient groups.

The repeated-measures MANOVA indicated a significant 3-way interaction between **Group**, **Measure** and **Time** (defined in Methods) [$F(1, 14) = 5.7, p < 0.03$]. Post-hoc testing revealed a significant difference in NAA/Cr values at 12 months

between the treated and untreated groups (treated, 2.89 (0.24), untreated, 2.65 (0.14), mean (SD), $p = 0.03$), and a borderline-significant increase of NAA/Cr over time for the treated group (2.74 (0.16), 2.89 (0.24), p = 0.05). There was no significant difference in lesion volume between the two groups, and there was no significant change in lesion volume over time in either group.

	Baseline		**12 months**	
	Untreated	*Treated*	*Untreated*	*Treated*
NAA/Cr Mean (SD)	2.76 (0.1)	†2.74(0.16)	*2.65 (0.14)	*†2.89 (0.24)
Lesion Volume (cc) Mean (SD)	16.1 (20)	11.4 (10.5)	16.9 (20.2)	12.4 (10.9)
EDSS Mean (SD)	3.0 (1.4)	3.1 (1.9)	3.0 (1.8)	2.45 (1.4)
Median (Range)	3.25 (1-5.5)	3.5 (1-5.5)	3.25 (1-5.5)	2.5 (1-5.5)
Disease Duration (years) Mean (SD)	10.8 (7.4)	9.2 (8.9)		
No. of attacks‡ Median (Range)	0 (0)	1 (0-4)	0 (0)	1 (0-3)
N	6	10	6	10

‡in the preceding 12 months *p = 0.03 †p = 0.05

Table 4-1: Mean (standard deviation) NAA/Cr, lesion volume, EDSS and disease duration at baseline and at 12 months for the untreated and treated patient groups. The median and range are reported for the number of attacks/year and EDSS.

The repeated-measures ANOVA performed on NAA/Cr in the subgroup of 8 treated patients having interim examinations at 6 months did not reveal a significant change of NAA/Cr [$F(2, 14) = 2.01$, $p = 0.17$]. It appears that most of the NAA/Cr increase occurred in the second 6 months of the study. Figure 4-3 plots the mean and standard errors of NAA/Cr for this group.

There was no correlation between NAA/Cr change and lesion volume change over one year (Pearson r = 0.24, p = 0.74) in the entire patient cohort.

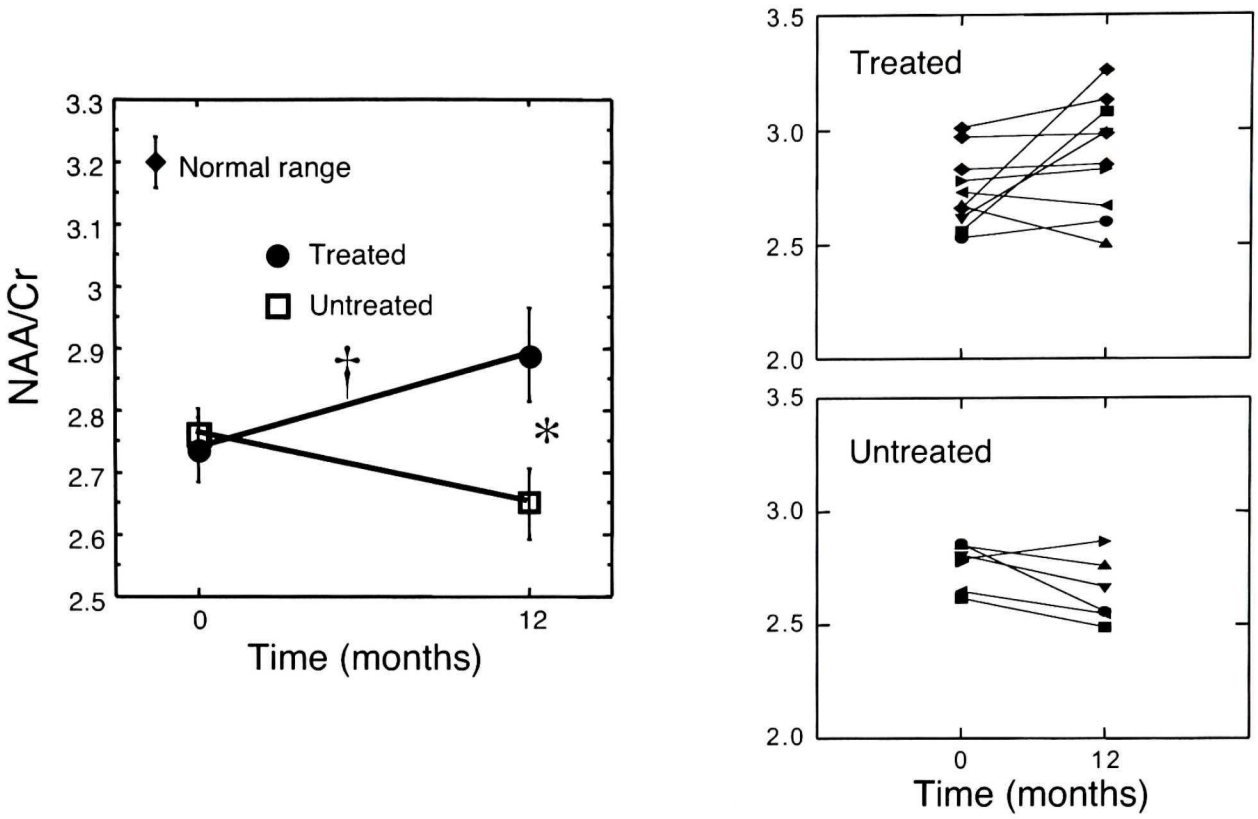

Figure 4-2: Plots illustrating the change of mean NAA/Cr over one year for the treated and untreated patient groups (left) and for individuals within each group (right). The error bars represent one standard error of the mean. (* p = 0.03, † p = 0.05).

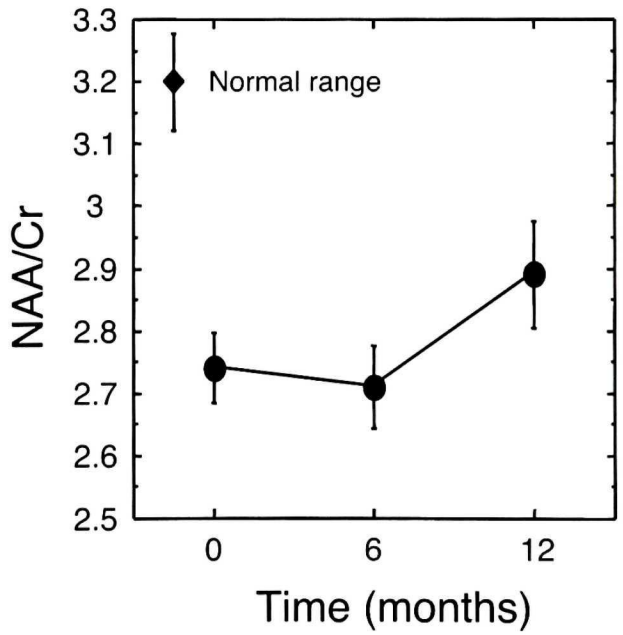

Figure 4-3: Plot of mean NAA/Cr over time for the subgroup of 8 treated patients who underwent interim examinations 6 months after the start of treatment. The error bars represent one standard error of the mean.

Discussion

The principal finding of this pilot study was that IFNβ-1b (Betaseron®) not only slowed, but actually reversed axonal injury in a group of patients with relapsing-remitting MS. Since the spectroscopic volume-of-interest used in this study predominantly contained normal-appearing brain (the mean percentage of the VOI occupied by lesion was 3.5% [range 1% to 9.6%]), the increase in NAA over time under treatment most likely represents recovery of NAA in the NAWM. NAA/Cr change did not correlate with lesion volume change. Thus, the observed 5.5% increase of NAA/Cr within the whole VOI, in the absence of any change in normal-appearing brain, would have required the NAA/Cr within lesions to rise to over two times normal. In addition, if we consider only those patients with very low lesion burdens (< 4 cc), this subgroup of three patients still exhibited recovery of mean NAA/Cr (2.66 to 2.84) over the study period. The latter observation also suggests that recovery of projection axons with connections to lesions was not the primary factor underlying the observed recovery of NAA/Cr after treatment.

There are a number of possible explanations for the rise in NAA/Cr. A chronic low-grade encephalitis is likely present in MS. There is pathological evidence for increased inflammatory cells in the NAWM (Allen and McKeown, 1979). A recent study using gadolinium-enhanced MRI suggests that the blood-brain barrier is diffusely impaired in the NAWM of MS patients (Silver et al., 1999). Such chronic, low-level inflammation could result in widespread, partially reversible axonal dysfunction superimposed upon more permanent axonal damage and loss. The fact that soluble factors associated with inflammation can be found in the cerebrospinal fluid of MS patients indicates that these factors diffuse away from focal sites of inflammation.

A number of tissue-injury mediating factors have been implicated in symptom production in MS (Moreau et al., 1996; Moreau et al., 1994). IFNβ directly or indirectly inhibits production of a number of these inflammation-associated factors, including interferon gamma (Becher et al., 1999), and its ability to stimulate nitric oxide release from astrocytes (Stewart et al., 1997). Elevated nitric oxide/peroxynitrate levels due to raised cytokine levels have been associated with significant damage to neuronal mitochondria (Stewart et al., 1998). IFNβ and a nitric oxide inhibitor both prevent this mitochondrial damage from occurring *in vitro* (Stewart et al., 1998). This suggests that suppression of nitric oxide production and the consequent mitigation of damage to mitochondria in surrounding neurons may be a mechanism of action of IFNβ in MS (Stewart et al., 1998). Since NAA is produced by neuronal mitochondria (Patel and Clark, 1979; Truckenmiller et al., 1985), this could explain the recovery of NAA seen in MS patients treated with IFNβ-1b.

Increases of NAA/Cr could also be associated with reversal of axonal metabolic dysfunction associated with inapparent myelin pathology in the NAWM. Recent magnetization transfer (MT) imaging studies report significantly lower MT ratios in the NAWM of MS patients relative to white matter in normal controls (Filippi et al., 1995a; Filippi et al., 1998; Pike et al., 1999; Pike et al., 2000; Richert et al., 1998). The myelin abnormality could be associated with Wallerian degeneration or low-grade inflammation (Lassmann, 1999).

In view of the relatively high attack rate at baseline in the treated group, one could question whether the observed recovery of NAA was mainly due to slow recovery from attacks (taking longer than the one month exclusion period). This is unlikely for several reasons. If we exclude the three patients who had an attack between one and three months

prior to MR examination, we still observe recovery of NAA/Cr (2.57 to 2.8). The plot of NAA/Cr vs. time in Figure 3 suggests that most of the recovery of NAA/Cr in this subgroup of 8 patients occurred between 6 months and 1 year after the initiation of treatment. Since post-attack recovery of NAA/Cr occurs on the order of weeks to months (De Stefano et al., 1995b; De Stefano et al., 1999; Narayana et al., 1998), and only one patient had an attack less than 5 months prior to the 6 month scan (but still greater than the 1 month exclusion period), it is unlikely that attack recovery could account for the apparent increase of NAA/Cr seen in the second six months after treatment.

A reduction in inflammation-associated cerebral edema following interferon treatment could contribute to the observed increase of NAA/Cr. However, the ratio of brain parenchymal volume to intra-cranial capacity (Collins et al., 2000) decreased over one year in the treated group by 1% (data not shown), which is comparable to previously reported rates of whole-brain atrophy in RRMS patients (Fox et al., 2000; Rudick et al., 1999). This loss of brain volume includes contributions from myelin, glial and axonal loss as well as water loss, so resolution of edema likely represents only a fraction of this 1% volume change. Thus, in our study, the potential contribution of reduced edema could not have been of sufficient magnitude to account for the NAA/Cr recovery observed.

The NAA/Cr in the untreated control group decreased by 4% over one year. Although this was not significant, in a previous study with a larger cohort of untreated, more severely affected patients with RRMS, we demonstrated a significant annual decrease of 5.8%/yr in NAWM (Fu et al., 1998). Since the natural history of MS includes a decrease of NAA/Cr over time, our estimate of the treatment effect may be conservative. A control group with comparable disease activity to our treated group on

entry likely would have exhibited a greater decline over one year than our relatively benign control group.

Sarchielli and co-workers have recently published the results of a study in which they performed short-echo spectroscopy on patients treated with interferon beta-1a (Sarchielli et al., 1998). Over the course of 6 months, they found no change in NAA or Cr levels within lesions or NAWM. In 8 of the patients in the present study, we acquired interim data 6 months after initiation of treatment, and also failed to find any change in NAA/Cr levels at this time point. Our results are therefore consistent with the data of Sarchielli *et al.* The majority of the recovery of NAA reported in the present study seems to have occurred between 6 and 12 months after the start of treatment. This could represent a delay in the onset of the effect of IFNβ on the pathology responsible for diffuse axonal dysfunction.

We have presumed that the increases in NAA/Cr observed are due to increases of NAA and not decreases in Cr. This is highly probable in view of the known sensitivity of NAA to demyelinating injury and the relative stability of Cr under these circumstances. (De Stefano et al., 1995a). *In vivo* MRS studies attempting absolute quantitation of NAA usually require assumptions about coil radiofrequency homogeneity, coil coupling, metabolite relaxation times, tissue composition of each voxel, point spread function, slice selection profile and standards that may not be justified in pathological tissue and often lead to excessive variance in the data. Studies attempting absolute quantitation *in vivo* have reported discrepant results as to whether Cr changes in the NAWM in MS (Husted et al., 1994; Narayana et al., 1998; Pan et al., 1996; Rooney et al., 1997; Sarchielli et al., 1999; van Walderveen et al., 1999). In a post-mortem study performed *in vitro* using high-resolution proton NMR spectroscopy, decreases in Cr were limited to MS plaques,

whereas Cr levels were unchanged in the NAWM (Davies et al., 1995). Since lesion occupied an average of 3.5% of the volume of our VOI, changes of Cr in lesion are unlikely to have affected our overall NAA/Cr measures. Consistent with this, the ratios of the tetra-methyl amine resonance (usually attributed to choline-containing compounds) to Cr did not change over time (data not shown).

Concerns over the specificity of NAA for neurons and neuronal processes in mature brain have been raised with the demonstration of NAA in cultured O2A progenitor cells (Urenjak et al., 1992; Urenjak et al., 1993) and in mature oligodendrocytes grown from cultured O2A progenitor cells exposed to neurotrophic factors (Bhakoo and Pearce, 2000). In contrast, immunohistochemistry studies have shown that antibodies directed against NAA or NAAG stain neurons strongly *in situ* without staining glial cells or glial cell precursors that are normally present in brain (Moffett et al., 1991; Simmons et al., 1991). In NAWM, which constitutes the majority of the tissue in our spectroscopic VOI, the density of oligodendrocyte precursors is low (Scolding et al., 1998) and in lesions, their ability to mature into oligodendrocytes is inhibited (Wolswijk, 1998). Thus, the potential for possible NAA expression in oligodendrocytes or their precursors confounding our results appears to be minimal.

Conclusions

Our results suggest that NAA/Cr in a VOI that predominantly contains normal-appearing brain may increase in MS patients after one year of treatment with interferon beta-1b. Recent evidence supports the notion that axonal pathology begins early in the course of MS (De Stefano et al., 2001). Interferon therapy may be able to reverse part of this early axonal dysfunction and thus delay the accumulation of permanent axonal loss. Treatment of MS with IFNβ-1b may not only slow the accumulation of axonal damage,

which eventually will have clinical consequences, but may also reverse diffuse, sublethal axonal injury.

Acknowledgments

Berlex Canada provided partial support for this study. S.N. received an FRSQ-FCAR-Santé scholarship from the Fonds de la recherche en santé du Québec. D.L.A was supported in part by the Killam Foundation and N.D.S by a grant from the Progetto Sclerosi Multipla, Istituto Superiore di Sanità, Roma.

The authors thank Maria Carmela Tartaglia and Simon Francis for their help in data analysis, and Dr. David MacDonald, Dr. Alan Evans and their colleagues at the Montreal Neurological Institute's Brain Imaging Centre for the development of lesion segmentation software. The assistance of Drs. Tal Arbel and Johan Montagnat in the brain atrophy measurements is greatly appreciated. We thank Drs. Yves Lapierre and W. J. Barkas for referring patients to us and for performing clinical evaluations. Finally, we extend our thanks and appreciation to the study participants for their time and cooperation.

References

1. Allen IV, McKeown SR. A histological, histochemical and biochemical study of the macroscopically normal white matter in multiple sclerosis. J Neurol Sci 1979; 41: 81-91.
2. Arnold DL. Reversible reduction of N-acetylaspartate after acute central nervous system damage. Society of Magnetic Resonance in Medicine. Vol 1, 1992: 643.
3. Arnold DL, Matthews PM, Francis G, Antel J. Proton magnetic resonance spectroscopy of human brain in vivo in the evaluation of multiple sclerosis: assessment of the load of disease. Magnetic Resonance in Medicine 1990; 14: 154-159.

4. Bates TE, Strangward M, Keelan J, Davey GP, Munro PM, Clark JB. Inhibition of N-acetylaspartate production: implications for 1H MRS studies in vivo. Neuroreport 1996; 7: 1397-400.

5. Becher B, Giacomini PS, Pelletier D, McCrea E, Prat A, Antel JP. Interferon-gamma secretion by peripheral blood T-cell subsets in multiple sclerosis: correlation with disease phase and interferon-beta therapy. Ann Neurol 1999; 45: 247-50.

6. Bhakoo KK, Pearce D. In vitro expression of N-acetyl aspartate by oligodendrocytes: implications for proton magnetic resonance spectroscopy signal in vivo. Journal of Neurochemistry 2000; 74: 254-62.

7. Brenner RE, Munro PM, Williams SC, Bell JD, Barker GJ, Hawkins CP, et al. The proton NMR spectrum in acute EAE: the significance of the change in the Cho:Cr ratio. Magnetic Resonance in Medicine 1993; 29: 737-745.

8. Bruhn H, Frahm J, Merboldt KD, Hanicke W, Hanefeld F, Christen HJ, et al. Multiple sclerosis in children: cerebral metabolic alterations monitored by localized proton magnetic resonance spectroscopy in vivo. Ann Neurol 1992; 32: 140-50.

9. Charcot M. Histologie de la sclerose en plaques. Gaz Hosp 1868; 141: 554-5, 557-8.

10. Collins DL, Narayanan S, Caramanos Z, De Stefano N, Tartaglia MC, Arnold DL. Relation of cerebral atrophy in multiple sclerosis to severity of disease and axonal injury. American Academy of Neurology, 52nd Annual Meeting, San Diego, CA. Neurology 2000; 54 Supp. 3: A17.

11. Dautry C, Vaufrey F, Brouillet E, Bizat N, Henry PG, Conde F, et al. Early N-acetylaspartate depletion is a marker of neuronal dysfunction in rats and primates chronically treated with the mitochondrial toxin 3- nitropropionic acid. J Cereb Blood Flow Metab 2000; 20: 789-99.

12. Davie CA, Hawkins CP, Barker GJ, Brennan A, Tofts PS, Miller DH, et al. Serial proton magnetic resonance spectroscopy in acute multiple sclerosis lesions. Brain 1994; 117: 49-58.

13. Davies SE, Newcombe J, Williams SR, McDonald WI, Clark JB. High resolution proton NMR spectroscopy of multiple sclerosis lesions. J Neurochem 1995; 64: 742-8.

14. de Beer R, van Ormondt D. Analysis of NMR data using time domain fitting procedures. NMR Basic Principles and Progress. Vol 26. Berlin: Springer-Verlag, 1992: 204-248.

15. De Stefano N, Matthews PM, Antel JP, Preul M, Francis G, Arnold DL. Chemical pathology of acute demyelinating lesions and its correlation with disability. Annals of Neurology 1995a; 38: 901-909.

16. De Stefano N, Matthews PM, Arnold DL. Reversible decreases in N-acetylaspartate after acute brain injury. Magn Reson Med 1995b; 34: 721-7.

17. De Stefano N, Narayanan S, Francis GS, Arnaoutelis R, Tartaglia MC, Antel JP, et al. Evidence of axonal damage in the early stages of multiple sclerosis and its relevance to disability. Arch Neurol 2001; 58: 65-70.

18. De Stefano N, Narayanan S, Matthews PM, Francis GS, Antel JP, Arnold DL. In vivo evidence for axonal dysfunction remote from focal cerebral demyelination of the type seen in multiple sclerosis. Brain 1999; 122: 1933-1939.

19. Ferguson B, Matyszak MK, Esiri MM, Perry VH. Axonal damage in acute multiple sclerosis lesions. Brain 1997; 120: 393-9.

20. Filippi M, Campi A, Dousset V, Baratti C, Martinelli V, Canal N, et al. A magnetization transfer imaging study of normal-appearing white matter in multiple sclerosis. Neurology 1995; 45: 478-82.

21. Filippi M, Rocca MA, Martino G, Horsfield MA, Comi G. Magnetization transfer changes in the normal appearing white matter precede the appearance of enhancing lesions in patients with multiple sclerosis. Ann Neurol 1998; 43: 809-14.

22. Fox NC, Jenkins R, Leary SM, Stevenson VL, Losseff NA, Crum WR, et al. Progressive cerebral atrophy in MS: a serial study using registered, volumetric MRI [see comments]. Neurology 2000; 54: 807-12.

23. Fu L, Matthews PM, De Stefano N, Worsley KJ, Narayanan S, Francis GS, et al. Imaging axonal damage of normal-appearing white matter in multiple sclerosis. Brain 1998; 121: 103-13.

24. Haase A, Frahm J. Multiple chemical shift selective NMR imaging using stimulated echoes. J. Magn. Reson. 1985: 94-102.

25. Husted CA, Goodin DS, Hugg JW, Maudsley AA, Tsuruda JS, de Bie SH, et al. Biochemical alterations in multiple sclerosis lesions and normal-appearing white matter detected by in vivo 31P and 1H spectroscopic imaging. Annals of Neurology 1994; 36: 157-165.

26. Larsson HB, Christiansen P, Jensen M, Frederiksen J, Heltberg A, Olesen J, et al. Localized in vivo proton spectroscopy in the brain of patients with multiple sclerosis. Magn Reson Med 1991; 22: 23-31.

27. Lassmann H. The pathology of multiple sclerosis and its evolution. Philos Trans R Soc Lond B Biol Sci 1999; 354: 1635-40.

28. Matthews PM, Cianfaglia L, McLaurin J, Cashman N, Sherwin D, Arnold D, et al. Demonstration of reversible decreases in N-Acetylaspartate (NAA) in a neuronal cell line: NAA decreases as a marker of sublethal neuronal dysfunction [abstract]. Proc Soc Magn Reson Med 1995; 1: 147.

29. Matthews PM, De Stefano N, Narayanan S, Francis GS, Wolinsky JS, Antel JP, et al. Putting magnetic resonance spectroscopy studies in context: axonal damage and disability in multiple sclerosis. Semin Neurol 1998; 18: 327-36.

30. Matthews PM, Francis G, Antel J, Arnold DL. Proton magnetic resonance spectroscopy for metabolic characterization of plaques in multiple sclerosis. Neurology 1991; 41: 1251-1256.

31. McDonald WI. Rachelle Fishman-Matthew Moore Lecture. The pathological and clinical dynamics of multiple sclerosis. [Review]. Journal of Neuropathology & Experimental Neurology 1994; 53: 338-343.

32. Moffett JR, Namboodiri MAA, Cangro CB, Neale JH. Immunohistochemical localization of N-acetylaspartate in rat brain. NeuroReport 1991; 2: 131-134.

33. Moreau T, Coles A, Wing M, Isaacs J, Hale G, Waldmann H, et al. Transient increase in symptoms associated with cytokine release in patients with multiple sclerosis. Brain 1996; 119: 225-37.

34. Moreau T, Thorpe J, Miller D, Moseley I, Hale G, Waldmann H, et al. Preliminary evidence from magnetic resonance imaging for reduction in disease

activity after lymphocyte depletion in multiple sclerosis [published erratum appears in Lancet 1994 Aug 13;344(8920):486]. Lancet 1994; 344: 298-301.

35. Narayana PA, Doyle TJ, Lai D, Wolinsky JS. Serial proton magnetic resonance spectroscopic imaging, contrast- enhanced magnetic resonance imaging, and quantitative lesion volumetry in multiple sclerosis. Ann Neurol 1998; 43: 56-71.

36. Narayanan S, Fu L, Pioro E, De Stefano N, Collins DL, Francis GS, et al. Imaging of axonal damage in multiple sclerosis: spatial distribution of magnetic resonance imaging lesions. Ann Neurol 1997; 41: 385-91.

37. Ordidge RJ, Mansfield P, Lohman JA, Prime SB. Volume selection using gradients and selective pulses. Ann N Y Acad Sci 1987; 508: 376-85.

38. Pan JW, Hetherington HP, Vaughan JT, Mitchell G, Pohost GM, Whitaker JN. Evaluation of multiple sclerosis by 1H spectroscopic imaging at 4.1 T. Magn Reson Med 1996; 36: 72-7.

39. Patel TB, Clark JB. Synthesis of N-acetyl-L-aspartate by rat brain mitochondria and its involvement in mitochondrial/cytosolic carbon transport. Biochem J 1979; 184: 539-46.

40. Paty DW, Li DK. Interferon beta-1b is effective in relapsing-remitting multiple sclerosis. II. MRI analysis results of a multicenter, randomized, double-blind, placebo-controlled trial. UBC MS/MRI Study Group and the IFNB Multiple Sclerosis Study Group [see comments]. Neurology 1993; 43: 662-667.

41. Pike GB, de Stefano N, Narayanan S, Francis GS, Antel JP, Arnold DL. Combined magnetization transfer and proton spectroscopic imaging in the assessment of pathologic brain lesions in multiple sclerosis. AJNR Am J Neuroradiol 1999; 20: 829-37.

42. Pike GB, De Stefano N, Narayanan S, Worsley KJ, Pelletier D, Francis GS, et al. Multiple sclerosis: magnetization transfer MR imaging of white matter before lesion appearance on T2-weighted images. Radiology 2000; 215: 824-30.

43. Richert ND, Ostuni JL, Bash CN, Duyn JH, McFarland HF, Frank JA. Serial whole-brain magnetization transfer imaging in patients with relapsing-remitting multiple sclerosis at baseline and during treatment with interferon beta-1b. AJNR 1998; 19: 1705-13.

44. Rooney WD, Goodkin DE, Schuff N, Meyerhoff DJ, Norman D, Weiner MW. 1H MRSI of normal appearing white matter in multiple sclerosis. Multiple Sclerosis 1997; 3: 231-7.

45. Rudick RA, Fisher E, Lee JC, Simon J, Jacobs L. Use of the brain parenchymal fraction to measure whole brain atrophy in relapsing-remitting MS. Multiple Sclerosis Collaborative Research Group [In Process Citation]. Neurology 1999; 53: 1698-704.

46. Sarchielli P, Presciutti O, Pelliccioli GP, Tarducci R, Gobbi G, Chiarini P, et al. Absolute quantification of brain metabolites by proton magnetic resonance spectroscopy in normal-appearing white matter of multiple sclerosis patients [In Process Citation]. Brain 1999; 122: 513-21.

47. Sarchielli P, Presciutti O, Tarducci R, Gobbi G, Alberti A, Pelliccioli GP, et al. 1H-MRS in patients with multiple sclerosis undergoing treatment with interferon beta-1a: results of a preliminary study. J Neurol Neurosurg Psychiatry 1998; 64: 204-12.

48. Scolding N, Franklin R, Stevens S, Heldin CH, Compston A, Newcombe J. Oligodendrocyte progenitors are present in the normal adult human CNS and in the lesions of multiple sclerosis [see comments]. Brain 1998; 121: 2221-8.

49. Silver NC, Tofts PS, Symms MR, Barker GJ, Thompson AJ, Miller DH. Evidence of widespread subtle blood-brain barrier dysfunction associated with progressive MS. Proc Soc Magn Reson Med 1999; 1: 628.

50. Simmons ML, Frondoza CG, Coyle JT. Immunocytochemical localization of N-acetyl-aspartate with monoclonal antibodies. Neuroscience 1991; 45: 37-45.

51. Stewart VC, Giovannoni G, Land JM, McDonald WI, Clark JB, Heales SJ. Pretreatment of astrocytes with interferon-alpha/beta impairs interferon-gamma induction of nitric oxide synthase. J Neurochem 1997; 68: 2547-51.

52. Stewart VC, Land JM, Clark JB, Heales SJ. Pretreatment of astrocytes with interferon-alpha/beta prevents neuronal mitochondrial respiratory chain damage. J Neurochem 1998; 70: 432-4.

53. Stone LA, Frank JA, Albert PS, Bash C, Smith ME, Maloni H, et al. The effect of interferon-beta on blood-brain barrier disruptions demonstrated by contrast-

enhanced magnetic resonance imaging in relapsing-remitting multiple sclerosis. Ann Neurol 1995; 37: 611-9.

54. The IFNB multiple sclerosis study group. Interferon beta-1b is effective in relapsing-remitting multiple sclerosis. I. Clinical results of a multicenter, randomized, double-blind, placebo-controlled trial. Neurology 1993; 43: 655-661.

55. Trapp BD, Peterson J, Ransohoff RM, Rudick R, Mork S, Bo L. Axonal transection in the lesions of multiple sclerosis [see comments]. N Engl J Med 1998; 338: 278-85.

56. Truckenmiller ME, Namboodiri MA, Brownstein MJ, Neale JH. N-Acetylation of L-aspartate in the nervous system: differential distribution of a specific enzyme. J Neurochem 1985; 45: 1658-62.

57. Urenjak J, Williams SR, Gadian DG, Noble MD. Specific expression of N-acetylaspartate in neurons, oligodendrocyte-type-2 astrocyte progenitors, and immature oligodendrocytes in vitro. J Neurochem 1992; 59: 55-61.

58. Urenjak J, Williams SR, Gadian DG, Noble MD. Proton nuclear magnetic resonance spectroscopy unambiguously identifies different neural cell types. J Neurosci 1993; 13: 981-9.

59. van Walderveen MA, Barkhof F, Pouwels PJ, van Schijndel RA, Polman CH, Castelijns JA. Neuronal damage in T1-hypointense multiple sclerosis lesions demonstrated in vivo using proton magnetic resonance spectroscopy. Ann Neurol 1999; 46: 79-87.

60. Waxman SG. Demyelinating diseases--new pathological insights, new therapeutic targets [editorial; comment]. N Engl J Med 1998; 338: 323-5.

61. Wolswijk G. Chronic stage multiple sclerosis lesions contain a relatively quiescent population of oligodendrocyte precursor cells. J Neurosci 1998; 18: 601-9.

Chapter 5

Cortical adaptations to injury in MS

5.1 Preface

Clinicians are often confronted with patients who satisfy the clinical and paraclinical requirements for a diagnosis of MS, have significant brain T2-weighed lesion load, have suffered documented relapses, and yet recover fully from these relapses, without accruing any significant chronic disability, at least for a time. These anecdotal data are corroborated by the numerous studies reporting poor correlation between brain T2-weighted lesion load and disability measures (Filippi et al., 1994b; Filippi et al., 1995b; Khoury et al., 1994; Lycklama à Nijeholt et al., 1998; Miller, 1994) (Filippi, 2001; van Walderveen et al., 2001). Newer MR techniques have improved the correlations between MR markers of pathology and disability, but a large proportion of the variance in chronic EDSS remains unexplained by these *in vivo* surrogates of structural damage and metabolic dysfunction (Arnold et al., 2000; Filippi, 2001; Simon, 2001; van Walderveen et al., 2001).

The study of large, acute lesions with direct functional consequences can be instructive, as the relationships between MR and clinical variables are not as confounded as in the general case of MS. Early MRS studies have shown large, partially reversible decreases of NAA in such cases (Arnold, 1992; Davie et al., 1994; De Stefano et al., 1995b; Narayana et al., 1998). The recovery of NAA can be attributed principally to the recovery of sublethal axonal damage as levels of inflammatory mediators decline and, to a smaller degree, resolution of edema. The fact that NAA did not return to normal levels in these studies indicates the presence of permanent axonal damage or loss, a feature of MS lesions which has been demonstrated directly via sophisticated pathology studies (Ferguson et al., 1997; Trapp et al., 1998). Other mechanisms that can aid functional recovery from these large, symptomatic lesions are redistribution of sodium channels (Waxman, 1998) and remyelination (Prineas et al., 1993; Raine and Wu, 1993). Despite the significant amount of axonal transection and loss that must occur in these large lesions, clinical recovery can be remarkable (De Stefano et al., 1995a; De Stefano et al., 1995b).

Studies in ischemic disease have demonstrated the brain's ability to compensate for cortical damage, either by expansion of the cortical area responsible for a specific function (Seil, 1997), or by recruiting latent pathways such as ipsilateral motor tracts to restore motor function (Cao et al., 1998). A preliminary study applying fMRI techniques to MS patients found evidence of increased bilateral activation of primary motor cortex with performance of a finger-thumb opposition task (1Hz) in patients with partial hand weakness (Clanet et al., 1997), suggesting that compensatory mechanisms similar to that seen in stroke could occur in MS.

The study presented in this chapter was the first, to our knowledge, to directly demonstrate dynamic cortical adaptations in response to acute subcortical injury. We performed serial MRSI and fMRI examinations on a patient presenting with an acute relapse of MS, including right-sided hemiplegia referable to four large confluent lesions in the left hemisphere. The fMRI paradigm was a block design using a simple finger-thumb opposition task, which was known to produce a robust activation of the primary motor cortex. The large plaques intersected the cortico-spinal tract, and MRSI demonstrated them to be active, with elevated choline and large lactate peaks. NAA was greatly reduced in the plaque, indicating marked axonal injury. The initial fMRI scan was performed just as the patient was beginning to recover function in her right hand, and showed a remarkable degree of enlarged, bilateral activation. The patient then exhibited a strong and rapid clinical recovery that preceded recovery of left corticospinal tract NAA, while maintaining an elevated total volume of activation. Only when NAA levels in the left corticospinal tract began to recover did the total activated volume begin to decrease. The key points were that (1) cortical adaptations to injury were able to restore functional capacity to a striking degree; (2) as axonal function began to recover, the elevated cortical activation volume began to decline and (3) the patient regained essentially all her pre-relapse function at the end of the follow-up period, even though NAA in the left corticospinal tract remained low relative to controls values (indicative of substantial residual axonal damage). The total volume of activation remained elevated compared to controls at the end of the study period. This was a seminal study in that it clearly demonstrated that cortical adaptations could compensate for significant white matter injury, and could aid functional recovery from relapse.

We followed this work with a combined fMRI and MRSI study of 9 patients with chronic MS (between relapses) to determine whether cortical adaptations could contribute to maintaining motor function with progressive axonal injury (Reddy et al., 2000a). We selected patients with near-normal finger tapping abilities to avoid the confounding effect of a more "effortful" task. We found that patients showed decreased lateralization of sensorimotor cortex activation relative to controls, and a strong negative correlation ($r = -0.88$, $p < 0.01$) between the degree of lateralization ("lateralizaton index") and decreases in brain NAA. The decreasing lateralization of activation with decreasing NAA was due to increasing ipsilateral activation, particularly in the ipsilateral supplementary motor cortex. The results suggest that cortical re-organization or unmasking of latent pathways contribute to maintaining normal motor function with increasing axonal damage in MS, and may mask irreversible brain injury early in the disease.

Other fMRI studies have appeared in the literature that corroborate and extend our findings. Using a four-finger flexion task, the Oxford group demonstrated a similar relationship between the lateralization of sensorimotor cortical activation and total T2-weighted lesion volume in MS patients, affirming the presence of adaptive cortical responses to white matter injury in MS (Lee et al., 2000a). A recent Italian study of non-disabled but relapsing MS patients using combined fMRI (four-finger flexion task), MTR and diffusion imaging again found significant cortical adaptations to tissue injury (assessed by T2-weighed lesion volume, MTR metrics and mean diffusivity) (Rocca et al., 2002). In addition to increased activation in the primary sensorimotor cortex and the supplementary motor area, they also detected activation in the cingulate motor area, the contralateral ascending bank of the sylvian fissure and in the contralateral intraparietal sulcus, indicating that recruitment of cortex in adapting to white matter injury can be

widespread (Rocca et al., 2002). Cortical adaptations do not limit the clinical impact of brain injury only on motor performance in MS, but have also been associated with fatigue (Filippi et al., 2002) and performance on attention tasks (Staffen et al., 2002).

5.2 Manuscript 3

Published in Neurology 2000;54:236-239

Relating Axonal Injury to Functional Recovery in Multiple Sclerosis

H. Reddy[1,2], M.D., S. Narayanan[1], M.Sc., P.M. Matthews[2], M.D., DPhil., R.D. Hoge[1], Ph.D., G.B. Pike[1], Ph.D., P. Duquette[3], M.D., J. Antel[1], M.D., D.L. Arnold[1], M.D.

[1]Department of Neurology and Neurosurgery, Montreal Neurological Institute, McGill University,

[2]Centre for Functional Magnetic Resonance Imaging of the Brain, Dept. of Clinical Neurology, University of Oxford, and

[3]Department of Clinical Neurology, Hôpital Notre Dame, Université de Montréal

Correspondence to:

Prof. D.L. Arnold
Montreal Neurological Institute
3801 University Street
Montreal, PQ
Canada H3A 2B4
Tel: 514-398-8525, Fax: 514-398-2975
Email: doug@mrs.mni.mcgill.ca

Running Title: **Combined MRSI and fMRI in MS**

Key words: multiple sclerosis; disability; magnetic resonance spectroscopy; functional magnetic resonance imaging; axon

Abstract

A patient was followed after the new onset of hemiparesis from relapse of MS with serial MR spectroscopy and functional MRI. The association of clinical improvement with recovery of N-acetylaspartate, a marker of neuronal integrity, and progressive reduction of abnormally large functional MRI cortical activation with movement demonstrates that dynamic reorganization of the motor cortex accompanies remission of MS.

Introduction

Relapsing-remitting MS is associated clinically with recurrent attacks, after which patients show remission of symptoms. Pathologically, lesions of MS show demyelination and axonal injury. Remyelination and repair of axonal dysfunction probably contribute to functional recovery. However, it also is possible that adaptive mechanisms in the cortex (e.g., reorganization) may augment functional recovery, as has been suggested for patients with focal ischemic disease. If such cortical reorganization follows axonal damage in MS, then evolution of abnormal patterns of brain activation associated with acute relapses should occur in the subsequent period of recovery.

MR spectroscopic imaging (MRSI) can be used to measure the extent of axonal injury or loss in white matter based on the relative resonance intensity of N-acetylaspartate (NAA), a compound found only in neurons and their processes in the mature brain (Matthews et al., 1998). Functional MRI (fMRI) can be used to map regions of brain activation during motor tasks and can define abnormal patterns of activation in disease (Cao et al., 1998; Seil, 1997).

We performed neurologic follow-up and serial MRSI and fMRI studies of a patient after an acute attack of relapsing-remitting MS to relate measures of axonal injury and task-related brain activation to functional impairment of the affected limb. This allowed us to test whether there are dynamic, adaptive changes in the motor cortex that could contribute to functional recovery after a relapse of MS.

Methods

Patient history

This 39-year-old, righthanded woman had been diagnosed with relapsing-remitting MS 7 years earlier and had been without significant disability (Expanded Disability Status Scale = 0) until 6 weeks before the start of this study. She developed a mild right-sided motor deficit, which progressed to right hemiplegia at presentation. There had been word-finding difficulties for the preceding 4 weeks. No symptoms or clinical deficits that could be localized to the right hemisphere were found on any examination. T2-weighted MRI showed four large, confluent demyelinating lesions extending almost the full length of the left hemisphere. The T1- weighted image showed a small mass effect and hypointense signal changes of edema, confirming that this was an acute lesion.

There were several smaller T2-hyperintense lesions in the right hemisphere that appeared to be chronic. She was treated with a one-week course of methylprednisolone and showed gradual, almost complete recovery of motor function over the subsequent 6 weeks. Follow-up MRI studies showed progressive resolution of the large, active left-hemisphere lesions. Lesions in the right hemisphere did not change size, shape, or appearance, confirming their chronic nature.

Controls

Controls were 6 healthy, right-handed adult volunteers (4 men, 2 women; ages 18-35 years old). Consent for study was obtained from all participants with a protocol approved by the local institutional ethics committee.

Functional Assessments

Motor functional assessments were performed on the controls and the patient at the time of each imaging study by measurement of maximum finger and foot tapping speeds and the time for completion of the nine-hole peg test. A neurologist examined the patient and disability was scored with the Expanded Disability Status Scale (EDSS).

Imaging

Conventional proton MRI (dual spin-echo, 3 mm slices parallel to the AC-PC line, repetition time [TR] 2075 msec, echo time [TE] 32/90) and MRSI (84 x 100 x 20 mm^3 slab parallel to the AC-PC line centered on the corpus callosum, 32 x 32 matrix with interpolated 16 x 16 non-suppressed water spectrum, TR 2 sec, TE 272 msec) examinations of the brain were performed using a 1.5 T Philips Gyroscan ACS II (Philips Medical Systems, Best, the Netherlands) (Arnold et al., 1992). Volumes of interest in the corticospinal tract were determined from intersection of the spectroscopy volume with the corticospinal tract as identified on each set of this patient's brain images according to anatomical landmarks on the structural image (Riahi et al., 1998). As validated in previous studies (Arnold et al., 1992; Sarchielli et al., 1999), NAA resonance intensities were normalized to intra-voxel creatine (Cr) resonance intensities for the right hemisphere and to the Cr resonance intensity in the corresponding contralateral voxels for the left hemisphere.

FMRI studies were performed using a "boxcar" design in which cued index finger-thumb opposition (1.5 Hz) was alternated with rest periods while acquiring images with a 1.5 T Siemens Magnetom Vision (gradient echo-planar imaging, 128 x 96 mm matrix, 300 mm FOV, TE 51 msec, TR 4 sec for 15 x 5 mm slices registered to a T1-weighted gradient-echo structural scan acquired with 1 mm^3 isotropic voxels, TR 22 msec, TE 10 msec, flip angle 30°). A total of 120 volumes each were obtained for studies of right and left hand movements with alternating blocks of 20 volumes.

t-Statistic activation images were generated with software developed in-house based on Spearman Rank Order correlation of image signal changes with the time-course of the cueing stimulus. The raw data set was initially motion-corrected (automated image registration), then intensity normalized, low-pass filtered, and spatially smoothed (3D gaussian kernel with full width at half maximum of 6 mm). Correcting for multiple comparisons, a threshold of $t > 4.9$ was calculated to correspond to a significance level of $p < 0.01$. Activation images then were overlaid on anatomic scans. Numbers of pixels achieving threshold in the anatomically defined regions of interest drawn around the primary sensorimotor/premotor and supplementary motor cortices in the left and right hemispheres then were measured.

A motor-task activation lateralization index (LI) was defined from the number of pixels activated in contralateral (C) and ipsilateral (I) primary sensorimotor/premotor regions ($LI = (C-I)/(C+I)$), where $LI = 1$ for fully contralateral and $LI = -1$ for fully ipsilateral activations.

Where mean results are reported, the standard deviations are noted.

Results

At presentation the patient was unable to move the right hand or foot. Movements of the limbs returned almost completely to the pre-relapse level of function over the subsequent six weeks (Table 5-1).

Time After Presentation (Weeks)	Disability Measures			NAA/Cr Signal Intensity Ratio by Hemisphere		Side of Finger-Thumb Opposition Movement	Total Volume of Sensorimotor Activation in a Hemisphere (number of pixels)	Hemispheric Activation Laterality Index
	EDSS	*Maximum Finger Tapping Rate by Hand (Hz)*						
		Right	Left	Right	Left			
0	8	0	3.6	**2.6**	**1.9**	-	-	-
2	7.5	**2.2**	3.8	2.8	**1.7**	-	-	-
3	7	**3.3**	4.5	-	-	Right Left	**14.9** **17.8**	**0.5** 1.0
4	2	**5.4**	**5.2**	**2.5**	**1.7**	-	-	-
10	1.5	**4.5**	**4.7**	-	-	Right Left	**16.0** **16.8**	0.9 0.7
24	1.5	**4.7**	**4.7**	3.0	**2.1**	Right Left	8.6 16.0	1.0 1.0
Control Values (±SD)	-	3.8 ± 0.1	3.6 ± 0.5	3.2 ± 0.2	3.0 ± 0.2	Right Left	4.3 ± 2.8 7.2 ± 4.5	0.9 ± 0.1 0.8 ±0.2

Table 5-1: Changes in disability, relative NAA concentration in voxels within the segmented corticospinal tract of the affected and unaffected hemispheres, and fMRI activation volume and hemispheric lateralization during the period of recovery after an acute relapse of MS. Disability is expressed in terms of the Expanded Disability Status Scale (EDSS) and the maximum index-finger thumb-tapping rate averaged over a 10 sec period. The concentration of N-acetylaspartate (NAA) was measured relative to creatine (Cr) in the same volumes for the unaffected right hemisphere. NAA in the left hemisphere was measured relative to the Cr concentration in the homologous volume of the unaffected hemisphere. fMRI was performed with simple index-finger thumb opposition with either the left or right hand. The total volume of significant activation with the motor task relative to a resting baseline was measured and a laterality index (LI) calculated as described in the Methods (non-lateralized LI=0, fully left lateralized LI = 1). Values in bold are greater than two standard deviations outside the normal control range.

MRSI was performed four times during the 6 months after presentation. Overall, the relative NAA concentration in the corticomotor area in both hemispheres increased in association with recovery from functional impairment (see Table 5-1 and Figure 5-1). However, at the last examination, the relative NAA concentration in the left hemisphere

was still reduced by over 30% relative to controls. The relative NAA concentration in homologous volumes in the right hemisphere recovered to the normal range by the final examination.

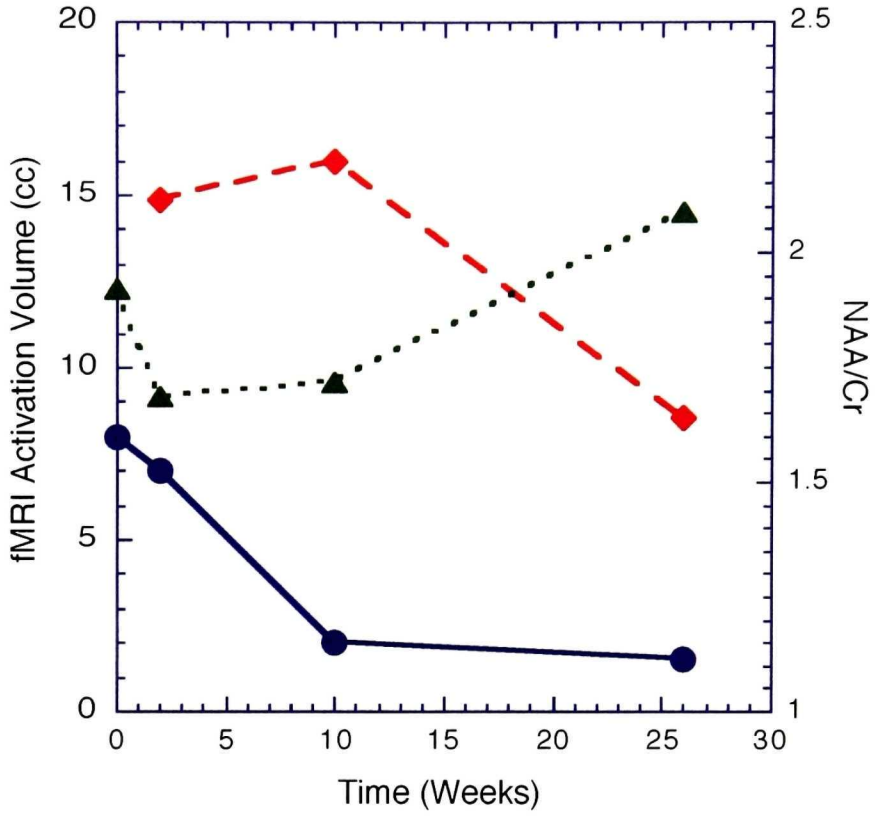

Figure 5-1: Relationship between changes in disability (Expanded Disability Status Scale [●]) and measures of axonal injury (N-acetylaspartate/creatine ratio [NAA/Cr [▲]) and functional MRI activation volumes (◆) in motor cortex. Decreasing disability over the study period is associated with a decrease in the volume of fMRI activation in the motor cortex and increasing NAA/Cr (a measure of axonal recovery) after the hyperacute period. Time after presentation is shown on the abscissa.

FMRI studies were performed three times during the period of recovery of right hand function, beginning about two weeks after presentation, when the patient could perform the task adequately. In each of the serial studies, the patient showed activation of ipsi- and contralateral primary sensorimotor and premotor cortices and the supplementary motor cortex with finger-thumb opposition of the paretic right hand (Figure 5-1). In the

first two studies, the volume of activation in the patient was substantially greater than that found with right hand movements in the normal (right-handed) controls (4.3 ± 2.8 cm^3). The total volume of activation in these areas decreased by almost 50% in both the right and left hemispheres over the period of study (Table 5-1 and Figure 5-2). However, the decrease in the fMRI activation volume lagged behind recovery of maximum finger tapping rate: the greatest improvement in finger tapping rate occurred between the first two completed fMRI studies, which showed essentially identical, abnormally increased volumes of activation.

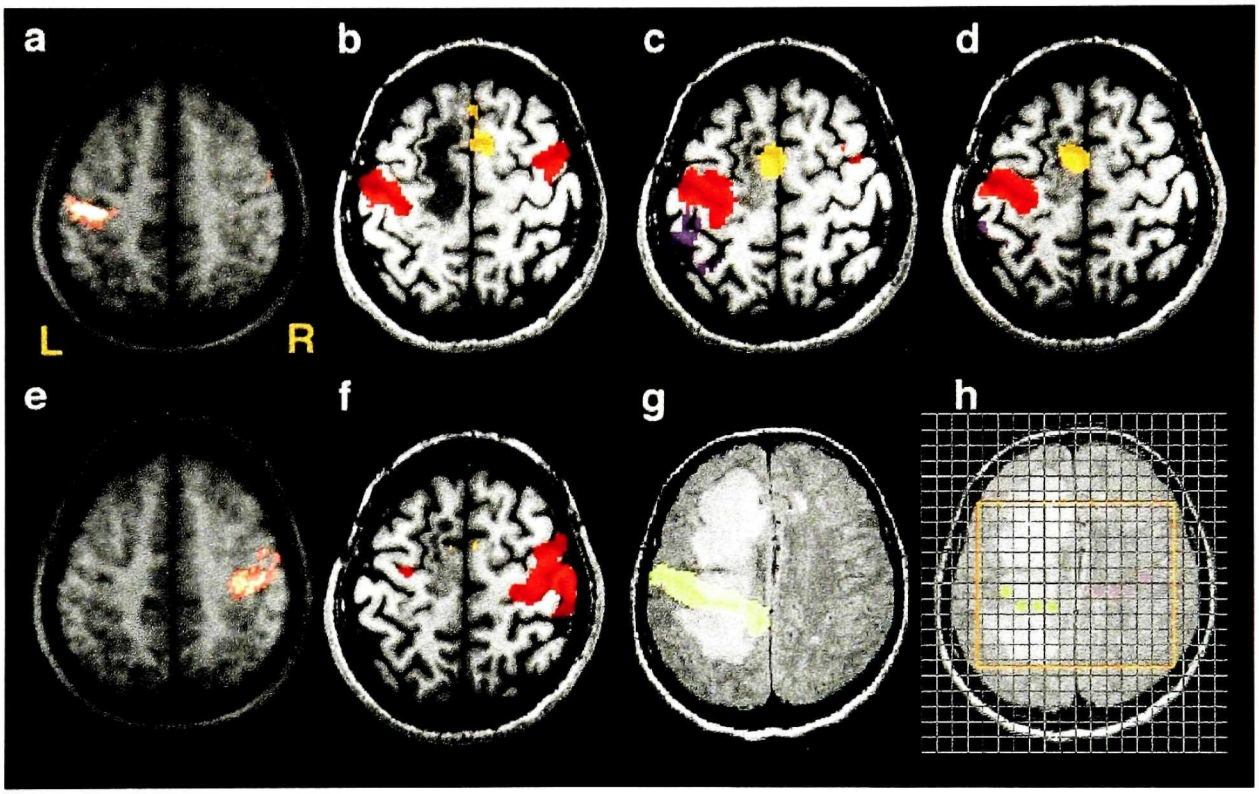

Figure 5-2: Anatomical representation of functional MRI motor activations for normal controls and the patient, and chosen areas of interest for MR spectroscopic imaging. "Hot metal" representation of the proportion of normal controls exhibiting activation in the motor cortex with right (a) or left (e) hand movements. Pixel brightness increases with frequency of activation at that location. Areas activated by the patient during movements of the impaired right hand at the first (b), second (c), and third (d) fMRI examinations. Areas (f) activated by the patient with movement of the unimpaired (left) hand. These did not change significantly over the course of the study. Activations are segmented on the basis of anatomical landmarks to identify those in sensorimotor (red), supplementary motor (yellow), or other cortex (blue). The corticospinal tract mask (g) used to select voxels of interest (h) for analysis of spectroscopy data.

The patient showed a more bihemispheric pattern of motor cortex activation with this simple movement than did control subjects. The lateralization index increased from an abnormally low value (0.5) at the first examination to an average of 1.0 (controls, 0.9 ± 0.1) in the later two completed studies. This increase in left-sided lateralization was caused primarily by a decrease of activation in the primary sensorimotor area of the ipsilateral hemisphere.

The volume of activation in the right hemisphere with left-hand movement was higher than that found for any of the normal controls but did not change significantly (Table 5-1 and Figure 5-2). The laterality index for left-hand movement was not different from that for the normal controls.

Discussion

This serial study of a patient after an acute relapse of MS allowed us to test the relation between axonal dysfunction, cortical activation, and recovery from functional impairments after a relapse of MS. Consistent with our previous MRSI observations (De Stefano et al., 1995b), the relapse was associated with a partially reversible decrease in relative NAA concentration, suggesting a degree of reversible axonal dysfunction or damage.

The most striking finding in the parallel fMRI studies was an increased volume of contralateral sensorimotor cortex activation with movement of the affected hand. A significant decrease in the total volume of activation occurred between the last two studies over a similar time period to increases in the relative NAA signal intensity in the segmented corticospinal tract voxels. We interpret this as evidence that cortical motor activation responses changed dynamically during recovery. Because the maximum finger

tapping rate by the affected hand did not change significantly from 4 weeks after presentation, the decrease in activation volume observed between the 6- and 24-week studies (Table 5-1) is consistent with the notion that cortical motor activity dynamically adapts locally to maintain functional capacity after subcortical injury from a relapse of MS. Previous studies have shown that cortical motor areas in normal subjects are modifiable as a result of central or peripheral neural injury, learning, or stimulation (Cao et al., 1998; Caramia et al., 1996; Jenkins and Merzenich, 1987; Seil, 1997).

Finger-thumb opposition by the affected hand also was associated with increased relative activation of the ipsilateral motor cortex. Ipsilateral pathways may play a role in functional recovery after brain injury (Cao et al., 1998; Seil, 1997). Increased ipsilateral activation may reflect mirror movements, although we did not see any mirror movements in the patient in this study during practice or during fMRI task performance. Other workers have reported significant ipsilateral motor cortex activation without mirror movements in patients with stroke (Cao et al., 1998). If undetectable movements of the unaffected hand were responsible for activation ipsilateral to the paretic hand, then these might be expected to be similar to changes seen with imagined hand movements in normal subjects, which lead to a much lower mean activation than do overt limb movements (imagined movements show only about 30% of the activation response seen with movement and this only in some subjects (Roth et al., 1996)).

A critical factor in interpretation of serial studies is the reproducibility of the measurement. Long-echo time (TE 272 msec) MRSI minimizes baseline artifacts and overlap of resonance peaks from short-T2 species with the NAA and Cr peaks, which have relatively long T2 relaxation times. Changes in NAA/Cr values of individual control subjects over time are less than 5% in our laboratory, suggesting that changes of greater

than 10% can be detected reliably in serial studies. FMRI studies can show substantial variations between volumes of activation associated with motor tasks in different individuals, as reflected in the large variance seen in our control values (Table 5-1). However, variance of activation volumes in serial studies of the same individual is much smaller (e.g., with a finger tapping task, the mean variance of sensorimotor cortical activation volumes for normal single individuals studied serially can be almost two-fold lower than the variance across a group of similar subjects; M. Lee, H. Reddy, P. M. Matthews, unpublished data, 1999). The good reproducibility of fMRI measurements in this study is confirmed by the small differences in activation volumes (16.9±0.9 pixels) measured with movements of the clinically unaffected hand during the three studies.

Special caution is needed when interpretating fMRI results in or around areas of pathology. The Blood Oxygenation Level-Dependent response is determined by the changes in blood flow, blood volume and blood oxygenation that occur secondary to neuronal activation. Vasoactive substances from inflammatory lesions conceivably could alter the relation between neuronal activation and the hemodynamic response. We have expressed our results in terms of the number of pixels activated rather than an intensity of activation in an effort to minimize the influence of these possible effects on our interpretation. The conclusion that there is a dynamic cortical response to MS relapse is based in part on observation of activation changes in the unaffected hemisphere ipsilateral to the paretic hand.

The concept that cortical changes may contribute to recovery from relapses in MS has intriguing clinical implications. In stroke, techniques such as proprioceptive stimulation and rehabilitation or treatment with neurotrophic factors may enhance recovery. Similar strategies also could facilitate functional recovery in MS.

Acknowledgements

Supported in part by the Multiple Sclerosis Society of Canada and the Medical Research Council (Canada). PMM is supported by the Medical Research Council (UK).

References

1. Arnold DL, Matthews PM, Francis GS, O'Connor J, Antel JP. Proton magnetic resonance spectroscopic imaging for metabolic characterization of demyelinating plaques. Ann Neurol 1992; 31: 235-41.
2. Cao Y, D'Olhaberriague L, Vikingstad EM, Levine SR, Welch KM. Pilot study of functional MRI to assess cerebral activation of motor function after poststroke hemiparesis. Stroke 1998; 29: 112-22.
3. Caramia MD, Iani C, Bernardi G. Cerebral plasticity after stroke as revealed by ipsilateral responses to magnetic stimulation. Neuroreport 1996; 7: 1756-60.
4. De Stefano N, Matthews PM, Arnold DL. Reversible decreases in N-acetylaspartate after acute brain injury. Magn Reson Med 1995; 34: 721-7.
5. Jenkins WM, Merzenich MM. Reorganization of neocortical representations after brain injury: a neurophysiological model of the bases of recovery from stroke. Prog Brain Res 1987; 71: 249-66.
6. Matthews PM, De Stefano N, Narayanan S, Francis GS, Wolinsky JS, Antel JP, et al. Putting magnetic resonance spectroscopy studies in context: axonal damage and disability in multiple sclerosis. Semin Neurol 1998; 18: 327-36.
7. Riahi F, Zijdenbos A, Narayanan S, Arnold D, Francis G, Antel J, et al. Improved correlation between scores on the expanded disability status scale and cerebral lesion load in relapsing-remitting multiple sclerosis. Results of the application of new imaging methods. Brain 1998; 121: 1305-12.
8. Roth M, Decety J, Raybaudi M, Massarelli R, Delon-Martin C, Segebarth C, et al. Possible involvement of primary motor cortex in mentally simulated movement: a functional magnetic resonance imaging study. Neuroreport 1996; 7: 1280-4.
9. Sarchielli P, Presciutti O, Pelliccioli GP, Tarducci R, Gobbi G, Chiarini P, et al. Absolute quantification of brain metabolites by proton magnetic resonance

spectroscopy in normal-appearing white matter of multiple sclerosis patients [In Process Citation]. Brain 1999; 122: 513-21.

10. Seil FJ. Recovery and repair issues after stroke from the scientific perspective. Curr Opin Neurol 1997; 10: 49-51.

Chapter 6

Relationship of axonal injury to demyelination

6.1 Preface

The data presented in previous chapters affirm the link between axonal injury and chronic disability, although as shown in Chapter 5, this relationship can be mitigated by cortical adaptations to axonal injury. Axons can also enter a state of chronic dysfunction, as evidenced by the fact that chronically low levels of NAA can be partially reversed by treatment in some patients. The manuscript presented in this chapter addresses the issue of whether chronic axonal injury in the cerebral NAWM of MS patients is linked to inapparent myelin pathology in the NAWM, as assessed by quantitative magnetization transfer (QMT) techniques.

Magnetization transfer imaging has generally been performed semi-quantitatively, by generating images of the percent change in signal intensity between two scans, one performed with an MT saturation pulse and the other without, as discussed in Section 2.5.2. MTR imaging has improved specificity to disturbances of myelin (Dousset et al., 1992; Kucharczyk et al., 1994) compared to conventional imaging, and has now been

used extensively to study myelin pathology both within MS lesions and the NAWM, documenting, in particular, abnormal MTR in the NAWM (Filippi et al., 1995a; Gass et al., 1994; Loevner et al., 1995; Pike et al., 1999; Pike et al., 2000; Richert and Frank, 1999; Richert et al., 1998; Rocca et al., 1999; Rovaris et al., 2001).

The specificity of MTR decreases to myelin pathology is not perfect, however. Vavasour *et al.* reported reduced computed myelin water percentages from relaxometry data (the "short T2" component is also a putative MR index of myelin) as well as reduced MTR both in NAWM and lesions of MS (Vavasour et al., 1998). However, the measures were uncorrelated in WM and GM, and showed a significant but small correlation in MS lesions. These authors concluded that the two techniques provided largely independent measures of MS lesion pathology, raising questions about the myelin specificity of both techniques. However, review of these data have revealed that at least part of this lack of correlation may have been due to the combining together of data from different regions of brain that had different slopes to their correlations (Alex MacKay and Corree Laule, personal communication). In an experimental allergic encephalomyelitis (EAE) model of MS in guinea pigs, Gareau *et al.* correlated MTR with relaxometry and histopathology and concluded that MTR was sensitive to inflammation, while the short T2 component was a more specific indicator of myelin content in tissue (Gareau et al., 2000). Given the prominent role of MT in WM, both of these studies highlight the weakness of the commonly used MTR technique and provide strong motivation to collect quantitative MT data in order to better understand these potentially valuable measures.

A recent study by Pendlebury *et al.* compared the relationships between NAA loss, MTR decrease and clinical impairment in both stroke and MS (Pendlebury et al., 1999). They found that NAA loss in the posterior internal capsule correlated with motor

impairment in both stroke and MS patients, but that MTR decrease correlated with motor impairment and NAA loss only in stroke patients. The close relationship between MTR decrease and NAA loss in stroke is consistent with demyelination secondary to wallerian degeneration of axons distal to the infarct. The relationship between axonal loss and demyelination in MS is clouded since demyelination can occur with variable amounts of axonal loss (Pendlebury et al., 1999). In both stroke and MS patients, axonal damage as assessed by NAA loss correlated with motor impairment (Pendlebury et al., 1999).

We have previously performed combined MRS and MTR imaging in MS patients, and found that mean NAA/Cr in a large central brain volume containing a large proportion of NAWM correlated well (SROC=0.7, p=0.016) with mean lesion MTR in RR patients, but not in SP patients (Pike et al., 1999). This suggests that wallerian degeneration of axons transected in more active lesions contributes significantly to the loss of NAA in the NAWM in RR patients, but that demyelination within lesions becomes less important to diffuse axonal damage in the SP stage. A weaker correlation ($r=0.45$, $p<0.0001$) was found in a voxel-by-voxel correlation between NAA/Cr and the mean MTR in each spectroscopic voxel in RR patients, reiterating the fact that local NAA/Cr levels can be sensitive to pathology at a distance as well as local pathology.

A recent study combining post-mortem MRI and MTI scanning with histopathology in 17 end-stage progressive MS patients reported that MTR decreases correlated with demyelination, but correlated better with axonal loss (van Waesberghe et al., 1999). The authors suggested that this was mainly because of T1 effects due to enlargement of the extracellular spaces following axonal loss, as well as loss of axonal membranes. Thus it appears that MTR can be sensitive to general tissue destruction as well as demyelination, particularly in late stage MS.

The interpretation of changes in MTR is made difficult by the fact that it reduces a complex combination of sequence, relaxation and MT parameters to a single number. Henkelman *et al.* have developed methods to explicitly quantify the sizes of the liquid and semisolid pools, individual relaxation rates as well as the cross-relaxation rate, based on the binary spin-bath model of MT (Henkelman et al., 1993; Morrison and Henkelman, 1995). Sled and Pike have recently extended these techniques to allow for quantitative, *in vivo* assessment of the observable parameters of the binary spin-bath model (Sled and Pike, 2000; Sled and Pike, 2001). Given the uncertainty in the interpretation of MTR decreases in MS, particularly the small decreases seen in NAWM, we set out to assess the relationship in NAWM between axonal injury as assessed by MRS and demyelination as assessed by quantitative MT imaging.

6.2 Manuscript 4

Presented at the 10th Annual Meeting of the International Society for Magnetic Resonance in Medicine.

Manuscript to be submitted.

Assessment of Axonal Injury and Demyelination in the Cerebral Normal-Appearing White Matter of Patients with Multiple Sclerosis

Sridar Narayanan, MSc, Simon J. Francis, BSc, John G. Sled, PhD, A. C. Santos, MD, Samson Antel, MSc, Ives Levesque, BSc, Steven Brass, MD, Yves Lapierre, MD, *Dominique Sappey-Marinier, PhD, G. Bruce Pike, PhD and *Douglas L. Arnold, MD

Department of Neurology and Neurosurgery,
Montreal Neurological Institute and Hospital,
Montreal, Quebec, Canada, (514) 398-8185,

and

*CERMEP, Hôpital Neurologique
Université Claude Bernard-Lyon1
Lyon, France

Reprint requests and correspondence to:

Dr. Douglas L. Arnold,
Montreal Neurological Institute,
3801 University Street, Montreal,
Quebec, Canada, H3A 2B4
Tel: (514) 398-8185
Fax: (514) 398-2975
E-mail: doug@mrs.mni.mcgill.ca

Running title: Axonal injury and demyelination in MS NAWM

Abstract

We assessed the normal-appearing white matter (NAWM) of MS patients with proton MRS and quantitative MT. NAA/Cr in NAWM was estimated by regression against WM fraction and extrapolation. The fractional size of the semi-solid pool (F) was obtained from the binary spin bath model of MT by computing the model parameters from multiple MT-weighted and relaxometry acquisitions. F in NAWM was significantly smaller in the patients [0.109 (0.009)] relative to controls [0.123 (0.007), p=0.011], but was not different between RR [0.1085] and SP [0.1087] patients [p>0.99]. NAA/Cr and F in the NAWM were not correlated (r=0.16, p > 0.7), mainly due to a lack of variation in F among patients. This may indicate a floor to the extent of myelin pathology that can occur in NAWM before a lesion appears, or that axonal damage is not strictly related to demyelination in NAWM. The correlation between NAA/Cr and T2w lesion volume did not reach significance (p > 0.1) in this small group. However, dividing the lesion volumes by the mean F in T2w lesions (weighting the lesion volumes by an index of lesion destructiveness) resulted in a quantity that correlated well with NAWM NAA/Cr (r = -0.78, p = 0.038), likely reflecting Wallerian degeneration in the NAWM associated with axonal transection within lesions.

Introduction

Multiple sclerosis (MS) is an inflammatory disease of the central nervous system (CNS) characterized by deficits referable to multiple lesions within the CNS disseminated in both space and time. While the primary target of the immunologic attack appears to be myelin / oligodendrocytes, secondary axonal damage also occurs and is likely the substrate for chronic, irreversible neurological impairment (Arnold et al., 2001; Bjartmar and Trapp, 2001; Trapp et al., 1998). The hallmark of MS on magnetic

resonance imaging (MRI) studies is the appearance of multiple regions of hyperintense signal on T2-weighted images (Miller et al., 1998).

In recent years, numerous magnetic resonance (MR) studies of the white matter that appears normal on conventional imaging (NAWM) have demonstrated abnormalities using more pathologically specific MR techniques. In particular, studies employing MR spectroscopy (MRS) have demonstrated low levels of N-acetylaspartate (NAA) in MS NAWM compared to healthy control white matter (WM), indicating loss of axonal density or axonal metabolic dysfunction extending far beyond visible lesions (Matthews and Arnold, 2001). Similarly, magnetization transfer imaging (MTI) experiments have repeatedly demonstrated low magnetization transfer ratios (MTR) in the cerebral NAWM of MS patients (Filippi, 2001). MTI generates contrast dependent upon the exchange of magnetization between semi-solid macromolecular hydrogen nuclei and free water protons, allowing semi-solids such as protein structures and cell membranes, whose relaxation times are too short to be imaged directly, to be indirectly probed (Edzes and Samulski, 1978; Wolff and Balaban, 1989). The MT effect is usually quantified by generating MT ratio images, which provide voxel by voxel maps of the percent decrease in signal caused by the MT prepulse used (Filippi and Grossman, 2002). In white matter, the MT effect appears to be mainly driven by exchange with constituents of myelin (Dousset et al., 1992; Kucharczyk et al., 1994), and so the prevailing view is that low MTR in MS NAWM indicates diffuse or distributed myelin pathology. However, MTR change can also be affected by non-specific changes in water content or physical state, and has been shown to be sensitive to inflammation (Gareau et al., 2000; Vavasour et al., 1998).

In order to overcome some of the limitations of the MTR measure, a more complete characterization of the MT phenomenon has been developed by Henkelman et al. (Henkelman et al., 1993; Morrison and Henkelman, 1995). This approach has been recently adapted and extended for human *in vivo* imaging studies (Sled and Pike, 2000; Sled and Pike, 2001). Using this new technique, it is now possible to produce parametric images of all the observable properties of the binary spin bath model for MT, namely, the fractional size of the restricted, or "bound water" pool, F, the magnetization exchange rate, the T2 of the restricted pool and the relaxation times in the free pool. The methodology has been termed "quantitative magnetization transfer imaging" or QMTI and is generating significant interest in the MRI-MS community, with other groups now implementing their own *in vivo* techniques (Dalton et al., 2002; Ropele et al., 2002). The fractional size of the restricted pool, F, quantifies the macromolecular content in each voxel. In white matter, F provides a putative index of myelination. In this report, we examine the relationship between these *in vivo* measures of axonal damage (NAA) and demyelination (F) in the cerebral NAWM of MS patients.

Methods

Subjects

Eight patients aged 24 to 57 years [38.8 (11.7) years, mean (standard deviation); range 24 to 57] with definite MS were selected from the Multiple Sclerosis Clinic of the Montreal Neurological Hospital. Four patients had relapsing-remitting (RR) MS and four had secondary-progressive (SP) disease. Patients underwent MR examination and concurrent clinical evaluation, and in a separate session, data for qMT analyses were acquired. Five healthy laboratory and hospital workers of similar mean age [40.8 (12.1), $p>0.8$; range 25 to 54] served as normal control subjects.

Proton MRI/MRSI of brain

MRSI examinations were performed using a 1.5T, Philips Gyroscan ACS II (Philips Medical Systems, Best, The Netherlands). PD/T2 images were obtained using a dual-echo turbo spin-echo sequence (TR/TE1/TE2=2075/32/90, 256×256, 1 signal average, 250mm FOV) yielding two sets of 50 contiguous 3mm slices parallel to the anterior-posterior commissural (AC-PC) line, followed by a matching T1w gradient recalled-echo sequence (TR/TE = 35/10 ms). These images were used to select a VOI for MRSI of approximately 90×90×20 mm3 centered on the body of the corpus callosum (Figure 6-1). MRSI data were acquired using a double spin-echo excitation method (TR 2000, TE 272ms, 32×32 phase-encodes, field of view 250×250mm, slab thickness 20mm), and post-processed as previously described (De Stefano et al., 2001). Metabolite resonance intensities were determined automatically from fitted peak areas and expressed relative to intra-voxel creatine (Cr).

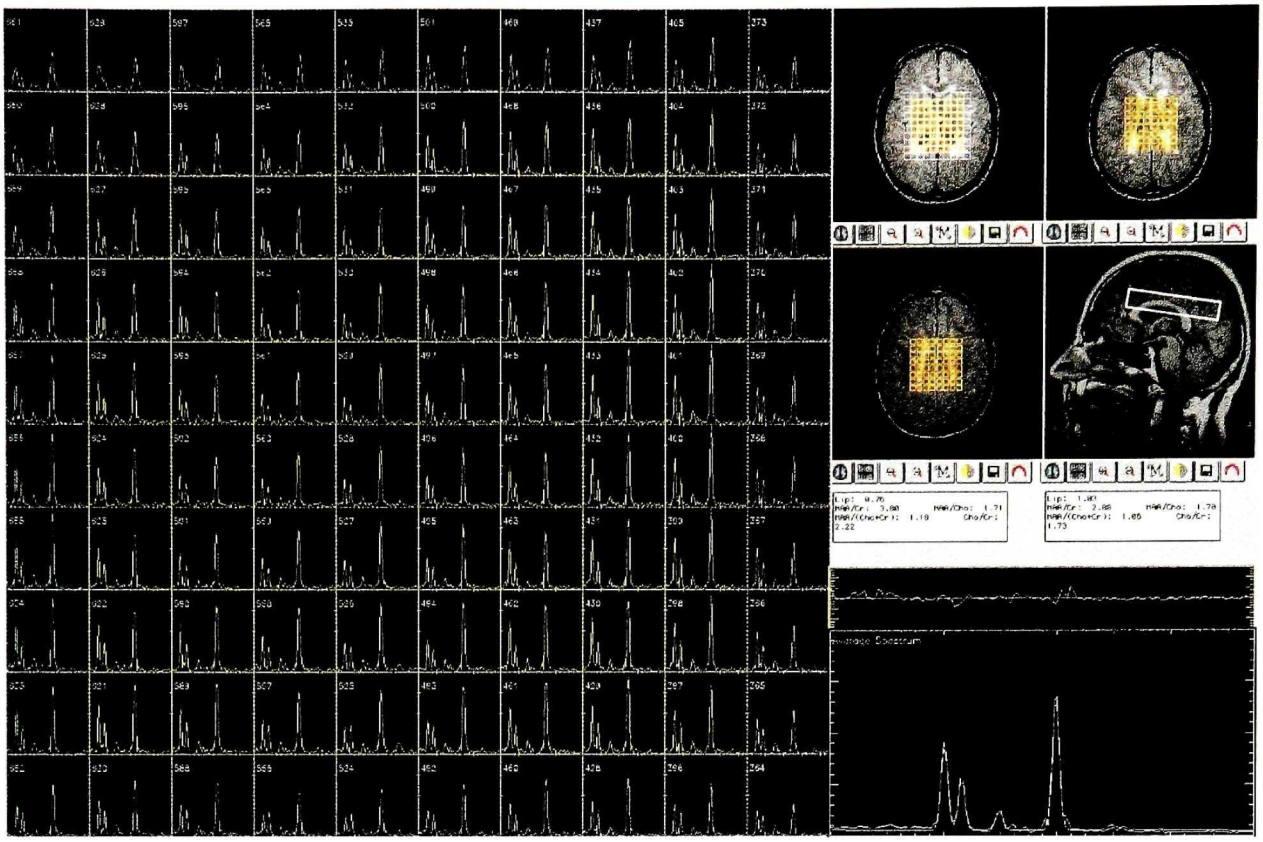

Figure 6-1: MRI images of a patient with multiple sclerosis illustrating the volume of interest (VOI) used for spectroscopic imaging (right), and the resulting spectra (left). Voxels at the edge of the VOI were omitted from analysis since they can show artifactual relative amplitudes.

MRI images were automatically segmented using a multispectral Bayesian technique and classified into WM/NAWM, grey matter (GM), cerebro-spinal fluid (CSF) and T2w lesion. Classified maps were verified and manually corrected where necessary.

Metabolite levels in NAWM were obtained via regression of the metabolite ratio in each MRSI voxel against the fraction of WM contributing to the signal in that voxel, computed using the classified tissue maps and weighted by the point-spread function (PSF) of the MRSI (Sappey-Marinier et al., 2001). For our acquisition and post-processing, the PSF was well represented by a 2D Gaussian with a full width at half-maximum (FWHM) of 12mm. For each nominal MRSI voxel, the tissue maps were multiplied by the PSF (centred on the centre of the voxel) to obtain the volume of each tissue type contributing to the signal in that voxel. Values in "pure" NAWM were

obtained by extrapolating the regression of metabolite ratio versus WM fraction to a WM fraction of 1 (Figure 6-2). To allow linear regression to provide a reasonable model of the change of metabolite ratio with partial volume, we excluded voxels with > 20% lesion content, so that GM and WM were the two tissues mainly present in the mixed voxels. Since NAA, Cho and Cr are not present in CSF in MR detectable quantities, the use of ratios to intravoxel Cr controlled for the presence of CSF in the voxels.

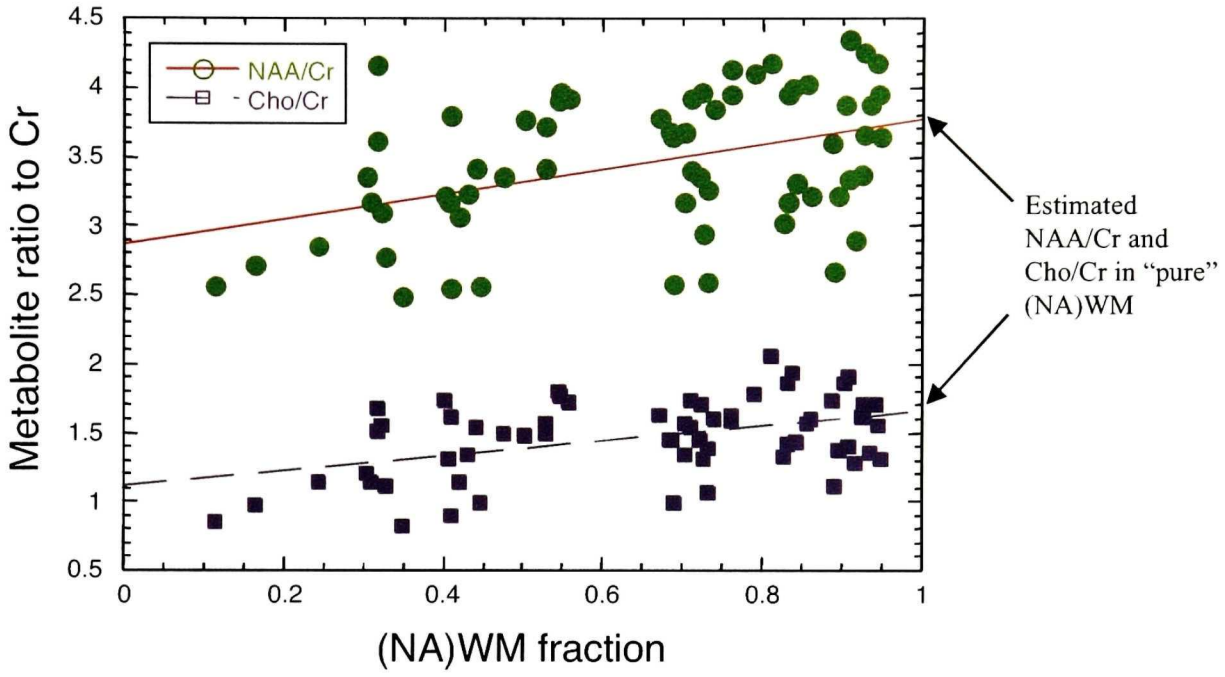

Figure 6-2: Example of the regression lines for NAA/Cr and Cho/Cr resonance intensity ratio versus WM fraction for all voxels containing < 20% lesion on T2w images. The metabolite ratio in "pure" WM or NAWM is the extrapolated intercept at a (NA)WM fraction = 1.

Quantitative MT imaging:

Conventional PD/T2 and T1 images were first acquired and used to plan the quantitative MT acquisitions on a 7mm oblique transverse slice at the level of the genu and splenium of the corpus callosum (Figure 6-3), using the protocol described in (Sled and Pike, 2001). Briefly, the protocol consisted of 60 variably weighted MT acquisitions, quantitative T2 and T1 sequences, and B0 and B1 field mapping. The modified binary

spin bath model was then fit to these data, and images of each of the model parameters were computed. A detailed description of the data acquisition and parameter estimation can be found in (Sled and Pike, 2001). For the present study, the fractional size of the restricted pool, F, is of particular interest since it reflects the macromolecular content in each voxel relative to water and is a putative measure of myelination in white matter.

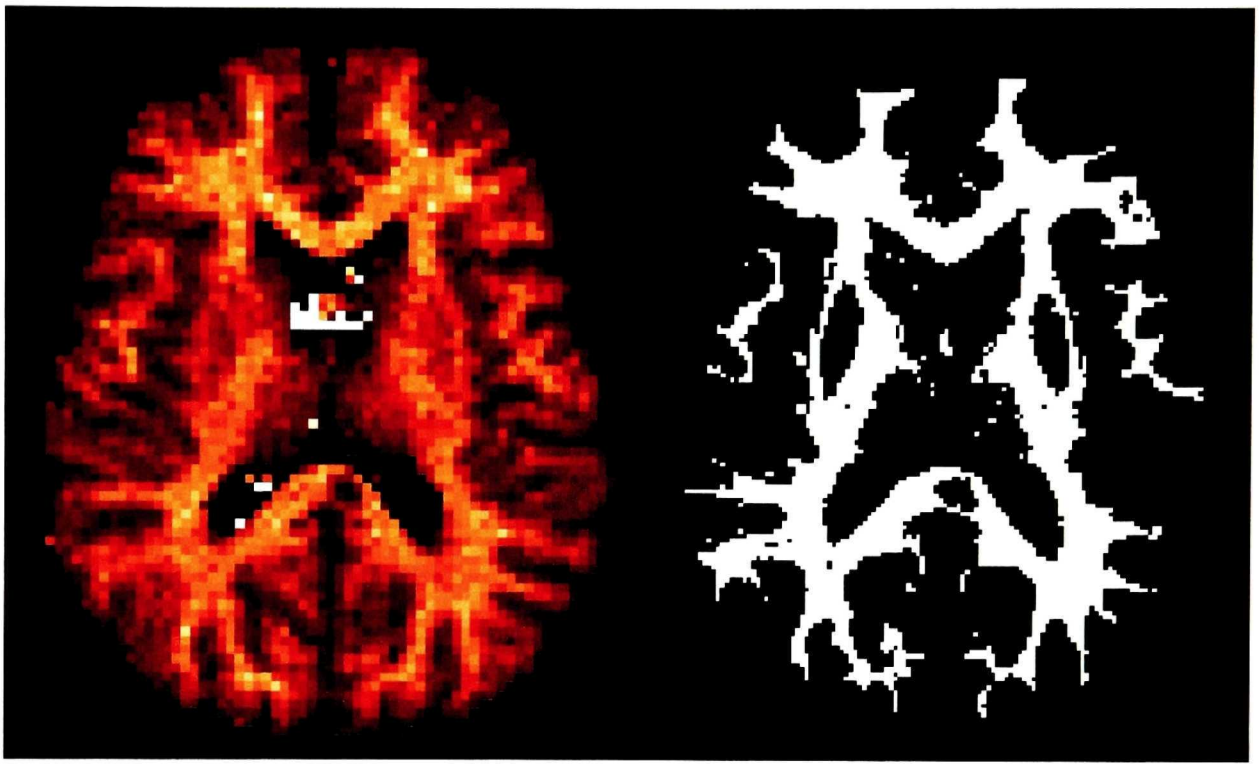

Figure 6-3: (*left*) Map of the fractional size of the restricted water pool, F, obtained in a 7mm thick transverse slice at the level of the genu and splenium of the corpus callosum. (*right*) Map of WM tissue fraction, thresholded to display only voxels containing > 80% WM.

The conventional MRI images were segmented as above. To minimize partial volume effects in the qMT maps, we computed the fraction of each tissue class within the qMT voxels and thresholded these maps to create masks of relatively "pure" voxels (defined as containing > 80% of a specific tissue) (Figure 6-3). The masks were applied to the model parameter maps to obtain mean values for each tissue class.

Statistics

We assessed group differences using analysis of variance (ANOVA) followed by Tukey's post-hoc testing. Relationships between metabolite levels and MT model parameters were assessed using Pearson correlation.

Results

Group Differences:

The fractional size of the restricted pool in NAWM (F-NAWM) was significantly smaller in the patients [0.109 (0.009)] relative to controls [0.123 (0.007), p=0.011], but was not different between RR [0.1085] and SP [0.1087] patients [p>0.99]. Mean F within T2w lesions [0.031 (0.01)] was significantly lower than mean F in NAWM (p<0.001).

The decrease of NAWM NAA/Cr of the patients [2.88 (0.4), mean (standard deviation)] relative to controls [3.23 (0.27)] did not reach significance in this small group [p=0.11].

Correlations

The results of the correlative analysis appear in Table 6-1. No significant correlations were found between any of the quantities of interest. In fact, NAA/Cr and F appeared completely uncoupled in NAWM. There were trends for a relationship between NAWM NAA/Cr and T2wLV and between NAWM F and T2wLV, which may have achieved significance in a larger group. The lack of correlation between NAA/Cr and Cho/Cr in NAWM ($p > 0.5$) made it unlikely that changes in Cr were responsible for the observed variation of NAA/Cr, since that would entail concomitant changes in the Cho/Cr ratio and hence at least some correlation between the two ratios.

	Cho/Cr	T2w LV	F-NAWM	F-Lesion
NAA/Cr	r = –0.27 p > 0.5	r = –0.67 p > 0.1	r = 0.16 p > 0.7	r = 0.42 p > 0.3
Cho/Cr		r = -0.09 p > 0.8	r = 0.50 p > 0.2	r = 0.54 p > 0.2
T2w LV			r = –0.60 p > 0.1	r = –0.27 p > 0.6
F-NAWM				r = 0.67 p > 0.1

Table 6-1: Pair-wise Pearson correlation coefficient (r) and associated measure of significance (p) for the extrapolated NAA/Cr in NAWM, the extrapolated Cho/Cr in NAWM, total T2w LV, the mean F in NAWM and the mean F in T2w lesions.

We hypothesized whether a potential surrogate for the total lesion-associated burden of disease might be obtained by dividing the total lesion volume by the mean F in T2w lesion, thereby weighting the lesion volumes by a measure of the extent of demyelination within lesions. This "demyelination-weighted lesion volume" (DWLV) correlated strongly with NAA/Cr in NAWM [r = –0.78, p=0.038] (Figure 6-4).

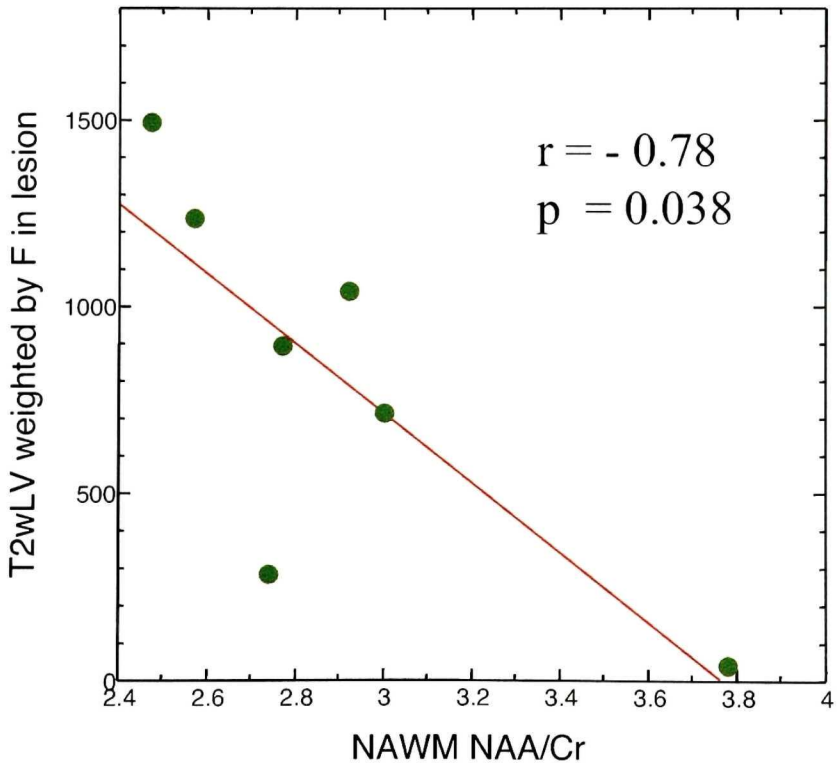

Figure 6-4: Correlation of "demyelination-weighted lesion volume" or DWLV (total T2w LV divided by mean F in lesion) with NAA/Cr in the NAWM.

Discussion

The fractional size of the restricted water pool, F, was found to be low in MS NAWM compared to healthy control WM. This result concurs with the widely reported findings of abnormal MTR in the NAWM of patients with established MS [see (Rovaris et al., 2001) for a review]. The magnitude of the decrease in F was small, but the low variance of the measure across subjects in both the control and MS groups led to the difference being significant. The small variation of F in NAWM across MS patients could indicate that there is a limit to the degree of disturbance of myelin integrity that can occur in NAWM before a lesion appears. This notion is supported by the previously reported progressive decline of MTR (Filippi et al., 1998; Goodkin et al., 1998; Pike et al., 2000) and apparent diffusion coefficient (Werring et al., 2000) as well as the increase of choline resonance intensity (Tartaglia et al., 2002]) in regions of NAWM that subsequently became lesions on follow-up. As to whether focal reductions in NAWM F precede lesion formation, this will be addressed in a future longitudinal study. As expected, mean lesion F in the current patient group was lower and more variable (range 0.01 – 0.05) than mean NAWM F (range 0.095 – 0.123). It may be that one mechanism of lesion formation is an inflammatory reaction to accumulated myelin damage in the NAWM effected by more subtle means, for example, by cytokines diffusing away from sites of existing lesions, or possibly by an increase of blood-brain barrier permeability throughout the NAWM (Silver et al., 1999). Local blood-brain barrier breakdown and large-scale infiltration of inflammatory cells may not always be the initiating events in lesion formation.

We did not find a correlation in MS NAWM between F, a putative index of myelination, and NAA/Cr, a marker of axonal integrity. In fact, F and NAA/Cr in the NAWM appeared to be uncoupled to such an extent ($r = 0.16$, $p > 0.7$), that if a

relationship existed (and were perhaps demonstrable in a much larger group of patients), it would likely be extremely weak. The lack of correlation between NAWM F and NAA/Cr may be simply the result of the lack of variation of F in NAWM discussed above. Given that there was a reasonable spread of NAA/Cr values in the patients (2.47-3.78), it also suggests that axonal injury or dysfunction in the NAWM may not strictly be secondary to the extent of demyelination within the NAWM itself. The good correlation between NAWM NAA/Cr and DWLV (T2wLV weighted by the mean F in lesion) likely indicates that a sizable portion of the NAA/Cr decrease in NAWM was due to Wallerian degeneration of axons transected within lesions. Greater numbers of axons per unit volume of lesion would be transected in the more destructive lesions, leading to greater associated Wallerian degeneration in the NAWM and hence an additional lowering of NAA/Cr. Since the time lag between degeneration of axons and the subsequent degradation of their myelin sheathes is likely non-trivial (Griffin et al., 1992; Simon et al., 2000), the contribution of this process to the *concurrent* relationship between F and NAA/Cr within the NAWM should be small. Conversely, given that decreases of NAA/Cr reflect axonal metabolic dysfunction as well as axonal loss, and that disturbances of axonal metabolism in the NAWM may be mediated by soluble factors diffusing though the brain (Silber and Sharief, 1999), it is possible for axonal injury to occur in NAWM without concurrent extra-lesional demyelination.

Conclusions

Quantitative MT imaging is a promising new technique that enables us to better characterize the MT effect *in vivo*. The fractional size of the semi-solid pool, F, is a putative marker of myelination in white matter, while NAA/Cr provides an index of

axonal integrity. In this study, we found no correlation between axonal damage and demyelination in the NAWM. Although preliminary, this suggests that the NAWM may be able to sustain only a limited degree of myelin pathology before a lesion appears (removing those voxels from being considered as NAWM). It also suggests that axonal damage may not strictly be secondary to local, concurrent demyelination. The good correlation between NAWM NAA/Cr and lesion volume weighted by lesion F likely reflects Wallerian degeneration of axons transected within lesions. Weighting T2w lesion volume by the associated myelin pathology (as reflected by F), may provide an improved metric for the burden of disease in MS.

References

1. Arnold DL, Narayanan S, De Stefano N, Reddy H, Matthews PM. Magnetic resonance spectroscopy of multiple sclerosis: Imaging axonal damage. In: Kappos L, Kesselring J, Radu EW and Johnson K, editors. Multiple Sclerosis: Understanding Tissue Destruction and Repair and New Immunological Treatments. London: Martin Duntz Ltd, 2001: 77-90.
2. Bjartmar C, Trapp BD. Axonal and neuronal degeneration in multiple sclerosis: mechanisms and functional consequences. Curr Opin Neurol 2001; 14: 271-8.
3. Dalton CM, Ramani A, Wheeler-Kingshott CA, Barker GJ, Miller DH, Tofts PS. Bound water magnetization transfer measurements in patients with multiple sclerosis: a pilot study. ISMRM. Honolulu, HI, 2002.
4. De Stefano N, Narayanan S, Francis GS, Arnaoutelis R, Tartaglia MC, Antel JP, et al. Evidence of axonal damage in the early stages of multiple sclerosis and its relevance to disability. Arch Neurol 2001; 58: 65-70.
5. Dousset V, Grossman RI, Ramer KN, Schnall MD, Young LH, Gonzalez-Scarano F, et al. Experimental allergic encephalomyelitis and multiple sclerosis: lesion characterization with magnetization transfer imaging [published erratum appears in Radiology 1992 Jun;183(3):878]. Radiology 1992; 182: 483-91.

6. Edzes HT, Samulski ET. The measurement of cross-relaxation effects in the proton NMR spin-lattice relaxation of water in biological systems:hydrated collagen and muscle. Journal of Magnetic Resonance 1978; 31: 207-29.
7. Filippi M. Linking structural, metabolic and functional changes in multiple sclerosis. Eur J Neurol 2001; 8: 291-7.
8. Filippi M, Grossman RI. MRI techniques to monitor MS evolution: the present and the future. Neurology 2002; 58: 1147-53.
9. Filippi M, Rocca MA, Martino G, Horsfield MA, Comi G. Magnetization transfer changes in the normal appearing white matter precede the appearance of enhancing lesions in patients with multiple sclerosis. Ann Neurol 1998; 43: 809-14.
10. Gareau PJ, Rutt BK, Karlik SJ, Mitchell JR. Magnetization transfer and multicomponent T2 relaxation measurements with histopathologic correlation in an experimental model of MS. J Magn Reson Imaging 2000; 11: 586-595.
11. Goodkin DE, Rooney WD, Sloan R, Bacchetti P, Gee L, Vermathen M, et al. A serial study of new MS lesions and the white matter from which they arise. Neurology 1998; 51: 1689-97.
12. Griffin JW, George R, Lobato C, Tyor WR, Yan LC, Glass JD. Macrophage responses and myelin clearance during Wallerian degeneration: relevance to immune-mediated demyelination. J Neuroimmunol 1992; 40: 153-65.
13. Henkelman RM, Huang X, Xiang QS, Stanisz GJ, Swanson SD, Bronskill MJ. Quantitative interpretation of magnetization transfer. Magn Reson Med 1993; 29: 759-66.
14. Kucharczyk W, Macdonald PM, Stanisz GJ, Henkelman RM. Relaxivity and magnetization transfer of white matter lipids at MR imaging: importance of cerebrosides and pH. Radiology 1994; 192: 521-9.
15. Matthews PM, Arnold DL. Magnetic resonance imaging of multiple sclerosis: new insights linking pathology to clinical evolution. Curr Opin Neurol 2001; 14: 279-87.
16. Miller DH, Grossman RI, Reingold SC, McFarland HF. The role of magnetic resonance techniques in understanding and managing multiple sclerosis. Brain 1998; 121: 3-24.

17. Morrison C, Henkelman RM. A model for magnetization transfer in tissues. Magn Reson Med 1995; 33: 475-82.

18. Pike GB, De Stefano N, Narayanan S, Worsley KJ, Pelletier D, Francis GS, et al. Multiple sclerosis: magnetization transfer MR imaging of white matter before lesion appearance on T2-weighted images. Radiology 2000; 215: 824-30.

19. Ropele S, Strasser-Fuchs S, Seifert T, Enzinger C, Fazekas F. Development of active multiple sclerosis lesions: a quantitative MT study. ISMRM. Honolulu, HI, 2002.

20. Rovaris M, Comi G, Filippi M. The role of non-conventional MR techniques to study multiple sclerosis patients. J Neurol Sci 2001; 186 Suppl 1: S3-9.

21. Sappey-Marinier D, Antel SB, Tartaglia CM, Narayanan S, Francis S, Arbel T, et al. Quantification métabolique dans la sclérose en plaques par imagerie spectroscopique RMN. Journée Neurologique Francaise. Lyons, 2001.

22. Silber E, Sharief MK. Axonal degeneration in the pathogenesis of multiple sclerosis. J Neurol Sci 1999; 170: 11-8.

23. Silver NC, Tofts PS, Symms MR, Barker GJ, Thompson AJ, Miller DH. Evidence of widespread subtle blood-brain barrier dysfunction associated with progressive MS. Proc Soc Magn Reson Med 1999; 1: 628.

24. Simon JH, Kinkel RP, Jacobs L, Bub L, Simonian N. A Wallerian degeneration pattern in patients at risk for MS. Neurology 2000; 54: 1155-60.

25. Sled JG, Pike GB. Quantitative interpretation of magnetization transfer in spoiled gradient echo MRI sequences. J Magn Reson 2000; 145: 24-36.

26. Sled JG, Pike GB. Quantitative imaging of magnetization transfer exchange and relaxation properties in vivo using MRI. Magn Reson Med 2001; 46: 923-31.

27. Tartaglia MC, Narayanan S, DeStefano N, Arnaoutelis R, Antel SB, Francis SJ, et al. Choline is increased in prelesional normal-appearing white matter in Multiple Sclerosis. J Neurology 2002; In Press.

28. Trapp BD, Peterson J, Ransohoff RM, Rudick R, Mork S, Bo L. Axonal transection in the lesions of multiple sclerosis [see comments]. N Engl J Med 1998; 338: 278-85.

29. Vavasour IM, Whittall KP, MacKay AL, Li DK, Vorobeychik G, Paty DW. A comparison between magnetization transfer ratios and myelin water percentages in normals and multiple sclerosis patients. Magn Reson Med 1998; 40: 763-8.

30. Werring DJ, Brassat D, Droogan AG, Clark CA, Symms MR, Barker GJ, et al. The pathogenesis of lesions and normal-appearing white matter changes in multiple sclerosis: a serial diffusion MRI study. Brain 2000; 123: 1667-76.

31. Wolff SD, Balaban RS. Magnetization transfer contrast (MTC) and tissue water proton relaxation in vivo. Magn Reson Med 1989; 10: 135-44.

Chapter 7

The need to use different tools to understand progression at different stages of disease

7.1 Preface

The data presented in the preceding chapters and the relevant literature cited within have highlighted the importance of axonal injury to the development of chronic disability in MS. While early axonal injury can be compensated for almost completely by adaptive mechanisms (Chapter 5), once disability becomes evident, cerebral NAA levels have shown good correlations with clinical status both in acute and chronic MS (Davie et al., 1995; Davie et al., 1999; De Stefano et al., 1995a; De Stefano et al., 1998; Fu et al., 1998; Lee et al., 2000b). In particular, chronic disability as measured by the EDSS is strongly correlated to levels of NAA in central brain NAWM (De Stefano et al., 1998; Fu et al., 1998; Sarchielli et al., 1999; Tourbah et al., 1999). This region of the brain is rich in long axons, containing crossing fibres of the corpus callosum and descending motor tracts. We have detected NAA decreases remote from the site of focal injury (De Stefano et al., 1999), suggesting that central brain NAA can be sensitive to axonal injury in a

substantially larger volume of brain than that directly sampled. However, the correlation between EDSS and central brain NAA is substantially stronger in patients with RR versus SP MS (De Stefano et al., 1998; Fu et al., 1998). We sought to better characterize the extent of axonal damage and its relationship to disability as a function of disease stage (more finely graded than RR vs. SP), and to assess whether axonal injury was evident early in MS. This issue is addressed in the manuscript, "Evidence of axonal damage in the early stages of multiple sclerosis and its relevance to disability." We found that NAA decreases began and were relevant to disability from the early stages of MS. In the later stages of MS, NAA loss appeared to decelerate and no longer correlated with disability.

NAA measured within a volume of brain tissue is essentially a measure of the *density* of NAA (and, by extension, the functional density of axons and neurons), so a possible explanation for these results is that progressive MS is associated with a greater degree of atrophy than RRMS, which serves to mitigate the decline of NAA density in SP patients. Spinal cord atrophy has been shown to correlate well with disability (Losseff and Miller, 1998; Losseff et al., 1996b; Stevenson et al., 1998), and so we explored the relationships of brain axonal injury and spinal cord atrophy to disability at varying disease stages in Manuscript 6, "Disease duration influences the relationship between brain axonal injury, spinal cord atrophy and disability in multiple sclerosis."

Finally, although the data presented in Manuscripts 5 and 6 support the existence and importance of early axonal damage, the mechanisms of early axonal damage in NAWM require further elucidation. Axonal damage can occur as a bystander effect secondary to inflammatory demyelination, as demonstrated by the fact that transected axons can be found in lesions of varying activity, and the number of transected axons appears to be related to the degree of inflammation (Trapp et al., 1998). Wallerian

degeneration of axons transected within lesions would then contribute to the diffuse axonal damage found in NAWM. However, this is not necessarily the only mechanism contributing to diffuse axonal damage. To further explore this question, we applied *in vivo* MRS, MTR and brain volume measurement techniques to assess diffuse axonal damage, myelin pathology and tissue loss in the brains of non-disabled MS patients with low cerebral lesion volume. The results of this work is described in Manuscript 7, "Diffuse axonal and tissue injury in patients with multiple sclerosis with low cerebral lesion load and no disability." We found that diffuse axonal injury and myelin pathology were present even in MS patients with no disability and trivial lesion loads, suggesting that, to some degree, diffuse axonal injury and tissue destruction occur independently of focal demyelination in the white matter. This diffuse pathology may be due to widespread but subtle inflammation or to invisible grey matter pathology and wallerian degeneration from grey matter lesions (Peterson et al., 2001). Cortical adaptations are likely responsible for maintaining the favourable clinical status of these patients.

7.2 Manuscript 5

Published in Archives of Neurology 2001;58(1):65-70

Evidence of Axonal Damage in the Early Stages of Multiple Sclerosis and its Relevance to Disability

Nicola De Stefano*^, MD; Sridar Narayanan*, MSc; Gordon S. Francis*, MD; Rozie Arnaoutelis*, BSc; Maria C. Tartaglia*, BSc; Jack P. Antel*, MD; Paul M. Matthews*#, MD; Douglas L. Arnold*, MD

*Department of Neurology and Neurosurgery, Montreal Neurological Institute and Hospital, Montreal, Canada
^Institute of Neurological Sciences & NMR Centre, University of Siena, Siena, Italy
#Centre for Functional Magnetic Resonance Imaging of the Brain, Deptartment of Clinical Neurology, University of Oxford, Oxford, England

Reprint requests and correspondence to:
Dr. Nicola De Stefano
Institute of Neurological Science
Viale Bracci 2
53100, Siena, Italy
Tel: +39-0577-233432
Fax: +39-0577-40327
Email: destefano@unisi.it

Running title: Early axonal damage in MS

Key words: axons, axonal damage, magnetic resonance spectroscopy, multiple sclerosis, N-Acetylaspartate

Acknowledgements
The study was supported by grants from the Multiple Sclerosis Society of Canada and the Medical Research Council of Canada, and a pilot grant from the National Multiple Sclerosis Society. N.D.S. was supported in part by a grant from the Progetto Sclerosi Multipla, Istituto Superiore di Sanita', Roma. PMM acknowledges support from the Medical Research Council (UK) and the Multiple Sclerosis Society of Great Britain and Northern Ireland.

Abstract

Objective: To assess axonal damage and its contribution to disability at different stages of multiple sclerosis (MS).

Background: Recent *in vivo* imaging and *in situ* pathologic studies have demonstrated that substantial axonal damage accompanies the inflammatory lesions of MS. However, the relationship of axonal damage to the duration of MS and its contribution to disability at different stages of the disease remain poorly defined.

Design: We performed proton magnetic resonance spectroscopic imaging in 88 patients with a wide range of clinical disability and disease duration to measure N-acetylaspartate (NAA, an index of axonal integrity) relative to creatine (Cr) in a large central brain volume that included mostly normal-appearing white matter on magnetic resonance imaging.

Results: We observed that the NAA/Cr values were abnormally low in the early stages of MS, even before significant disability (measured using the Expanded Disability Status Scale [EDSS]) was evident clinically, and declined more rapidly with respect to EDSS at lower than at higher levels of EDSS ($p<0.001$). The correlation of NAA/Cr with EDSS was significantly ($p<0.03$) stronger in patients with mild disability (EDSS <5, Spearman rank order correlation = –0.54, $p< 0.001$) than in patients with more severe disability (EDSS ≥5, Spearman rank order correlation = -0.1, p<0.9). When similar analyses were performed in patients with MS grouped for duration of disease, the subgroup with early disease duration (<5 years) also showed central brain NAA/Cr resonance intensity ratios significantly lower than normal controls ($p<0.0001$).

Conclusion: Cerebral axonal damage begins and contributes to disability from the earliest stages of the disease.

Introduction

The importance of axonal injury in multiple sclerosis (MS) is being increasingly appreciated (Matthews et al., 1998; McDonald, 1994; Trapp et al., 1999b; Waxman, 2000b). Neuropathologic techniques have demonstrated that sparing of axons is only relative in MS (Ferguson et al., 1997; Trapp et al., 1998). Pathologic evidence of injured or transected axons is common in active MS lesions, and chronic lesions show clear evidence of axonal injury (Silber and Sharief, 1999; Trapp et al., 1998). Although there is increasing agreement that axonal loss is a major factor contributing to disability in the later stages of MS (Barnes et al., 1991; Scolding and Franklin, 1998; Silber and Sharief, 1999), the relation of axonal damage to disability in the early stages of MS is less clear.

Magnetic resonance spectroscopy (MRS) is particularly useful for the study of axonal damage because it allows *in vivo* assessment of axonal dysfunction or loss based on the signal intensity of *N*-acetylaspartate (NAA), the main component of the peak dominating the normal proton spectrum, which is localized almost exclusively in neurons and axons in mature human brains (Birken and Oldendorf, 1989; Simmons et al., 1991). Large decreases of NAA not restricted to brain lesions were observed in the earliest proton MRS studies of patients with well established MS (Arnold et al., 1990a) and have been confirmed in many subsequent reports (for review see Matthews et al (Matthews et al., 1998)). Spectroscopic studies also have demonstrated a strong relation between changes in NAA and clinical disability both in acute and chronic MS (Davie et al., 1995; Davie et al., 1999; De Stefano et al., 1995a; De Stefano et al., 1998; Fu et al., 1998; Lee et al., 2000b). Interestingly, in these studies, it was NAA in normal-appearing white matter that correlated best with disability.

Generalization from data reported so far, however, has been limited by the small numbers of patients and the restricted disability range studied. Therefore, we performed proton magnetic resonance spectroscopic imaging (MRSI) examinations and concurrent clinical evaluations in a relatively large group of patients with MS with a wide range of clinical disability and disease duration. We then assessed the levels of NAA relative to creatine (Cr) in different patient subgroups and examined the relevance of axonal injury to disability in initial vs later stages of MS.

Patients and Methods

Study Population

Eighty-eight patients with clinically definite MS (Poser et al., 1983) (48 women and 40 men; age range, 25-58 years) were chosen from the population followed in the Montreal Neurological Hospital MS clinic. Patients were classified according to clinical course as having either recurrent relapses (RR) with complete or partial remission (n=55; 32 women and 23 men) or secondary progressive (SP) disease with progression in the absence of discrete relapses after earlier relapsing-remitting disease (n=33; 16 women and 17 men). Patients were entered into the study only if they had been free from attacks in the previous month to study a clinically relatively stable MS population and reduce the potential confound of reversible NAA and Cr changes occurring after acute relapses (De Stefano et al., 1995a). Patients were stratified across a wide range of disability (Expanded Disability Status Scale [EDSS] score (Kurtzke, 1983); range, 0-9) and disease duration (range, 0.5-33 years). The whole patient group could therefore be subdivided into smaller subgroups according to either their EDSS score or their disease duration (Table 7-1). The Montreal Neurological Hospital Ethics Committee approved the study, and informed consent was obtained from all participating subjects.

Patients	No.	NAA/Cr Mean ± SD
Whole MS group	88	2.71 ± 0.31*
RR	55	2.77 ± 0.33*
SP	33	2.61 ± 0.25*
DD < 5y	21 (20 RR, 1 SP)	2.73 ± 0.35*
DD 5-10y	21 (18 RR, 3 SP)	2.79 ± 0.33*
DD 10-15y	22 (11 RR, 11 SP)	2.73 ± 0.26*
DD > 15	24 (6 RR, 18 SP)	2.60 ± 0.29*
EDSS 0-1	17 (17 RR, 0 SP)	3.01 ± 0.31
EDSS 2-3	19 (18 RR, 1 SP)	2.84 ± 0.20*
EDSS 4-5	20 (12 RR 8 SP)	2.58 ± 0.28*
EDSS 6-7	25 (8 RR, 17 SP)	2.59 ± 0.23*
EDSS 8-9	7 (0 RR, 7 SP)	2.45 ± 0.28*
Normal Controls	17	3.2 ± 0.24

Table 7-1: N-acetylaspartate-creatine (NAA/Cr) values relative to the whole group of patients with multiple sclerosis (MS) and different subgroups. *RR* indicates relapsing remitting; *SP*, secondary progressive; and *EDSS*, Expanded Disability Status Scale. *$p<.001$ compared with healthy controls.

Proton MRI and MRSI of brain

Combined proton MRI and MRSI examinations of the brain were obtained in a single session for each examination using a scanner operating at 1.5 T (Philips Gyroscan; Philips Medical Systems, Best, the Netherlands). A transverse dual-echo, turbo spin-echo sequence (repetition time [TR], 2075 milliseconds; echo time [TE] 1, 32 milliseconds; TE2, 90 milliseconds, 256x256 matrix, 1 signal average, 250-mm field of view), yielding proton density-weighted and T2-weighted images with 50 contiguous 3-mm slices, was acquired parallel to the line connecting the anterior and posterior commissures. These MRIs were used to select an intracranial volume of interest (VOI) for spectroscopy measuring approximately 100 mm anteroposteriorly by 20 mm craniocaudally by 90 mm

left to right (Figure 7-1). This was centered on the corpus callosum to include mostly white matter and some mesial cortex of both hemispheres. Although the VOI used in this study comprised only a limited portion of the whole brain, this included regions where axonal projections converge after traversing large brain volumes. Thus, NAA/Cr measures from this deep central brain region should reflect axonal status in a fairly large volume of brain beyond that contained within the spectroscopic VOI. Two-dimensional spectroscopic images were obtained using a 90°, 180°, 180° pulse sequence (TR, 2000 milliseconds; TE, 272 milliseconds; 250-mm field of view; 32x32 phase-encoding steps; 1 signal average per step) as previously described (De Stefano et al., 1995b). Magnetic field homogeneity was optimized to a line width of about 5 Hz over the VOI using the proton signal from water. Water suppression was achieved by placing frequency-selective excitation pulses at the beginning of the MRSI sequence (Haase et al., 1985). Before the water-suppressed acquisition, another MRSI was acquired without water suppression (TR, 850 milliseconds; TE, 272 milliseconds; 250-mm field of view; and 16x16 phase-encoding steps) to allow for B_0 homogeneity correction.

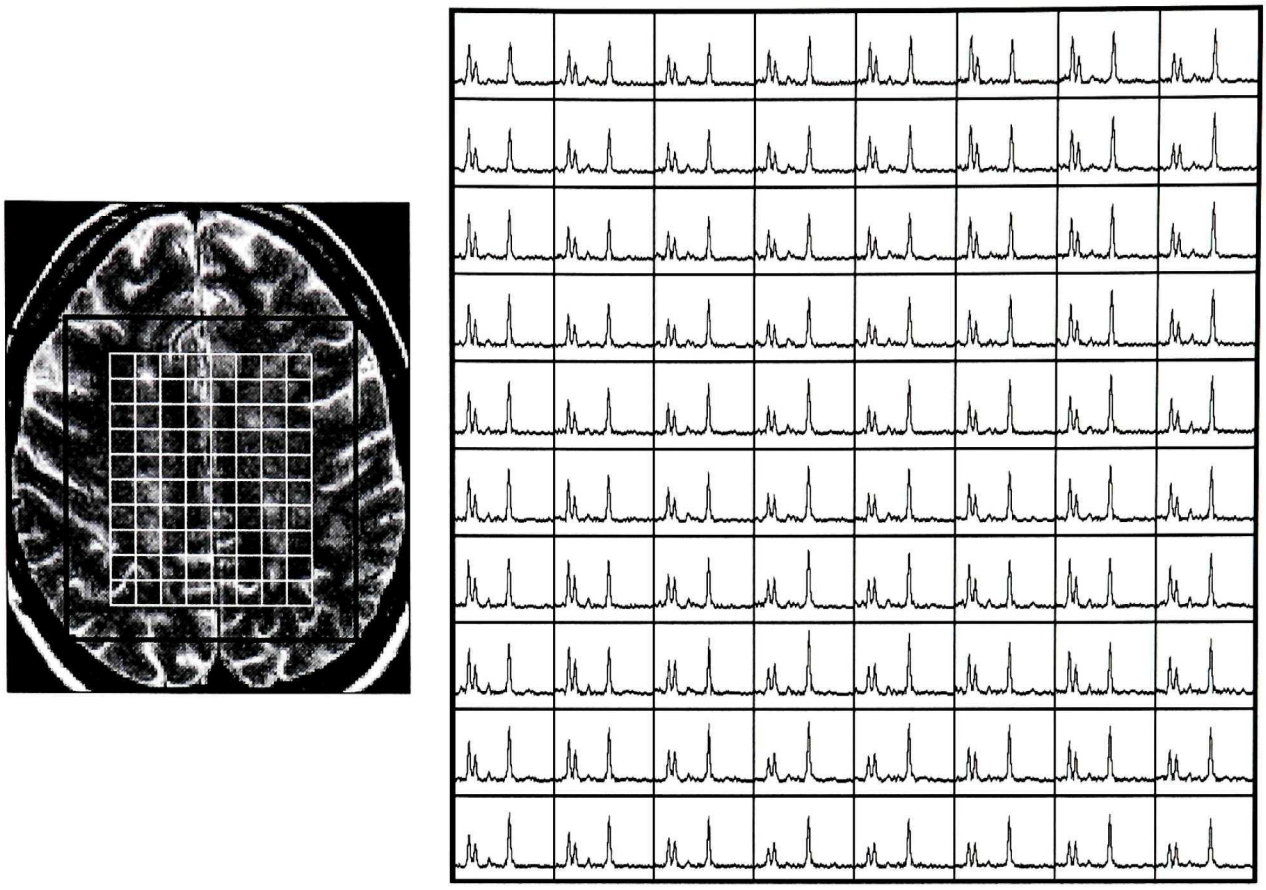

Figure 7-1: Conventional T2-weighted magnetic resonance imaging (MRI) scan of a patient with multiple sclerosis illustrating the volume of interest (VOI, black box inside the MRI) used for spectroscopy (left) and a set of proton spectra corresponding to the brain voxels (right). Voxels at the edges of the VOI were not used because they can show artifactual relative amplitudes. In the remaining voxels (white boxes inside the MRI), N-acetylaspartate (NAA) values were normalized to intravoxel creatine (Cr) to correct for magnetic resonance inhomogeneities through the VOI. The NAA/Cr values of the whole brain region were obtained by averaging NAA/Cr values for all the voxels in the spectroscopic VOI for each subject.

Proton MRSI data analysis

Postprocessing of the raw MRSI data included zero filling the non–water-suppressed MRSI to obtain 32x32 profiles, followed by a mild gaussian k-space filter and an inverse 2-dimensional Fourier transformation to both the water suppressed and unsuppressed MRSI. Artifacts present in the time domain water-suppressed signal due to static magnetic field inhomogeneities and time-varying gradients were corrected by dividing the water-suppressed MRSI signal by the non–water-suppressed signal (den Hollander et al., 1991), a procedure that does not affect relative signal intensities. The

residual water signal was then fitted and removed from the water-suppressed data using the Hankel singular-value decomposition procedure (de Beer et al., 1992). To enhance the resolution of the spectral peaks, a lorentzian-to-gaussian transformation was applied before Fourier transformation in the spectral domain. The nominal voxel size was 8x8x20 mm, giving a resolution of about 12x12x20 mm after k-space filtering. Metabolite resonance intensities of NAA and Cr were determined automatically from peak areas relative to a spline-corrected baseline. Results were expressed as the intravoxel ratio of NAA to Cr (a signal arising mainly from both Cr and phosphocreatine). In vitro MRS analysis of MS brains has demonstrated that Cr does not change in normal appearing tissue (Davies et al., 1995). In the present study, we refer to Cr in the normal-appearing white matter rather than in the lesions, because in the large central VOIs examined, lesions accounted for only about 6% of the VOI in the whole group of patients (range, 0.5%-25%; data not shown).

In our analysis, the relative NAA/Cr values of the whole brain region were obtained by averaging the NAA/Cr values for all the voxels in the spectroscopic VOI for each subject. Spectra at the edges of the VOI can be affected by chemical shift artifacts associated with selective excitation and were deleted before averaging (Figure 7-1). The average NAA/Cr values of the MS patient group were compared with those of a group of healthy adult controls (n=17; age range, 24-56 years) using the nonparametric Kruskal-Wallis test of variance. Central brain NAA/Cr values of the different patient subgroups were compared using analysis of variance followed by pairwise post hoc comparison using the Tukey honestly significant difference procedure to account for multiple comparisons. Values of NAA/Cr of the whole MS patient group and the different subgroups were then correlated with their corresponding EDSS scores using the

nonparametric Spearman rank order correlation (SROC). Data were considered significant at the .05 level.

Results

In the 88 patients with MS studied, the central brain NAA/Cr ratio was significantly lower than in healthy controls (mean±SD NAA/Cr ratio, 2.71±0.31 and 3.20±0.24, respectively; $p < .001$) (Table 7-1) and was inversely correlated with disability (SROC= –0.55, $p < .001$). In this group of patients with MS, age did not correlate with NAA/Cr levels (SROC=0.04, $p > .6$), and there were no differences in NAA/Cr values between men and women (mean±SD NAA/Cr ratio=2.71±0.33 for men with MS and 2.71±0.29 for women with MS).

Analyses of subgroups based on clinical course, disability level, and duration of disease were performed. Both the RR and SP subgroups exhibited significantly lower NAA/Cr ratios than healthy controls (mean±SD NAA/Cr ratio=2.77±0.33 in patients with RR MS and 2.61±0.25 in patients with SP MS; $p < .001$ for both groups). Central brain NAA/Cr ratio was significantly lower in patients with SP MS than in those with RR MS ($p = .05$). As in previous studies (De Stefano et al., 1998; Fu et al., 1998), the correlation between decreasing NAA/Cr resonance intensity ratios and increasing EDSS scores was stronger in patients with RR MS than in those with SP MS (SROC=-0.64 in RR MS patients, $p < .001$; SROC= -0.28 in SP MS patients, $p < .1$).

When a subgroup of MS patients with milder disability (EDSS score<5, n=50) was considered alone, central brain NAA/Cr resonance intensity ratios were still significantly lower than healthy controls (mean±SD NAA/Cr ratio=2.83±0.28; $p < .001$). Further dividing this patient subgroup into smaller EDSS groups revealed that decreases in central brain NAA/Cr ratios were significant in patients with MS in the earliest stages

of the disease (Table 7-1). Changes in NAA/Cr ratios as a function of EDSS were greater for patients with mild disease than for the more severely affected patients. For example, the mean decrease in NAA/Cr ratio between the patient subgroup with EDSS scores of 0 to 1 and the subgroup with EDSS scores of 4 to 5 was about 15% (p=.001), whereas the decrease was only 5% between the patient subgroup with EDSS scores of 4 to 5 and the subgroup with EDSS scores of 8 to 9 (p=.1) (Figure 7-2). The correlation between NAA/Cr ratio and EDSS score was significantly ($p < .03$) stronger in patients with mild disability (EDSS score <5, SROC=-0.54, $p < .001$) than in the more disabled group (EDSS score ≥5, n=38, SROC=-0.1, p=.9) (Figure 7-3).

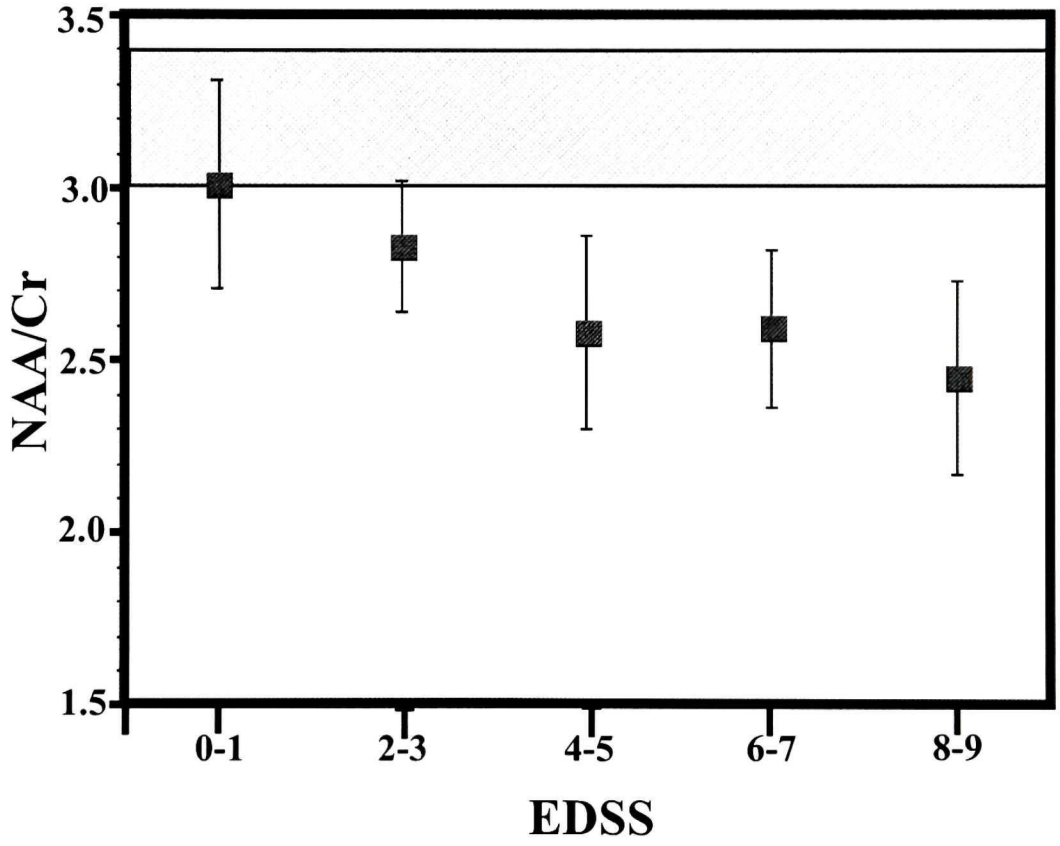

Figure 7-2: Mean N-acetylaspartate-creatine (NAA/Cr) ratios for patients with multiple sclerosis grouped by Expanded Disability Status Scale (EDSS) score. In the different patient subgroups, analysis of variance followed by pairwise post hoc comparison (Tukey honestly significant difference procedure) showed that changes in NAA/Cr ratio with respect to EDSS score are greater for patients with lower EDSS scores than for more disabled patients (see the "Results" section). Shaded area indicates mean ± SD of healthy controls.

When similar analyses were performed in patients with MS grouped for duration of disease, the subgroup with short disease duration (<5 years, n=21) also showed central brain NAA/Cr resonance intensity ratios (2.73±0.35) significantly lower than healthy controls ($p < .001$) and a close correlation between cerebral NAA/Cr ratio and EDSS score (SROC=-0.70, $p < .001$) was found (Figure 7-4). A significant correlation was not found in patients with more long-standing disease.

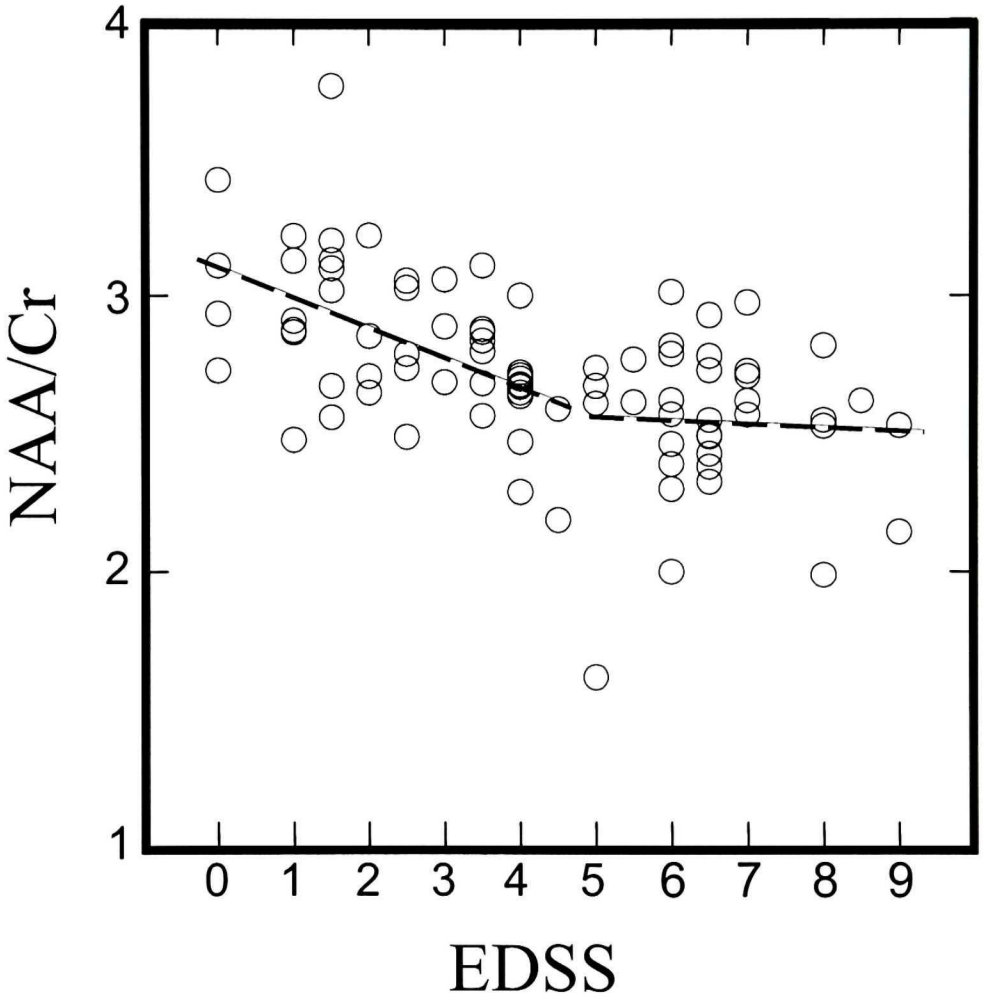

Figure 7-3: Data from 88 patients with multiple sclerosis illustrating the nonlinear decrease of N-acetylaspartate-creatine (NAA/Cr) ratio with respect to Expanded Disability Status Scale (EDSS) score. A significant relationship can be seen in the group of patients with milder disability (EDSS score <5, Spearman rank order coefficient = –0.54, $p<.001$) but cannot be seen in the more disabled group (EDSS ≥5, Spearman rank order coefficient =-0.1, $p= .9$).

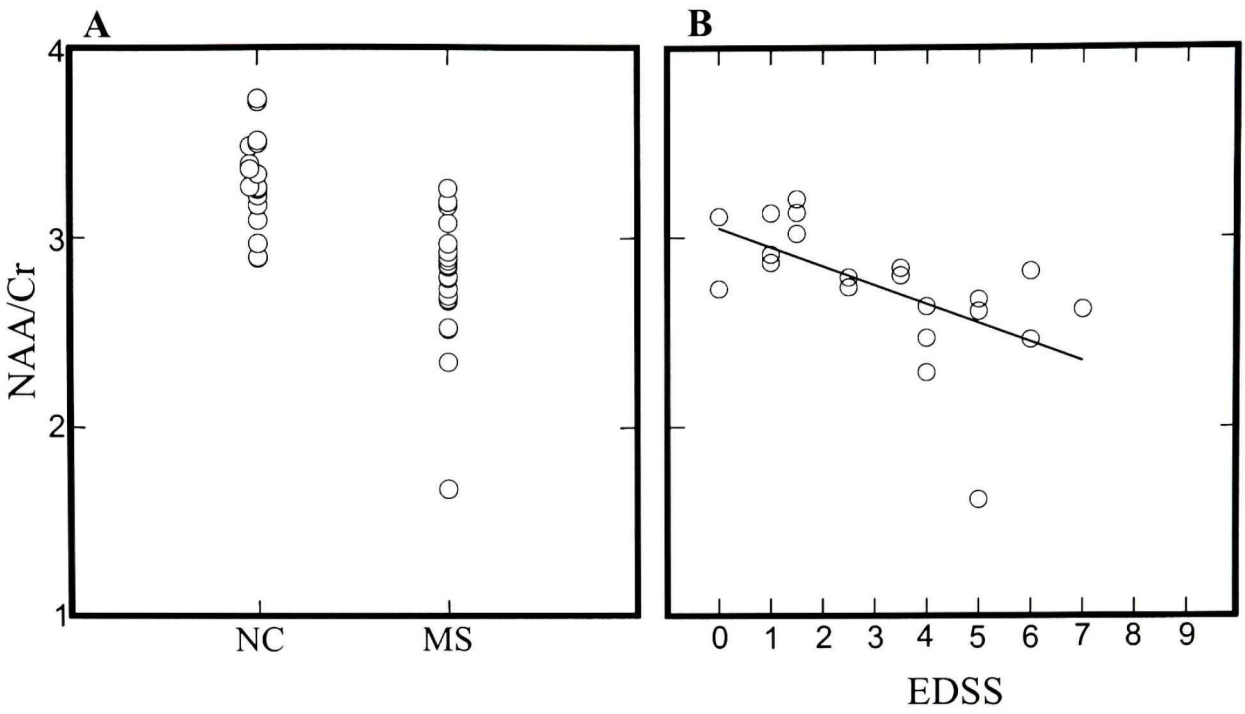

Figure 7-4: Data from patients with multiple sclerosis (MS) with disease duration of less than 5 years illustrating the following: (A) the significant decrease in N-acetylaspartate-creatine (NAA/Cr) ratio relative to the healthy control group ($p<.001$) and (B) a very strong correlation between NAA/Cr ratio and Expanded Disability Status Scale (EDSS) score (Spearman rank order correlation = –0.70, $p<.001$).

Discussion

Early axonal damage in MS

By assessing central brain NAA in a relatively large, clinically stable MS population with a wide range of disability and disease duration, we showed that diffuse cerebral axonal damage (1) begins in the early stages of MS, (2) develops more rapidly in the earlier clinical stages of the disease, and (3) correlates more strongly with disability in patients with mild disease than in patients with more severe disease.

Our results emphasize that significant axonal pathology is not confined to lesions and must occur early in the evolution of MS, ie, axonal injury and loss is not restricted to the end stages of the disease. Even complete clinical recovery from acute attacks in early MS does not mean that axonal damage has not occurred. In the initial stages of MS, in

addition to functional recovery due to reversal of axonal conduction block associated with inflammation and release of soluble factors (Smith et al., 1999), functional impairment due to axonal damage and dysfunction may be compensated for by mechanisms such as sodium channel redistribution (Black et al., 1991; Moll et al., 1991) and brain plasticity (Reddy et al., 2000b; Waxman, 1997). In fact, the presence of early axonal damage in MS has been suggested in recent histological studies that showed that (1) axon degeneration can accompany acute demyelination (Silver et al., 1997), (2) milder axonal changes can occur before inflammation (Zhu et al., 1999), and (3) axon degeneration can be evident in MS lesions of individuals with no history of neurologic symptoms (Mews et al., 1998; Trapp et al., 1999b). These in vitro observations lend support to our *in vivo* findings in suggesting that axonal damage does accumulate and is relevant to disability from the early stages of MS.

An interesting finding reported herein is that the decreases in NAA/Cr ratio were faster with respect to EDSS score in earlier stages of MS than in later stages. This should not be interpreted as evidence that axonal damage contributes less to disability later in the course of MS. In fact, with the progression of the disease, other mechanisms of axonal damage may become important and be more sensitively assessed by other magnetic resonance measures (ie, loss of brain and spinal cord parenchymal volume (Filippi et al., 1997)) (Losseff and Miller, 1998; Lycklama à Nijeholt et al., 1998; Stevenson et al., 1998). The loss of spinal cord volume, for example, appears to be more evident in patients with SPMS than in those with the relapsing form of the disease (Stevenson et al., 1998). Recent studies also have suggested that brain atrophy, although detectable in patients with RR MS (Simon et al., 1999), is more prominent in the progressive phase of MS. In addition, marked brain volume changes in the later stages of MS might affect, to

some extent, the sensitivity of NAA measurements. Thus, the presence of more pronounced brain atrophy and spinal cord pathology in late disease stages may explain, at least in part, the weaker relation between NAA/Cr ratio and EDSS score found in our study of patients with MS and severe disability.

NAA/Cr ratio as a marker of axonal damage

We believe that NAA is a reliable marker of axonal integrity in the adult brain. Antibodies directed against NAA or *N*-acetylaspartylglutamate stain neurons strongly without staining glial cells (Moffett et al., 1991; Simmons et al., 1991). The fact that O2A progenitor cells in culture express NAA (Urenjak et al., 1993) has raised some concerns about the specificity of NAA changes *in vivo*. However, O2A progenitor cells have been characterized only in culture. Related A2B5-positive cells are believed to occur *in vivo* but do not appear to be abundant enough to be able to contribute substantially to the total amount of NAA measured (Scolding et al., 1998). A recent report (Bhakoo and Pearce, 2000) has demonstrated that NAA can be detected in cultured, rat-derived O2A progenitor cells and mature oligodendrocytes derived from them. However, it is not clear that these in vitro conditions are relevant to the situation *in vivo*. There is a need to reconcile the antibody data with these high-performance liquid chromatography and nuclear magnetic resonance–based analyses. Regarding the results presented herein, oligodendrocyte density appears not to be reduced in normal-appearing white matter, which constitutes the majority of the tissue in our spectroscopic VOI. Thus, the potential for NAA expression in oligodendrocytes confounding our results appears to be minimal (Wolswijk, 1998).

Proton MRSI results are expressed in this study as NAA/Cr ratios. The resonance intensity of intravoxel Cr has been widely used as an internal standard in MRS studies *in*

vivo, since it is relatively equally present in all brain cells and tends to be stable in chronic (ie, nonacute (De Stefano et al., 1995a)) pathologic conditions. Changes in apparent brain Cr concentrations have been reported in chronic MS in recent MRS studies that attempted absolute quantitation. However, all current quantitative approaches have important limitations when applied to clinical studies and, in patients with MS, have shown discrepant results, reporting in turn increases, decreases, and absence of Cr changes in MRI lesions and in the normal-appearing white matter (Davie et al., 1997; Davie et al., 1999; Husted et al., 1994; Narayana et al., 1998; Pan et al., 1996; Sarchielli et al., 1999; van Walderveen et al., 1999). We believe that the most reliable data come from a study using high-resolution *in vitro* proton nuclear magnetic resonance spectroscopy (which does not have the same limitations as *in vivo* quantitation) on postmortem MS tissue (Davies et al., 1995). This study showed that Cr was decreased in MS plaques and that Cr levels were un-changed in the normal-appearing brain. In the present study, lesions occupied, on average, about 6% of the brain VOI used for spectroscopy (see the "Patients and Methods" section), suggesting that significant changes in Cr resonance intensities are unlikely. Consistent with this, ratios of choline to Cr resonance intensities in the group of patients with MS did not differ from controls (data not shown).

Conclusion

Central brain NAA/Cr ratios reveal that axonal injury begins in the early stages of MS. The strong correlation between NAA/Cr ratio and EDSS score in patients with low disability and disease duration adds to accumulating evidence that axonal damage is a primary determinant of disability from the early stages of the disease. To better understand the contribution of axonal loss to disability through the full course of the

disease, the use of new measures (Gonen et al., 2000) and the integration of multiple magnetic resonance modalities (ie, brain NAA, cerebral and spinal cord volumes) will be necessary. The close relation between axonal pathology and clinical disability in the early stages of the disease argues for the early treatment of MS with agents directed not only against inflammation but also toward axonal protection (Compston, 1998; Demerens et al., 1999; Trapp et al., 1999b).

References

1. Arnold DL, Matthews PM, Francis G, Antel J. Proton magnetic resonance spectroscopy of human brain in vivo in the evaluation of multiple sclerosis: assessment of the load of disease. Magnetic Resonance in Medicine 1990; 14: 154-159.
2. Barnes D, Munro PM, Youl BD, Prineas JW, McDonald WI. The longstanding MS lesion. A quantitative MRI and electron microscopic study. Brain 1991; 114 (Pt 3): 1271-80.
3. Bhakoo KK, Pearce D. In vitro expression of N-acetyl aspartate by oligodendrocytes: implications for proton magnetic resonance spectroscopy signal in vivo. Journal of Neurochemistry 2000; 74: 254-62.
4. Birken DL, Oldendorf WH. N-acetyl-L-aspartic acid: a literature review of a compound prominent in 1H-NMR spectroscopic studies of brain. Neurosci Biobehav Rev 1989; 13: 23-31.
5. Black JA, Felts P, Smith KJ, Kocsis JD, Waxman SG. Distribution of sodium channels in chronically demyelinated spinal cord axons: immuno-ultrastructural localization and electrophysiological observations. Brain Res 1991; 544: 59-70.
6. Compston A. Future options for therapies to limit damage and enhance recovery. Semin Neurol 1998; 18: 405-14.
7. Davie CA, Barker GJ, Thompson AJ, Tofts PS, McDonald WI, Miller DH. 1H magnetic resonance spectroscopy of chronic cerebral white matter lesions and normal appearing white matter in multiple sclerosis. J Neurol Neurosurg Psychiatry 1997; 63: 736-42.

8. Davie CA, Barker GJ, Webb S, Tofts PS, Thompson AJ, Harding AE, et al. Persistent functional deficit in multiple sclerosis and autosomal dominant cerebellar ataxia is associated with axon loss. Brain 1995; 118: 1583-1592.

9. Davie CA, Silver NC, Barker GJ, Tofts PS, Thompson AJ, McDonald WI, et al. Does the extent of axonal loss and demyelination from chronic lesions in multiple sclerosis correlate with the clinical subgroup? [In Process Citation]. J Neurol Neurosurg Psychiatry 1999; 67: 710-5.

10. Davies SE, Newcombe J, Williams SR, McDonald WI, Clark JB. High resolution proton NMR spectroscopy of multiple sclerosis lesions. J Neurochem 1995; 64: 742-8.

11. de Beer R, Van den Boogaart A, van Ormondt D, Pijnappel WW, den Hollander JA, Marien AJ, et al. Application of time-domain fitting in the quantification of in vivo 1H spectroscopic imaging data sets. NMR in Biomedicine 1992; 5: 171-178.

12. De Stefano N, Matthews PM, Antel JP, Preul M, Francis G, Arnold DL. Chemical pathology of acute demyelinating lesions and its correlation with disability. Annals of Neurology 1995a; 38: 901-909.

13. De Stefano N, Matthews PM, Arnold DL. Reversible decreases in N-acetylaspartate after acute brain injury. Magn Reson Med 1995b; 34: 721-7.

14. De Stefano N, Matthews PM, Fu L, Narayanan S, Stanley J, Francis GS, et al. Axonal damage correlates with disability in patients with relapsing- remitting multiple sclerosis. Results of a longitudinal magnetic resonance spectroscopy study. Brain 1998; 121: 1469-77.

15. Demerens C, Stankoff B, Zalc B, Lubetzki C. Eliprodil stimulates CNS myelination: new prospects for multiple sclerosis? Neurology 1999; 52: 346-50.

16. den Hollander JA, Oosterwall B, van Vroonhoven H, Luyten PR. Elimination of magnetic field distortions in ^{1}H NMR spectroscopic imaging. Soc Maggn Reson Med. Vol 1, 1991: 472.

17. Ferguson B, Matyszak MK, Esiri MM, Perry VH. Axonal damage in acute multiple sclerosis lesions. Brain 1997; 120: 393-9.

18. Filippi M, Colombo B, Rovaris M, Pereira C, Martinelli V, Comi G. A longitudinal magnetic resonance imaging study of the cervical cord in multiple sclerosis. J Neuroimaging 1997; 7: 78-80.

19. Fu L, Matthews PM, De Stefano N, Worsley KJ, Narayanan S, Francis GS, et al. Imaging axonal damage of normal-appearing white matter in multiple sclerosis. Brain 1998; 121: 103-13.

20. Gonen O, Catalaa I, Babb JS, Ge Y, Mannon LJ, Kolson DL, et al. Total brain N-acetylaspartate: a new measure of disease load in MS. Neurology 2000; 54: 15-9.

21. Haase A, Frahm J, Hanicke W, Matthaei D. 1H NMR chemical shift selective (CHESS) imaging. Phys Med Biol 1985; 30: 341-4.

22. Husted CA, Goodin DS, Hugg JW, Maudsley AA, Tsuruda JS, de Bie SH, et al. Biochemical alterations in multiple sclerosis lesions and normal-appearing white matter detected by in vivo 31P and 1H spectroscopic imaging. Annals of Neurology 1994; 36: 157-165.

23. Kurtzke JF. Rating neurologic impairment in multiple sclerosis: an expanded disability status scale (EDSS). Neurology 1983; 33: 1444-1452.

24. Lee MA, Blamire AM, Pendlebury S, Ho KH, Mills KR, Styles P, et al. Axonal injury or loss in the internal capsule and motor impairment in multiple sclerosis [see comments]. Arch Neurol 2000; 57: 65-70.

25. Losseff NA, Miller DH. Measures of brain and spinal cord atrophy in multiple sclerosis. J Neurol Neurosurg Psychiatry 1998; 64 Suppl 1: S102-5.

26. Lycklama à Nijeholt GJ, van Walderveen MA, Castelijns JA, van Waesberghe JH, Polman C, Scheltens P, et al. Brain and spinal cord abnormalities in multiple sclerosis. Correlation between MRI parameters, clinical subtypes and symptoms. Brain 1998; 121: 687-97.

27. Matthews PM, De Stefano N, Narayanan S, Francis GS, Wolinsky JS, Antel JP, et al. Putting magnetic resonance spectroscopy studies in context: axonal damage and disability in multiple sclerosis. Semin Neurol 1998; 18: 327-36.

28. McDonald WI. Rachelle Fishman-Matthew Moore Lecture. The pathological and clinical dynamics of multiple sclerosis. [Review]. Journal of Neuropathology & Experimental Neurology 1994; 53: 338-343.

29. Mews I, Bergmann M, Bunkowski S, Gullotta F, Bruck W. Oligodendrocyte and axon pathology in clinically silent multiple sclerosis lesions. Mult Scler 1998; 4: 55-62.

30. Moffett JR, Namboodiri MAA, Cangro CB, Neale JH. Immunohistochemical localization of N-acetylaspartate in rat brain. NeuroReport 1991; 2: 131-134.

31. Moll C, Mourre C, Lazdunski M, Ulrich J. Increase of sodium channels in demyelinated lesions of multiple sclerosis. Brain Res 1991; 556: 311-6.

32. Narayana PA, Doyle TJ, Lai D, Wolinsky JS. Serial proton magnetic resonance spectroscopic imaging, contrast- enhanced magnetic resonance imaging, and quantitative lesion volumetry in multiple sclerosis. Ann Neurol 1998; 43: 56-71.

33. Pan JW, Hetherington HP, Vaughan JT, Mitchell G, Pohost GM, Whitaker JN. Evaluation of multiple sclerosis by 1H spectroscopic imaging at 4.1 T. Magn Reson Med 1996; 36: 72-7.

34. Poser CM, Paty DW, Scheinberg L, McDonald WI, Floyd AD, Ebers GC, et al. New diagnostic criteria for multiple sclerosis: Guidelines for research protocols. Annals of Neurology 1983; 13: 227-231.

35. Reddy H, Narayanan S, Matthews PM, Hoge RD, Pike GB, Duquette P, et al. Relating axonal injury to functional recovery in MS. Neurology 2000; 54: 236-9.

36. Sarchielli P, Presciutti O, Pelliccioli GP, Tarducci R, Gobbi G, Chiarini P, et al. Absolute quantification of brain metabolites by proton magnetic resonance spectroscopy in normal-appearing white matter of multiple sclerosis patients [In Process Citation]. Brain 1999; 122: 513-21.

37. Scolding N, Franklin R. Axon loss in multiple sclerosis. Lancet 1998; 352: 340-1.

38. Scolding N, Franklin R, Stevens S, Heldin CH, Compston A, Newcombe J. Oligodendrocyte progenitors are present in the normal adult human CNS and in the lesions of multiple sclerosis [see comments]. Brain 1998; 121: 2221-8.

39. Silber E, Sharief MK. Axonal degeneration in the pathogenesis of multiple sclerosis. J Neurol Sci 1999; 170: 11-8.

40. Silver NC, Barker RA, MacManus DG, Barker GJ, Thom M, Thomas DG, et al. Proton magnetic resonance spectroscopy in a pathologically confirmed acute demyelinating lesion. J Neurol 1997; 244: 204-7.

41. Simmons ML, Frondoza CG, Coyle JT. Immunocytochemical localization of N-acetyl-aspartate with monoclonal antibodies. Neuroscience 1991; 45: 37-45.

42. Simon JH, Jacobs LD, Campion MK, Rudick RA, Cookfair DL, Herndon RM, et al. A longitudinal study of brain atrophy in relapsing multiple sclerosis. The

Multiple Sclerosis Collaborative Research Group (MSCRG). Neurology 1999; 53: 139-48.

43. Smith KJ, Kapoor R, Felts PA. Demyelination: the role of reactive oxygen and nitrogen species. Brain Pathol 1999; 9: 69-92.

44. Stevenson VL, Leary SM, Losseff NA, Parker GJ, Barker GJ, Husmani Y, et al. Spinal cord atrophy and disability in MS: a longitudinal study. Neurology 1998; 51: 234-8.

45. Trapp BD, Peterson J, Ransohoff RM, Rudick R, Mork S, Bo L. Axonal transection in the lesions of multiple sclerosis [see comments]. N Engl J Med 1998; 338: 278-85.

46. Trapp BD, Ransohoff R, Rudick R. Axonal pathology in multiple sclerosis: relationship to neurologic disability. Curr Opin Neurol 1999a; 12: 295-302.

47. Trapp BD, Ransohoff RM, Fisher E, Rudick RA. Neurodegenration in multiple sclerosis: relationship to neurological disability. Neuroscientist 1999b; 5: 48-57.

48. Urenjak J, Williams SR, Gadian DG, Noble MD. Proton nuclear magnetic resonance spectroscopy unambiguously identifies different neural cell types. J Neurosci 1993; 13: 981-9.

49. van Walderveen MA, Barkhof F, Pouwels PJ, van Schijndel RA, Polman CH, Castelijns JA. Neuronal damage in T1-hypointense multiple sclerosis lesions demonstrated in vivo using proton magnetic resonance spectroscopy. Ann Neurol 1999; 46: 79-87.

50. Waxman SG. Molecular remodeling of neurons in multiple sclerosis: what we know, and what we must ask about brain plasticity in demyelinating diseases. Adv Neurol 1997; 73: 109-20.

51. Waxman SG. Multiple sclerosis as a neuronal disease. Arch Neurol 2000; 57: 22-4.

52. Wolswijk G. Chronic stage multiple sclerosis lesions contain a relatively quiescent population of oligodendrocyte precursor cells. J Neurosci 1998; 18: 601-9.

53. Zhu B, Moore GR, Zwimpfer TJ, Kastrukoff LF, Dyer JK, Steeves JD, et al. Axonal cytoskeleton changes in experimental optic neuritis. Brain Res 1999; 824: 204-17.

7.3 Preface to Manuscript 6

In Manuscript 5, we found that NAA decreases began and were relevant to disability from the early stages of MS. In the later stages of MS, NAA loss appeared to decelerate and no longer correlated with disability.

NAA measured within a volume of brain tissue is essentially a measure of the *density* of NAA (and, by extension, the functional density of axons and neurons). Thus, a possible explanation for the results of Manuscript 5 is that progressive MS is associated with a greater degree of atrophy than RRMS, which serves to mitigate the decline of NAA density in SP patients. If compensatory atrophy is less pronounced in RRMS, then axonal damage and dysfunction will be more fully represented by decreased NAA. Stated another way, if damaged axons and associated glia are completely cleared from a region of brain, and the surrounding tissue is displaced to fill the space, then the decline of NAA will be much smaller than if no compensatory atrophy were to take place. Thus, concurrent measures of axonal density and tissue loss are needed to fully assess the extent of axonal loss (Evangelou et al., 2000). Spinal cord cross-sectional area has been shown to correlate well with disability (Losseff and Miller, 1998; Losseff et al., 1996b; Stevenson et al., 1998), particularly in patients with SPMS. Spinal cord atrophy is thought to reflect mainly axonal degeneration, and so we explored the relationships of brain axonal injury and spinal cord atrophy to disability at varying disease stages in Manuscript 6, "Disease duration influences the relationship between brain axonal injury, spinal cord atrophy and disability in multiple sclerosis."

7.4 Manuscript 6

Presented at the 8th Annual Meeting of the International Society for Magnetic Resonance in Medicine.

Manuscript to be submitted.

Disease Duration Influences the Relationship between Brain Axonal Injury, Spinal Cord Atrophy and Disability in Multiple Sclerosis

Sridar Narayanan, MSc, [1]Nicola De Stefano, MD, PhD, Simon Francis, BSc,
M. Carmela Tartaglia, BSc, Rozie Arnaoutelis, BSc,
Yves Lapierre, MD and Douglas L. Arnold, MD

Department of Neurology and Neurosurgery,
Montreal Neurological Institute and Hospital,
Montreal, Quebec, Canada, (514) 398-8185,

and

[1]Institute of Neurological Sciences and NMR Centre
University of Siena
Siena, Italy

Reprint requests and correspondence to:

Dr. Douglas L. Arnold,
Montreal Neurological Institute,
3801 University Street, Montreal,
Quebec, Canada, H3A 2B4
Tel: (514) 398-8185
Fax: (514) 398-2975
E-mail: doug@mrs.mni.mcgill.ca

Running title: Axonal injury and demyelination in MS NAWM

Abstract

Proton magnetic resonance spectroscopic imaging (MRSI) of the brain provides a method of assessing axonal injury *in vivo* via measurement of the neuronal/axonal marker N-acetylaspartate (NAA). Spinal cord cross-sectional area at the level of C2 is a measure of spinal cord atrophy that has been shown to correlate with clinical disability scores. We performed proton MRSI of a large, central brain volume and high-resolution cervical spinal cord imaging in 56 multiple sclerosis patients [39 with relapsing remitting (RR) and 17 with secondary progressive (SP) disease] to examine the relevance to disability of brain axonal injury and spinal cord atrophy as a function of disease stage. We found that central brain NAA/Cr was reduced in both RR [2.7 (0.3), mean (standard deviation)] and SP [2.6 (0.3)] subgroups relative to controls [3.1 (0.2), $p<0.005$]. Spinal cord cross-sectional area at the level of C2 was reduced in SP patients [59.5 (14.8)] relative to controls [81.0 (6.9), $p<0.01$] and the RR group [77.8 (10.3), $p<0.01$]. Spearman correlation between Expanded Disability Status Scale (EDSS) and central brain NAA/Cr was strongest in early stage MS (SRCC = –0.75, $p<0.01$), whereas spinal cord atrophy correlated better with EDSS late in the disease course (SRCC = –0.84, $p<0.01$). These results suggest that chronic axonal dysfunction is an important contributor to disability in early stage MS, but that axonal degeneration and loss (represented by spinal cord atrophy) determine disability in the late stages of MS.

Introduction

Multiple sclerosis (MS) is an idiopathic inflammatory disease characterised by lesions distributed throughout the central nervous system. Magnetic resonance imaging (MRI) has had a great impact on our understanding of multiple sclerosis, as well as in

aiding diagnosis. However, while conventional MRI can sensitively detect the focal lesions of MS, it cannot differentiate between demyelination, axonal loss, edema and inflammation. In an effort to overcome the limitations of conventional MRI, a variety of pathogically more specific magnetic resonance (MR) techniques have been employed to study MS (Miller et al., 1998). MR spectroscopy (MRS) has been particularly informative as it provides an *in-vivo* measure of axonal impairment through the measurement of the neuronal/axonal metabolite N-acetylaspartate (NAA) (Arnold et al., 2000). Relative resonance intensities of NAA have been shown to correlate well with clinical disability, particularly in the early stages of the disease (De Stefano et al., 2001). Measures of spinal cord atrophy also have shown good correlations with disability (Liu et al., 1999; Losseff and Miller, 1998; Losseff et al., 1996b; Stevenson et al., 1998). Given that different MR modalities are sensitive to different underlying pathological processes, the relevance of each modality to disability can be expected to be different at different stages of a heterogeneous disease such as MS, providing some clues as to the mechanisms of progression in this disease. The purpose of the present study was to evaluate the relationship of brain axonal damage and spinal cord atrophy to clinical disability at various stages of MS.

Methods

Patient Population

Fifty-six patients (36 women and 20 men) aged 20 to 61 years [39.6 (8.8) years, mean (standard deviation)] with definite MS were selected from the Multiple Sclerosis Clinic of the Montreal Neurological Hospital to span the entire range (0-9) of the Expanded Disability Status Scale (EDSS). Patients with either relapsing-remitting (RR, N=39) or secondary-progressive (SP, N=17) disease were asked to undergo magnetic

resonance examination and concurrent clinical evaluation, including recording of EDSS scores and any recent exacerbations. Patients were not on immunomodulatory therapy, and examinations were timed to be no less than 1 month after an exacerbation. A group of 17 healthy laboratory and hospital workers of similar mean age [35.3 (9.2), p=0.1] served as normal control subjects. The ethics committee of the Montreal Neurological Institute approved the study, and informed consent was obtained from all participants.

Magnetic Resonance Imaging and Spectroscopy of Brain

Combined proton MRI and MRSI examinations of the brain were obtained in a single session for each examination using a Philips Gyroscan ACS II operating at 1.5 T (Philips Medical Systems, Best, The Netherlands). A transverse dual-echo, turbo spin-echo sequence (TR/TE1/TE2 = 2075/32/90 ms, 256x256 matrix, 1 signal average, 250mm field of view) yielding proton density-weighted (PDW) and T2-weighted (T2W) images with 50 contiguous 3 mm slices was acquired parallel to the line connecting the inferior aspects of the genu and splenium of the corpus callosum (callosal line), followed by a matching T1-weighted (T1W) fast field-echo (FFE) sequence (TR/TE = 35/10 ms).

These conventional MR images were used to position a spectroscopic volume of interest (VOI) of approximately 90x90x20 mm^3 to include the corpus callosum and adjacent periventricular white matter (Figure 7-5). MR spectroscopic images parallel to the AC-PC line were acquired (32x32 phase-encodes, 250x250 mm field-of-view, 20 mm slab thickness) using a double spin-echo excitation method (Ordidge et al., 1987) (TR 2000, TE 272ms). To suppress the intense water resonance, frequency selective excitation pulses were placed at the beginning of the MRSI sequence (Haase and Frahm, 1985). To allow for correction of B_0 inhomogeneity during post-processing, a quick MRSI without

water-suppression was also acquired (TR 850ms, TE 272ms, 16x16 phase-encodes, 250x250 mm field-of-view and one signal average).

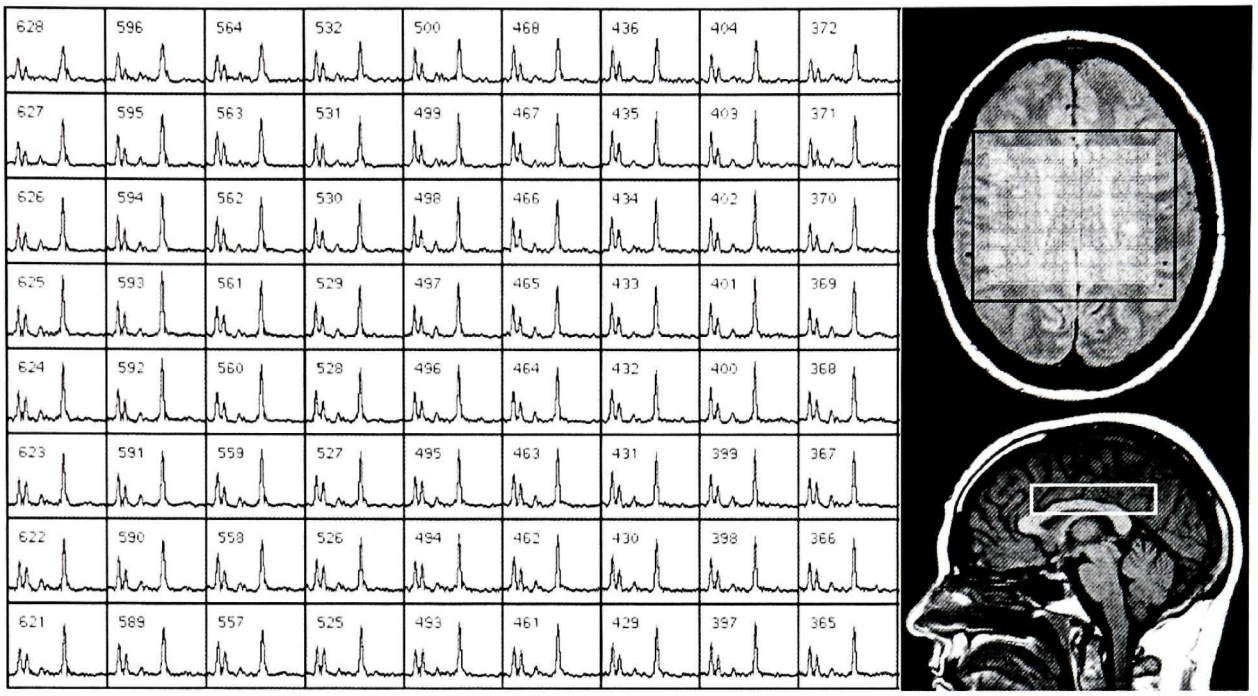

Figure 7-5: The spectroscopic volume of interest is shown in black on the transverse proton density-weighted MRI (upper right) and in white on the sagittal T1-weighted MRI (lower right). The phase-encoded voxel grid is shown (semi-transparent) superimposed on the transverse MRI (upper right) and enlarged (left). Voxels at the edge of the excited volume were excluded from analysis since they can show artifactual relative intensities.

Post-Processing

Post-processing of the raw MRSI data was performed as previously described (Fu et al., 1998), with the exception that in the present study the residual water signal was fitted and removed from the water-suppressed data using the Hankel singular-value decomposition procedure (de Beer and van Ormondt, 1992). The nominal voxel size in-plane was approximately 8x8 mm, which yielded a spatial resolution of approximately 12x12 mm after filtering.

Metabolite resonance intensities were determined by integration of Gaussian-fitted peak areas relative to a baseline computed from a moving average of the noise regions of each spectrum (AVIS, Samson Antel, MRS Unit, MNI). Metabolite signals

were expressed as ratios to creatine (Cr) in the same voxel and then averaged over the entire VOI to obtain mean metabolite ratios for each examination.

Lesions were manually segmented using locally developed software (Display, David MacDonald, Brain Imaging Centre, MNI), which provided simultaneous access to PD, T2 and T1-weighted image sets. Lesion boundaries were primarily determined on the PD images.

Measurement of Spinal Cord Atrophy

T1W images of the cervical spine at the level of the second cervical segment (C2) were obtained with a quadrature neck coil, using a 3D T1W-FFE sequence (TR=27ms, TE=7.5ms, 256×256 matrix, 150mm FOV, 20° flip angle, and 6 SA). Twenty-five 1mm thick transverse slices (producing 0.6 mm × 0.6 mm × 1 mm voxels) were acquired perpendicular to the cord, with the level of the most inferior slice positioned at the top of C3. Post-processing consisted of rotating and resampling this volume data set to ensure that the slices were perpendicular to the cord and applying a box filter of dimensions 1×1×4 mm to improve the signal-to-noise ratio. Twelve slices were then extracted, with the bottom of the most inferior slice retained aligned with the inferior margin of C2, using the intervertebral disk as a landmark. The data were then resampled to yield three 4 mm thick slices for cross-sectional area measurements. This procedure aids in consistent placement of the slices used for quantitation and avoids intensity artifacts at the edges of the excitation volume. The cord was labeled on each slice by applying a threshold equal to the signal intensity halfway between the average intensity of CSF and cord. The cross-sectional areas of the 3 slices were then averaged to yield the final mean cross-sectional area of the cord at C2. The procedure is illustrated in Figure 7-6.

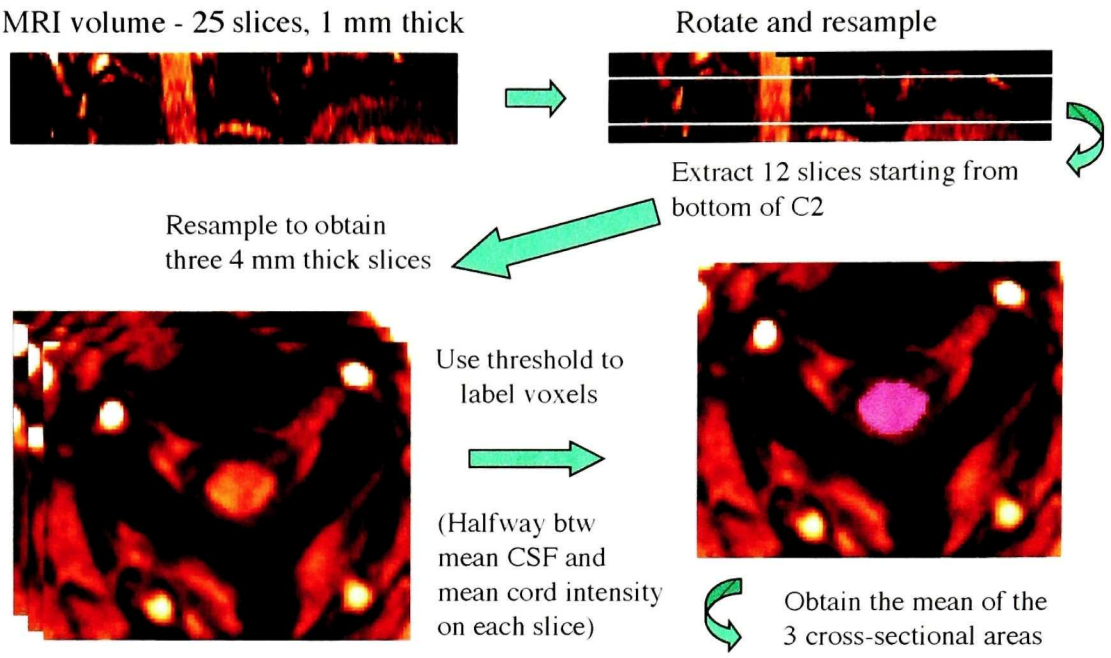

Figure 7-6: Calculation of spinal cord cross-sectional area. The original high resolution MRI (top left) is rotated and resampled so that the slices are perpendicular to the cord. Twelve slices are extracted starting from the bottom of C2, using the intervertebral disk as the caudal landmark. The data are box filtered and resampled to improve signal-to-noise and reduce the number of slices to three. A threshold halfway between the mean intensity of CSF and spinal cord is used to segment the cord on each slice. The cord cross-sectional area is obtained for each slice by voxel counting, and the mean of the three values is taken as the mean cross-sectional area at C2.

Statistics

We examined group differences of NAA/Cr and spinal cord cross-sectional area between controls, RR and SP patients using analysis of variance (ANOVA) followed by Tukey's post-hoc testing.

We then performed Spearman rank-order correlations of NAA/Cr and spinal cord cross-sectional area with EDSS for patients grouped by duration of disease.

Results

Group Differences

Central brain NAA/Cr ratios of the patient group with RR [2.7 (0.3), mean (standard deviation), N=39] and SP [2.6 (0.3), N=17] disease both were significantly

lower than normal controls [3.1 (0.20), p<0.005]. The decrease of NAA/Cr in the SP patients relative to the RR patients did not reach significance (p=0.1) in this study (Figure 7-7).

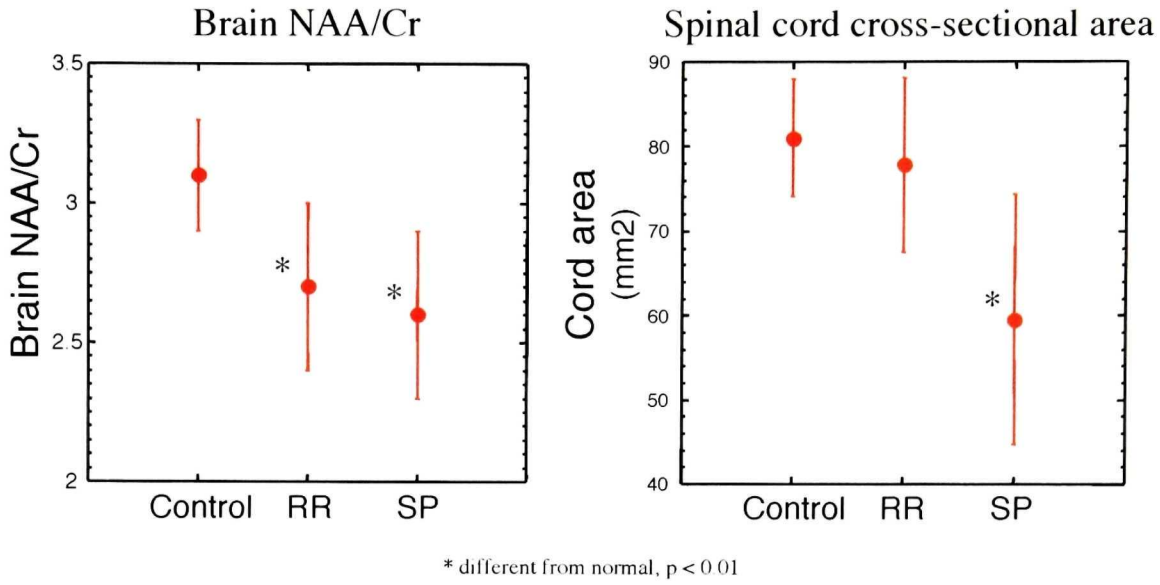

Figure 7-7: Comparison of central brain NAA/Cr (left) and spinal cord cross sectional area (right) between control, RR and SP patient groups.

The difference in spinal cord cross-sectional area between controls [81.0 (6.9) mm^2, mean (SD)]) and the whole patient cohort [71.7 (13.3) mm^2] trended toward significance (p = 0.06). Spinal cord cross-sectional area was not reduced in the RR subgroup [77.8 (10.3)] compared to controls (p = 0.47). However, the SP subgroup had significantly lower spinal cord cross-sectional areas [59.5 (14.8)] than controls (p < 0.01) or the RR subgroup (p < 0.01) (Figure 7-7).

Correlational analysis

Over the entire EDSS range, EDSS correlated with both NAA/Cr and spinal cord atrophy (see Table 7-2 and Figure 7-8). The correlation between NAA/Cr and EDSS was

stronger earlier in the disease than later, while the initially weak correlation between spinal cord area and EDSS became stronger with increasing disease duration.

	Dur < 5	5≤ Dur ≤ 20	Dur ≥ 20	Overall
NAA/Cr	**-0.75**	**-0.44**	-0.30	**-0.53**
Cord	-0.29	**-0.53**	**-0.84**	**-0.58**
N	15	33	8	56

Table 7-2: Correlation (Spearman Rank-Order Correlation) with EDSS as a function of disease duration. Coefficients in bold were significant ($p < 0.01$).

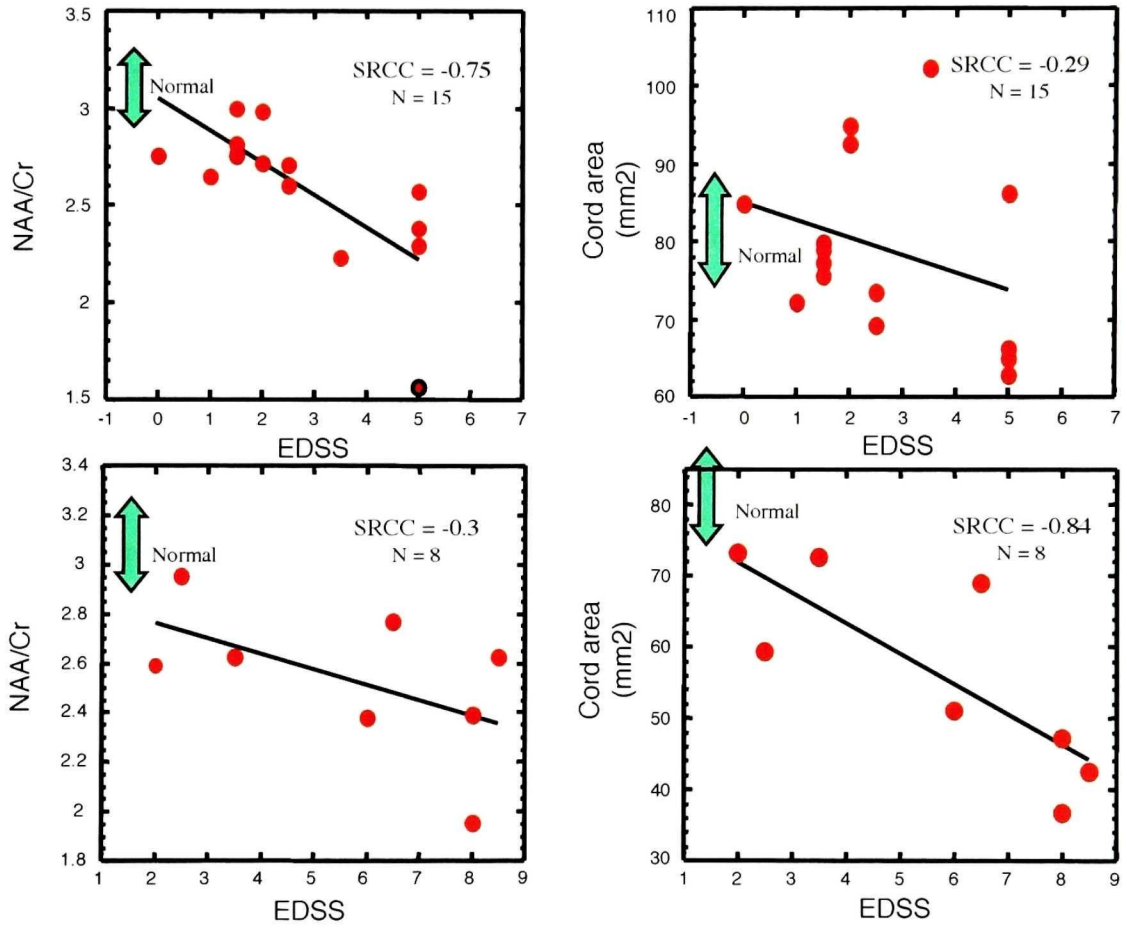

Figure 7-8: NAA/Cr (left) and spinal cord cross-sectional area (right) vs. EDSS for MS patients with disease duration < 5 yrs (top pair) and > 20 years (bottom pair).

Discussion

We have previously shown that cerebral axonal damage begins and contributes significantly to clinical disability from the early stages of MS (De Stefano et al., 2001). Our present results confirm the strong correlation between central brain NAA/Cr and EDSS early in the course of MS, and the weakening of this relationship in later stages of the disease. Given that the measurement of NAA/Cr in a defined volume yields a measure of the functional density of axons (Matthews et al., 1998), the likely explanation for this behaviour is that the early decrease of NAA represents chronic axonal dysfunction and loss of axonal density, with relatively little change in the overall volume of tissue. A recent post-mortem study by Bjartmar *et al.* has shown that in the spinal cord of paralyzed MS patients, NAA per axonal volume is reduced not only within lesions, but in NAWM, providing direct evidence of decreased NAA in non-demyelinated but functionally impaired axons (Bjartmar et al., 2000). While brain atrophy has been detected in relatively early MS (Rudick et al., 1999; Simon et al., 1999), it is generally more pronounced in progressive MS (Collins et al., 2000). The compensatory atrophy of the brain in later stages of MS likely serves to limit the decrease of axonal density measured by MRS (Collins et al., 2000), illustrating the utility of obtaining measures both of axonal density and volume of tissue.

Conversely, atrophy of the cervical spinal cord at the level of C2 was not found to be abnormal in the RR group, but was significantly low in the SP group. The finding of normal cord cross-sectional area in the RR group should be approached with caution, however, since spinal cord cross-sectional area was found to be variable even in the control group. Unlike brain atrophy measures, we did not find a way to perform normalization for natural variability in cord size, due to the lack of correlation of cord

size with body size metrics such as weight or height (Losseff et al., 1996b). In fact, longitudinal studies have suggested that the rate of spinal cord atrophy is faster in RR patients than in SP patients, perhaps due to a more active disease process in the earlier, relapsing-remitting stage of MS (Liu et al., 1999; Stevenson et al., 1998). However, it is clear from our results and previous studies that the amount of accumulated spinal cord atrophy is greater in patients with secondary progressive MS than in patients with relapsing-remitting disease (Liu et al., 1999; Losseff et al., 1996b; Lycklama à Nijeholt et al., 1998; Stevenson et al., 1998). Since both demyelination and axonal loss can contribute to spinal cord atrophy, one could speculate that the cross sectional area loss seen in the RR group is linked more to demyelination and associated axonal shinkage, while in the more disabled SP group, the atrophy represents a greater proportion of axonal loss.

Consistent with this notion, we found that atrophy of the cervical spinal cord at the level of C2 did not correlate with EDSS in the initial stages of MS, but that the relationship strengthened with more longstanding disease. In mice infected with Theiler's encephalomyelitis virus, functional impairment did not result from spinal cord demyelination only, but appeared to require axonal damage (Rivera-Quinones et al., 1998). This group then showed that large-calibre axonal loss results only after prolonged demyelination in these mice, and that this loss correlates strongly with spinal cord atrophy (McGavern et al., 2000). In a study of post-mortem spinal cord samples from SPMS patients, Lovas *et al.* found a significant reduction in axonal density in both lesions and NAWM of the spinal cord compared to normal control samples, but no difference in axonal density between spinal cord plaque and contralateral NAWM (Lovas et al., 2000). From this they suggest that loss of axonal density in the spinal cord is the

final result of chronic inflammation at multiple sites along the descending tracts (Lovas et al., 2000). Multiple "hits" on individual, large calibre corticospinal axons would indeed be more likely in patients with longer-standing, progressive disease, in part due to their larger lesion loads, but also because diffuse, widespread axonal damage of NAWM is more pronounced in the brains of SP patients than of RR patients (Fu et al., 1998) (De Stefano et al., 2001; Tourbah et al., 1999). Chronically demyelinated axons may degenerate after being sufficiently deprived of trophic support from myelin, and gradual loss of axons over time may occur without the requirement for new inflammatory lesions (Bjartmar et al., 2000). Spinal cord atrophy may correlate strongly with EDSS in longstanding MS because cord atrophy provides a measure of the degree of axonal degeneration that has occurred, along with the fact that EDSS in the later stages of MS is based on gait, which is particularly sensitive to spinal pathology.

References

1. Arnold DL, De Stefano N, Narayanan S, Matthews PM. Proton MR spectroscopy in multiple sclerosis. Neuroimaging Clin N Am 2000; 10: 789-98 ,ix-x.
2. Bjartmar C, Kidd G, Mork S, Rudick R, Trapp BD. Neurological disability correlates with spinal cord axonal loss and reduced N-acetyl aspartate in chronic multiple sclerosis patients. Ann Neurol 2000; 48: 893-901.
3. Collins DL, Narayanan S, Caramanos Z, De Stefano N, Tartaglia MC, Arnold DL. Relation of cerebral atrophy in multiple sclerosis to severity of disease and axonal injury. American Academy of Neurology, 52nd Annual Meeting, San Diego, CA. Neurology 2000; 54 Supp. 3: A17.
4. de Beer R, van Ormondt D. Analysis of NMR data using time domain fitting procedures. NMR Basic Principles and Progress. Vol 26. Berlin: Springer-Verlag, 1992: 204-248.

5. De Stefano N, Narayanan S, Francis GS, Arnaoutelis R, Tartaglia MC, Antel JP, et al. Evidence of axonal damage in the early stages of multiple sclerosis and its relevance to disability. Arch Neurol 2001; 58: 65-70.

6. Fu L, Matthews PM, De Stefano N, Worsley KJ, Narayanan S, Francis GS, et al. Imaging axonal damage of normal-appearing white matter in multiple sclerosis. Brain 1998; 121: 103-13.

7. Haase A, Frahm J. Multiple chemical shift selective NMR imaging using stimulated echoes. J. Magn. Reson. 1985: 94-102.

8. Liu C, Edwards S, Gong Q, Roberts N, Blumhardt LD. Three dimensional MRI estimates of brain and spinal cord atrophy in multiple sclerosis. J Neurol Neurosurg Psychiatry 1999; 66: 323-30.

9. Losseff NA, Miller DH. Measures of brain and spinal cord atrophy in multiple sclerosis. J Neurol Neurosurg Psychiatry 1998; 64 Suppl 1: S102-5.

10. Losseff NA, Webb SL, O'Riordan JI, Page R, Wang L, Barker GJ, et al. Spinal cord atrophy and disability in multiple sclerosis. A new reproducible and sensitive MRI method with potential to monitor disease progression. Brain 1996; 119: 701-8.

11. Lovas G, Szilagyi N, Majtenyi K, Palkovits M, Komoly S. Axonal changes in chronic demyelinated cervical spinal cord plaques [see comments]. Brain 2000; 123: 308-17.

12. Lycklama à Nijeholt GJ, van Walderveen MA, Castelijns JA, van Waesberghe JH, Polman C, Scheltens P, et al. Brain and spinal cord abnormalities in multiple sclerosis. Correlation between MRI parameters, clinical subtypes and symptoms. Brain 1998; 121: 687-97.

13. Matthews PM, De Stefano N, Narayanan S, Francis GS, Wolinsky JS, Antel JP, et al. Putting magnetic resonance spectroscopy studies in context: axonal damage and disability in multiple sclerosis. Semin Neurol 1998; 18: 327-36.

14. McGavern DB, Murray PD, Rivera-Quinones C, Schmelzer JD, Low PA, Rodriguez M. Axonal loss results in spinal cord atrophy, electrophysiological abnormalities and neurological deficits following demyelination in a chronic inflammatory model of multiple sclerosis. Brain 2000; 123 Pt 3: 519-31.

15. Miller DH, Grossman RI, Reingold SC, McFarland HF. The role of magnetic resonance techniques in understanding and managing multiple sclerosis. Brain 1998; 121: 3-24.

16. Ordidge RJ, Mansfield P, Lohman JA, Prime SB. Volume selection using gradients and selective pulses. Ann N Y Acad Sci 1987; 508: 376-85.

17. Rivera-Quinones C, McGavern D, Schmelzer JD, Hunter SF, Low PA, Rodriguez M. Absence of neurological deficits following extensive demyelination in a class I-deficient murine model of multiple sclerosis. Nat Med 1998; 4: 187-93.

18. Rudick RA, Fisher E, Lee JC, Simon J, Jacobs L. Use of the brain parenchymal fraction to measure whole brain atrophy in relapsing-remitting MS. Multiple Sclerosis Collaborative Research Group [In Process Citation]. Neurology 1999; 53: 1698-704.

19. Simon JH, Jacobs LD, Campion MK, Rudick RA, Cookfair DL, Herndon RM, et al. A longitudinal study of brain atrophy in relapsing multiple sclerosis. The Multiple Sclerosis Collaborative Research Group (MSCRG). Neurology 1999; 53: 139-48.

20. Stevenson VL, Leary SM, Losseff NA, Parker GJ, Barker GJ, Husmani Y, et al. Spinal cord atrophy and disability in MS: a longitudinal study. Neurology 1998; 51: 234-8.

21. Tourbah A, Stievenart JL, Gout O, Fontaine B, Liblau R, Lubetzki C, et al. Localized proton magnetic resonance spectroscopy in relapsing remitting versus secondary progressive multiple sclerosis. Neurology 1999; 53: 1091-7.

7.5 Preface to Manuscript 7

The results presented in Manuscripts 5 and 6 have helped establish the existence and importance of early axonal damage. However, the question remained as to what the mechanisms of this damage were. Evidence of transected axons can be found in lesions of varying activity, and the number of transected axons appears to be related to the degree of inflammation (Trapp et al., 1998), suggesting that axonal damage occurs as a bystander effect secondary to inflammatory demyelination. The diffuse axonal damage found in NAWM could then be postulated to result from wallerian degeneration of axons transected within lesions. While this undoubtedly contributes to axonal pathology in NAWM, it is not necessarily the only mechanism of diffuse axonal damage. To elucidate this question, we applied *in vivo* MRS, MTR and brain volume measurement techniques to assess diffuse axonal damage, myelin pathology and tissue loss in the brains of non-disabled MS patients with low cerebral lesion volume. The results of this work, described in Manuscript 7, "Diffuse axonal and tissue injury in patients with multiple sclerosis with low cerebral lesion load and no disability," suggest that, to some degree, diffuse axonal injury and tissue destruction occur independently of focal demyelination in the white matter, perhaps due to widespread but subtle inflammation or alternatively, due to invisible grey matter pathology and wallerian degeneration from grey matter lesions (Peterson et al., 2001). These results also confirm that diffuse axonal injury and myelin pathology are present even in MS patients with no disability. Cortical adaptations are likely responsible for maintaining the favourable clinical status of these patients.

7.6 Manuscript 7

Published in Archives of Neurology 2002;59(10):1565-71.

Diffuse Axonal and Tissue Injury in Patients with Multiple Sclerosis with Low Cerebral Lesion Load and No Disability

Nicola De Stefano*, MD, Sridar Narayanan^, MSc, Simon J. Francis^, BSc, Steve Smith~, Dphil, Marzia Mortilla*, MD, M. Carmela Tartaglia^, BSc, Maria L. Bartolozzi#, MD, Leonello Guidi#, MD, Antonio Federico*, MD and Douglas L. Arnold^, MD

*Institute of Neurological Sciences & NMR Centre, University of Siena, Italy
^Department of Neurology and Neurosurgery, Montreal Neurological Institute and Hospital, Quebec, Canada
~Centre for Functional Magnetic Resonance Imaging of the Brain, Dept. of Clinical Neurology, University of Oxford, UK
#Neurology Unit, Hospital of Empoli, Italy

Reprint requests and correspondence to:
Dr. Nicola De Stefano
Institute of Neurological Science
Viale Bracci 2
53100, Siena, Italy
Tel: +39-0577-233432
Fax: +39-0577-40327
Email: destefano@unisi.it

Running title: Diffuse axonal and tissue injury in MS

Key words: multiple sclerosis, axonal damage, magnetic resonance spectroscopy, magnetization transfer, brain atrophy

Acknowledgements
The study was supported by grants from the Multiple Sclerosis Society of Canada and the Medical Research Council of Canada. A.F was supported in part by a grant from MURST (Rome). NDS was supported by grants by the PAR grant of the University of Siena.

Abstract

Objective. To determine whether diffuse axonal and tissue injury is present in patients with definite multiple sclerosis (MS) who do not show clinically significant disability. **Background**. Although both *in situ* pathologic studies and *in vivo* MR investigations have shown that axonal injury can be significant in the early stages of MS, diffuse axonal injury is generally considered a secondary event that becomes meaningful only after substantial brain demyelination has occurred. Cerebral axonal damage can be specifically assessed *in vivo* by measuring levels of brain N-acetylaspartate (NAA, a specific index of axonal integrity detected by MR spectroscopy). Other new MR metrics such as magnetization transfer ratio (MTr) or computed estimation of brain volume can provide less specific indices of tissue damage. **Methods**. We measured brain NAA levels (normalized to creatine [Cr]), MTr values and cerebral volumes in patients with definite MS, who were selected to have low T_2-weighted MRI lesion volumes and no clinical disability, and also in age-matched normal subjects. **Results**. Values of central brain NAA/Cr and MTr in normal-appearing white matter were significantly lower in the MS patients than in normal controls ($p<0.0001$). In contrast, total brain volumes were not significantly different between these groups. Similar results were found for MS patients with very early disease (duration <3 years) and with particularly low cerebral T_2-weighted MRI lesion load (≤2 cc, i.e., <0.2% of the total volume of brain tissue). **Conclusions**. Results of our study indicate that cerebral NAA/Cr and MTr values are diffusely decreased in MS patients with very early disease, low demyelinating lesion load and no significant disability. This suggests that axonal/tissue injury begins very early in the course of MS and might be at least partially independent of focal cerebral demyelination. The absence of disability associated with this pathology suggests that it

can be initially compensated for by adaptive cortical reorganization. Values of NAA and total brain volume do not always change in parallel and both should be assessed to better estimate the true extent of axonal injury and loss.

Introduction

Multiple sclerosis (MS) is an inflammatory demyelinating disease of the central nervous system (CNS) that causes severe clinical disability in young adults. Traditionally, the CNS impairment and the related loss of function have been considered to be largely due to the demyelination and consequent delay or block of electrical conduction by axons that are otherwise substantially preserved. Over the past decade, however, *in vivo* magnetic resonance spectroscopy (MRS) studies of N-acetylaspartate (NAA) (Arnold et al., 1990a; Davie et al., 1994; De Stefano et al., 1995a; Gonen et al., 2000; Narayana et al., 1998) and *in situ* post-mortem studies (Ferguson et al., 1997; Silber and Sharief, 1999; Trapp et al., 1998) have demonstrated that sparing of axons is only relative in MS and injured or transected axons are a common finding in this disorder. This has led to a reconsideration of the role of axonal injury in MS and, in particular, its relevance to clinical disability (Bjartmar and Trapp, 2001; De Stefano et al., 1998).

There is an increasing agreement that axonal loss plays a major role in the pathology of MS (Waxman, 2000a) and there exists both *in vivo* and *in situ* evidence that axonal injury can be significant from the early stages of the disease. However, the mechanisms by which axonal injury occurs are not fully understood. For example, if axonal injury is simply a bystander effect secondary to demyelination, then the degree of axonal injury should be strongly related to the degree of demyelination. However, several experimental studies suggest that axonal injury and dysfunction in MS may be

independent of the degree of demyelination (Bitsch et al., 2000; Lightman et al., 1987; Rivera-Quinones et al., 1998; Youl et al., 1991; Zhu et al., 1999) and might begin to accumulate before clinical disability is evident (Mews et al., 1998).

Axonal injury inside and beyond MS lesions can be evaluated with MRS by measuring brain levels of NAA (Matthews et al., 1998) (an amino acid localized almost exclusively in neurons and axons in mature CNS (Bjartmar et al., 2000; Simmons et al., 1991) and, more indirectly, by means of other MR indices of tissue damage such as the magnetization transfer ratio (MTr) (van Waesberghe et al., 1999) or the computed estimation of brain volume (Rudick et al., 1999). In a number of recent studies, these MR indices have been demonstrated to be very sensitive in detecting early pathologic changes in MS brains (Brex et al., 2000; De Stefano et al., 2001; Filippi et al., 1999a; Fox et al., 2000; Narayana et al., 1998) . Thus, our goal in the present study was to assess *in vivo* whether diffuse cerebral axonal and tissue injury accrues in non-disabled MS patients with little evidence of focal demyelination. To do this, we evaluated values of NAA/Cr, MTr and total cerebral volumes in the brains of a selected group of patients with established MS who showed low volumes of cerebral T_2-weighted (T_2-W) lesions on conventional MRI and absence of disability at clinical examination.

Methods.

Study Population

Sixty patients (41 females and 19 males; age range = 18-54 years, mean = 35 years) with clinically definite MS (Poser et al., 1983), but without clinical disability (Expanded Disability Status Scale [EDSS] (Kurtzke, 1983): < 2) were chosen from the population followed at the MS clinics of the Montreal Neurological Hospital (MNH, n = 26) and of the Institute of Neurological Sciences of the University of Siena (n = 34).

Patients from both sites had a relatively short disease duration (range = 0.4-13 years, median = 2.7 years) and were all classified as having the relapsing remitting (RR) form of the disease. All patients were relapse- and drug treatment-free for at least one month before study entry. Both the Montreal Neurological Hospital (MNH) Ethics Committee and the Ethics Committee of the Faculty of Medicine of the University of Siena approved the study. Informed consent was obtained from all participating subjects.

MR examinations

All patients were examined using the same MR protocol, which included combined proton MRI and MRSI examinations of the brain. A transverse dual-echo, turbo spin-echo sequence (TR/TE1/TE2 = 2075/30/90 ms, 256x256 matrix, 1 signal average, 250mm field of view) yielding proton density (PD) and T2-weighted images with 50 contiguous 3mm slices was acquired parallel to the line connecting the anterior and posterior commissures. Subsequently, an MT sequence was performed acquiring two transverse T1-weighted, gradient echo images, one without (No Sat) and one with (Sat) MT saturation pulses (TR/TE=35 ms/10, 256x256 matrix, 1 signal average, 250mm field of view). This sequence yielded image volumes of 50 slices, 3mm thick, oriented to match the PD/T2 acquisition exactly. The MT pulse was a 1.2-millisecond on-resonance, $1\bar{2}1$ binomial pulse (radio-frequency field strength = 20 μT) placed just before each slice-selective excitation (Pike et al., 1993).

The MR images were used to select an intracranial volume of interest (VOI) for spectroscopy measuring approximately 100 mm anteroposterior x 20 mm craniocaudal x 90 mm left-right. This was centred on the corpus callosum to include mostly white matter of both hemispheres. Two-dimensional spectroscopic images were obtained using a 90^0-

180^0-180^0 pulse sequence (TR = 2000 ms, TE = 272 ms, 250mm field of view, 32x32 phase-encoding steps, 1 signal average per step) as previously described (De Stefano et al., 1995b). Water suppression was achieved by placing frequency-selective excitation pulses at the beginning of the MRSI sequence (Haase et al., 1985). Prior to the water-suppressed acquisition, another MRSI was acquired without water suppression (TR 850, TE 272, 250mm field of view, and 16x16 phase-encoding steps) to allow for B_0 homogeneity correction.

MR data analysis

Lesion Volumes and MT. T_2-W lesions were classified by a single observer (S.F.) employing a user-supervised thresholding technique. Lesion borders were determined primarily on PD-W images, but information from T2 and T1-weighted images were also considered. As the aim of the study was to study a population with established MS and low disease burden, MS patients were included only if they had a T_2-W lesion volume of less than 20cc (about 1.5% of the total brain tissue volume). This condition was met in 57 out of the 60 MS patients, and so data from 3 patients were excluded from the analysis. Percent difference MT ratio images were calculated on a voxel-by-voxel basis according to the equation: MTr = 100 x (noSat - Sat) /noSat (after thresholding above the noise background), as previously described (Pike et al., 1999). Once T_2-W lesions and normal appearing brain were classified, the MTr values of these regions were calculated. Only values of MTr in the normal-appearing white matter (NAWM) were considered here. These were calculated by taking consistent samples of white matter from five regions (corona radiata and centrum semiovale, frontal lobe, genu of the corpus callosum, splenium of the corpus callosum and occipital lobe) (Figure 7-9: Examples of MTr

percentage difference images of a healthy control illustrating (dark regions) the five white matter regions (corona radiata and centrum semiovale, frontal lobe, genu of the corpus callosum, splenium of the corpus callosum and occipital lobe) used for the calculation of white matter MTr values. In each subject, these ROIs span six slices, but only two are illustrated for brevity.). The MTr for NAWM was then obtained by averaging the mean MTr from each region. Values of MTr for normal white matter in the control group were obtained in the same way.

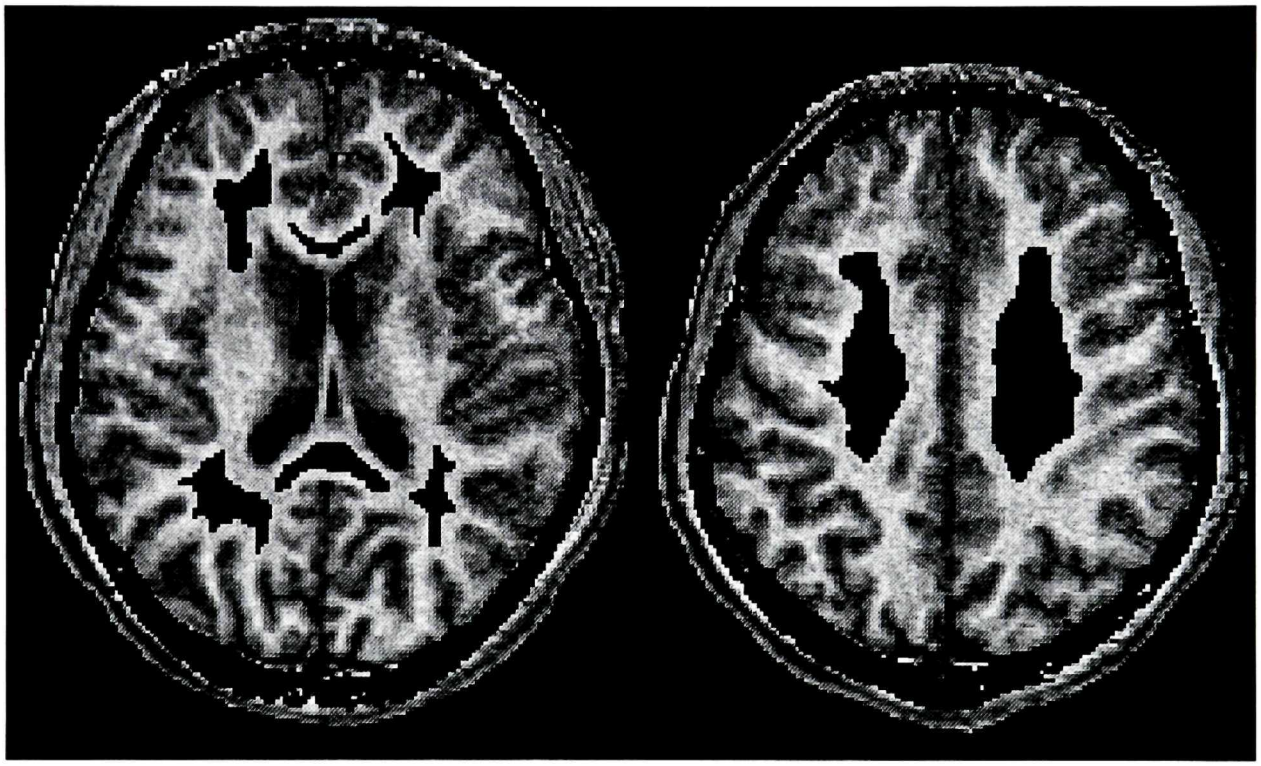

Figure 7-9: Examples of MTr percentage difference images of a healthy control illustrating (dark regions) the five white matter regions (corona radiata and centrum semiovale, frontal lobe, genu of the corpus callosum, splenium of the corpus callosum and occipital lobe) used for the calculation of white matter MTr values. In each subject, these ROIs span six slices, but only two are illustrated for brevity.

^{1}H-MRSI. Post-processing of the raw ^{1}H-MRSI data was performed as previously described (De Stefano et al., 2001). Metabolite resonance intensities of NAA were determined automatically from peak areas relative to a spline-corrected baseline and expressed as ratios to Cr (Figure 7-10). The resonance intensity of intravoxel Cr has been

widely used as internal standard in MR spectroscopy studies *in vivo*, as it is relatively equally present in all brain cells and tends to be stable in non-acute pathology (De Stefano et al., 1995a). Changes in apparent brain Cr concentrations have been reported in MS in recent MR spectroscopy studies attempting absolute quantitation. However, all current quantitative approaches have important limitations when applied to clinical studies and, in MS patients, have shown discrepant results in both lesions and normal appearing white matter (Davie et al., 1997; Husted et al., 1994; Narayana et al., 1998; Pan et al., 1996; Sarchielli et al., 1999; van Walderveen et al., 1999) . *In vitro* MR spectroscopy, which does not suffers from the limitations of *in vivo* quantitation, has demonstrated that Cr does not change in normal appearing tissues of MS brains (Davies et al., 1995). Thus, as lesions accounted for only a minimal portion of the large central VOI (mean = 1.5%, range 0% to 3%, data not shown) in this group of MS patients, changes in Cr, although possible, are unlikely and results were expressed as the intravoxel ratio of NAA to Cr. The relative NAA/Cr values of the whole brain region were obtained by averaging the NAA/Cr for all the voxels in the spectroscopic VOI for each subject. Spectra at the edges of the VOI affected by chemical shift artifacts associated with selective excitation were deleted before averaging.

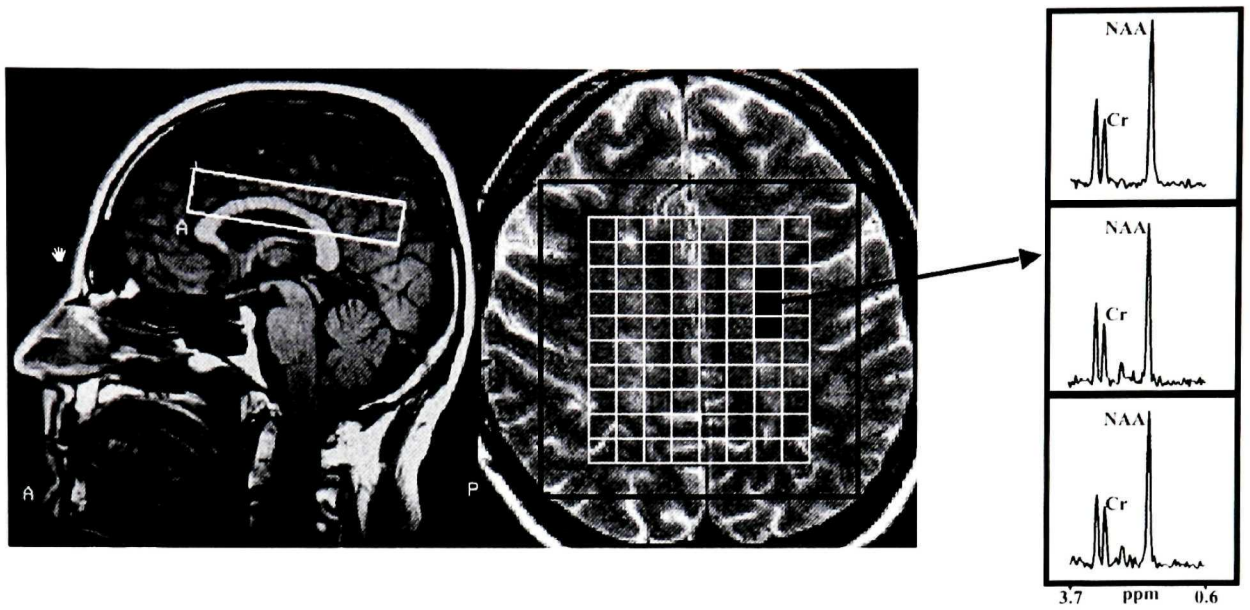

Figure 7-10: MRI images in sagittal and transversal orientation of a patient with multiple sclerosis illustrating the volume of interest (VOI) used for spectroscopic imaging (*right*) and an example of the resulting spectra (*left*) from deep white matter voxels (■). Voxels at the edge of the VOI were omitted from analysis since they can show artifactual relative amplitudes. The ratios of NAA to intravoxel Cr in the remaining voxels were averaged to obtain one value for each examination.

Total brain volumes. On T1-weighted MR images, normalized volumes of the whole of the brain parenchyma were measured using a method for brain volume measurement (the cross-sectional version of the SIENA software (Smith et al., 2001) [SIENAX]) (Figure 7-11). SIENAX uses a method to extract the brain and skull from the MR images, as previously described (Smith et al., 2002). A tissue segmentation program (Zhang et al., 2001) is then used to segment the extracted brain image into brain tissue, CSF and background, yielding an estimate of total brain tissue volume. The original MR images are registered to a canonical image in a standardized space (using the skull image to provide the scaling cue), a procedure that provides a spatial normalisation factor for each subject. The estimate of brain tissue volume for a subject is then multiplied by the normalisation factor to yield the normalised brain volume (NBV).

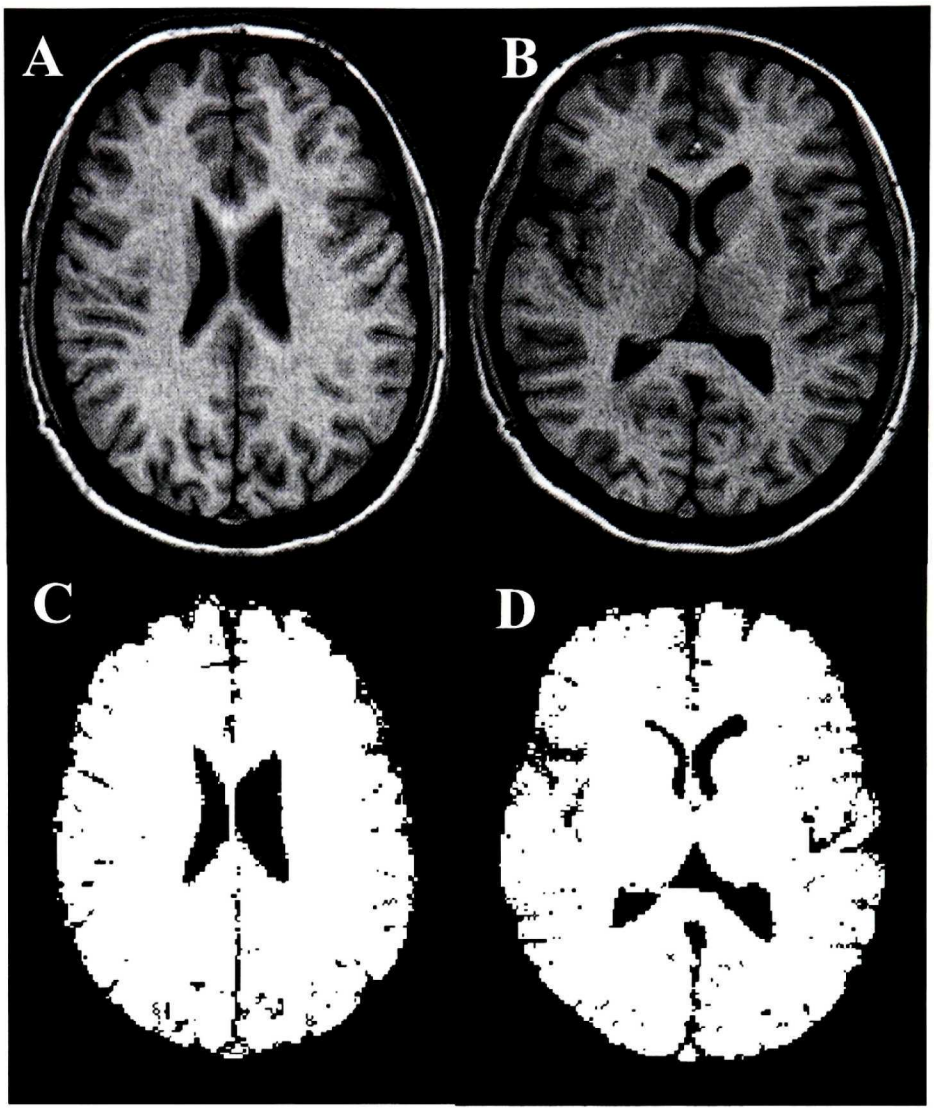

Figure 7-11: Typical transverse T1 weighted MR images of a normal control (**a, b**) and an illustrative example of the SIENAX output (**c, d**). The normalized brain volume includes only brain parenchyma and discards CSF and other non-brain tissues, yielding an estimate of total brain tissue volume (see Methods section).

Statistical Analysis

At each site, MR data of MS patients were compared to those of an age-matched normal control (NC) group: n = 21 for the Canadian site (13 females and 8 males; age range = 22-57 years, mean = 35 years) and 21 for the Italian site (12 females and 9 males; age range = 21-52 years, mean = 35 years). Comparisons were made between corresponding normal populations of each site (i.e., Siena-NC versus MNH-NC) and

between the whole group of MS patients and NC of both sites. In the latter case, MR data were standardized at each site using a z-score transformation relative to the corresponding control group. This avoided potentially spurious results due to machine-related differences between sites. The nonparametric Kruskal-Wallis one-way analysis of variance on ranks was used for the statistical analysis and values were considered significant at the 0.05 level. The SYSTAT software version 9 running on Windows (copyright SPSS Inc. 1998) was used to perform statistical calculations.

Results

The comparison of MR metrics from each center showed that NAA/Cr and NBV values of the NC groups were not different between the two sites (NAA/Cr in Siena-NC = 3.06±0.2, NAA/Cr in MNH-NC = 3.14±0.16; NBV in Siena-NC = 1467±41, NBV in MNH-NC = 1476±68, $p > 0.1$ for both). However, white matter MTr values were significantly lower in the Siena normal control group than in the MNH control group (MTr in Siena-NC = 35.3±0.9, MTr in MNH-NC = 36.4±0.4, $p<0.001$). This was probably due to the sensitivity of MTr measurements to subtle differences in hardware between MR scanners. However, as mentioned before, all MR data measurements were standardized at each site using a z-score transformation to correct for differences in NC at different sites and allow comparisons between the whole groups of NC and MS patients.

In the whole group of MS patients without clinical disability, the standardized levels of central brain NAA/Cr were significantly lower than those of normal controls ($p<0.0001$, Figure 7-12). Similarly, standardized MTr values were lower in the NAWM of MS patients than in the white matter of normal controls ($p<0.0001$, Figure 7-12). However, while the fully automated estimation of standardized NBV showed a trend

towards decreased values in the MS group with respect to the age-matched normal control group, this did not reach statistical significance (*p=0.07,* Figure 7-12).

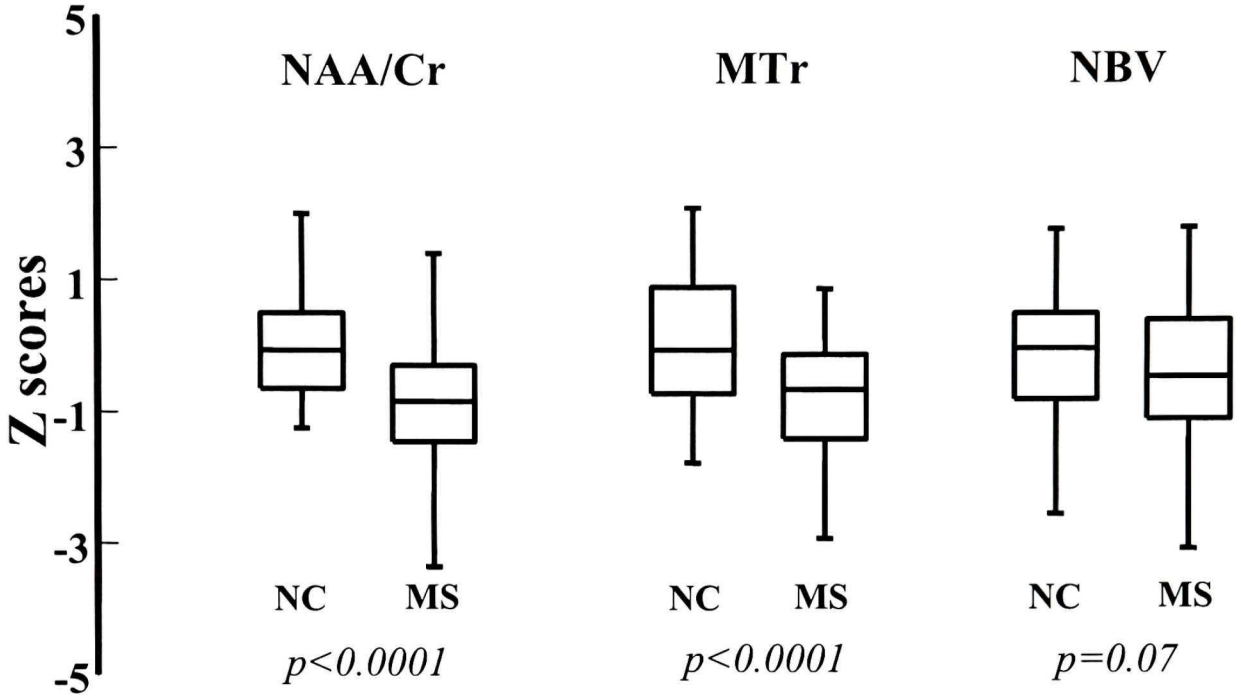

Figure 7-12: Box plots comparing the standardized MR measurements (NAA/Cr, MTr and NBV) in the whole group of MS patients (*right boxes,* **MS**) to a group of age-matched normal controls (*left boxes,* **NC**).

When similar analyses were performed in MS patients grouped according to duration of disease, the subgroup with very early disease duration (<3 years, number of patients = 36) still showed significantly lower brain NAA/Cr and MTr values than normal controls (*p<0.001 and p<0.005,* respectively; Figure 7-13). Furthermore, a subgroup (number = 26) of patients with minimal lesion volume (≤2 cc of T_2-W MRI lesions, about 0.15 % of the total brain volume) also showed significantly low NAA/Cr and MTr (*p<0.05,* for both; Figure 7-14). In both subgroups, patient values of NBV were not different from those of normal controls (*p> 0.5*).

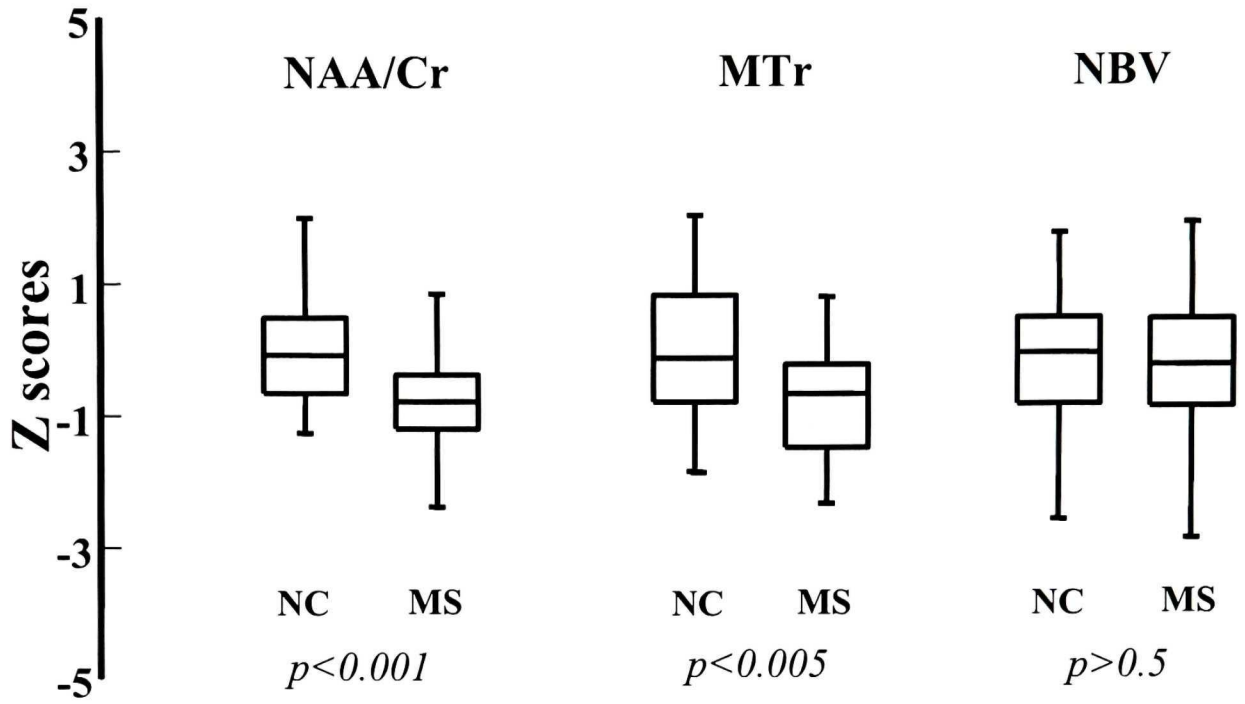

Figure 7-13: Box plots of the standardized MR measurements (NAA/Cr, MTr and NBV) in a selected patient subgroup (n=36) with short disease duration (< 3years, *right boxes,* **MS**)

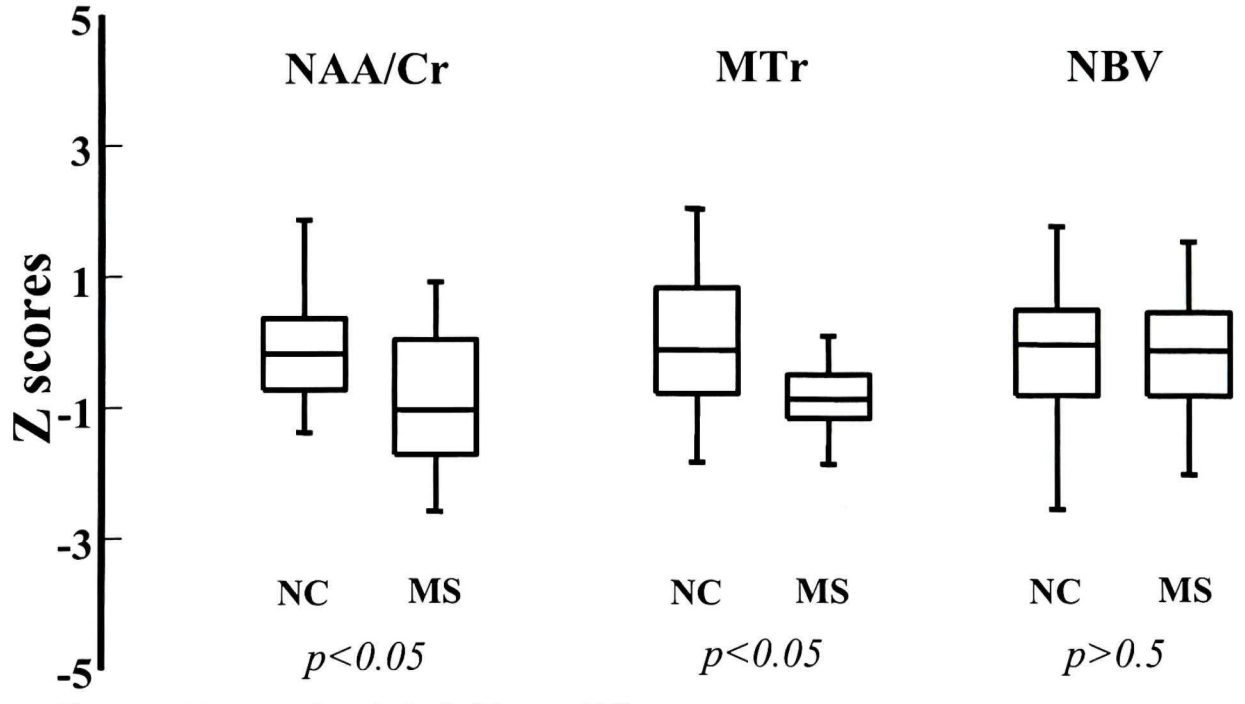

with respect to normal controls (*left boxes,* **NC**).

Figure 7-14: Box plots of the standardized MR measurements (NAA/Cr, MTr and NBV) in a selected patient subgroup (n=26) with very low volume (≤ 2 cc) of cerebral T_2-W MRI lesion (*right boxes,* **MS**) with respect to normal controls (*left boxes,* **NC**).

Discussion

As NAA is localized to neurons and axons in adult human brain (Moffett et al., 1991; Simmons et al., 1991) and correlates strongly with axonal density (Bjartmar et al., 2000; Nakano et al., 1998), levels of brain NAA detected by ^{1}H-MRSI can be interpreted, with some rare exceptions (Austin et al., 1991; Martin et al., 2001), as a surrogate of neuronal and axonal integrity. Large decreases of NAA have been observed in numerous spectroscopic studies inside and beyond MS lesions (Arnold et al., 1990a; Davie et al., 1994; Gonen et al., 2000; Matthews et al., 1998; Narayana et al., 1998) and have been demonstrated to occur, to a lesser degree, also in the NAWM of MS patients from the early disease stages (De Stefano et al., 2001). Results of the present study extend our and others' previous observations by showing that significant decreases of NAA can be detected in the NAWM of MS patients with very low disease duration, in the absence of substantial focal brain demyelination and before permanent clinical disability becomes evident. Given that NAA decreases were confined to demyelinating lesions in brains of patients with clinically isolated syndromes who subsequently developed MS (Brex et al., 1999), our observations also suggest that diffuse cerebral axonal injury rapidly accumulates in the early stages of the disease.

In addition to decreases of NAA/Cr, we also found decreases of MTr in NAWM in this group of non-disabled MS patients. MT imaging of the brain is based on the interactions between the free water protons and protons attached to macromolecules, and low MTr indirectly reflects tissue (matrix) damage (Dousset et al., 1992; McGowan et al., 1998). Several studies have demonstrated marked MTr reductions in lesions and NAWM of patients with MS (Filippi et al., 1995a; Filippi et al., 1999b). As recent studies have shown that focal MTr decreases in NAWM can occur before lesion appearance on

conventional MRI (Filippi et al., 1998; Goodkin et al., 1998; Pike et al., 2000), low MTr in the NAWM may reflect subtle, microscopic or molecular pathology of myelin in macroscopically normal white matter. Edema, astrocytic proliferation, perivascular inflammation and demyelination may all contribute to a decreased amount of water bound to macromolecules in the NAWM and, as a consequence, reduced MTr (Dousset et al., 1992). These pathological features, however, are not prominent in NAWM of early MS. A potential mechanism for subtle molecular alteration of myelin remains to be determined, but its presence is suggested by the fact that MTr values are decreased in the white matter of patients with MS who have completely normal conventional MRI of their brain (Filippi et al., 1999a). In addition, since MTr decreases in post-mortem brain of MS patients also correlates with axonal loss (van Waesberghe et al., 1999), it may be possible that membrane alterations associated with axonal injury also contribute to the decreases in MTr.

In this cross-sectional study, we did not find significant differences in NBV between MS patients and age- matched normal subjects, although there was a trend suggesting the presence of modest brain atrophy in the patient group as a whole. Using automated or semi-automated measures of brain volume, significant atrophy has been recently reported in the brains of MS patients in both cross-sectional and longitudinal studies (Fox et al., 2000; Liu et al., 1999; Losseff et al., 1996a; Rudick et al., 1999; Simon et al., 1999). In particular, significant brain volume losses have been found in MS patients with mild disability (Rudick et al., 1999), and significantly increased rates of ventricular enlargement have been reported both in early-stage MS patients (Luks et al., 2000) and patients with clinically isolated syndromes who later developed MS (Brex et al., 2000). Differences between these published data and those presented here could be

due to the lower sensitivity of cross-sectional measurements of total brain volume with respect to measurements of atrophy rates and the particularly mild clinical condition of the patients included in our study. Indeed, by showing a trend towards NBV decreases in MS patients with low lesion load and absence of disability, we suspect that the present results are not really in conflict with previous findings. Importantly, the differences in the relative magnitude of decreases in NAA/Cr and NBV in our study suggest that decreases in NAA (which can result from axonal dysfunction, decreases in axonal density and axonal loss), and decreases in NBV (which reflect a less pathologically specific tissue loss) do not always occur in parallel. Brain atrophy should be considered a later event that is not necessarily proportional to axonal injury. It follows that *in vivo* measures of *total* axonal injury and loss should be based on measurements of both decreases in brain volume and decreases of NAA density in remaining brain tissue.

By restricting our analysis to MS patients with low volume of T_2W lesion, we sought evidence that the abnormalities in NAWM could occur independently of focal demyelinating lesions. As reported in a number of previous studies (Filippi et al., 1995a; Fu et al., 1998; Goodkin et al., 1998; Narayana et al., 1998; Pike et al., 1999), decreases of NAA and MTr are more pronounced inside demyelinating lesions than in the NAWM of MS patients. However, the presence of significant decreases of NAA/Cr and MTr in our subgroup of patients in whom lesions occupied less than 0.2% of the total brain tissue (patient subgroup with ≤2 cc of T_2-W MRI lesions) suggest that axonal and tissue injury in MS might accrue, at least in part, independently of focal cerebral demyelination. Since Wallerian degeneration of axons traversing lesions is unlikely to account for much of the NAA decrease seen in these patients with very low lesion loads, the diffuse axonal abnormality must result from non-lesional abnomalities either associated with subtle

myelin pathology that is not visible on conventional MRI or with subtle axonal pathology, possibly due to the indirect effects of inflammation (Hohlfeld, 1997). The fact that diffuse decreases of NAA are to some extent reversible with immunomodulatory therapy (Narayanan et al., 2001) is consistent with a role for inflammation in these decreases.

How can widespread axonal injury occur in the brains of MS patients without clinical evidence of disability? Experimental and functional MRI data may provide an answer to this. Neurons can function as dynamic electrogenic machines with electroresponsive properties that change in response to pathological insults (Waxman, 2000c). However, in the initial disease stages, both adaptive cortical reorganization (by "unmasking" of latent pathways) (Waxman, 1997) and ion channel redistribution (Black et al., 1991; Moll et al., 1991) can achieve complete functional recovery and cause neuronal degeneration to remain subclinical. Development of permanent disability occurs later, when a threshold of axonal loss is reached and compensatory resources of the CNS are exhausted (Lee et al., 2000a; Reddy et al., 2000a; Trapp et al., 1999a). Thus, axonal injury does occur in MS, even in the absence of clinical disability, and can be detected and monitored by pathologically specific MR measures.

In conclusion, results of our study indicate that cerebral NAA/Cr and MTr values are diffusely decreased in brains of patients with early MS, minimal focal T_2W lesion volume and no clinical evidence of disability. This suggests that axonal/tissue injury might be to some extent independent of focal cerebral demyelination and is probably initially well compensated for by brain plasticity. Decreases of total brain volume do not necessarily occur in parallel with decreases of NAA and, therefore, both NAA and brain atrophy should be assessed to determine the true total extent of axonal injury and loss.

Reference List

1. Arnold DL, Matthews PM, Francis G, Antel J. Proton magnetic resonance spectroscopy of human brain in vivo in the evaluation of multiple sclerosis: assessment of the load of disease. Magnetic Resonance in Medicine 1990; 14: 154-159.
2. Austin SJ, Connelly A, Gadian DG, Benton JS, Brett EM. Localized 1H NMR spectroscopy in Canavan's disease: a report of two cases. Magn Reson Med 1991; 19: 439-45.
3. Bitsch A, Schuchardt J, Bunkowski S, Kuhlmann T, Bruck W. Acute axonal injury in multiple sclerosis. Correlation with demyelination and inflammation. Brain 2000; 123 (Pt 6): 1174-83.
4. Bjartmar C, Kidd G, Mork S, Rudick R, Trapp BD. Neurological disability correlates with spinal cord axonal loss and reduced N-acetyl aspartate in chronic multiple sclerosis patients. Ann Neurol 2000; 48: 893-901.
5. Bjartmar C, Trapp BD. Axonal and neuronal degeneration in multiple sclerosis: mechanisms and functional consequences. Curr Opin Neurol 2001; 14: 271-8.
6. Black JA, Felts P, Smith KJ, Kocsis JD, Waxman SG. Distribution of sodium channels in chronically demyelinated spinal cord axons: immuno-ultrastructural localization and electrophysiological observations. Brain Res 1991; 544: 59-70.
7. Brex PA, Gomez-Anson B, Parker GJ, Molyneux PD, Miszkiel KA, Barker GJ, et al. Proton MR spectroscopy in clinically isolated syndromes suggestive of multiple sclerosis. J Neurol Sci 1999; 166: 16-22.
8. Brex PA, Jenkins R, Fox NC, Crum WR, O'Riordan JI, Plant GT, et al. Detection of ventricular enlargement in patients at the earliest clinical stage of MS. Neurology 2000; 54: 1689-91.
9. Davie CA, Barker GJ, Thompson AJ, Tofts PS, McDonald WI, Miller DH. 1H magnetic resonance spectroscopy of chronic cerebral white matter lesions and normal appearing white matter in multiple sclerosis. J Neurol Neurosurg Psychiatry 1997; 63: 736-42.

10. Davie CA, Hawkins CP, Barker GJ, Brennan A, Tofts PS, Miller DH, et al. Serial proton magnetic resonance spectroscopy in acute multiple sclerosis lesions. Brain 1994; 117: 49-58.

11. Davies SE, Newcombe J, Williams SR, McDonald WI, Clark JB. High resolution proton NMR spectroscopy of multiple sclerosis lesions. J Neurochem 1995; 64: 742-8.

12. De Stefano N, Matthews PM, Antel JP, Preul M, Francis G, Arnold DL. Chemical pathology of acute demyelinating lesions and its correlation with disability. Annals of Neurology 1995a; 38: 901-909.

13. De Stefano N, Matthews PM, Arnold DL. Reversible decreases in N-acetylaspartate after acute brain injury. Magn Reson Med 1995b; 34: 721-7.

14. De Stefano N, Matthews PM, Fu L, Narayanan S, Stanley J, Francis GS, et al. Axonal damage correlates with disability in patients with relapsing- remitting multiple sclerosis. Results of a longitudinal magnetic resonance spectroscopy study. Brain 1998; 121: 1469-77.

15. De Stefano N, Narayanan S, Francis GS, Arnaoutelis R, Tartaglia MC, Antel JP, et al. Evidence of axonal damage in the early stages of multiple sclerosis and its relevance to disability. Arch Neurol 2001; 58: 65-70.

16. Dousset V, Grossman RI, Ramer KN, Schnall MD, Young LH, Gonzalez-Scarano F, et al. Experimental allergic encephalomyelitis and multiple sclerosis: lesion characterization with magnetization transfer imaging [published erratum appears in Radiology 1992 Jun;183(3):878]. Radiology 1992; 182: 483-91.

17. Ferguson B, Matyszak MK, Esiri MM, Perry VH. Axonal damage in acute multiple sclerosis lesions. Brain 1997; 120: 393-9.

18. Filippi M, Campi A, Dousset V, Baratti C, Martinelli V, Canal N, et al. A magnetization transfer imaging study of normal-appearing white matter in multiple sclerosis. Neurology 1995; 45: 478-82.

19. Filippi M, Rocca MA, Martino G, Horsfield MA, Comi G. Magnetization transfer changes in the normal appearing white matter precede the appearance of enhancing lesions in patients with multiple sclerosis. Ann Neurol 1998; 43: 809-14.

20. Filippi M, Rocca MA, Minicucci L, Martinelli V, Ghezzi A, Bergamaschi R, et al. Magnetization transfer imaging of patients with definite MS and negative conventional MRI. Neurology 1999a; 52: 845-8.

21. Filippi M, Tortorella C, Bozzali M. Normal-appearing white matter changes in multiple sclerosis: the contribution of magnetic resonance techniques. Mult Scler 1999b; 5: 273-82.

22. Fox NC, Jenkins R, Leary SM, Stevenson VL, Losseff NA, Crum WR, et al. Progressive cerebral atrophy in MS: a serial study using registered, volumetric MRI [see comments]. Neurology 2000; 54: 807-12.

23. Fu L, Matthews PM, De Stefano N, Worsley KJ, Narayanan S, Francis GS, et al. Imaging axonal damage of normal-appearing white matter in multiple sclerosis. Brain 1998; 121: 103-13.

24. Gonen O, Catalaa I, Babb JS, Ge Y, Mannon LJ, Kolson DL, et al. Total brain N-acetylaspartate: a new measure of disease load in MS. Neurology 2000; 54: 15-9.

25. Goodkin DE, Rooney WD, Sloan R, Bacchetti P, Gee L, Vermathen M, et al. A serial study of new MS lesions and the white matter from which they arise. Neurology 1998; 51: 1689-97.

26. Haase A, Frahm J, Hanicke W, Matthaei D. 1H NMR chemical shift selective (CHESS) imaging. Phys Med Biol 1985; 30: 341-4.

27. Hohlfeld R. Biotechnological agents for the immunotherapy of multiple sclerosis. Principles, problems and perspectives. Brain 1997; 120 (Pt 5): 865-916.

28. Husted CA, Goodin DS, Hugg JW, Maudsley AA, Tsuruda JS, de Bie SH, et al. Biochemical alterations in multiple sclerosis lesions and normal-appearing white matter detected by in vivo 31P and 1H spectroscopic imaging. Annals of Neurology 1994; 36: 157-165.

29. Kurtzke JF. Rating neurologic impairment in multiple sclerosis: an expanded disability status scale (EDSS). Neurology 1983; 33: 1444-1452.

30. Lee M, Reddy H, Johansen-Berg H, Pendlebury S, Jenkinson M, Smith S, et al. The motor cortex shows adaptive functional changes to brain injury from multiple sclerosis. Ann Neurol 2000; 47: 606-13.

31. Lightman S, McDonald WI, Bird AC, Francis DA, Hoskins A, Batchelor JR, et al. Retinal venous sheathing in optic neuritis. Its significance for the pathogenesis of multiple sclerosis. Brain 1987; 110 (Pt 2): 405-14.

32. Liu C, Edwards S, Gong Q, Roberts N, Blumhardt LD. Three dimensional MRI estimates of brain and spinal cord atrophy in multiple sclerosis. J Neurol Neurosurg Psychiatry 1999; 66: 323-30.

33. Losseff NA, Wang L, Lai HM, Yoo DS, Gawne-Cain ML, McDonald WI, et al. Progressive cerebral atrophy in multiple sclerosis. A serial MRI study. Brain 1996; 119: 2009-19.

34. Luks TL, Goodkin DE, Nelson SJ, Majumdar S, Bacchetti P, Portnoy D, et al. A longitudinal study of ventricular volume in early relapsing-remitting multiple sclerosis. Mult Scler 2000; 6: 332-7.

35. Martin E, Capone A, Schneider J, Hennig J, Thiel T. Absence of N-acetylaspartate in the human brain: impact on neurospectroscopy? Ann Neurol 2001; 49: 518-21.

36. Matthews PM, De Stefano N, Narayanan S, Francis GS, Wolinsky JS, Antel JP, et al. Putting magnetic resonance spectroscopy studies in context: axonal damage and disability in multiple sclerosis. Semin Neurol 1998; 18: 327-36.

37. McGowan JC, Filippi M, Campi A, Grossman RI. Magnetisation transfer imaging: theory and application to multiple sclerosis. J Neurol Neurosurg Psychiatry 1998; 64 Suppl 1: S66-9.

38. Mews I, Bergmann M, Bunkowski S, Gullotta F, Bruck W. Oligodendrocyte and axon pathology in clinically silent multiple sclerosis lesions. Mult Scler 1998; 4: 55-62.

39. Moffett JR, Namboodiri MAA, Cangro CB, Neale JH. Immunohistochemical localization of N-acetylaspartate in rat brain. NeuroReport 1991; 2: 131-134.

40. Moll C, Mourre C, Lazdunski M, Ulrich J. Increase of sodium channels in demyelinated lesions of multiple sclerosis. Brain Res 1991; 556: 311-6.

41. Nakano M, Ueda H, Li JY, Matsumoto M, Yanagihara T. Measurement of regional N-acetylaspartate after transient global ischemia in gerbils with and without ischemic tolerance: an index of neuronal survival. Ann Neurol 1998; 44: 334-40.

42. Narayana PA, Doyle TJ, Lai D, Wolinsky JS. Serial proton magnetic resonance spectroscopic imaging, contrast- enhanced magnetic resonance imaging, and quantitative lesion volumetry in multiple sclerosis. Ann Neurol 1998; 43: 56-71.

43. Narayanan S, De Stefano N, Francis GS, Arnaoutelis R, Caramanos Z, Collins DL, et al. Axonal metabolic recovery in multiple sclerosis patients treated with interferon beta-1b. J Neurol 2001; 248: 979-86.

44. Pan JW, Hetherington HP, Vaughan JT, Mitchell G, Pohost GM, Whitaker JN. Evaluation of multiple sclerosis by 1H spectroscopic imaging at 4.1 T. Magn Reson Med 1996; 36: 72-7.

45. Pike GB, de Stefano N, Narayanan S, Francis GS, Antel JP, Arnold DL. Combined magnetization transfer and proton spectroscopic imaging in the assessment of pathologic brain lesions in multiple sclerosis. AJNR Am J Neuroradiol 1999; 20: 829-37.

46. Pike GB, De Stefano N, Narayanan S, Worsley KJ, Pelletier D, Francis GS, et al. Multiple sclerosis: magnetization transfer MR imaging of white matter before lesion appearance on T2-weighted images. Radiology 2000; 215: 824-30.

47. Pike GB, Glover GH, Hu BS, Enzmann DR. Pulsed magnetization transfer spin-echo MR imaging. J Magn Reson Imaging 1993; 3: 531-9.

48. Poser CM, Paty DW, Scheinberg L, McDonald WI, Floyd AD, Ebers GC, et al. New diagnostic criteria for multiple sclerosis: Guidelines for research protocols. Annals of Neurology 1983; 13: 227-231.

49. Reddy H, Narayanan S, Arnoutelis R, Jenkinson M, Antel J, Matthews PM, et al. Evidence for adaptive functional changes in the cerebral cortex with axonal injury from multiple sclerosis. Brain 2000; 123: 2314-20.

50. Rivera-Quinones C, McGavern D, Schmelzer JD, Hunter SF, Low PA, Rodriguez M. Absence of neurological deficits following extensive demyelination in a class I-deficient murine model of multiple sclerosis. Nat Med 1998; 4: 187-93.

51. Rudick RA, Fisher E, Lee JC, Simon J, Jacobs L. Use of the brain parenchymal fraction to measure whole brain atrophy in relapsing-remitting MS. Multiple Sclerosis Collaborative Research Group [In Process Citation]. Neurology 1999; 53: 1698-704.

52. Sarchielli P, Presciutti O, Pelliccioli GP, Tarducci R, Gobbi G, Chiarini P, et al. Absolute quantification of brain metabolites by proton magnetic resonance spectroscopy in normal-appearing white matter of multiple sclerosis patients [In Process Citation]. Brain 1999; 122: 513-21.

53. Silber E, Sharief MK. Axonal degeneration in the pathogenesis of multiple sclerosis. J Neurol Sci 1999; 170: 11-8.

54. Simmons ML, Frondoza CG, Coyle JT. Immunocytochemical localization of N-acetyl-aspartate with monoclonal antibodies. Neuroscience 1991; 45: 37-45.

55. Simon JH, Jacobs LD, Campion MK, Rudick RA, Cookfair DL, Herndon RM, et al. A longitudinal study of brain atrophy in relapsing multiple sclerosis. The Multiple Sclerosis Collaborative Research Group (MSCRG). Neurology 1999; 53: 139-48.

56. Smith SM, De Stefano N, Jenkinson M, Matthews PM. Normalized accurate measurement of longitudinal brain change. J Comput Assist Tomogr 2001; 25: 466-75.

57. Smith SM, Zhang Y, Jenkinson M, Chen JT, Matthews PM, Federico A, et al. Accurate, robust and automated longitudinal and cross-sectional brain change analysis. NeuroImage 2002; In Press.

58. Trapp BD, Bo L, Mork S, Chang A. Pathogenesis of tissue injury in MS lesions. J Neuroimmunol 1999; 98: 49-56.

59. Trapp BD, Peterson J, Ransohoff RM, Rudick R, Mork S, Bo L. Axonal transection in the lesions of multiple sclerosis [see comments]. N Engl J Med 1998; 338: 278-85.

60. van Waesberghe JH, Kamphorst W, De Groot CJ, van Walderveen MA, Castelijns JA, Ravid R, et al. Axonal loss in multiple sclerosis lesions: magnetic resonance imaging insights into substrates of disability. Ann Neurol 1999; 46: 747-54.

61. van Walderveen MA, Barkhof F, Pouwels PJ, van Schijndel RA, Polman CH, Castelijns JA. Neuronal damage in T1-hypointense multiple sclerosis lesions demonstrated in vivo using proton magnetic resonance spectroscopy. Ann Neurol 1999; 46: 79-87.

62. Waxman SG. Molecular remodeling of neurons in multiple sclerosis: what we know, and what we must ask about brain plasticity in demyelinating diseases. Adv Neurol 1997; 73: 109-20.

63. Waxman SG. Do 'demyelinating' diseases involve more than myelin? Nat Med 2000a; 6: 738-9.

64. Waxman SG. The neuron as a dynamic electrogenic machine: modulation of sodium-channel expression as a basis for functional plasticity in neurons. Philos Trans R Soc Lond B Biol Sci 2000b; 355: 199-213.

65. Youl BD, Turano G, Miller DH, Towell AD, MacManus DG, Moore SG, et al. The pathophysiology of acute optic neuritis. An association of gadolinium leakage with clinical and electrophysiological deficits. Brain 1991; 114 (Pt 6): 2437-50.

66. Zhang Y, Brady M, Smith S. Segmentation of brain MR images through a hidden Markov random field model and the expectation maximization algorithm. (Abstract). IEEE Transactions on Biomedical Imaging 2001; 20: 45-57.

67. Zhu B, Moore GR, Zwimpfer TJ, Kastrukoff LF, Dyer JK, Steeves JD, et al. Axonal cytoskeleton changes in experimental optic neuritis. Brain Res 1999; 824: 204-17.

Chapter 8

Summary and Conclusions

The preceding chapters have illustrated the value of multiple magnetic resonance techniques as *in vivo* windows on the pathology and pathophysiology of multiple sclerosis. Each modality provides a different view of the disease processes in MS, and each has its strengths and weaknesses with regards to pathological specificity, sensitivity, resolution and relevance to clinical deficits. Central to this thesis has been the prime role of proton MRS for *in vivo* monitoring of axonal functional integrity via measurement of N-acetylaspartate levels in the brain. The early work of Arnold and colleagues has been seminal in "rediscovering" the importance of axonal pathology and its relationship to disability in MS (Arnold et al., 1990a; Arnold et al., 1991; Arnold et al., 1992; Matthews et al., 1991a). Carrying on the tradition, the work presented in Chapter 1 employed image processing techniques borrowed from PET analysis and applied in a novel way to MRSI and segmented lesion data to demonstrate widespread decreases of NAA/Cr extending beyond regions with high lesion probability into areas of low lesion probability across a group of MS patients. Averaging the MRSI data in a standardized, anatomically based coordinate system and generating lesion probability distributions in stereotaxic space

allowed us to visualize aspects of the data that would have not been readily apparent in individual metabolite and lesion maps. The results of this analysis also demonstrated that the greater axonal damage per unit lesion volume in SP patients vs. RR patients reported previously by our group (Matthews et al., 1996) was not due to differences in the distribution of lesions between the two groups. NAA decrease in NAWM was subsequently confirmed by our group using sophisticated statistical modeling techniques developed specifically for the purpose (Fu et al., 1998). This paper also showed that the NAWM of the SP patients exhibited greater axonal injury than the NAWM of RR patients, thus explaining the greater axonal damage per unit lesion volume found in the SP group (Matthews et al., 1996). These and previous MRS studies appear to have helped motivate pathologists to develop new methodologies for detecting axonal damage in pathological specimens, and consequently establish conclusively that significant axonal damage does occur in MS (Ferguson et al., 1997; Trapp et al., 1998; Waxman, 1998).

NAA decreases have been shown to be partially reversible in acute demyelinating lesions (Davie et al., 1994; De Stefano et al., 1995a; De Stefano et al., 1995b). Studies in culture (Matthews et al., 1995) and in animals (Dautry et al., 2000) have demonstrated that NAA concentrations can be induced to decline by interfering with axonal metabolism, and subsequently recover when the interference is removed. We questioned in Chapter 4 whether part of the chronically decreased NAA seen in NAWM could be due to chronically dysfunctional axons. We tested this hypothesis by longitudinally following a small group of patients starting interferon β-1b therapy with MRI and MRSI, and showed that chronic decreases of NAA could be reversed in these patients. The issue of whether this could be due to resolution of edema was addressed by measuring the change in brain volume over the study period using the brain to intracranial capacity ratio

developed by Louis Collins (Collins et al., 2000). The 1% change in volume over the 1-year study period was comparable to previous reports of brain atrophy in RRMS, and was not of sufficient magnitude to account for the recovery of NAA/Cr. A recent combined pathology and HPLC post-mortem study found reduced NAA even in myelinated axons in paralyzed patients, corroborating the interpretation of MRS data suggesting that axons can be chronically functionally impaired (Bjartmar et al., 2000).

Functional MRI is an advanced MR technique that allows one to image activation of cortical regions in response to a functional task. The most common technique utilizes the blood oxygenation level-dependent (BOLD) response to image localized regions of increased blood flow that occur in response to increased neuronal energy demand. The increased blood flow overcompensates for the increased energy demand, leading to an increase in the ratio of oxyhemoglogin to deoxyhemoglobin. The resulting change in local magnetic susceptibility leads to a small increase in signal on T2*-weighted imaging. Activations are regions of statistically significant, stimulus-correlated changes of MR intensity between baseline and active task conditions. This powerful, non-invasive probe of neuronal function has been used extensively in neuropsychological experiments and, to a lesser extent, in studies of cortical adaptations to stroke. The study presented in Chapter 5 was one of the first applications of this technique to study cortical responses to white matter injury in MS. The strength of the study was the serial acquisition of combined fMRI, MRSI and clinical data to elucidate the temporal evolution of cortical adaptation to axonal injury from a new, large, evolving plaque producing major motor impairment. The results clearly demonstrated that cortical adaptations could return motor function to the patient before recovery of axonal injury. Subsequent studies in chronic patients showed that progressively greater recruitment of alternate pathways could maintain motor

function in the face of increasing axonal impairment. The implications are that axonal damage can be accumulating in early MS even in patients exhibiting full recovery from relapses. Therapies aimed at reducing inflammatory demyelination as well as improving axonal survival may have the greatest long-term benefit early in the disease.

Axonal damage within lesions is likely the byproduct of the tissue-destructive factors released in the process of inflammatory demyelination, at least in active and chronic-active plaques (Trapp et al., 1998). The mechanisms for axonal injury in NAWM are less clear, but the fact that "demyelination-weighted lesion volume" correlated well with NAWM NAA/Cr in the combined MRS and quantitative MT study presented in Chapter 6 suggest that wallerian degeneration and chronic dysfunction of axons damaged within lesions makes a significant contribution. However, given that 40% of the variation of NAWM NAA/Cr was unexplained by demyelination-weighted lesion volume, this is unlikely to be the only mechanism for axonal damage in NAWM. The finding of significantly low central brain NAA/Cr and NAWM MTR even in patients with no disability and trivial lesion burden (Manuscript 7) suggest that a mechanism for direct pathology of white matter may exist in MS, independent of focal, macroscopic lesions of white matter. The lack of brain atrophy in this low lesion load subgroup further suggests that what we are observing is diffuse axonal dysfunction, perhaps due to subtle but widespread myelin pathology or inflammation. Alternatively, it is possible that wallerian degeneration of axons damaged in invisible grey matter lesions contribute to the observed diffuse white matter abnormalities, to the extent that grey matter lesions do not contribute to global atrophy. The development of MRI techniques to directly visualize grey matter lesions, or image processing techniques to estimate cortical atrophy (Chen et al., 2002)

would help resolve this issue. Again, these observations illustrate the additional insight gained by using multiple *in vivo* tools to investigate the pathophysiology of MS.

The close relationship between central brain NAA/Cr and EDSS in the early stages of MS observed in Manuscripts 5 and 6 probably largely reflects the clinical impact of chronic axonal dysfunction more than outright axonal loss. In the later stages of MS, characterized by a decrease in inflammatory activity, the increased clinical relevance of spinal cord atrophy suggests that chronically injured axons eventually degenerate, perhaps due to insufficient trophic support. This new perspective of progressive MS as a neurodegenerative disorder has been driven to a significant extent by recent findings from neuroimaging as well as from pathology (Bjartmar and Trapp, 2001), and has important implications for the design of new therapies aimed at slowing the inexorable clinical decline of MS patients. Study of the mechanisms of progression will likely come to the forefront of MS research in the coming years. The combined application of multiple advanced magnetic resonance acquisition and analysis techniques will play a crucial role in future studies of multiple sclerosis.

Bibliography

1. Allen IV, Glover G, Anderson R. Abnormalities in the macroscopically normal white matter in cases of mild or spinal multiple sclerosis (MS). Acta Neuropathol Suppl 1981; 7: 176-8.
2. Allen IV, McKeown SR. A histological, histochemical and biochemical study of the macroscopically normal white matter in multiple sclerosis. J Neurol Sci 1979; 41: 81-91.
3. Arnold DL. Reversible reduction of N-acetylaspartate after acute central nervous system damage. Society of Magnetic Resonance in Medicine. Vol 1, 1992: 643.
4. Arnold DL, De Stefano N, Narayanan S, Matthews PM. Proton MR spectroscopy in multiple sclerosis. Neuroimaging Clin N Am 2000; 10: 789-98 ,ix-x.
5. Arnold DL, Matthews PM, Francis G, Antel J. Proton magnetic resonance spectroscopy of human brain in vivo in the evaluation of multiple sclerosis: assessment of the load of disease. Magnetic Resonance in Medicine 1990a; 14: 154-159.
6. Arnold DL, Matthews PM, Francis G, Antel J. Magnetic resonance spectroscopic imaging (MRSI) allows metabolic characterization of brain lesions. MedicaMundi 1991; 36: 111-116.
7. Arnold DL, Matthews PM, Francis GS, O'Connor J, Antel JP. Proton magnetic resonance spectroscopic imaging for metabolic characterization of demyelinating plaques. Ann Neurol 1992; 31: 235-41.
8. Arnold DL, Narayanan S, De Stefano N, Reddy H, Matthews PM. Magnetic resonance spectroscopy of multiple sclerosis: Imaging axonal damage. In: Kappos L, Kesselring J, Radu EW and Johnson K, editors. Multiple Sclerosis: Understanding Tissue Destruction and Repair and New Immunological Treatments. London: Martin Duntz Ltd, 2001: 77-90.

9. Arnold DL, Shoubridge EA, Villemure JG, Feindel W. Proton and phosphorus magnetic resonance spectroscopy of human astrocytomas *in vivo*. Preliminary observations on tumor grading. NMR Biomed 1990b; 3: 184-189.

10. Austin SJ, Connelly A, Gadian DG, Benton JS, Brett EM. Localized 1H NMR spectroscopy in Canavan's disease: a report of two cases. Magn Reson Med 1991; 19: 439-45.

11. Barkhof F, Filippi M, Miller DH, Tofts P, Kappos L, Thompson AJ. Strategies for optimizing MRI techniques aimed at monitoring disease activity in multiple sclerosis treatment trials. J Neurol 1997; 244: 76-84.

12. Barnes D, Munro PM, Youl BD, Prineas JW, McDonald WI. The longstanding MS lesion. A quantitative MRI and electron microscopic study. Brain 1991; 114 (Pt 3): 1271-80.

13. Bates TE, Strangward M, Keelan J, Davey GP, Munro PM, Clark JB. Inhibition of N-acetylaspartate production: implications for 1H MRS studies in vivo. Neuroreport 1996; 7: 1397-400.

14. Becher B, Giacomini PS, Pelletier D, McCrea E, Prat A, Antel JP. Interferon-gamma secretion by peripheral blood T-cell subsets in multiple sclerosis: correlation with disease phase and interferon-beta therapy. Ann Neurol 1999; 45: 247-50.

15. Bhakoo KK, Pearce D. In vitro expression of N-acetyl aspartate by oligodendrocytes: implications for proton magnetic resonance spectroscopy signal in vivo. Journal of Neurochemistry 2000; 74: 254-62.

16. Birken DL, Oldendorf WH. N-acetyl-L-aspartic acid: a literature review of a compound prominent in 1H-NMR spectroscopic studies of brain. Neurosci Biobehav Rev 1989; 13: 23-31.

17. Bitsch A, Schuchardt J, Bunkowski S, Kuhlmann T, Bruck W. Acute axonal injury in multiple sclerosis. Correlation with demyelination and inflammation. Brain 2000; 123 (Pt 6): 1174-83.

18. Bjartmar C, Battistuta J, Terada N, Dupree E, Trapp BD. N-acetylaspartate is an axon-specific marker of mature white matter in vivo: A biochemical and immunohistochemical study on the rat optic nerve. Annals of Neurology 2002; 51: 51-58.

19. Bjartmar C, Kidd G, Mork S, Rudick R, Trapp BD. Neurological disability correlates with spinal cord axonal loss and reduced N-acetyl aspartate in chronic multiple sclerosis patients. Ann Neurol 2000; 48: 893-901.

20. Bjartmar C, Trapp BD. Axonal and neuronal degeneration in multiple sclerosis: mechanisms and functional consequences. Curr Opin Neurol 2001; 14: 271-8.

21. Black JA, Felts P, Smith KJ, Kocsis JD, Waxman SG. Distribution of sodium channels in chronically demyelinated spinal cord axons: immuno-ultrastructural localization and electrophysiological observations. Brain Res 1991; 544: 59-70.

22. Brenner RE, Munro PM, Williams SC, Bell JD, Barker GJ, Hawkins CP, et al. The proton NMR spectrum in acute EAE: the significance of the change in the Cho:Cr ratio. Magnetic Resonance in Medicine 1993; 29: 737-745.

23. Brex PA, Gomez-Anson B, Parker GJ, Molyneux PD, Miszkiel KA, Barker GJ, et al. Proton MR spectroscopy in clinically isolated syndromes suggestive of multiple sclerosis. J Neurol Sci 1999; 166: 16-22.

24. Brex PA, Jenkins R, Fox NC, Crum WR, O'Riordan JI, Plant GT, et al. Detection of ventricular enlargement in patients at the earliest clinical stage of MS. Neurology 2000; 54: 1689-91.

25. Bruhn H, Frahm J, Merboldt KD, Hanicke W, Hanefeld F, Christen HJ, et al. Multiple sclerosis in children: cerebral metabolic alterations monitored by localized proton magnetic resonance spectroscopy in vivo. Ann Neurol 1992; 32: 140-50.

26. Cao Y, D'Olhaberriague L, Vikingstad EM, Levine SR, Welch KM. Pilot study of functional MRI to assess cerebral activation of motor function after poststroke hemiparesis. Stroke 1998; 29: 112-22.

27. Caramia MD, Iani C, Bernardi G. Cerebral plasticity after stroke as revealed by ipsilateral responses to magnetic stimulation. Neuroreport 1996; 7: 1756-60.

28. Cendes F, Andermann F, Preul MC, Arnold DL. Lateralization of temporal lobe epilepsy based on regional metabolic abnormalities in proton magnetic resonance spectroscopic images. Annals of Neurology 1994; 35: 211-216.

29. Chang A, Tourtellotte WW, Rudick R, Trapp BD. Premyelinating oligodendrocytes in chronic lesions of multiple sclerosis. N Engl J Med 2002; 346: 165-73.

30. Charcot M. Histologie de la sclerose en plaques. Gaz Hosp 1868; 141: 554-5, 557-8.

31. Chen JT, Smith SM, Arnold DL, Matthews PM. Quantification of change in cortical grey matter thickness in multiple sclerosis. Tenth Annual Meeting of the International Society for Magnetic Resonance in Medicine. Honolulu, HI, USA: ISMRM, 2002.

32. Cifelli A, Matthews PM. Cerebral plasticity in multiple sclerosis: insights from fMRI. Mult Scler 2002; 8: 193-9.

33. Clanet M, Berry I, Boulanouar K. Functional imaging in multiple sclerosis. International MS Journal 1997; 4: 26-32.

34. Collins DL, Narayanan S, Caramanos Z, De Stefano N, Tartaglia MC, Arnold DL. Relation of cerebral atrophy in multiple sclerosis to severity of disease and axonal injury. American Academy of Neurology, 52nd Annual Meeting, San Diego, CA. Neurology 2000; 54 Supp. 3: A17.

35. Compston A. Future options for therapies to limit damage and enhance recovery. Semin Neurol 1998; 18: 405-14.

36. Dalton CM, Ramani A, Wheeler-Kingshott CA, Barker GJ, Miller DH, Tofts PS. Bound water magnetization transfer measurements in patients with multiple sclerosis: a pilot study. ISMRM. Honolulu, HI, 2002.

37. Dautry C, Vaufrey F, Brouillet E, Bizat N, Henry PG, Conde F, et al. Early N-acetylaspartate depletion is a marker of neuronal dysfunction in rats and primates chronically treated with the mitochondrial toxin 3- nitropropionic acid. J Cereb Blood Flow Metab 2000; 20: 789-99.

38. Davie CA, Barker GJ, Thompson AJ, Tofts PS, McDonald WI, Miller DH. 1H magnetic resonance spectroscopy of chronic cerebral white matter lesions and normal appearing white matter in multiple sclerosis. J Neurol Neurosurg Psychiatry 1997; 63: 736-42.

39. Davie CA, Barker GJ, Webb S, Tofts PS, Thompson AJ, Harding AE, et al. Persistent functional deficit in multiple sclerosis and autosomal dominant cerebellar ataxia is associated with axon loss. Brain 1995; 118: 1583-1592.

40. Davie CA, Hawkins CP, Barker GJ, Brennan A, Tofts PS, Miller DH, et al. Serial proton magnetic resonance spectroscopy in acute multiple sclerosis lesions. Brain 1994; 117: 49-58.

41. Davie CA, Silver NC, Barker GJ, Tofts PS, Thompson AJ, McDonald WI, et al. Does the extent of axonal loss and demyelination from chronic lesions in multiple sclerosis correlate with the clinical subgroup? [In Process Citation]. J Neurol Neurosurg Psychiatry 1999; 67: 710-5.

42. Davies SE, Newcombe J, Williams SR, McDonald WI, Clark JB. High resolution proton NMR spectroscopy of multiple sclerosis lesions. J Neurochem 1995; 64: 742-8.

43. Dawson-Saunders B, Trapp RG. Basic and Clinical Biostatistics. Norwalk, CT: Appleton and Lange, 1990.

44. de Beer R, Van den Boogaart A, van Ormondt D, Pijnappel WW, den Hollander JA, Marien AJ, et al. Application of time-domain fitting in the quantification of in vivo 1H spectroscopic imaging data sets. NMR in Biomedicine 1992; 5: 171-178.

45. de Beer R, van Ormondt D. Analysis of NMR data using time domain fitting procedures. NMR Basic Principles and Progress. Vol 26. Berlin: Springer-Verlag, 1992: 204-248.

46. De Stefano N, Matthews PM, Antel JP, Preul M, Francis G, Arnold DL. Chemical pathology of acute demyelinating lesions and its correlation with disability. Annals of Neurology 1995a; 38: 901-909.

47. De Stefano N, Matthews PM, Arnold DL. Reversible decreases in N-acetylaspartate after acute brain injury. Magn Reson Med 1995b; 34: 721-7.

48. De Stefano N, Matthews PM, Fu L, Narayanan S, Stanley J, Francis GS, et al. Axonal damage correlates with disability in patients with relapsing- remitting multiple sclerosis. Results of a longitudinal magnetic resonance spectroscopy study. Brain 1998; 121: 1469-77.

49. De Stefano N, Matthews PM, Narayanan S, Francis GS, Antel JP, Arnold DL. Axonal dysfunction and disability in a relapse of multiple sclerosis: longitudinal study of a patient. Neurology 1997; 49: 1138-41.

50. De Stefano N, Narayanan S, Francis GS, Arnaoutelis R, Tartaglia MC, Antel JP, et al. Evidence of axonal damage in the early stages of multiple sclerosis and its relevance to disability. Arch Neurol 2001; 58: 65-70.

51. De Stefano N, Narayanan S, Matthews PM, Francis GS, Antel JP, Arnold DL. In vivo evidence for axonal dysfunction remote from focal cerebral demyelination of the type seen in multiple sclerosis. Brain 1999; 122: 1933-1939.

52. Demerens C, Stankoff B, Zalc B, Lubetzki C. Eliprodil stimulates CNS myelination: new prospects for multiple sclerosis? Neurology 1999; 52: 346-50.

53. den Hollander JA, Oosterwall B, van Vroonhoven H, Luyten PR. Elimination of magnetic field distortions in ^{1}H NMR spectroscopic imaging. Soc Maggn Reson Med. Vol 1, 1991: 472.

54. Dousset V, Grossman RI, Ramer KN, Schnall MD, Young LH, Gonzalez-Scarano F, et al. Experimental allergic encephalomyelitis and multiple sclerosis: lesion characterization with magnetization transfer imaging [published erratum appears in Radiology 1992 Jun;183(3):878]. Radiology 1992; 182: 483-91.

55. Edzes HT, Samulski ET. The measurement of cross-relaxation effects in the proton NMR spin-lattice relaxation of water in biological systems:hydrated collagen and muscle. Journal of Magnetic Resonance 1978; 31: 207-29.

56. Evangelou N, Esiri MM, Smith S, Palace J, Matthews PM. Quantitative pathological evidence for axonal loss in normal appearing white matter in multiple sclerosis. Ann Neurol 2000; 47: 391-5.

57. Evans AC, Marrett S, Neelin P, Collins L, Worsley KJ, Dai W, et al. Anatomical mapping of functional activation in stereotactic coordinate space. NeuroImage 1992; 1: 43-63.

58. Evans AC, Marrett S, Torrescorzo J, Ku S, Collins L. MRI-PET correlation in three dimensions using a volume-of-interest (VOI) atlas. Journal of Cerebral Blood Flow & Metabolism 1991; 11: A69-A78.

59. Ferguson B, Matyszak MK, Esiri MM, Perry VH. Axonal damage in acute multiple sclerosis lesions. Brain 1997; 120: 393-9.

60. Filippi M. Linking structural, metabolic and functional changes in multiple sclerosis. Eur J Neurol 2001; 8: 291-7.

61. Filippi M, Barker GJ, Horsfield MA, Sacares PR, MacManus DG, Thompson AJ, et al. Benign and secondary progressive multiple sclerosis: a preliminary quantitative MRI study. Journal of Neurology 1994a; 241: 246-251.

62. Filippi M, Campi A, Dousset V, Baratti C, Martinelli V, Canal N, et al. A magnetization transfer imaging study of normal-appearing white matter in multiple sclerosis. Neurology 1995a; 45: 478-82.

63. Filippi M, Colombo B, Rovaris M, Pereira C, Martinelli V, Comi G. A longitudinal magnetic resonance imaging study of the cervical cord in multiple sclerosis. J Neuroimaging 1997; 7: 78-80.

64. Filippi M, Grossman RI. MRI techniques to monitor MS evolution: the present and the future. Neurology 2002; 58: 1147-53.

65. Filippi M, Horsfield MA, Morrissey SP, MacManus DG, Rudge P, McDonald WI, et al. Quantitative brain MRI lesion load predicts the course of clinically isolated syndromes suggestive of multiple sclerosis. Neurology 1994b; 44: 635-641.

66. Filippi M, Paty DW, Kappos L, Barkhof F, Compston DA, Thompson AJ, et al. Correlations between changes in disability and T2-weighted brain MRI activity in multiple sclerosis: a follow-up study. Neurology 1995b; 45: 255-60.

67. Filippi M, Rocca MA, Colombo B, Falini A, Codella M, Scotti G, et al. Functional magnetic resonance imaging correlates of fatigue in multiple sclerosis. Neuroimage 2002; 15: 559-67.

68. Filippi M, Rocca MA, Martino G, Horsfield MA, Comi G. Magnetization transfer changes in the normal appearing white matter precede the appearance of enhancing lesions in patients with multiple sclerosis. Ann Neurol 1998; 43: 809-14.

69. Filippi M, Rocca MA, Minicucci L, Martinelli V, Ghezzi A, Bergamaschi R, et al. Magnetization transfer imaging of patients with definite MS and negative conventional MRI. Neurology 1999a; 52: 845-8.

70. Filippi M, Tortorella C, Bozzali M. Normal-appearing white matter changes in multiple sclerosis: the contribution of magnetic resonance techniques. Mult Scler 1999b; 5: 273-82.

71. Fischer JS, Rudick RA, Cutter GR, Reingold SC. The Multiple Sclerosis Functional Composite Measure (MSFC): an integrated approach to MS clinical outcome assessment. National MS Society Clinical Outcomes Assessment Task Force. Mult Scler 1999; 5: 244-50.

72. Foong J, Rozewicz L, Davie CA, Thompson AJ, Miller DH, Ron MA. Correlates of executive function in multiple sclerosis: the use of magnetic resonance spectroscopy as an index of focal pathology [In Process Citation]. J Neuropsychiatry Clin Neurosci 1999; 11: 45-50.

73. Fox NC, Jenkins R, Leary SM, Stevenson VL, Losseff NA, Crum WR, et al. Progressive cerebral atrophy in MS: a serial study using registered, volumetric MRI [see comments]. Neurology 2000; 54: 807-12.

74. Fox PT. Functional brain mapping with positron emission tomography. [Review]. Seminars in Neurology 1989; 9: 323-329.

75. Fox PT, Mintun MA, Reiman EM, Raichle ME. Enhanced detection of focal brain responses using intersubject averaging and change-distribution analysis of subtracted PET images. Journal of Cerebral Blood Flow & Metabolism 1988; 8: 642-653.

76. Fox PT, Perlmutter JS, Raichle ME. A stereotactic method of anatomical localization for positron emission tomography. Journal of Computer Assisted Tomography 1985; 9: 141-153.

77. Fralix TA, Ceckler TL, Wolff SD, Simon SA, Balaban RS. Lipid bilayer and water proton magnetization transfer: effect of cholesterol. Magn Reson Med 1991; 18: 214-23.

78. Fu L, Matthews PM, De Stefano N, Worsley KJ, Narayanan S, Francis GS, et al. Imaging axonal damage of normal-appearing white matter in multiple sclerosis. Brain 1998; 121: 103-13.

79. Fu L, Wolfson C, Worsley KJ, De Stefano N, Collins DL, Narayanan S, et al. Statistics for investigation of multimodal MR imaging data and an application to multiple sclerosis patients. NMR Biomed 1996; 9: 339-46.

80. Gadian DG. NMR and its applications to living systems. Oxford: Oxford University Press, 1995.

81. Gareau PJ, Rutt BK, Karlik SJ, Mitchell JR. Magnetization transfer and multicomponent T2 relaxation measurements with histopathologic correlation in an experimental model of MS. J Magn Reson Imaging 2000; 11: 586-595.

82. Gass A, Barker GJ, Kidd D, Thorpe JW, MacManus D, Brennan A, et al. Correlation of magnetization transfer ratio with clinical disability in multiple sclerosis. Annals of Neurology 1994; 36: 62-67.

83. Gonen O, Catalaa I, Babb JS, Ge Y, Mannon LJ, Kolson DL, et al. Total brain N-acetylaspartate: a new measure of disease load in MS. Neurology 2000; 54: 15-9.

84. Goodkin DE, Rooney WD, Sloan R, Bacchetti P, Gee L, Vermathen M, et al. A serial study of new MS lesions and the white matter from which they arise. Neurology 1998; 51: 1689-97.

85. Graham GD, Blamire AM, Howseman AM, Rothman DL, Fayad PB, Brass LM, et al. Proton magnetic resonance spectroscopy of cerebral lactate and other metabolites in stroke patients. Stroke 1992; 23: 333-40.

86. Graham SJ, Henkelman RM. Understanding pulsed magnetization transfer. J Magn Reson Imaging 1997; 7: 903-12.

87. Green JB, Bialy Y, Sora E, Ricamato A. High-resolution EEG in poststroke hemiparesis can identify ipsilateral generators during motor tasks [In Process Citation]. Stroke 1999; 30: 2659-65.

88. Griffin JW, George R, Lobato C, Tyor WR, Yan LC, Glass JD. Macrophage responses and myelin clearance during Wallerian degeneration: relevance to immune-mediated demyelination. J Neuroimmunol 1992; 40: 153-65.

89. Grossman RI. Magnetization transfer in multiple sclerosis. Annals of Neurology 1994; 36 Suppl: S97-S99.

90. Grossman RI, Gomori JM, Ramer KN, Lexa FJ, Schnall MD. Magnetization transfer: theory and clinical applications in neuroradiology. RadioGraphics 1994; 14: 279-290.

91. Haase A, Frahm J. Multiple chemical shift selective NMR imaging using stimulated echoes. J. Magn. Reson. 1985: 94-102.

92. Haase A, Frahm J, Hanicke W, Matthaei D. 1H NMR chemical shift selective (CHESS) imaging. Phys Med Biol 1985; 30: 341-4.

93. Henkelman RM, Huang X, Xiang QS, Stanisz GJ, Swanson SD, Bronskill MJ. Quantitative interpretation of magnetization transfer. Magn Reson Med 1993; 29: 759-66.

94. Henkelman RM, Stanisz GJ, Graham SJ. Magnetization transfer in MRI: a review. NMR Biomed 2001; 14: 57-64.

95. Hohlfeld R. Biotechnological agents for the immunotherapy of multiple sclerosis. Principles, problems and perspectives. Brain 1997; 120 (Pt 5): 865-916.

96. Hu BS, Conolly SM, Wright GA, Nishimura DG, Macovski A. Pulsed saturation transfer contrast. Magn Reson Med 1992; 26: 231-40.

97. Husted CA, Goodin DS, Hugg JW, Maudsley AA, Tsuruda JS, de Bie SH, et al. Biochemical alterations in multiple sclerosis lesions and normal-appearing white matter detected by in vivo 31P and 1H spectroscopic imaging. Annals of Neurology 1994; 36: 157-165.

98. Jenkins WM, Merzenich MM. Reorganization of neocortical representations after brain injury: a neurophysiological model of the bases of recovery from stroke. Prog Brain Res 1987; 71: 249-66.

99. Jones SJ. Visual evoked potentials after optic neuritis. Effect of time interval, age and disease dissemination. J Neurol 1993; 240: 489-94.

100. Kamber M. Automated Detection of Multiple Sclerosis Lesions in Magnetic Resonance Images of the Human Brain. Montreal, Quebec: Master's thesis, Dept. of Computer Science, Concordia University, 1991.

101. Kapeller P, McLean MA, Griffin CM, Chard D, Parker GJ, Barker GJ, et al. Preliminary evidence for neuronal damage in cortical grey matter and normal appearing white matter in short duration relapsing-remitting multiple sclerosis: a quantitative MR spectroscopic imaging study. J Neurol 2001; 248: 131-8.

102. Kastrukoff LF, Oger JJ, Hashimoto SA, Sacks SL, Li DK, Palmer MR, et al. Systemic lymphoblastoid interferon therapy in chronic progressive multiple sclerosis. I. Clinical and MRI evaluation. Neurology 1990; 40: 479-86.

103. Khoury SJ, Guttmann CR, Orav EJ, Hohol MJ, Ahn SS, Hsu L, et al. Longitudinal MRI in multiple sclerosis: correlation between disability and lesion burden. Neurology 1994; 44: 2120-2124.

104. Kidd D, Thorpe JW, Thompson AJ, Kendall BE, Moseley IF, MacManus DG, et al. Spinal cord MRI using multi-array coils and fast spin echo. II. Findings in multiple sclerosis. Neurology 1993; 43: 2632-7.

105. Koenig SH, Brown RD, 3rd, Spiller M, Lundbom N. Relaxometry of brain: why white matter appears bright in MRI. Magn Reson Med 1990; 14: 482-95.

106. Kucharczyk W, Macdonald PM, Stanisz GJ, Henkelman RM. Relaxivity and magnetization transfer of white matter lipids at MR imaging: importance of cerebrosides and pH. Radiology 1994; 192: 521-9.

107. Kurtzke JF. Rating neurologic impairment in multiple sclerosis: an expanded disability status scale (EDSS). Neurology 1983; 33: 1444-1452.

108. Larsson HB, Christiansen P, Jensen M, Frederiksen J, Heltberg A, Olesen J, et al. Localized in vivo proton spectroscopy in the brain of patients with multiple sclerosis. Magn Reson Med 1991; 22: 23-31.

109. Lassmann H. The pathology of multiple sclerosis and its evolution. Philos Trans R Soc Lond B Biol Sci 1999; 354: 1635-40.

110. Leary SM, Davie CA, Parker GJ, Stevenson VL, Wang L, Barker GJ, et al. 1H magnetic resonance spectroscopy of normal appearing white matter in primary progressive multiple sclerosis. J Neurol 1999; 246: 1023-6.

111. Lee JH, Arcinue E, Ross BD. Brief report: organic osmolytes in the brain of an infant with hypernatremia. N Engl J Med 1994; 331: 439-42.

112. Lee M, Reddy H, Johansen-Berg H, Pendlebury S, Jenkinson M, Smith S, et al. The motor cortex shows adaptive functional changes to brain injury from multiple sclerosis. Ann Neurol 2000a; 47: 606-13.

113. Lee MA, Blamire AM, Pendlebury S, Ho KH, Mills KR, Styles P, et al. Axonal injury or loss in the internal capsule and motor impairment in multiple sclerosis [see comments]. Arch Neurol 2000b; 57: 65-70.

114. Lightman S, McDonald WI, Bird AC, Francis DA, Hoskins A, Batchelor JR, et al. Retinal venous sheathing in optic neuritis. Its significance for the pathogenesis of multiple sclerosis. Brain 1987; 110 (Pt 2): 405-14.

115. Liu C, Edwards S, Gong Q, Roberts N, Blumhardt LD. Three dimensional MRI estimates of brain and spinal cord atrophy in multiple sclerosis. J Neurol Neurosurg Psychiatry 1999; 66: 323-30.

116. Loevner LA, Grossman RI, Cohen JA, Lexa FJ, Kessler D, Kolson DL. Microscopic disease in normal-appearing white matter on conventional MR images in patients with multiple sclerosis: assessment with magnetization-transfer measurements. Radiology 1995; 196: 511-5.

117. Losseff NA, Miller DH. Measures of brain and spinal cord atrophy in multiple sclerosis. J Neurol Neurosurg Psychiatry 1998; 64 Suppl 1: S102-5.

118. Losseff NA, Wang L, Lai HM, Yoo DS, Gawne-Cain ML, McDonald WI, et al. Progressive cerebral atrophy in multiple sclerosis. A serial MRI study. Brain 1996a; 119: 2009-19.

119. Losseff NA, Webb SL, O'Riordan JI, Page R, Wang L, Barker GJ, et al. Spinal cord atrophy and disability in multiple sclerosis. A new reproducible and sensitive MRI method with potential to monitor disease progression. Brain 1996b; 119: 701-8.

120. Lovas G, Szilagyi N, Majtenyi K, Palkovits M, Komoly S. Axonal changes in chronic demyelinated cervical spinal cord plaques [see comments]. Brain 2000; 123: 308-17.

121. Luks TL, Goodkin DE, Nelson SJ, Majumdar S, Bacchetti P, Portnoy D, et al. A longitudinal study of ventricular volume in early relapsing-remitting multiple sclerosis. Mult Scler 2000; 6: 332-7.

122. Lycklama à Nijeholt GJ, van Walderveen MA, Castelijns JA, van Waesberghe JH, Polman C, Scheltens P, et al. Brain and spinal cord abnormalities in multiple sclerosis. Correlation between MRI parameters, clinical subtypes and symptoms. Brain 1998; 121: 687-97.

123. MacKay A, Whittall K, Adler J, Li D, Paty D, Graeb D. In vivo visualization of myelin water in brain by magnetic resonance. Magn Reson Med 1994; 31: 673-7.

124. Manly BFJ. Randomization and Monte Carlo Methods in Biology. New York: Chapman and Hall, 1991.

125. Martin E, Capone A, Schneider J, Hennig J, Thiel T. Absence of N-acetylaspartate in the human brain: impact on neurospectroscopy? Ann Neurol 2001; 49: 518-21.

126. Matthews PM, Andermann F, Silver K, Karpati G, Arnold DL. Proton MR spectroscopic characterization of differences in regional brain metabolic

abnormalities in mitochondrial encephalomyopathies. Neurology 1993; 43: 2484-90.

127. Matthews PM, Arnold DL. Magnetic resonance imaging of multiple sclerosis: new insights linking pathology to clinical evolution. Curr Opin Neurol 2001; 14: 279-87.

128. Matthews PM, Cianfaglia L, McLaurin J, Cashman N, Sherwin D, Arnold D, et al. Demonstration of reversible decreases in N-Acetylaspartate (NAA) in a neuronal cell line: NAA decreases as a marker of sublethal neuronal dysfunction [abstract]. Proc Soc Magn Reson Med 1995; 1: 147.

129. Matthews PM, De Stefano N, Narayanan S, Francis GS, Wolinsky JS, Antel JP, et al. Putting magnetic resonance spectroscopy studies in context: axonal damage and disability in multiple sclerosis. Semin Neurol 1998; 18: 327-36.

130. Matthews PM, Francis G, Antel J, Arnold DL. Proton magnetic resonance spectroscopy for metabolic characterization of plaques in multiple sclerosis. Neurology 1991a; 41: 1251-1256.

131. Matthews PM, Pioro E, Narayanan S, De Stefano N, Fu L, Francis G, et al. Assessment of lesion pathology in multiple sclerosis using quantitative MRI morphometry and magnetic resonance spectroscopy. Brain 1996; 119: 715-22.

132. Matthews WB, Compston A, Allen IV, Martyn CN. Pathology of multiple sclerosis. In: Matthews WB, editor. McAlpine's Multiple Sclerosis. New York: Churchill Livingstone, 1991b: 341-378.

133. McAlpine D, Compston NC, Lumsden CE. Course and prognosis. In: McAlpine D, Compston NC and Lumsden CE, editors. Multiple Sclerosis. Edinburgh: Livingstone, 1955: 135-155.

134. McDonald WI. Rachelle Fishman-Matthew Moore Lecture. The pathological and clinical dynamics of multiple sclerosis. [Review]. Journal of Neuropathology & Experimental Neurology 1994; 53: 338-343.

135. McGavern DB, Murray PD, Rivera-Quinones C, Schmelzer JD, Low PA, Rodriguez M. Axonal loss results in spinal cord atrophy, electrophysiological abnormalities and neurological deficits following demyelination in a chronic inflammatory model of multiple sclerosis. Brain 2000; 123 Pt 3: 519-31.

136. McGowan JC, Filippi M, Campi A, Grossman RI. Magnetisation transfer imaging: theory and application to multiple sclerosis. J Neurol Neurosurg Psychiatry 1998; 64 Suppl 1: S66-9.

137. Menon DK, Baudouin CJ, Tomlinson D, Hoyle C. Proton MR spectroscopy and imaging of the brain in AIDS: evidence of neuronal loss in regions that appear normal with imaging. J Comput Assist Tomogr 1990; 14: 882-5.

138. Mews I, Bergmann M, Bunkowski S, Gullotta F, Bruck W. Oligodendrocyte and axon pathology in clinically silent multiple sclerosis lesions. Mult Scler 1998; 4: 55-62.

139. Miller BL, Chang L, Booth R, Ernst T, Cornford M, Nikas D, et al. In vivo 1H MRS choline: correlation with in vitro chemistry/histology. Life Sci 1996; 58: 1929-35.

140. Miller DH. Magnetic resonance in monitoring the treatment of multiple sclerosis. [Review]. Annals of Neurology 1994; 36 Suppl: S91-S94.

141. Miller DH, Frank JA. Magnetic resonance imaging techniques to monitor short term evolution of multiple sclerosis and to use in preliminary trials. J Neurol Neurosurg Psychiatry 1998; 64 Suppl 1: S44-6.

142. Miller DH, Grossman RI, Reingold SC, McFarland HF. The role of magnetic resonance techniques in understanding and managing multiple sclerosis. Brain 1998; 121: 3-24.

143. Moffett JR, Namboodiri MAA, Cangro CB, Neale JH. Immunohistochemical localization of N-acetylaspartate in rat brain. NeuroReport 1991; 2: 131-134.

144. Moll C, Mourre C, Lazdunski M, Ulrich J. Increase of sodium channels in demyelinated lesions of multiple sclerosis. Brain Res 1991; 556: 311-6.

145. Moreau T, Coles A, Wing M, Isaacs J, Hale G, Waldmann H, et al. Transient increase in symptoms associated with cytokine release in patients with multiple sclerosis. Brain 1996; 119: 225-37.

146. Moreau T, Thorpe J, Miller D, Moseley I, Hale G, Waldmann H, et al. Preliminary evidence from magnetic resonance imaging for reduction in disease activity after lymphocyte depletion in multiple sclerosis [published erratum appears in Lancet 1994 Aug 13;344(8920):486]. Lancet 1994; 344: 298-301.

147. Morrison C, Henkelman RM. A model for magnetization transfer in tissues. Magn Reson Med 1995; 33: 475-82.

148. Muller RA, Chugani HT, Muzik O, Mangner TJ. Brain organization of motor and language functions following hemispherectomy: a [(15)O]-water positron emission tomography study. J Child Neurol 1998; 13: 16-22.

149. Nakano M, Ueda H, Li JY, Matsumoto M, Yanagihara T. Measurement of regional N-acetylaspartate after transient global ischemia in gerbils with and without ischemic tolerance: an index of neuronal survival. Ann Neurol 1998; 44: 334-40.

150. Narayana PA, Doyle TJ, Lai D, Wolinsky JS. Serial proton magnetic resonance spectroscopic imaging, contrast- enhanced magnetic resonance imaging, and quantitative lesion volumetry in multiple sclerosis. Ann Neurol 1998; 43: 56-71.

151. Narayanan S, De Stefano N, Francis GS, Arnaoutelis R, Caramanos Z, Collins DL, et al. Axonal metabolic recovery in multiple sclerosis patients treated with interferon beta-1b. J Neurol 2001; 248: 979-86.

152. Narayanan S, De Stefano N, Francis GS, Tartaglia MC, Arnaoutelis R, Arnold DL. Disease duration influences the relationship between brain axonal injury, spinal cord atrophy and disability in multiple sclerosis. Eighth Annual Meeting of the International Society for Magnetic Resonance in Medicine. Vol 1. Denver, CO: ISMRM, 2000: 297.

153. Narayanan S, Fu L, Pioro E, De Stefano N, Collins DL, Francis GS, et al. Imaging of axonal damage in multiple sclerosis: spatial distribution of magnetic resonance imaging lesions. Ann Neurol 1997; 41: 385-91.

154. Newcombe J, Hawkins CP, Henderson CL, Patel HA, Woodroofe MN, Hayes GM, et al. Histopathology of multiple sclerosis lesions detected by magnetic resonance imaging in unfixed postmortem central nervous system tissue. Brain 1991; 114 (Pt 2): 1013-23.

155. Nudo RJ, Friel KM. Cortical plasticity after stroke: implications for rehabilitation. Rev Neurol (Paris) 1999; 155: 713-7.

156. Ogawa S, Menon RS, Tank DW, Kim SG, Merkle H, Ellermann JM, et al. Functional brain mapping by blood oxygenation level-dependent contrast

magnetic resonance imaging. A comparison of signal characteristics with a biophysical model. Biophys J 1993; 64: 803-12.

157. Ordidge RJ, Mansfield P, Lohman JA, Prime SB. Volume selection using gradients and selective pulses. Ann N Y Acad Sci 1987; 508: 376-85.

158. Pan JW, Hetherington HP, Vaughan JT, Mitchell G, Pohost GM, Whitaker JN. Evaluation of multiple sclerosis by 1H spectroscopic imaging at 4.1 T. Magn Reson Med 1996; 36: 72-7.

159. Patel TB, Clark JB. Synthesis of N-acetyl-L-aspartate by rat brain mitochondria and its involvement in mitochondrial/cytosolic carbon transport. Biochem J 1979; 184: 539-46.

160. Paty DW. Magnetic resonance in multiple sclerosis. Curr Opin Neurol Neurosurg 1993; 6: 202-8.

161. Paty DW, Li DK. Interferon beta-1b is effective in relapsing-remitting multiple sclerosis. II. MRI analysis results of a multicenter, randomized, double-blind, placebo-controlled trial. UBC MS/MRI Study Group and the IFNB Multiple Sclerosis Study Group [see comments]. Neurology 1993; 43: 662-667.

162. Paty DW, Li DK, Oger JJ, Kastrukoff L, Koopmans R, Tanton E, et al. Magnetic resonance imaging in the evaluation of clinical trials in multiple sclerosis. Annals of Neurology 1994; 36 Suppl: S95-S96.

163. Pendlebury ST, Blamire AM, Lee MA, Styles P, Matthews PM. Axonal injury in the internal capsule correlates with motor impairment after stroke. Stroke 1999; 30: 956-62.

164. Peters AR, Geelen JA, den Boer JA, Prevo RL, Minderhoud JM, s Gravenmade EJ. A study of multiple sclerosis patients with magnetic resonance spectroscopic imaging. Mult Scler 1995; 1: 25-31.

165. Peterson JW, Bo L, Mork S, Chang A, Trapp BD. Transected neurites, apoptotic neurons, and reduced inflammation in cortical multiple sclerosis lesions. Ann Neurol 2001; 50: 389-400.

166. Pierce WB, Harms SE, Flamig DP, Griffey RH, Evans WP, Hagans JE. Three-dimensional gadolinium-enhanced MR imaging of the breast: pulse sequence with fat suppression and magnetization transfer contrast. Work in progress. Radiology 1991; 181: 757-63.

167. Pike GB. Pulsed magnetization transfer contrast in gradient echo imaging: a two-pool analytic description of signal response. Magn Reson Med 1996; 36: 95-103.

168. Pike GB, de Stefano N, Narayanan S, Francis GS, Antel JP, Arnold DL. Combined magnetization transfer and proton spectroscopic imaging in the assessment of pathologic brain lesions in multiple sclerosis. AJNR Am J Neuroradiol 1999; 20: 829-37.

169. Pike GB, De Stefano N, Narayanan S, Worsley KJ, Pelletier D, Francis GS, et al. Multiple sclerosis: magnetization transfer MR imaging of white matter before lesion appearance on T2-weighted images. Radiology 2000; 215: 824-30.

170. Pike GB, Glover GH, Hu BS, Enzmann DR. Pulsed magnetization transfer spin-echo MR imaging. J Magn Reson Imaging 1993; 3: 531-9.

171. Pike GB, Hu BS, Glover GH, Enzmann DR. Magnetization transfer time-of-flight magnetic resonance angiography. Magn Reson Med 1992; 25: 372-9.

172. Pitt D, Werner P, Raine CS. Glutamate excitotoxicity in a model of multiple sclerosis. Nat Med 2000; 6: 67-70.

173. Poser CM, Paty DW, Scheinberg L, McDonald WI, Floyd AD, Ebers GC, et al. New diagnostic criteria for multiple sclerosis: Guidelines for research protocols. Annals of Neurology 1983; 13: 227-231.

174. Preul MC, Caramanos Z, Collins DL, Villemure JG, Leblanc R, Olivier A, et al. Accurate, noninvasive diagnosis of human brain tumors by using proton magnetic resonance spectroscopy. Nat Med 1996; 2: 323-5.

175. Prineas JW, Barnard RO, Kwon EE, Sharer LR, Cho ES. Multiple sclerosis: remyelination of nascent lesions. Annals of Neurology 1993; 33: 137-151.

176. Prineas JW, Connell F. The fine structure of chronically active multiple sclerosis plaques. Neurology 1978; 28 (Suppl.2): 68-75.

177. Prineas JW, Connell F. Remyelination in multiple sclerosis. Ann Neurol 1979; 5: 22-31.

178. Quarles RH, Morell P, McFarlin DE. Diseases involving myelin. In: Siegel J, Agranoff BW, Albers RW and Molinoff PB, editors. Basic Neurochemistry: molecular, cellular and medical aspects. New York: Raven Press, 1993: 771-792.

179. Raine CS. The neuropathology of multiple sclerosis. In: Raine CS, McFarland HF and Tourtellotte WW, editors. Multiple Sclerosis : Clinical and Pathogenetic Basis. London: Chapman & Hall, 1997a: 151-171.

180. Raine CS. The Norton Lecture: a review of the oligodendrocyte in the multiple sclerosis lesion. J Neuroimmunol 1997b; 77: 135-52.

181. Raine CS, Cross AH. Axonal dystrophy as a consequence of long-term demyelination. Laboratory Investigation 1989; 60: 714-725.

182. Raine CS, Wu E. Multiple sclerosis: remyelination in acute lesions. J Neuropathol Exp Neurol 1993; 52: 199-204.

183. Rasminsky M. Pathophysiology of demyelination. Ann N Y Acad Sci 1984; 436: 68-85.

184. Rasminsky M, Kearney RE, Aguayo AJ, Bray GM. Conduction of nervous impulses in spinal roots and peripheral nerves of dystrophic mice. Brain Res 1978; 143: 71-85.

185. Rasminsky M, Sears TA. Internodal conduction in undissected demyelinated nerve fibres. J Physiol (Lond) 1972; 227: 323-50.

186. Reddy H, Narayanan S, Arnoutelis R, Jenkinson M, Antel J, Matthews PM, et al. Evidence for adaptive functional changes in the cerebral cortex with axonal injury from multiple sclerosis. Brain 2000a; 123: 2314-20.

187. Reddy H, Narayanan S, Matthews PM, Hoge RD, Pike GB, Duquette P, et al. Relating axonal injury to functional recovery in MS. Neurology 2000b; 54: 236-9.

188. Riahi F, Zijdenbos A, Narayanan S, Arnold D, Francis G, Antel J, et al. Improved correlation between scores on the expanded disability status scale and cerebral lesion load in relapsing-remitting multiple sclerosis. Results of the application of new imaging methods. Brain 1998; 121: 1305-12.

189. Richert ND, Frank JA. Magnetization transfer imaging to monitor clinical trials in multiple sclerosis. Neurology 1999; 53: S29-32.

190. Richert ND, Ostuni JL, Bash CN, Duyn JH, McFarland HF, Frank JA. Serial whole-brain magnetization transfer imaging in patients with relapsing-remitting multiple sclerosis at baseline and during treatment with interferon beta-1b. AJNR 1998; 19: 1705-13.

191. Richert ND, Ostuni JL, Bash CN, Leist TP, McFarland HF, Frank JA. Interferon beta-1b and intravenous methylprednisolone promote lesion recovery in multiple sclerosis. Mult Scler 2001; 7: 49-58.

192. Rivera-Quinones C, McGavern D, Schmelzer JD, Hunter SF, Low PA, Rodriguez M. Absence of neurological deficits following extensive demyelination in a class I-deficient murine model of multiple sclerosis. Nat Med 1998; 4: 187-93.

193. Rocca MA, Falini A, Colombo B, Scotti G, Comi G, Filippi M. Adaptive functional changes in the cerebral cortex of patients with nondisabling multiple sclerosis correlate with the extent of brain structural damage. Ann Neurol 2002; 51: 330-9.

194. Rocca MA, Mastronardo G, Rodegher M, Comi G, Filippi M. Long-term changes of magnetization transfer-derived measures from patients with relapsing-remitting and secondary progressive multiple sclerosis. AJNR Am J Neuroradiol 1999; 20: 821-7.

195. Rodriguez M, Scheithauer B. Ultrastructure of multiple sclerosis. Ultrastruct Pathol 1994; 18: 3-13.

196. Rooney WD, Goodkin DE, Schuff N, Meyerhoff DJ, Norman D, Weiner MW. 1H MRSI of normal appearing white matter in multiple sclerosis. Multiple Sclerosis 1997; 3: 231-7.

197. Ropele S, Strasser-Fuchs S, Seifert T, Enzinger C, Fazekas F. Development of active multiple sclerosis lesions: a quantitative MT study. ISMRM. Honolulu, HI, 2002.

198. Roth M, Decety J, Raybaudi M, Massarelli R, Delon-Martin C, Segebarth C, et al. Possible involvement of primary motor cortex in mentally simulated movement: a functional magnetic resonance imaging study. Neuroreport 1996; 7: 1280-4.

199. Rovaris M, Comi G, Filippi M. The role of non-conventional MR techniques to study multiple sclerosis patients. J Neurol Sci 2001; 186 Suppl 1: S3-9.

200. Rudick RA, Fisher E, Lee JC, Simon J, Jacobs L. Use of the brain parenchymal fraction to measure whole brain atrophy in relapsing-remitting MS. Multiple Sclerosis Collaborative Research Group [In Process Citation]. Neurology 1999; 53: 1698-704.

201. Sappey-Marinier D, Antel SB, Tartaglia CM, Narayanan S, Francis S, Arbel T, et al. Quantification métabolique dans la sclérose en plaques par imagerie spectroscopique RMN. Journée Neurologique Francaise. Lyons, 2001.

202. Sarchielli P, Presciutti O, Pelliccioli GP, Tarducci R, Gobbi G, Chiarini P, et al. Absolute quantification of brain metabolites by proton magnetic resonance spectroscopy in normal-appearing white matter of multiple sclerosis patients [In Process Citation]. Brain 1999; 122: 513-21.

203. Sarchielli P, Presciutti O, Tarducci R, Gobbi G, Alberti A, Pelliccioli GP, et al. 1H-MRS in patients with multiple sclerosis undergoing treatment with interferon beta-1a: results of a preliminary study. J Neurol Neurosurg Psychiatry 1998; 64: 204-12.

204. Schiepers C, Van Hecke P, Vandenberghe R, Van Oostende S, Dupont P, Demaerel P, et al. Positron emission tomography, magnetic resonance imaging and proton NMR spectroscopy of white matter in multiple sclerosis. Mult Scler 1997; 3: 8-17.

205. Schneider E, Prost RW, Glover GH. Pulsed magnetization transfer versus continuous wave irradiation for tissue contrast enhancement. J Magn Reson Imaging 1993; 3: 417-23.

206. Scolding N, Franklin R. Axon loss in multiple sclerosis. Lancet 1998; 352: 340-1.

207. Scolding N, Franklin R, Stevens S, Heldin CH, Compston A, Newcombe J. Oligodendrocyte progenitors are present in the normal adult human CNS and in the lesions of multiple sclerosis [see comments]. Brain 1998; 121: 2221-8.

208. Scolding NJ, Rayner PJ, Compston DA. Identification of A2B5-positive putative oligodendrocyte progenitor cells and A2B5-positive astrocytes in adult human white matter. Neuroscience 1999; 89: 1-4.

209. Seil FJ. Recovery and repair issues after stroke from the scientific perspective. Curr Opin Neurol 1997; 10: 49-51.

210. Seitz RJ, Azari NP, Knorr U, Binkofski F, Herzog H, Freund HJ. The role of diaschisis in stroke recovery. Stroke 1999; 30: 1844-50.

211. Silber E, Sharief MK. Axonal degeneration in the pathogenesis of multiple sclerosis. J Neurol Sci 1999; 170: 11-8.

212. Silver NC, Barker RA, MacManus DG, Barker GJ, Thom M, Thomas DG, et al. Proton magnetic resonance spectroscopy in a pathologically confirmed acute demyelinating lesion. J Neurol 1997; 244: 204-7.

213. Silver NC, Tofts PS, Symms MR, Barker GJ, Thompson AJ, Miller DH. Evidence of widespread subtle blood-brain barrier dysfunction associated with progressive MS. Proc Soc Magn Reson Med 1999; 1: 628.

214. Simmons ML, Frondoza CG, Coyle JT. Immunocytochemical localization of N-acetyl-aspartate with monoclonal antibodies. Neuroscience 1991; 45: 37-45.

215. Simon JH. Brain and spinal cord atrophy in multiple sclerosis: role as a surrogate measure of disease progression. CNS Drugs 2001; 15: 427-36.

216. Simon JH, Jacobs LD, Campion MK, Rudick RA, Cookfair DL, Herndon RM, et al. A longitudinal study of brain atrophy in relapsing multiple sclerosis. The Multiple Sclerosis Collaborative Research Group (MSCRG). Neurology 1999; 53: 139-48.

217. Simon JH, Kinkel RP, Jacobs L, Bub L, Simonian N. A Wallerian degeneration pattern in patients at risk for MS. Neurology 2000; 54: 1155-60.

218. Sled JG, Pike GB. Quantitative interpretation of magnetization transfer in spoiled gradient echo MRI sequences. J Magn Reson 2000; 145: 24-36.

219. Sled JG, Pike GB. Quantitative imaging of magnetization transfer exchange and relaxation properties in vivo using MRI. Magn Reson Med 2001; 46: 923-31.

220. Smith KJ, Kapoor R, Felts PA. Demyelination: the role of reactive oxygen and nitrogen species. Brain Pathol 1999; 9: 69-92.

221. Smith SM, De Stefano N, Jenkinson M, Matthews PM. Normalized accurate measurement of longitudinal brain change. J Comput Assist Tomogr 2001; 25: 466-75.

222. Smith SM, Zhang Y, Jenkinson M, Chen JT, Matthews PM, Federico A, et al. Accurate, robust and automated longitudinal and cross-sectional brain change analysis. NeuroImage 2002; In Press.

223. Staffen W, Mair A, Zauner H, Unterrainer J, Niederhofer H, Kutzelnigg A, et al. Cognitive function and fMRI in patients with multiple sclerosis: evidence for compensatory cortical activation during an attention task. Brain 2002; 125: 1275-82.

224. Stevenson VL, Leary SM, Losseff NA, Parker GJ, Barker GJ, Husmani Y, et al. Spinal cord atrophy and disability in MS: a longitudinal study. Neurology 1998; 51: 234-8.

225. Stewart VC, Giovannoni G, Land JM, McDonald WI, Clark JB, Heales SJ. Pretreatment of astrocytes with interferon-alpha/beta impairs interferon-gamma induction of nitric oxide synthase. J Neurochem 1997; 68: 2547-51.

226. Stewart VC, Land JM, Clark JB, Heales SJ. Pretreatment of astrocytes with interferon-alpha/beta prevents neuronal mitochondrial respiratory chain damage. J Neurochem 1998; 70: 432-4.

227. Stone LA, Frank JA, Albert PS, Bash C, Smith ME, Maloni H, et al. The effect of interferon-beta on blood-brain barrier disruptions demonstrated by contrast-enhanced magnetic resonance imaging in relapsing-remitting multiple sclerosis. Ann Neurol 1995; 37: 611-9.

228. Suhy J, Rooney WD, Goodkin DE, Capizzano AA, Soher BJ, Maudsley AA, et al. 1H MRSI comparison of white matter and lesions in primary progressive and relapsing-remitting MS. Mult Scler 2000; 6: 148-55.

229. Talairach J, Tournoux P. Co-planar stereotactic atlas of the human brain: 3-dimensional proportional system: an approach to cerebral imaging. Stuttgart: Georg Thieme Verlag, 1988.

230. Tartaglia MC, Narayanan S, DeStefano N, Arnaoutelis R, Antel SB, Francis SJ, et al. Choline is increased in prelesional normal-appearing white matter in Multiple Sclerosis. J Neurology 2002; In Press.

231. The IFNB multiple sclerosis study group. Interferon beta-1b is effective in relapsing-remitting multiple sclerosis. I. Clinical results of a multicenter, randomized, double-blind, placebo-controlled trial. Neurology 1993; 43: 655-661.

232. Thomas DJ, Pennock JM, Hajnal JV, Young IR, Bydder GM, Steiner RE. Magnetic resonance imaging of spinal cord in multiple sclerosis by fluid-attenuated inversion recovery [see comments]. Lancet 1993; 341: 593-594.

233. Thompson AJ, Montalban X, Barkhof F, Brochet B, Filippi M, Miller DH, et al. Diagnostic criteria for primary progressive multiple sclerosis: a position paper. Ann Neurol 2000; 47: 831-5.

234. Thorpe JW, Kidd D, Kendall BE, Tofts PS, Barker GJ, Thompson AJ, et al. Spinal cord MRI using multi-array coils and fast spin echo. I. Technical aspects and findings in healthy adults. Neurology 1993; 43: 2625-31.

235. Thorpe JW, Kidd D, Moseley IF, Kenndall BE, Thompson AJ, MacManus DG, et al. Serial gadolinium-enhanced MRI of the brain and spinal cord in early relapsing-remitting multiple sclerosis. Neurology 1996a; 46: 373-8.

236. Thorpe JW, Kidd D, Moseley IF, Thompson AJ, MacManus DG, Compston DA, et al. Spinal MRI in patients with suspected multiple sclerosis and negative brain MRI. Brain 1996b; 119 (Pt 3): 709-14.

237. Tourbah A, Stievenart JL, Gout O, Fontaine B, Liblau R, Lubetzki C, et al. Localized proton magnetic resonance spectroscopy in relapsing remitting versus secondary progressive multiple sclerosis. Neurology 1999; 53: 1091-7.

238. Tourbah A, Stievenart JL, Iba-Zizen MT, Zannoli G, Lyon-Caen O, Cabanis EA. In vivo localized NMR proton spectroscopy of normal appearing white matter in patients with multiple sclerosis. J Neuroradiol 1996; 23: 49-55.

239. Trapp BD, Bo L, Mork S, Chang A. Pathogenesis of tissue injury in MS lesions. J Neuroimmunol 1999a; 98: 49-56.

240. Trapp BD, Peterson J, Ransohoff RM, Rudick R, Mork S, Bo L. Axonal transection in the lesions of multiple sclerosis [see comments]. N Engl J Med 1998; 338: 278-85.

241. Trapp BD, Ransohoff R, Rudick R. Axonal pathology in multiple sclerosis: relationship to neurologic disability. Curr Opin Neurol 1999b; 12: 295-302.

242. Trapp BD, Ransohoff RM, Fisher E, Rudick RA. Neurodegenration in multiple sclerosis: relationship to neurological disability. Neuroscientist 1999c; 5: 48-57.

243. Truckenmiller ME, Namboodiri MA, Brownstein MJ, Neale JH. N-Acetylation of L-aspartate in the nervous system: differential distribution of a specific enzyme. J Neurochem 1985; 45: 1658-62.

244. Truyen L, van Waesberghe JH, van Walderveen MA, van Oosten BW, Polman CH, Hommes OR, et al. Accumulation of hypointense lesions ("black holes") on T1 spin-echo MRI correlates with disease progression in multiple sclerosis. Neurology 1996; 47: 1469-76.

245. Urenjak J, Williams SR, Gadian DG, Noble MD. Specific expression of N-acetylaspartate in neurons, oligodendrocyte-type-2 astrocyte progenitors, and immature oligodendrocytes in vitro. J Neurochem 1992; 59: 55-61.

246. Urenjak J, Williams SR, Gadian DG, Noble MD. Proton nuclear magnetic resonance spectroscopy unambiguously identifies different neural cell types. J Neurosci 1993; 13: 981-9.

247. van Waesberghe JH, Kamphorst W, De Groot CJ, van Walderveen MA, Castelijns JA, Ravid R, et al. Axonal loss in multiple sclerosis lesions: magnetic resonance imaging insights into substrates of disability. Ann Neurol 1999; 46: 747-54.

248. van Walderveen MA, Barkhof F, Pouwels PJ, van Schijndel RA, Polman CH, Castelijns JA. Neuronal damage in T1-hypointense multiple sclerosis lesions demonstrated in vivo using proton magnetic resonance spectroscopy. Ann Neurol 1999; 46: 79-87.

249. van Walderveen MA, Kamphorst W, Scheltens P, van Waesberghe JH, Ravid R, Valk J, et al. Histopathologic correlate of hypointense lesions on T1-weighted spin-echo MRI in multiple sclerosis. Neurology 1998; 50: 1282-8.

250. van Walderveen MA, Lycklama ANGJ, Ader HJ, Jongen PJ, Polman CH, Castelijns JA, et al. Hypointense lesions on T1-weighted spin-echo magnetic resonance imaging: relation to clinical characteristics in subgroups of patients with multiple sclerosis. Arch Neurol 2001; 58: 76-81.

251. Vavasour IM, Whittall KP, MacKay AL, Li DK, Vorobeychik G, Paty DW. A comparison between magnetization transfer ratios and myelin water percentages in normals and multiple sclerosis patients. Magn Reson Med 1998; 40: 763-8.

252. Waxman SG. Molecular remodeling of neurons in multiple sclerosis: what we know, and what we must ask about brain plasticity in demyelinating diseases. Adv Neurol 1997; 73: 109-20.

253. Waxman SG. Demyelinating diseases--new pathological insights, new therapeutic targets [editorial; comment]. N Engl J Med 1998; 338: 323-5.

254. Waxman SG. Do 'demyelinating' diseases involve more than myelin? Nat Med 2000a; 6: 738-9.

255. Waxman SG. Multiple sclerosis as a neuronal disease. Arch Neurol 2000b; 57: 22-4.

256. Waxman SG. The neuron as a dynamic electrogenic machine: modulation of sodium-channel expression as a basis for functional plasticity in neurons. Philos Trans R Soc Lond B Biol Sci 2000c; 355: 199-213.

257. Weiller C, Ramsay SC, Wise RJ, Friston KJ, Frackowiak RS. Individual patterns of functional reorganization in the human cerebral cortex after capsular infarction. Annals of Neurology 1993; 33: 181-189.

258. Werner P, Pitt D, Raine CS. Glutamate excitotoxicity--a mechanism for axonal damage and oligodendrocyte death in Multiple Sclerosis? J Neural Transm Suppl 2000: 375-85.

259. Werring DJ, Brassat D, Droogan AG, Clark CA, Symms MR, Barker GJ, et al. The pathogenesis of lesions and normal-appearing white matter changes in multiple sclerosis: a serial diffusion MRI study. Brain 2000; 123: 1667-76.

260. Wolff SD, Balaban RS. Magnetization transfer contrast (MTC) and tissue water proton relaxation in vivo. Magn Reson Med 1989; 10: 135-44.

261. Wolswijk G. Chronic stage multiple sclerosis lesions contain a relatively quiescent population of oligodendrocyte precursor cells. J Neurosci 1998; 18: 601-9.

262. Yeung HN, Aisen AM. Magnetization transfer contrast with periodic pulsed saturation. Radiology 1992; 183: 209-14.

263. Youl BD, Turano G, Miller DH, Towell AD, MacManus DG, Moore SG, et al. The pathophysiology of acute optic neuritis. An association of gadolinium leakage with clinical and electrophysiological deficits. Brain 1991; 114 (Pt 6): 2437-50.

264. Yousry TA, Berry I, Filippi M. Functional magnetic resonance imaging in multiple sclerosis. J Neurol Neurosurg Psychiatry 1998; 64 Suppl 1: S85-7.

265. Zhang Y, Brady M, Smith S. Segmentation of brain MR images through a hidden Markov random field model and the expectation maximization algorithm. (Abstract). IEEE Transactions on Biomedical Imaging 2001; 20: 45-57.

266. Zhu B, Moore GR, Zwimpfer TJ, Kastrukoff LF, Dyer JK, Steeves JD, et al. Axonal cytoskeleton changes in experimental optic neuritis. Brain Res 1999; 824: 204-17.

Appendix

Research Compliance Certificates

MONTREAL NEUROLOGICAL INSTITUTE AND HOSPITAL

INSTITUT ET HÔPITAL NEUROLOGIQUES DE MONTRÉAL

A Teaching and Research Institute of McGill University

Institut d'enseignement et de recherche de l'Université McGill

March 21, 1997

Dr. Douglas L. Arnold
Department of Neurology/Neurosurgery
MNI

Dear Dr. Arnold:

The Research Ethics Committee of the Montreal Neurological Institute and Hospital met the 13th of March 1997 and reviewed your request for renewal of the protocol. ***"Proton Magnetic Resonance Spectroscopy of Multiple Sclerosis".*** The Committee approves this request.

Attached please find an appendix outlining routine conditions of the approval.

Yours very truly,

Ronald Pokrupa, MD
Chairman, Research Ethics Committee
Montreal Neurological Institute and Hospital

3801, rue University
Montréal, Québec
Canada H3A 2B4
Téléphone (514) 398 6644

MONTREAL NEUROLOGICAL INSTITUTE AND HOSPITAL
INSTITUT ET HÔPITAL NEUROLOGIQUES DE MONTRÉAL

A Teaching and Research Institute of McGill University

Institut d'enseignement et de recherche de l'Université McGill

29 May 1998

Dr Douglas Arnold
Magnetic Resonance Spectroscopy
M N I

5.c. ARND 1991/3 **Proton Magnetic Resonance Spectroscopy of Multiple Sclerosis**

Your application names Christina Wolfson and Paul Matthews as associate investigators. Please promptly confirm that this is correct or forward a single corrected copy of the renewal application to the Research Ethics Committee office (Rm 686).

The committee approves renewal of the above protocol for a period of one year.

Attached please find an appendix outlining routine conditions of the approval.

Yours very truly,

Ronald Pokrupa, MD
Chairman, Research Ethics
/ve

3801, rue University
Montreal, Québec
Canada H3A 2B4
Téléphone (514) 398 1903
Télécopieur/Fax (514) 398 8248
Internet http://mcgill.ca/mni

MONTREAL NEUROLOGICAL INSTITUTE AND HOSPITAL

INSTITUT ET HÔPITAL NEUROLOGIQUES DE MONTRÉAL

A Teaching and Research Institute of McGill University

Institut d'enseignement et de recherche de l'Université McGill

20 November 1998

Dr Douglas Arnold
Magnetic Resonance Spectroscopy
M N I

3.e. ARND 1998/6 **Proton Magnetic Resonance Spectroscopy of Multiple Sclerosis**, undated English and 1998.11.10 French consent forms.

The committee approves the foregoing protocol and accompanying consent forms for a period of twelve months.

It suggests, however, that the consent form be reworded using the second person throughout except for the very last paragraph in which the subject signifies consent. Moreover, in the first paragraph of the consent forms the term "my" should be omitted.

It also requests that the consent form include the usual exclusion criteria or that an MRI consent form be appended.

Please promptly return a single copy embodying the foregoing.

Attached please find an appendix outlining routine conditions of the approval.

Yours very truly,

Ronald Pokrupa, MD
Chairman, Research Ethics
/ve

NOV 27 1998

3801, rue University
Montreal, Quebec
Canada H3A 2B4

Telephone (514) 398 6644
Telecopier/Fax (514) 398 8540

MONTREAL NEUROLOGICAL INSTITUTE AND HOSPITAL

INSTITUT ET HÔPITAL NEUROLOGIQUES DE MONTRÉAL

A Teaching and Research Institute of McGill University

Institut d'enseignement et de recherche de l'Université McGill

14 March 2000

Dr Douglas Arnold
Magnetic Resonance Spectroscopy
M N I

Meeting of 1998.11.19

3.e. ARND 1998/6 **Proton Magnetic Resonance Spectroscopy of Multiple Sclerosis**, undated English and 1998.11.10 French consent forms.

In our letter of 1998.11.20, account was not taken of the approval period requested in the initial application to the Research Ethics Committee.

The committee approves the foregoing protocol and accompanying consent forms for a period of twelve months. The specific 12-month period, as requested, is to run from1999.06.01 until 2000.05.31.

Please excuse this inadvertent oversight.

Yours very truly,

Ronald Pokrupa, MD
Chairman, Research Ethics
/ve

3801, rue University
Montréal, Québec
Canada H3A 2B4
Téléphone (514) 398-6644

MONTREAL NEUROLOGICAL INSTITUTE AND HOSPITAL
INSTITUT ET HÔPITAL NEUROLOGIQUES DE MONTRÉAL

A Teaching and Research Institute of McGill University

Institut d'enseignement et de recherche de l'Université McGill

18 April 2000

Dr Douglas Arnold
Magnetic Resonance Spectroscopy
Montreal Neurological Institute

Meeting of 2000.04.01

5.a. ARND 1991/3 **Proton Magnetic Resonance Spectroscopy of Multiple Sclerosis**

The committee has reviewed the protocol and consent forms that you submitted for renewal. Although the committee grants renewal, the following are considerations that require your attention.

1. The sheet the subject will be signing should bear the site of the study and its title or unique identifier.

2. A better title for item 7 of the consent form would be 'Termination for scientific reasons'.

Please promptly forward a single copy of both consent forms after revision.

Attached please find an appendix outlining routine conditions of the approval.

Yours very truly,

Ronald Pokrupa, MD, Chair
Research Ethics Committee
/ve

3801, rue University
Montréal, Québec
Canada H3A 2B4
Téléphone (514) 398-6644

Centre universitaire de santé McGill
McGill University Health Centre

29 May 2001

Sridar Narayanan, MSc
Research Assistant
MRS Unit, MNI

Meeting of 2001.05.28

3.a. ARND 1991/3 **Proton Magnetic Resonance Spectroscopy of Multiple Sclerosis (CIHR)** - D Arnold

(Documentation submitted: Signed Checklist of 2001.05.06; English and French consent forms both dated 2001.05.06)

The board has reviewed your request for renewal of the foregoing protocol and renews its approval for a one-year period, specifically from 2001.06.01 to 2002.05.31.

However, the renewal is based on the assumption that you are using the latest version of the MRI questionnaire and are reconsenting the subjects for every scanning session.

Yours very truly,

Paul Holland, PhD, Acting Chair
Research Ethics Board
/ve

JUN - 4 2001